Tim-3 as a signalling receptor expressed by leukaemia cells and potential target for highly specific drug delivery

Thesis by

Isabel Bernardo Gonçalves Oliveira Silva

A thesis submitted in partial fulfilment of the requirements of the University of Kent and the University of Greenwich for the Degree of Doctor of Philosophy

September 2017

DECLARATION

"I certify that this work has not been accepted in substance for any degree, and is not concurrently being submitted for any degree other that of Doctor of Philosophy being studied at the Universities of Greenwich and Kent. I also declare that this work is the result of my own investigations except where otherwise identified by references and that I have not plagiarised the work of others."

The Candidate

_____ Date_____

The Supervisor

_____ Date_____

ACKOWLEDGEMENTS

I would like to start thanking all our collaborators, whose participation in the project allowed me to perform essential experiments and made this work possible.

Many thanks to my colleagues, Dr Inna Yasinska and Svetlana Sakhnevych for allowing me to use some of their results, more specifically some of the results shown in “4.4 A fundamental molecular pathway controlling immune escape of human acute leukaemia cells”. Their participation allowed me to put together this puzzle.

Thanks to Dr Bernhard Gibbs for providing me with primary human NK cells, primary healthy human leukocytes and human blood plasma. Also I am grateful for his guidance during my PhD.

A big Thank you to Dr Vadim Sumbayev for all the guidance, help, encouragement and patience during my PhD programme. Without his help, I do not believe I would achieve the results I had.

Finally, I would like to thank my parents, my siblings, Eduard and my friends for supporting me in all the ways they could during this stage of my life.

A big and sincere thanks to all of you!

ABSTRACT

Leukaemia is a blood/bone marrow cancer caused by malignant immature hematopoietic precursors, and quickly becomes a systematic malignancy. The most severe type of leukaemia that has the highest number of lethal outcomes is Acute Myeloid Leukaemia (AML) where malignant cells escape host immune surveillance by inactivating cytotoxic lymphoid cells.

We discovered a fundamental biochemical mechanism in AML cells, which includes ligand-dependent (probably FLRT3) activation of ectopically expressed latrophilin 1 and possible other G-protein coupled receptors, leading to upregulated translation and secretion of the immune receptor Tim-3 and its ligand galectin-9. This process involved protein kinase C and the mammalian target of rapamycin (mTOR). Tim-3 was observed to participate in galectin-9 secretion, and was also released in a free soluble form. Galectin-9 impaired the anti-cancer activities of cytotoxic lymphoid cells including natural killer (NK) cells and soluble Tim-3 prevented the secretion of interleukin-2 (IL-2), which was required for the activation of cytotoxic lymphoid cells.

These results were validated in *ex vivo* experiments, using primary samples from AML patients. This fundamental pathway provides reliable targets for both highly specific diagnosis and immune therapy of AML.

Furthermore, we demonstrated that the Tim-3/galectin-9 autocrine loop has intracellular functions and promotes cell growth and proliferation by directly upregulating translational pathway controlled by mTOR.

CONTENTS

FIGURES

TABLES

ABREVIATIONS

4E-BP1: 4E binding protein

Akt: Protein kinase B

ALL: Acute lymphoid leukaemia

AML: Acute myeloid leukaemia

AMPK: AMP-activated protein kinase

ATG13: Autophagy-related gene 13

ATLL: T-cell leukaemias/lymphomas

ATP: Adenosine triphosphate

BSA: Bovine serum albumin

CLL: Chronic lymphoid leukaemia

CML: chronic myeloid leukaemia

Deptor: DEP-domain containing mTOR-interacting protein

DTT: Dithiothreitol

EDTA: Ethylenediaminetetraacetic acid

eEF2K: Eukaryotic elongation factor 2 kinase

eIFAE: Eukaryotic initiation factor 4E

ERK1/2: Extra cellular-signal-regulated kinase 1/2

FIP200: Focal adhesion kinase family-interacting protein of 200 kDa

FKBP12: FK06-binding protein of 12 kDa

GAP: GTPase-activating protein

G-CSF: Granulocyte colony-stimulation factor

GM-CSF: Granulocyte macrophage colony-stimulation factor

HIF-1: Hypoxia-inducible factor 1

HIF-1α/β: Hypoxia-inducible factor 1 α/β

HSC: Hematopoietic stem cells

ICA: In cell assay

ICW: In cell western

Ig: Immunoglobulin

IgSF: Immunoglobulin super family

IgV: Immunoglobulin variable domain

IL-1β: Interleukin 1β

IL-6: Interleukin 6

IL-8: Interleukin 8

IRS1/2: Insulin receptor substrate 1/2

LIC: Leukaemia initiating cells

LKB1: Serine-threonine kinase 11

LPHN: Latrophilin

LPS: Lypopolysaccharides

LTX: Latrotoxin

MGO: Methylglyoxal

mLST8: Mammalian lethal with Sec13 protein 8

mSIN1: Mammalian stress-activated protein kinase interacting protein

mTOR: Mammalian target of rapamycin

mTOR1/2: Mammalian target of rapamycin complex 1/2

NF1: Neurofibromatosis 1

NF-κB: Factor kappa-light-chain-enhancer of activated B cells

P70S6K1: p70 ribosomal S6 kinase 1

PBS: Phosphate-buffered saline

PDC4: Programmed cell death 4

PDGF: Platelet-derived growth factor

PDK1: Phosphoinositide-dependent kinase 1

PHL: Primary healthy leukocytes

PI-3K: Phosphatidylinositol-3 kinase

PKCα: Protein kinase Cα

PL: Primary leukocytes

PLC-1: Phospholipase C1

PMA: para-Methoxyamphetamine

PMSF: Phenylmethylsulfonyl fluoride

PPARγ: Peroxisome proliferation-activated receptor γ

PRAS40: Proline rich Akt substrate

Proctor-1: Protein observed with Rictor-1

qRT-PCR: Reverse transcription polymerase chain reaction

Raptor: Regulatory-associated protein of mTOR

Rheb: Ras homologue enriched in brain

Rictor: Rapamycin-insensitive companion of mTOR

RSK1: p90 ribosomal S6 kinase

SCF: Stem cell factor

SDS: Sodium dodecyl sulphate

SRCD: Synchrotron radiation circular dichroism

SREBP1: Sterol regulatory element binding protein

TBST: Tris-buffered saline, 0.1% Tween 20

Tc1: T cytotoxic type I cell

Th1: T-helper type 1

Tim-3: T-cell immunoglobulin mucin-3

TLR4: Toll-like receptor 4

TNF: Tumour necrosis factor

TNFα: Tumour necrosis factor α

TSC1/2: Tuberous sclerosis complex 1/2

ULK1: Unc-S1-like kinase 1

VEGF: Vascular endothelial growth factor

1. INTRODUCTION

Cancer is a severe disease associated with the transformation of healthy cells at any stage of differentiation or maturation. These malignant cells, unlike healthy ones, are non-differentiated and are unable to mature into specialised cells with normal biological functions and keep proliferating. Also, malignant cells are smaller than healthy ones, they have less cytoplasmic space and the cell to cell connection between malignant is weaker. This is due to the lack of specialisation of the cells that do not allow the proper development of desmosomes, structure responsible by the cell to cell adhesion. These phenomena can result in the breach off of cells and the entrance of these in circulation, leading to the formation of metastasis (Figure 1).

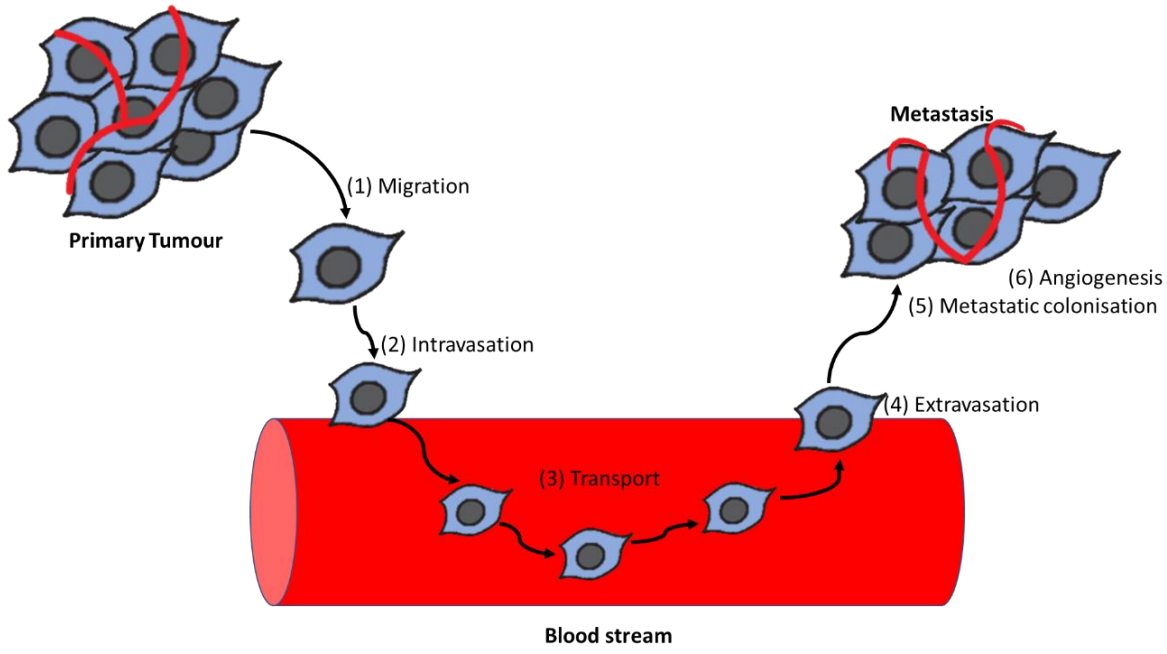

Figure 1 Steps of metastasis. *The cells migrate from primary tumour and through intravasation get into the circulation. They migrate together with the blood until extravasated to a different tissue where they form a metastatic colony which then develops into a secondary (metastatic) tumour.*

1.1 Epidemiology of cancer

Cancer is a serious medical burden worldwide, affecting both industrialised and developing countries. In 2015, cancer was the second leading cause of death worldwide, being only overcome by cardiovascular disease (Wang *et al.*, 2016). There were 17.5 million cancer cases worldwide and 8.7 million deaths cancer-related. In 2005, the number of cancer cases was much smaller, there were registers of 13 million. This means that between 2005 and 2015 there was an increase of 33% in the number of cancer cases. In 2015, 8.7 million people died from cancer, which represents 16% of all deaths worldwide. This was an increase of 3% in the number of deaths due to cancer, since 2005, where cancer was responsible for 13% of all deaths (Fitzmaurice *et al.*, 2016; Bray, 2016). The increase in the number of register cancer cases and deaths, not only raises concern in health levels but also in economical levels on a global scale. Since 1995, the cost of incident cancer cases suffered a 10-fold increase. And, in 2009, these values reached the value of $286 billion (Bray, 2016; Hill *et al.*, 2017).

In 2015, the type of cancer with the higher number of registered cases was the breast cancer, with 2.4 million cases. The type of cancer with the highest number of deaths was the tracheal, bronchus and lung cancer with 1.7 million of registered deaths (Fitzmaurice *et al.*, 2016). In the table below are the 10 most common types of cancer, according to the number of cases in 2015.

Table 1 10 Common types of cancer according to the number of cases and lethal outcomes. (Fitzmaurice *et al.*, 2016)

	Registered cases	**Registered deaths**
Breast cancer	2.4 million	533000
Tracheal, bronchus and lung cancer	2 million	1.7 million
Colon and rectum cancer	1.7 million	832000
Prostate cancer	1.6 million	360000
Stomach cancer	1.3 million	819000
Liver Cancer	854000	768000
Non-Hodgkin lymphoma	666000	231000
Leukaemia	606000	353000
Bladder cancer	541000	188000
Cervical cancer	526000	239000

Among the cancer types present in Table 1, leukaemia is the most poorly studied, and its mechanisms are not well understood. Unlike other types of cancer, it affects stem cells responsible for tissue (blood) development (haematopoiesis) and thus is considered a severe systemic disorder. It affects all the organ systems straight away since blood is required everywhere. Leukaemia also develops a strong and highly effective strategy, which allows malignant cells to escape immune attack. Therefore, understanding the mechanisms of this type of cancer will allow understanding the progression and immune escape of other types of cancer.

1.2 Leukaemia

Leukaemia is a blood/bone marrow cancer that has origin in self-renewing malignant immature precursors, which often becomes a systematic malignancy.

1.2.1 Epidemiology

Each year, 250,000 cases of leukaemia are reported worldwide. This is the 3rd most common type of cancer among children and young people, and the 8th in general. It represents 2.5% of the total number of cancer cases in the world (Fitzmaurice *et al.,* 2016). This type of cancer is more common in men (57%) than in women (43%), but in terms of mortality is about the same in both genders (75%) (IARC, 2017; World Cancer Research Fund International, n.d.). In 2012, Denmark was considered the country with the highest incidence of leukaemia, with 29 cases per 100,000 individuals.

Leukaemia causes are not clear, but several factors have been associated with the increased risk of developing it. Some of these factors are age, infection with some virus and exposure environmental hazards (like ionising radiation, pollution, benzene, etc.) (Pokharel, 2012; Estey and Döhner, 2006). Given the wide use/misuse of nuclear energy and the increase of the environmental pollution worldwide, this becomes one of the most serious problems of the modern society. That is why timely diagnostics and less aggressive cure against leukaemia are an important issues to address.

The risk of developing leukaemia increases with the age, except in acute lymphoid leukaemia (ALL) that has a high number of patients in the group age 2-7 years and then after 40 years. Chronic myeloid leukaemia (CML) is more common in patients around 50 years old and represents 15 to 20% of leukaemia cases in adult patients, acute myeloid leukaemia (AML) is

more common after 70 years old and chronic lymphoid leukaemia (CLL) in the age range between 65 to 70 years old (Pokharel, 2012; Chiorazzi *et al.*, 2005; Hehlmann *et al.*, 2007; Pui *et al.*, 2008; Estey and Döhner, 2006).

This risk of developing leukaemia is also related to the ethnic origin of a person. Almost all types of leukaemia are most common in white people. The exception is the chronic lymphoid leukaemia were white and black people have the same chances of developing it (Pui *et al.*, 2008; Pokharel, 2012).

The genetic background of the individual can be also an important risk factor for having leukaemia. For example, individuals with Down syndrome have a 20-fold increase chance of developing leukaemia. Other syndromes like ataxia-telangiectasia, bloom syndrome, Fanconi syndrome, Klinefelter syndrome and neurofibromatosis are known to increase the risk of leukaemia (Pokharel, 2012). Also, if there is a familiar history of some types of leukaemia (AML and CLL), there is a higher risk of having the disease (Chiorazzi *et al.*, 2005; Estey and Döhner, 2006).

Another factor that is known to increase the chances of developing leukaemia is exposure to radiation. Although exposure to high levels of radiation is a known risk factor, exposure to low levels of radiation is still not well investigated as a contribute factor for developing leukaemia (Pokharel, 2012).

Exposure to human T-cell lymphotropic virus-1 is linked to T-cell leukaemias/lymphomas (ATLL). This is not a common type of leukaemia or infection since the virus is only found in some areas of the world, namely the Caribbean Basin, Japan, some parts of south America and some parts of Africa (Pokharel, 2012).

As any other disease, diagnosis is essential for treating leukaemia. At the moment, the main diagnosis methods of leukaemia are physical exam, blood tests, bone marrow aspiration and biopsy, and lumbar puncture. In the physical exam, a medical doctor performs palpitation to identify any lumps or other abnormalities that can be identified as symptoms of leukaemia. There are three blood tests that can be done to diagnose leukaemia, the complete blood count, where the amount and quality of all blood cells is measured; the peripheral blood smear, that determines presence of blast cells and reveals the type and quantity of white blood cells; and the cytogenic analysis, used to identify lymphocytes chromosomes and changes in them. In the bone marrow aspiration, a small amount of bone marrow is removed from a bone through a needle and this sample is used to check for chromosomes problems and infection signs and the bone marrow biopsy, which is normally done after the aspiration, and it consists in removing bone with bone marrow for further analysis. Finally, the lumbar puncture consists in the removal of a small amount of the spinal fluid from the spaces between the vertebrae in the spine and the count of white blood cells is performed in this sample (Pokharel, 2012; Pui *et al.*, 2008; WebMD, 2005; Pinkel *et al.*, 1986; Baron, 2005).

After a positive diagnosis, it is important to proceed with treatment. Different treatments for leukaemia are available at the moment, such as surgery, where there is removal of the enlarged spleen or installation of a venous access device to give medication and withdraw blood. Radiotherapy, the use of ionising radiation to kill malignant cells, and chemotherapy, where a wide range of drugs (such as antimetabolites, genotoxic drugs, enzyme inhibitors and spindle inhibitors) are used to kill malignant cells. There is also immunotherapy, which consist of vaccines containing proteins found in or produced by cancer cells. These proteins will stimulate the body's defences against cancer by increasing its response and by stem cell transportation (hematopoietic stem cell, multipotent hematopoietic stem cells usually derived from bone

marrow, peripheral blood, or umbilical cord blood cells). Prior to stem cell transportation, the immune system of the recipient is destroyed with radiation or chemotherapy (Pokharel, 2012).

1.2.2 Pathophysiology

Haematopoiesis is the process that leads to the formation of mature blood cells. Mature blood cells, mostly, have a short lifetime, therefore stem cells are essential throughout life to restock blood cells (Orkin and Zon, 2008).

Haematopoietic stem cells (HSC) are the stem cells that undergo transformation into mature blood cells and are progenitors of all blood cells, due to its capacity of self-renewal and differentiation. During the differentiation process, these cells become progressively restricted to several or to a single lineage (Orkin and Zon, 2008; Jagannathan-Bogdan and Zon, 2013).

Haematopoiesis starts with the differentiation of $CD14^{+}$ HSC into myeloid stem cells or lymphoid stem cells. The lymphoid stem cells mature in to B lymphocytes (cells responsible for fabricating antibodies), T lymphocytes (help B lymphocytes to fabricate antibodies) and natural killer cells (responsible for the attack on cancer cells and viruses). The myeloid stem cells become erythrocytes (also known as red blood cells, which carry oxygen and nutrients to the body tissues), platelets (responsible for the formation of blood clots) and myeloid leukocytes (responsible for fighting pathogens) like basophils, neutrophils, monocytes and eosinophils (Orkin and Zon, 2008; Janeway *et al.*, 2001; National Cancer Institute, 2013).

In the following scheme (Figure 2) is a summary of the haematopoietic process.

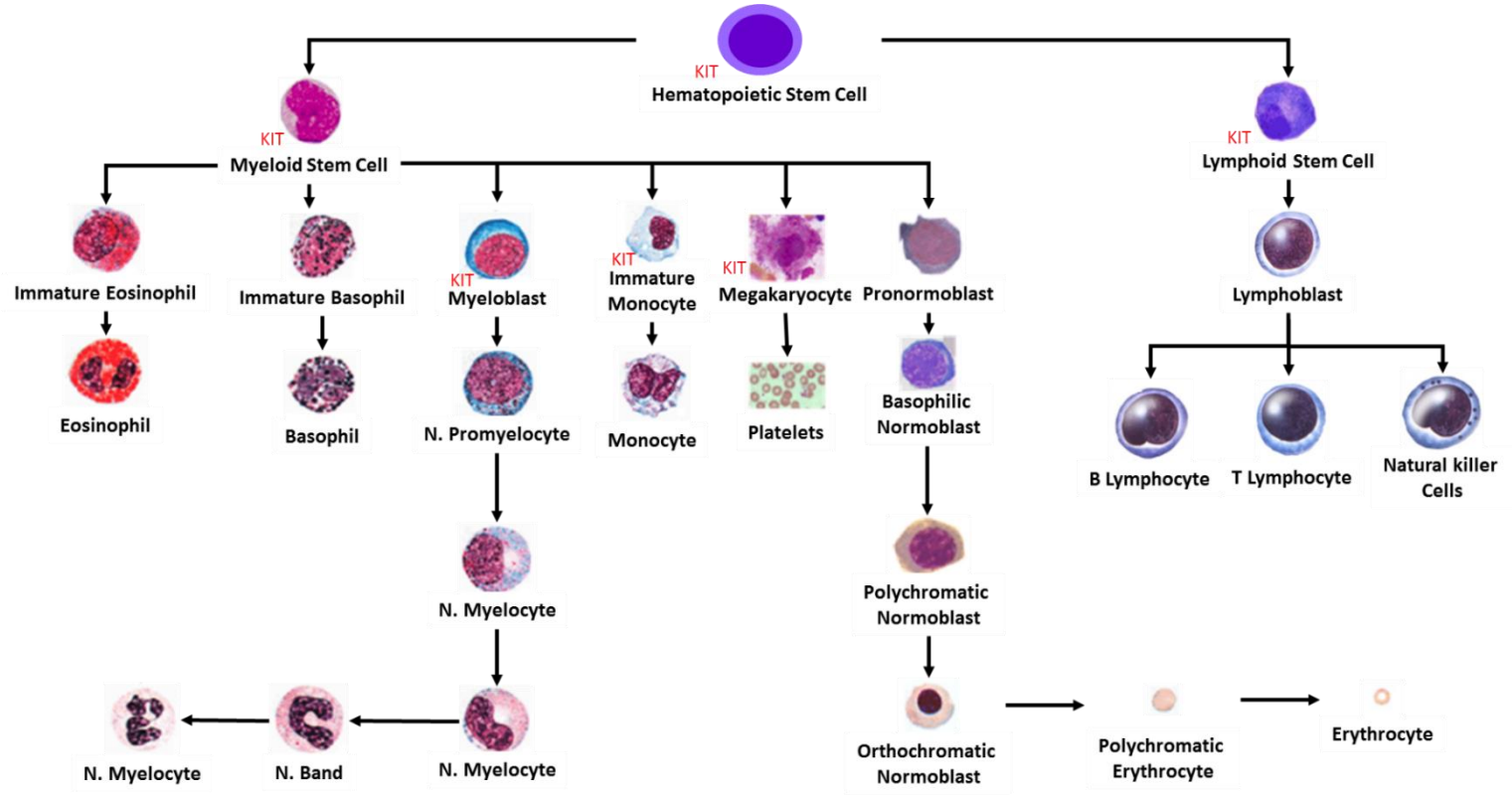

Figure 2 Normal blood cell development with indication of presence/absence of Kit receptor (stem cell factor receptor). *The hematopoietic stem cell originates a myeloid stem cell or lymphoid stem cell (beginning of myeloid and lymphoid lineages). These cells will differentiate into the main blood cell types. Image adapted from* (Wrock, 2011).

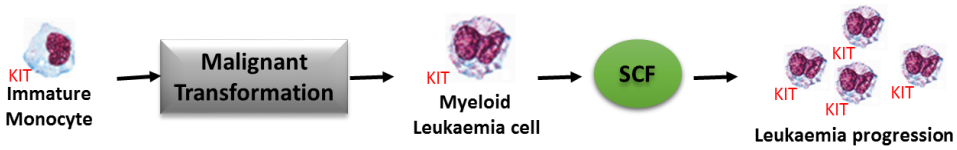

Figure 3 Representation of haematopoiesis in myeloid leukaemia. *The immature monocyte suffers malignant transformation and origins Myeloid Leukeamia cell, it expresses the Kit receptor contrary to what happens in normal haematopoiesis, so it is able to multiply* (Wrock, 2011).

In leukaemia, the normal process of haematopoiesis is disturbed and malignant transformation occurs (Figure 3). It is believed that leukaemia may be initiated by transforming events that occur in the hematopoietic stem cells, allowing the cells to keep their self-renewal abilities, such as retaining expression of the Kit receptor. Hematopoietic stem cells are a better hypothesis for being the precursor of leukaemia cells than more mature cells because they have all the machinery for self-renewal so it requires fewer mutations to keep it active than to activate it ectopically (Passegue *et al.*, 2003).

During or after cell division, haematopoietic stem cells must decide their fate, remain HSC, differentiate or die by apoptosis. These decisions must be a well-tuned process to maintain a steady state level of functional HSC in the bone marrow and a constant source of progenitors for the different hematopoietic lineages. Failing in doing these decisions lead to the formation of cancer cells. There is evidence showing that leukaemia cells arise from accumulated mutations in hematopoietic stem cells that allow them to keep the capacity of indefinite proliferation. Both cells have self-renewal ability, extensive proliferative potential and the ability to generate new hematopoietic tissues with a combination of heterogeneous cells, with different phenotypes and proliferation potentials (Passegue *et al.*, 2003).

The accumulation of mutations can be potentiated by external factors like ionising radiation and chemicals and/or internal factors like chromosomal abnormalities (for example, avoiding the telomere shortening trough action of the telomerase complex). Chromosomal rearrangements may alter the structure or regulation of cellular oncogenes (Passegue *et al.*, 2003; Wu, 2017; Spivak, 2017).

This leads to an overproduction of abnormal white blood cells,. These cells, unlike the healthy ones, do not die when they become old or damaged. This leads to an increase in the number of abnormal cells, overtaking the number of healthy cells. The fact that the number of healthy cells decreases makes harder for the body tissues to obtain oxygen, to control bleeding and to fight infections (National Cancer Institute, 2013; Spivak, 2017).

Most of the leukaemia symptoms result from the suppression of normal blood cell formation and the organ infiltration, the malignant cells spill into the circulation and infiltration of other organs. This infiltration results in enlargement of liver, spleen, and lymph nodes (Spivak, 2017; Wu, 2017).

1.2.2.1 Types of leukaemia

Leukaemia can be classified into four types, per the type of Leucocytes that are affected (myeloid or lymphoid) and according to the characteristics of the disease (acute or chronic). These types of leukaemia are acute myeloid leukaemia (AML), chronic myeloid leukaemia (CML), acute lymphoid leukaemia (ALL) and chronic lymphoid Leukaemia (CLL). In Table 2, the main characteristics of these four types of leukaemia are described.

Table 2 Schematic information about the four main types of leukaemia. (Cancer Treatment Centers of America, 2017; Chiorazzi *et al.*, 2005; Hehlmann *et al.*, 2007; Pui *et al.*, 2008; Dana-Farber cancer institute, 2014; Estey and Döhner, 2006; Pui *et al.*, 2004; Gao *et al.*, 2014)

	AML	**CML**	**ALL**	**CLL**
Affected Cells	• Myeloid Stem cells	• Myeloid stem cells	• Lymphoid stem cells	• B Lymphocytes
Epidemiology	• > 60 years	• > 50 years	• 2-7 years	• 65-70 years
Main Symptoms	• Pale skin • Tiredness • Breathlessness • Frequent infections • Unusual and frequent bleeding	• Tiredness • Weight loss • Night sweats • Tenderness and swelling in the left side of the abdomen • Pale skin • Shortness of breath • High temperature • Bleeding easily • Frequent infections • Bone pain	• Pale skin • Tiredness • Breathless • Frequent infections • Unusual and frequent bleeding • High temperature • Night sweats • Bone and joint pain • Swollen lymph nodes • Abdominal pain • Weight loss • Purple skin rash	• Anaemia • Leukopenia • Thrombocytopenia • Swollen lymph nodes • Enlarged liver or spleen
Causes	• Previous chemo/radiotherapy • Exposure to very high levels of radiation • Benzene exposure • Underlying blood or genetic disorder	• Genetic disorders	• Previous chemotherapy • Smoking • Obesity • Genetic disorders • Weakened immune system	• Genetic disorders • Chemical exposure
Therapeutic strategies applied	• Chemotherapy • Radiotherapy • Bone marrow transplant	• Chemotherapy • Chemo-immunotherapy • Stem cell transplants	• Chemotherapy • Drugs like glucocorticoid, and anthracycline • Stem Cell transplant	• Radiotherapy • Chemotherapy • Stem cell transplant • Immunotherapy
Survival Rate	• ≈26%	• 87%	• 80% in children • 40% in adults	• 82%

Acute myeloid leukaemia (AML) is the most common type of leukaemia in adults and the one with the highest mortality rate. Although the survival rate improved in younger patients, the prognosis in elderly patients continues to be very poor. Approximately, 60% of the patients are over 60 years old, which means that elderly patients are the majority (Deschler and Lübbert, 2006; Lu and Hassan, 2006).

Elderly patients do not respond well to conventional chemotherapy, due to the intrinsic resistant nature of their AML cells and/or their poor tolerance to conventional chemotherapy regimens. Untreated AML is uniformly a fatal disease that can kill in 12 to 20 weeks. Despite these facts, in the last 30 years, very little progress was made in the treatment of these patients (Lu and Hassan, 2006; Deschler and Lübbert, 2006). This shows that finding new treatments, less aggressive and more efficient and new diagnosis methods for acute myeloid leukaemia is important. In order to do it, understanding the mechanisms of this disease is essential.

1.3 Acute myeloid leukaemia

Acute myeloid leukaemia is a heterogeneous, haematological malignant disease that originates from the bone marrow and affects hematopoietic progenitor cells (blasts). It is the most common myeloid disorder in adults, killing two-thirds of young adults and 90% of older adults who have the disease (Lu and Hassan, 2006; Estey and Döhner, 2006; Shafat *et al.*, 2017). Even in patients who achieve remission with the available treatment strategies, like chemotherapy, there is a 60% chance of relapse. This occurs from minimal residual disease sequestered in protective niches in the bone marrow microenvironment (Gao *et al.*, 2014; Shafat *et al.*, 2017).

Acute myeloid leukaemia arises from myeloid haematopoietic progenitors and is characterised by the rapid accumulation of abnormal haematopoietic progenitor in the bone marrow. These

cells lose the ability to differentiate normally and respond to normal regulators of proliferation. This can lead to fatal infection, bleeding, or organ infiltration, normally within one year, in the absence of treatment (Estey and Döhner, 2006; Deschler and Lübbert, 2006; Shafat *et al.*, 2017). Some progress has been made in the treatment of younger patients, but the prospects for elderly patients have remained dismal (Estey and Döhner, 2006).

1.3.1 Epidemiology

Acute myeloid leukaemia represents 25% of all leukaemias in adults in the Western world and therefore is the most common form of leukaemia. Worldwide, its incidence is highest in United States, Australia, and Western Europe (Deschler and Lübbert, 2006; Estey and Döhner, 2006). AML is primarily a disease of later adulthood, being 60% of the cases in patients over 60 years old, being the median age of the newly diagnosed patients 65 years. Acute leukaemias represent less than 3% of all cancer, but it constitutes the leading cause of death due to cancer in children and people under 39 years old (Deschler and Lübbert, 2006; Gao *et al.*, 2014).

The incidence of AML varies with gender, being slightly more common in males than in females, approximately 3 men for 2 women. The mortality rate is also higher for males (Estey and Döhner, 2006; Deschler and Lübbert, 2006).

The development of AML has been associated with several risk factors. These include age, antecedent hematologic disease, genetic disorders (such as Down syndrome or Kinefelter syndrome) and exposure to radiation (nontherapeutic or therapeutic), chemicals (such as benzene and pesticides) and previous chemotherapy. 10 to 15% of AML patients develop it after treatment with cytotoxic chemotherapy for other types of cancer (Deschler and Lübbert, 2006; Estey and Döhner, 2006).

1.3.2 Pathophysiology

The haematopoietic stem cells reside in the bone marrow and remain there until maturation. The bone marrow is a soft viscous tissue that is located in the cavities of the bones. It is constituted by blood vessels and a heterogeneous population of cells, directly involved in the bone marrow's function of haematopoiesis, or act in support of haematopoietic cell function (Shafat *et al.*, 2017).

Leukaemia cells and leukaemia initiating cells (LICs) are a subpopulation of AML cells that have long-term repopulation potential, an ability for limitless self-renewal. These cells reside in the bone marrow microenvironment and contain one or more oncogenic mutations driving tumorigenesis (Shafat *et al.*, 2017; Darwish *et al.*, 2016).

Acute myeloid leukaemia blasts develop from normal blasts affected by two types of genetic damage first (class I) lesion and second (class II) lesion. The first (class I) lesion results in the activation of cell surface receptors like tyrosine kinase receptors like FLT3 and Kit. Using downstream pathways, it leads to a constitutive activation conferring a survival or proliferative advantage, leading to clonal expansion of the affected haematopoietic progenitors. The second (class II) lesion can be, for example, the overexpression of HOX genes or formation of fusion genes. AML might develop only when both classes of lesion are present (Estey and Döhner, 2006).

The genetic reprogramming of AML blasts reduces the capacity in generating mature red blood cells, neutrophils, monocytes, and platelets. This is due to the promotion of AML cells survival and proliferation by the bone marrow microenvironment (Estey and Döhner, 2006; Shafat *et al.*, 2017).

AML has diverse biological features have a major impact on the resistance to chemotherapy and relapse. AML blast cells have several unfavourable covariates such as high stem cell marker CD34 expression; minimally or undifferentiated features; high P-glycoprotein expression and bcl-2/bax ratio;; internal tandem duplications (ITDs); mutations of class III receptor-type tyrosine kinase for key haematopoietic cytokines (Flt-3 – Flt ligand, 25-35% of patients; Kit – SCF ligand, 10-20% of patients; fms – M-CSF ligand, 5-20% of patients) (Lu and Hassan, 2006; Gao *et al.*, 2014).

1.3.2.1 Diagnosis

The diagnosis of acute myeloid leukaemia is primarily done by the observation of accumulation of AML blasts. AML is confirmed when the percentage of blasts in the bone marrow is higher than 20% (Estey and Döhner, 2006).

1.3.2.2 Treatment

The most common treatment for AML consists in two phases. The first one attempts to produce complete remission, defined as bone marrow with less than 5% of blasts, neutrophils over one thousand and platelets over one hundred thousand. The complete remission is the only response that leads to cure and to an extension in survival. The second phase aims to prolong the complete remission. If a patient stays in these stage for 3 years the chances of a relapse decline to less than 10% (Estey and Döhner, 2006). Some of the present treatments for AML have as their goal the elimination of the affected blasts. This is more efficient on the blasts that are in circulation than on the blasts that are in the bone marrow. This is most likely the ones in the bone marrow that are protected from the apoptosis induced by the treatment, by the marrow stroma (Estey and Döhner, 2006).

The most common cause of death in AML patients is bone-marrow failure. The principal sign of this failure is infection (Estey and Döhner, 2006).

1.3.3 Biochemistry of AML

On the molecular level, acute myeloid leukaemia affects haematopoiesis. Healthy haematopoietic stem cells suffer malignant transformation and became leukaemia cells. This process is described in section 1.2.2.

The haematopoiesis requires several cytokines that promote survival, proliferation, and differentiation of haematopoietic stem cells. It is the balance of these cytokines within the microenvironment surrounding the hematopoietic stem cells that will determine the pathway of differentiation (Broudy, 1997; Hauke and Tarantolo, 2000). Cytokines and growth factors play a role in haematopoiesis not only by causing differentiation of stem cells toward a cell type but also by inducing proliferation of cells and regulating their differentiation (Hauke and Tarantolo, 2000).

The direct contact of leukaemia and stromal cells strongly inhibits apoptosis of leukaemia cells and enhances their survival. This may explain how, after chemotherapy, the small number of malignant cells remaining are protected *in vivo*. These stromal cells secret some cytokines and growth factors[1], including the following proteins (Giles, 2002; Shafat *et al.*, 2017; Waugh and Wilson, 2008):

[1] Growth factors are often confused with cytokines. They are both produce by cells, normally of the immune system, but while cytokines will act in the signally of inflammatory response, growth factor will stimulate the growth and proliferation of the cells.

Table 3 List of growth factors and cytokines secreted by stromal cells.

Designation	**Description**
Tumour necrosis factor alpha (TNFα)	It is a cytokine that acts during the inflammatory process as regulator of immune cells, for example, it can stimulate the apoptotic cell death.
Interleukin 6 (IL-6)	It is a pro-inflammatory cytokine that stimulates immune response during inflammation, which has been shown to protect AML cells against programmed cell death.
Interleukin 8 (IL-8)	It is a pro-inflammatory chemokine involved in chemotaxis, which regulates different stimuli including inflammatory signals like TNFα and IL-1β.
Interleukin 1 beta (IL-1β)	It is a mediator of inflammatory response that is involved in cell proliferation, differentiation, and apoptosis.
Granulocyte colony-stimulating factor (G-CSF)	It is a growth factor responsible for the stimulation of the bone marrow to produce and release granulocytes and stem cells.
Granulocyte macrophage colony-stimulating factor (GM-CSF)	It is a growth factor that stimulates stem cells to produce granulocytes and monocytes.
Stem cell factor (SCF)	It is a haematopoietic growth factor that promotes haematopoietic cell proliferation and differentiation, and regulates growth and development of these cells.

Some of these cytokines and growth factors, such as SCF, GM-CSF, and TNFα, in serum-free medium, produced by leukaemia and stromal cells can achieve a high degree of apoptosis inhibition (Giles, 2002). Stromal cells also secrete IL-6, to protect AML cells against programmed cell death. IL-8 has also been implicated in bone marrow stromal cell changes (Shafat *et al.*, 2017). There is evidence that the secretion of IL-1β by leukaemia cells can stimulate the release of G-CSF and GM-CSF from endothelial cells, which, in turn, may affect the proliferation of leukaemia blasts. The location of the endothelial cells in the sinusoid of the bone, close to other cell types in the bone marrow environment, suggests their role as gatekeepers. They may regulate the movement of cells between the bone marrow and the circulation (Shafat *et al.*, 2017; Giles, 2002).

The stem cell factor receptor, Kit was found to be over-expressed in 63% of AML cases, two-thirds of which are also $CD34^+$. CD34 may play an important role in cell survival and maturation because it is expressed mainly on progenitor cells and disappears with cell maturation. These are two known factors that lead to a low chance of complete remission and to a poor prognosis, thus to a low survival rate (Lu and Hassan, 2006; Darwish *et al.*, 2016).

It was found that $CD34^+$ cells also express T cell immunoglobulin mucin-3 (Tim-3, section 1.3.3.3), a cell-surface glycoprotein. Tim-3 overexpression is markedly correlated with poor prognosis of AML patients. Also, there is a correlation between the expression of Tim-3 and the aggressiveness of AML (Darwish *et al.*, 2016).

1.3.3.1 Kit receptor

The Kit receptor, also called CD117, is a member of the type III receptor tyrosine kinase family. This family of receptors also contains c-fms receptor, platelet-derived growth factor (PDGF) receptors and flk-2/flt3 receptor. It is a transmembrane protein, and its activity is encoded by the oncogene Kit (Broudy, 1997; Liang *et al.*, 2013).

This tyrosine kinase family causes specific expression of certain genes. It regulates cell differentiation, proliferation, and resistance to apoptosis. Kit receptor also plays a key role in tumour occurrence, development, migration, through activation of downstream molecules following interaction with stem cell factor (SCF) (Broudy, 1997; Liang *et al.*, 2013).

The Kit receptor (Figure 4) is a 145 kDa glycoprotein, with 976 amino acids (aa). 519 aa on the extracellular domain, 23 aa on the transmembrane domain and 433 aa at the intracellular tail, that consists of a juxta-membrane domain and a tyrosine kinase domain inserted by approximately 80 aa residues (Broudy, 1997; Liang *et al.*, 2013).

The extracellular domain of Kit receptor has five Ig-like motifs (D1~D5), a single short membrane-spanning domain, and a cytoplasmic domain with tyrosine kinase activity. The motifs D1~D3 are a key component of binding to SCF, and D4~D5 are the essential region of dimerization. This domain is interrupted by a kinase-insert-sequence that divides the kinase domain into an ATP (adenosine triphosphate)-binding region and a phosphotransferase region (Broudy, 1997; Liang *et al.*, 2013).

When SCF binds the Kit receptor, it triggers the homodimerization and intermolecular tyrosine phosphorylation of the receptor, creating docking sites for a number SH2-containing signal transduction molecules (Broudy, 1997). The SCF dimer forms complexes with two molecules of the extracellular domain of Kit to activate downstream signal transduction. Then it regulates

a variety of cells biological behaviour, such as normal cells proliferation and differentiation and tumour occurrence, development, migration, and recurrence (Liang *et al.*, 2013).

The Kit receptor is broadly distributed within the hierarchy of hematopoietic cells. It is also found in germ cells, mast cells, melanoma cells and gastrointestinal tract cajal cells, skin appendages, breast epithelial cells and small neurones in the brain. In healthy people, approximately 1% to 4% of bone marrow stem cells and 60% to 70% of $CD34^{+}$ haematopoietic cells express Kit receptor. About 85% of B cell progenitors also express Kit receptor, but it gradually disappears with the cell differentiation and maturation (Broudy, 1997; Liang *et al.*, 2013).

Studies show that Kit receptor is express in 68% of AML and in 80% of CML patients in blast phase. Only 2% of acute lymphoid leukaemia patients express it, what suggest that the receptor has a more important role in myeloid leukaemias than in lymphoid leukaemias. It was also found that AML patients that are Kit positive, survived much shorter time than Kit negative AML patients. In patients with low complete remission rate, Kit receptor has, normally, high levels of expression (Liang *et al.*, 2013).

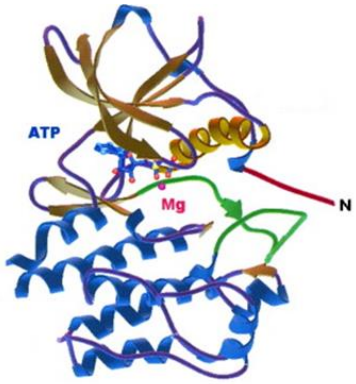

Figure 4 Ribbon diagram of the activated form of Kit showing the N-termini. A-helices are illustrated in blue, ß-strandsin amber and loops in purple. (Roskoski, 2005)

This data seems to show that Kit receptor has an important role in AML. It has influence in AML complete remission and recurrence, patients that express this receptor have low complete remission rate, tend to relapse despite complete remission and they also have a higher mortality rate (Liang *et al.*, 2013).

1.3.3.2 Stem Cell Factor

Stem cell factor (SCF) or Kit ligand is a hematopoietic cytokine that triggers its biologic effects by binding to its receptor (Kit receptor). The constitutive production of SCF by endothelial cells and fibroblast is required for the maintenance of normal basal haematopoiesis (Broudy, 1997).

SCF is a haematopoietic cytokine, which plays an important role in maintaining the survival of haematopoietic cells. It promotes haematopoietic cell proliferation and differentiation and regulates growth and development of haematopoietic cells (Liang *et al.*, 2013).

SCF can be found in two different forms, the soluble form, and the transmembrane form, that are generated by alternative splicing that includes or excludes a proteolytic cleavage site. Both forms are biologically active. The endothelial cells and the fibroblasts display the transmembrane form on its surface and release the soluble form (Broudy, 1997). The soluble form of SCF circulates as a non-covalently bonded dimer, it is glycosylated and has considerable secondary structure, including region α-helices and β-sheets. It has a molecular weight of 18500 Daltons. This value was calculated from its amino acid sequence (Broudy, 1997).

Enriched populations of human hematopoietic stem cells and progenitor cells ($CD34^+$ Kit $receptor^+$) are reported to have SCF mRNA. Some inflammatory stimuli such as interleukin-1 (IL-1) or tumour necrosis factor (TNF) may modestly enhance SCF protein production by marrow stromal cells (Broudy, 1997). SCF can act directly on an enriched population containing hematopoietic stem cells to accelerate their entry into cell cycle (Broudy, 1997).

Recent studies demonstrated that the use of the anti-SCF together with low dosage of chemotherapy enhance the effects of the treatment. The anti-SCF enhancing activity was associated with a further significant reduction in the expression of the anti-apoptotic gene, bcl-2 (Lu and Hassan, 2006).

1.3.3.3 T cell immunoglobulin mucin-3

T cell immunoglobulin mucin-3 (Tim-3) is a specific surface molecule expressed on leukaemia stem cells on most types of AML, thus being a candidate for AML leukaemia cells target therapies. It was first discovered in 2002 as a receptor expressed on interferon(IFN)-γ-producing $CD4^+$ T-helper type 1 (Th1) cells and on $CD8^+$ T cytotoxic type I (Tc1) cells and is a type I transmembrane protein. Its discovery led to the discovery of Tim family of genes (Gao *et al.*, 2014; Darwish *et al.*, 2016; Das *et al.*, 2017).

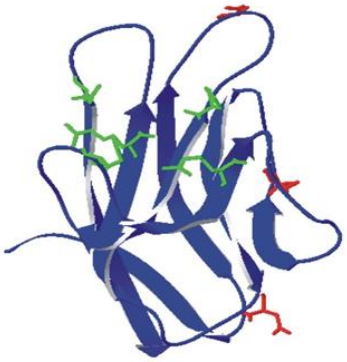

Figure 5 Structure of the Tim-3 extracellular domain created using Swiss pdb viewer. *Amino acids residues involved in galectin-9-independent binding are highlighted in green. Residues, which are potential targets for glycosylation, are highlighted in red* (Gonçalves Silva *et al.*, 2017)**.**

Human Tim-3 has 302 amino acids residues and belongs to the immunoglobulin superfamily (IgSF). It consists of four domains, the membrane-distal N-terminal immunoglobulin (IgV) variable domain, mucin domain, transmembrane domain, and a cytoplasmic tail. The membrane-distal N-terminal immunoglobulin (IgV) domain followed by a membrane-proximal mucin domain, that contains sites for O-linked glycosylation, form an extracellular domain. Between the mucin and the transmembrane domain, there is site for N-linked sugars, which are followed by the transmembrane domain and a cytoplasmic tail (Figure 5) (Das *et al.*, 2017; Darwish *et al.*, 2016).

Tim-3 protein has molecular weight of 33 KDa. It can be subjected to both N- and O-glycosylation. In each case the polysaccharide molecule attached has molecular weight of 2 kDa. Maximum number of glycoside molecules which can be attached to a single Tim-3 molecule is 11. Minimum – is one. So Molecular weight of this protein can vary from 33 kDa up to 55 kDa. In AML cells the WB band normally appears between 35 and 42 kDa also depending on the type of MW marker used (Clayton et al., 2015; Gonçalves Silva et al., 2017).

Tim-3 plays a key role in inhibiting Th1 responses and the expression of some cytokines like TNF and INF-γand non-T cells populations, such as NK cells. This was demonstrated by the expression of Tim-3 on tumour-infiltration and suppressing innate antitumour immune responses. In this way, Tim-3 is considered a negative regulatory checkpoint molecule associated with both T-cell exhaustion and suppression innate immune response (Das *et al.*, 2017). The analysis of these data leads to believe that Tim-3 may have a function as a signal transductor in AML leukaemia cells since it was reported that anti-Tim-3 antibody is able to interfere with leukaemia cells' proliferation (Darwish *et al.*, 2016).

It is hypothesised, that elevated Tim-3 expression may be a direct consequence of the molecular mutations presented in AML cells. Elevated expression levels of Tim-3 showed substantial correlation with patients' leukocyte count and a number of treatment cycles to complete remission. This seems to indicate Tim-3 as a potential prognostic factor for patients with AML (Li *et al.*, 2016). A higher expression of Tim-3 protein was suggested to promote a poor response to chemotherapy, which may be closely associated with primary resistance. This observation supports the idea that Tim-3 could be considered a potential predictor of chemotherapeutic sensitivity and prognosis in AML patients (Li *et al.*, 2016).

It was reported that Tim-3 also triggers growth factor type responses in AML cells by activating a phosphatidylinositol-3 kinase (PI-3K). This includes kinase cascade leading to activation of mammalian target of rapamycin (mTOR), a central regulator of cell growth and metabolism, via its phosphorylation at S2448. mTOR is known to upregulate glycolysis, proangiogenic responses and to induce the non-hypoxic activation of hypoxia-inducible factor 1 (HIF-1), a transcription complex essential for cellular adaptation to low oxygen availability (Gibbs *et al.*, 2015; Prokhorov *et al.*, 2015; Fitzmaurice *et al.*, 2016; Gibbs *et al.*, 2011).

HIF-1 is a heterodimeric complex containing two subunits, a constitutively expressed subunit hypoxia-inducible factor 1β (HIF-1β) and a hypoxically inducible subunit hypoxia-inducible factor 1α (HIF-1α). The non-hypoxic activation of HIF-1 leads to the accumulation of HIF-1α that will induce the secretion vascular endothelial growth factor (VEGF). VEGF is the most potent endothelial-specific mitogen that directly participates in angiogenesis, recruiting endothelial cells into hypoxia and avascular areas and stimulate their proliferation (Gibbs *et al.*, 2011; Ke and Costa, 2006). This is an essential process for the survival and proliferation of leukaemia cells.

A natural ligand of this receptor was recently identified, galectin-9.

1.3.3.4 Galectin-9

Galectins are a family of lectins that exhibit high affinity for β-galactosides, share conserved amino acids sequences in their carbohydrate recognition domains and modulate various biological events (Kobayashi *et al.*, 2010).

Galectin-9 was identified as a Tim-3 ligand. It is expressed as a soluble molecule that is widely expressed and upregulated by IFN-γ (Gao *et al.*, 2014). Galectin-9 induces phospholipase C (PLC-1) in a Bruton's tyrosine kinase-dependent way, which is required for Ca^{2+} mobilisation and the phosphatidylinositol 3-kinase (PI-3K) pathway. This process leads to mTOR activation and to an increase of intracellular mobilisation and upregulation of the transcriptional activity of HIF1 complex and its downstream processes, such as glycolysis, VEGF expression and release (Prokhorov *et al.*, 2015).

Figure 6 Galectin-9 structure created by swiss pdb viewer. *Sugar located close to a sugar binding site is shown in green* (Gonçalves Silva *et al.*, 2017)**.**

Galectin-9 is a soluble protein containing two tandem-repeat type of galectin with two carbohydrate recognition domains that specifically recognises the structure of N-linked sugar chains in the Tim-3 membrane distal immunoglobulin variable (IgV) domain (Figure 6). There normally three splice variants of galectin-9. In all cases sugar binding domains stay unchanged but the length of the linker polypeptide fusing them together varies. The one which is secreted by AML cells has molecular weight of 31.5 kDa and displays biochemical activity.

Galectin-9 has been shown to be involved in a variety of cellular functions, such as cell adhesion, proliferation and apoptosis (Darwish *et al.*, 2016; Das *et al.*, 2017; Kobayashi *et al.*, 2010; Chabot *et al.*, 2002a).

Galectin-9 is mainly released by the $CD34^+$ fraction of AML cells that contain leukaemia cells and primitive blasts (Darwish *et al.*, 2016; Kikushige *et al.*, 2015). It is expressed in various tissues involved in the immune system like spleen, thymus and lymphocytes, and in tissues of the endodermal origin like liver, intestine and lung (Kikushige *et al.*, 2015).

1.3.3.5 Tim-3-galectin-9 interaction

There is an evidence of correlation between Tim-3 and galectin-9 levels, which is increased in AML patients in comparison to the normal individuals (Darwish *et al.*, 2016). The two tandemly linked carbohydrate recognition domains of galectin-9, specifically recognise the structure of N-linked sugar chains in the Tim-3 IgV domain. It does not recognise the same place on other Tim proteins. Also, the interaction between the Tim-3 IgV domain and galectin-9 has the highest affinity when compared with other galectins. This suggests that the link between Galectin-9 and Tim-3 is specific (Das *et al.*, 2017).

The binding between Tim-3 and galectin-9 induces simultaneous activation of the nuclear factor kappa-light-chain-enhancer of activated B cells (NF-κB) and β-catenin signalling in leukaemic cells. This will trigger marked gene expression changes inducing upregulation of Mcl-1, an important survival factor for leukaemia cells, enhancing the pro-survival axis. The lack of galectin-9 accelerates apoptosis of leukaemic cells in AML cell lines (Darwish *et al.*, 2016; Kikushige *et al.*, 2015). This binding also triggers death in effector Th1 cells, dampening tissue inflammation and increases the Tim-3-mediated IFN-γ production in an NK cell line (NK92) (Das *et al.*, 2017; Kikushige *et al.*, 2015). The binding between Tim-3 and galectin-9, also, phosphorylates tyrosine residues of the cytoplasmic tail of Tim-3 and activates Src family of kinases through its Src homology 2 (SH2) binding motif in T-cells and monocytes (Kikushige *et al.*, 2015).

In AML cells, galectin-9 was found to be bound to Tim-3 on the cell surface, suggesting that AML cells may secrete galectin-9. The levels of intracellular galectin-9 in AML cells are higher than in normal haematopoietic stem cells, but since galectin-9 lacks a sequence essential for

secretion through ER-Golgi pathway, this does not mean that the cells will secrete it (Kikushige *et al.,* 2015).

It was found that, prior to secretion, galectin-9 seems to be translocated intermediate through the lipid bilayer of cell membraneand that Tim-3^+ leukaemic stem cells and blasts cells actively secrete galectin-9 while Tim-3^- do not. This suggeststhat Tim-3 and galectin-9 may form an autocrine loop critical for leukaemia stem cells self-renewal and development of human AML (Kikushige *et al.*, 2015).

Tim-3/galectin-9 autocrine loop activates both NF-κB, and the β-catenin signalling in mist leukaemias. NF-κB regulates expression of different but overlapping genes that are involved in innate and adaptive immunity, inflammation, anti-apoptosis, proliferation, and cancer progression. β-catenin is a key molecule for self-renewing machinery in haematopoietic stem cells and leukaemia cells. The signalling of these two molecules is critical in clonal selection, where the number of preleukaemic haematopoietic stem cells becomes much higher than the number of normal HSC. This autocrine loop is, probably, critical for the survival of leukaemia cells since deprivation of Galectin-9 accelerates apoptotic cell death of leukaemia cells (Kikushige *et al.*, 2015; Kawai and Akira, 2007).

Data suggest that the autocrine loop is essential for the secretion of galectin-9 from AML cells, and secretion of Galectin-9 is essential for AML cells survival and proliferation. However, the mechanism that these cells use, it is unclear.

It is important to understand the molecular events leading to the secretion of galectin-9. On one hand, galectin-9 as all other galectins lacks a signal sequence which is required for transport into cellular endoplasmic reticulum (ER) and thus requires a trafficking protein for its secretion (Hughes, 1999; Delacour *et al.*, 2009). On the other hand, exocytosis must be provoked to

induce not just generation of galectin-9, but its externalisation and secretion into the environment. One of the possible candidates is the neuronal G-protein-coupled receptor Latrophilin-1 (LPHN1).Its expression could possibly fail to be repressed during haematopoiesis in the case of malignant transformation. Importantly, one of the endogenous ligands of LPHN1 called fibronectin leucine rich transmembrane protein 3 (FLRT3) is expressed in a number of tissues and may function in cell adhesion and cell signalling (Boucard *et al.*, 2014). One could therefore hypothesise that FLRT3 and possibly other ligands of LPHN1 can induce secretion of galectin-9 thus protecting malignant cells against NK cells and cytotoxic T cells. Especially, because LPHN1 as a G-protein-coupled receptor acts through protein kinase C, which was suggested to be involved in galectin-9 secretion (Chabot *et al.*, 2002a). However, this hypothesis has not been studied experimentally and thus became the aim of the present study.

Importantly, there is evidence demonstrating that in myeloid leukaemia cell lines Tim-3/galectin-9 pathway triggers the key translational pathway controlled by the mammalian target of rapamycin (mTOR) (Prokhorov *et al.*, 2015). This suggests that the autocrine loop is also likely to have a growth/proliferation stimulatory function.

1.4 Mammalian Target of Rapamycin pathway

The mammalian target of rapamycin (mTOR) is an enzyme from the serine/threonine kinase family, which, like other kinases, phosphorylates substrates using ATP. It is allosterically regulated by covalent attachment of H_3PO_4 in the position S2448 for activation or in the position T2446 for inhibition (Yasinska *et al.*, 2014). If mTOR is active, it recruits different chaperones. These chaperones determine the structure of mTOR protein, allowing it to recognise different substrates. Also, depending on the group of chaperones that mTOR recruits,

it forms two types of multiprotein complexes, mTOR1 and mTOR2. These complexes regulate translation of different, but essential proteins like transcription factors that will control cell survival, differentiation, and death (Wang and Proud, 2006).

Some of the chaperones are common in both complexes, while others are different. These chaperones do not have any specific catalytic function in the complex but they determine the shape and conformation of the mTOR recognition site, thus controlling its capacity to recognise specific folded different amino acids sequences of its substrates (Laplante and Sabatini, 2009; Sabatini, 2006). In Figure 7 is a scheme showing the main components of both complexes. These complexes are described with more detail on section "1.4.1 Biochemistry of mTOR as an enzyme".

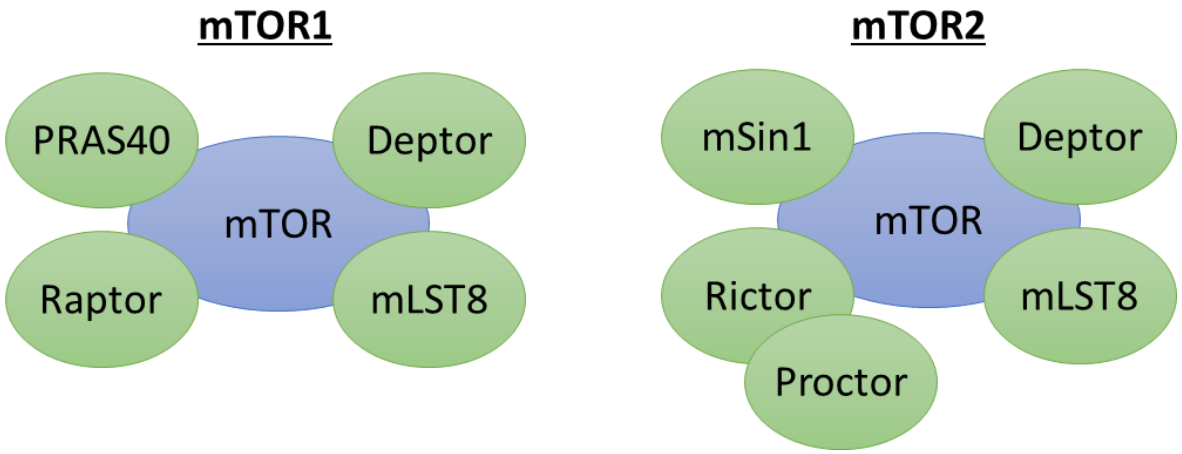

Figure 7 mTOR1 and mTOR2 complexes with their chaperones. *In both complexes mTOR is the main constituent recruiting different chaperones according to their function.*

mTOR pathway is activated during various cellular processes such as tumour formation, angiogenesis, insulin resistance, adipogenesis and T-lymphocyte activation. In diseases such as cancer and type 2 diabetes, mTOR is deregulated (Laplante and Sabatini, 2009). Due to this, mTOR inhibitors have been more and more used in the treatment of several diseases such as solid tumours, coronary restenosis and rheumatoid arthritis (Laplante and Sabatini, 2009).

1.4.1 Biochemistry of mTOR as an enzyme

The mTOR protein is a 289 kDa serine-therosine kinase that belongs to the phosphoinositide 3-kinase (PI3K)-related kinase family (Laplante and Sabatini, 2009). As mentioned before, mTOR is part of the mammalian target of rapamycin complex 1 and 2 (mTOR1 and mTOR2). Two multi-protein complexes responsible for important tasks in the cells (Laplante and Sabatini, 2009).

mTOR1 has five components: mTOR, regulatory-associated protein of mTOR (Raptor), mammalian lethal with Sec13 protein 8 (mLST8, also called GβL), proline-rich AKT substrate 40 kDa (PRAS40), and DEP-domain-containing mTOR-interacting protein (Deptor). The exact function of this proteins in mTOR1 signalling remains unclear (Laplante and Sabatini, 2009; Sabatini, 2006).

In this complex mTOR is the catalytic subunit and it is associated with Raptor and LST8 Figure 7). The Raptor might affect mTOR1 activity by regulating assembly of the complex and by recruiting substrates for mTOR. The function of LST8 in mTOR1 function is unclear since its deletion does not seem to affect the mTOR1 activity in vivo (Laplante and Sabatini, 2009; Sabatini, 2006).

PRAS40 and Deptor are proposed to be negative regulators of mTOR1. When the activity of mTOR1 is reduced these two proteins are recruited to the complex and they promote mTOR1 inhibition. It is hypothesised that PRAS40 affects mTOR1 kinase activity by acting as a direct inhibitor of substrate binding. When mTOR1 is activated, it phosphorylates PRAS40 and Deptor, reducing the physical interaction of these with mTOR1 and further activating mTOR1 signalling (Laplante and Sabatini, 2009).

Not much is known about mTOR2. Contrarily to mTOR1 few studies on mTOR2 have been done. mTOR2 comprises six different proteins, being three in common with mTOR1. These are mTOR, mLST8 and Deptor. In addition to these mTOR2 has the rapamycin-insensitive companion of mTOR (Rictor) instead of Raptor, the mammalian stress-activated protein kinase interacting protein (mSIN1) and the protein observed with Rictor-1 (Protor-1) (Laplante and Sabatini, 2009; Sabatini, 2006).

Studies seem to show that Rictor and mSIN1 stabilise each other and the structure of the mTOR2. Deptor regulates negatively mTOR2 activity, currently it is the only characterised endogenous inhibitor. The function of mLST8 is not clear but it is essential for the mTOR2 activity since its knockout severely reduces the stability and the activity of this complex (Laplante and Sabatini, 2009).

1.4.2 Functions of mTOR1

mTOR1 has a central role in cell growth and proliferation by promoting several anabolic processes like biosynthesis of proteins, lipids and organelles; and limiting catabolic processes like autophagy (Laplante and Sabatini, 2009; Sarbassov *et al.*, 2005).

1.4.2.1 Protein synthesis

mTOR1 induces protein synthesis used in cell growth, through various downstream effectors. This happens by phosphorylation of the eukaryotic initiation factor 4E (eIF4E)-binding protein (4E-BP1) and the p70 ribosomal S6 kinase 1 (P70S6K1). This phosphorylation prevents the binding of 4E-BP1 to eIF4E and in this way the later promotes cap-dependent translation and elongation, and translation of ribosomal proteins through regulation of the activity of many proteins such as P70S6K1, programmed cell death 4 (PDCD4), eukaryotic elongation factor 2

kinase (eEF2K) and ribosomal protein S6 (Figure 8) (Laplante and Sabatini, 2009; Sarbassov *et al.*, 2005).

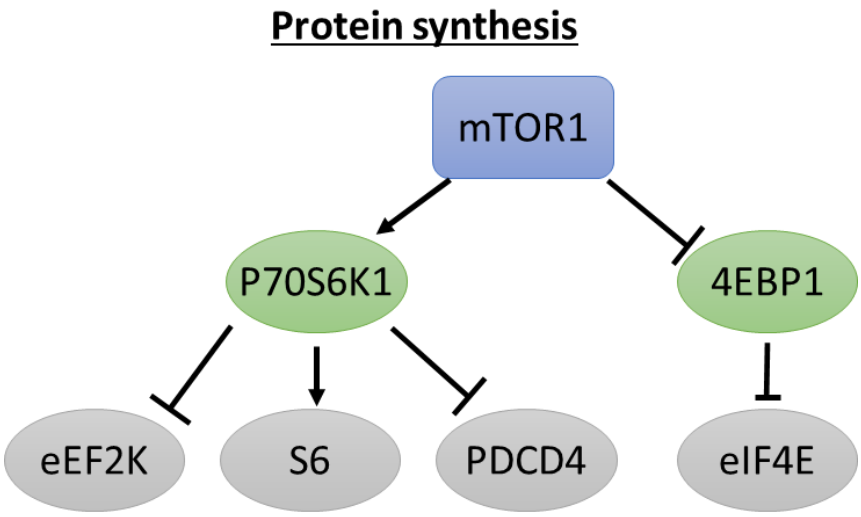

Figure 8 Schematic representation of mTOR1 protein synthesis (simplified scheme). *mTOR1 activates P70S6K1 that will inhibit eEF2K (inhibitor of protein elongation) and PDCD4 that supresses cell proliferation and activate S6 that is involved in translation. mTOR1 also inhibits 4EBP1, that is a translation repressor.*

1.4.2.2 Programmed cell death

There are two types of programmed cell death, apoptosis, and autophagy. mTOR pathway participates in the regulation of one of the, autophagy. Autophagy is a self-degradative process that leads to cell death. It removes misfolded or aggregated proteins and damaged organelles, like mitochondria, endoplasmic reticulum, and peroxisomes, by the formation of vesicles (Gozuacik and Kimchi, 2007; Glick *et al.*, 2010).

These vesicles have double or multiple membrane and appear in the cytoplasm. They engulf portions of the cytoplasm, aggregated/misfolded proteins and/or the damaged organelles, and then they fuse with lysosomes and deliver their cargo for degradation by lysosomal enzymes (Gozuacik and Kimchi, 2007; Glick *et al.*, 2010).

mTOR1 has an inhibitory role in autophagy. mTOR1 activation leads to an inhibition of autophagy while its activation leads to an increase of autophagy. This regulation is done through the regulation of a protein complex composed of unc-S1-like kinase 1 (ULK1), autophagy-related gene 13 (ATG13) and focal adhesion kinase family-interacting protein of 200 kDa (FIP200). mTOR1 promotes ULK1 and ATG13 phosphorylation and by consequence its repression. Repression of ULK1 and ATG13 leads to repression of autophagy (Figure 9) (Laplante and Sabatini, 2009).

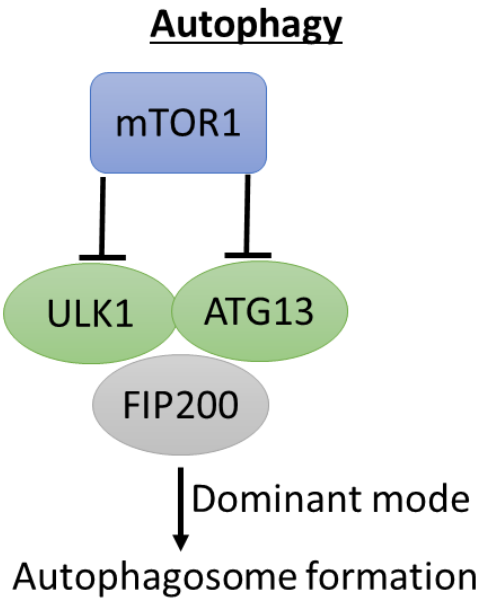

Figure 9 Schematic representation of mTOR1 autophagy (simplified scheme). *mTOR1 represses ULK1 and ATG13 thus represses autophagy process.*

1.4.2.3 Lipid synthesis

mTOR participates is a crucial regulator of steroid lipids, which on genomic level control both organic and mineral metabolism as well as embryonic development. Steroid lipids also support elasticity of cell membrane (cholesterol) and processes of lipid digestion (cholic acids). This happens by positive regulation of the activity of sterol regulatory element binding protein

(SREBP1) and of peroxisome proliferation-activated receptor-γ (PPARγ) by mTOR1. These two transcription factors control the expression of genes encoding proteins involved in lipid and cholesterol homoeostasis. Blocking mTOR with rapamycin reduces the expression and the transactivation of PPARγ (Figure 10) (Laplante and Sabatini, 2009).

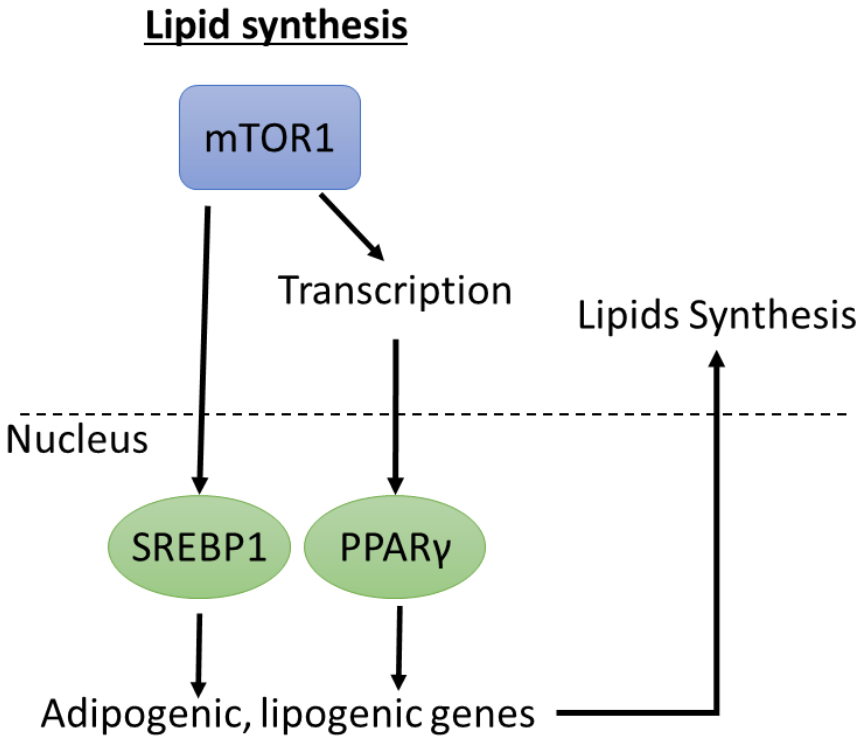

Figure 10 Schematic representation of mTOR1 lipids synthesis (simplified scheme). *mTOR activates SREBP1 and PPARγ that will activate adipogenic and lipogenic genes and thus activating the lipids synthesis.*

1.4.2.4 Mitochondrial metabolism

Inhibition of mTOR1 by rapamycin lowers mitochondrial membrane potential, consumption of oxygen, ATP level and alters mitochondrial phosphoproteome. It reduces the number of copies of mitochondrial DNA and expression of genes involved in oxidative metabolism.

1.4.2.5 mTOR1 signalling

mTOR1 integrates major signals in the cells: growth factors, energy status, and oxygen levels. These signals regulate several processes that are involved in the promotion of cell growth and proliferation (Figure 11) (Laplante and Sabatini, 2009).

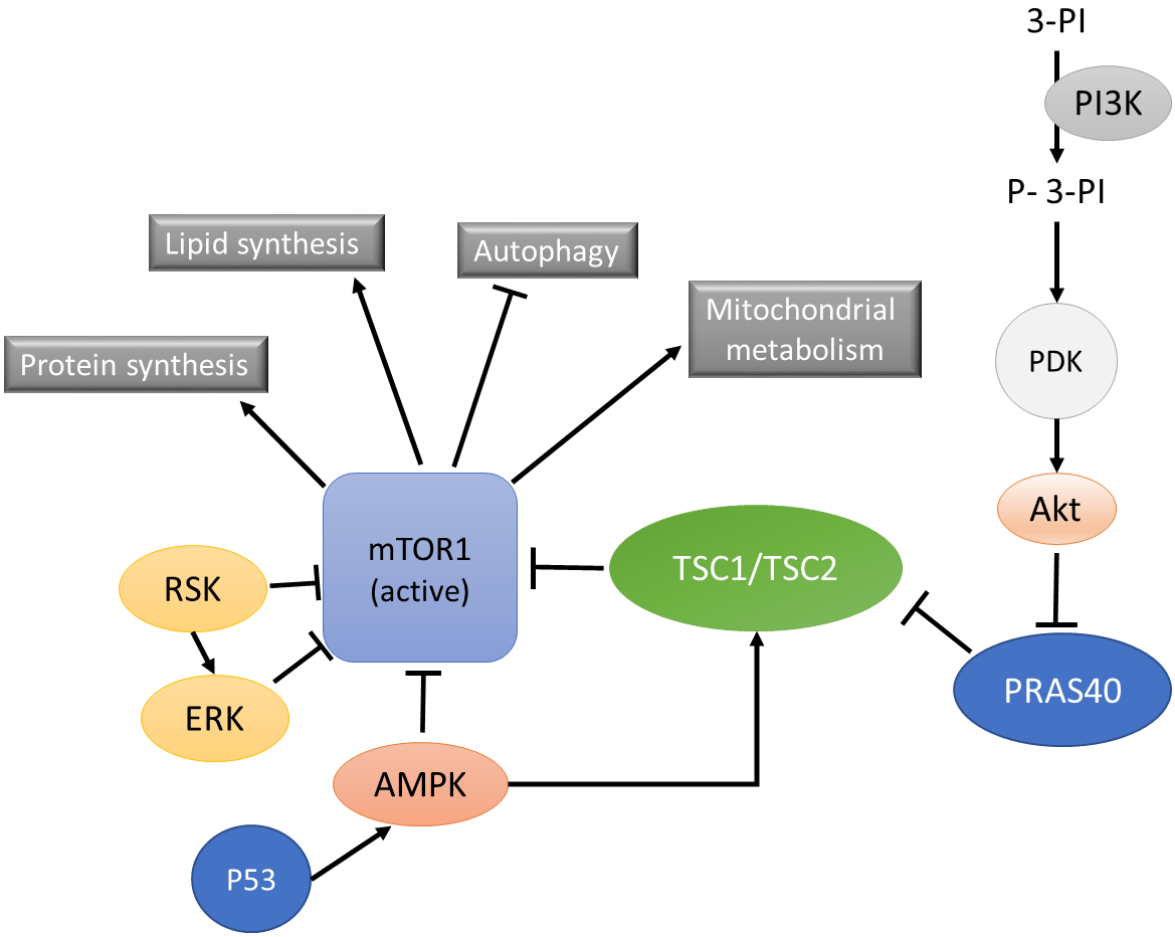

Figure 11 Schematic representation of mTOR1 (simplified scheme). *Main mechanism that activates/represses mTOR1 and the ones that mTOR1 activates/inhibits.*

One of the most important sensors of mTOR1 regulation is the tuberous sclerosis complex (TSC). This is a heterodimer that contains TSC1 (also called hamartin) and TSC2 (also called tuberin) (Laplante and Sabatini, 2009). TSC1-TSC2 is a GTPase-activating protein (GAP) for Ras homologue enriched in brain (Rheb). Rheb is a GTP-binding protein that activates mTOR1, by binding to it. TSC1-TC2 inhibits mTOR1 signalling by converting Rheb to its inactive GDP-bound form. TSC1-TSC2 and Rheb have an important role in the activation of mTOR1 when the cell loses the phosphate and tumour suppressors like neurofibromatosis 1 (NF1), serine-threonine kinase 11 (LKB1) or p53 tumour suppressor (Laplante and Sabatini, 2009; Sabatini, 2006).

1.4.2.5.1 Growth factors

The mTOR1 pathway regulates growth through downstream effectors, such as the regulators of translation eukaryotic translation initiation factor 4E binding protein 1 (4EBP1) and P70 ribosomal S6 kinase 1 (P70S6K1). P70S6K1 promotes protein synthesis and represses the phosphatidylinositol3-kinase (PI3K)-protein kinase B (AKT) pathway by inhibiting insulin receptor substrate 1 and 2 (IRS1 and IRS2) expression (Sabatini, 2006). P70S6K1 promotes the phosphorylation of IRS1 and reduces its stability (Laplante and Sabatini, 2009).

The activation of mTOR1 can happen when there is the phosphorylation of TSC2 by AKT, by extracellular-signal-regulated kinase 1/2 (ERK1/2) and by p90 ribosomal S6 kinase (RSK1). This will lead to inactivation of TSC1-TSC2 and by consequence to activation of mTOR1. The activation of mTOR1 can also happen in a TSC1-TSC2-independent manner by promoting the phosphorylation and dissociation of PRAS40 from mTOR1 (Laplante and Sabatini, 2009).

1.4.2.5.2 Energy status

AMP-activated protein kinase (AMPK), a master sensor of intracellular energy status, is responsible for signalling the energy status to mTOR1. When there is lack of energy in the cell (low ratio ATP: ADP), AMPK is activated and phosphorylates TSC2 to increase GAP activity towards Rheb and decreasing mTOR1 activity. Also, AMPK is able to decrease mTOR1 activity by phosphorylating Raptor (Laplante and Sabatini, 2009).

1.4.2.5.3 Oxygen levels

When the cell is under mild hypoxia the low level of ATP activates AMPK, that will activate TSC1-TSC2 and thus inhibit mTOR1 signalling (Laplante and Sabatini, 2009).

1.4.3 Functions of mTOR2

Very little is known about mTOR2 since its study has shown to be difficult to perform. Nevertheless, it is known that mTOR2 plays key roles in different biological processes like cell survival, metabolism, proliferation and cytoskeleton organisation (Laplante and Sabatini, 2009).

1.4.3.1 Cell survival, metabolism, and proliferation

Cell survival, metabolism and proliferation are processes that depend on the activation status of AKT. It positively regulates these processes through the phosphorylation of various effectors. AKT is active when it is phosphorylated at Ser308 by phosphoinositide-dependent kinase 1 (PDK1) and at Ser473 by mTOR2 (Laplante and Sabatini, 2009).

1.4.3.2 Cytoskeleton organization

The molecular mechanism that allows mTOR2 to regulate the cytoskeleton organisation is not determinate yet. However, it is known that the knockdown of mTOR2 affects the actin polymerization and perturbs cell morphology (Laplante and Sabatini, 2009). It is suggested that mTOR2 controls the actin cytoskeleton by promoting protein kinase Cα (PKCα) phosphorylation, phosphorylation of paxillin and its relocalization to focal adhesions (Laplante and Sabatini, 2009).

1.4.3.3 mTOR2 signalling

mTOR2 should be considered part of the PI3K-Akt pathway as it directly phosphorylates Akt on one of the two sites that are necessary for Akt activation in response to growth-factor signalling. This finding makes mTOR2 essential part of the pathway that activates Akt and, like PDK1 (3-phosphoinositide-dependent protein kinase1) and PI3K (Sabatini, 2006). The Akt-activation function of mTOR2 sets up the intriguing situation in which mTOR, as part of two distinct complexes, is potentially both upstream and downstream of itself (Figure 12) (Sabatini, 2006).

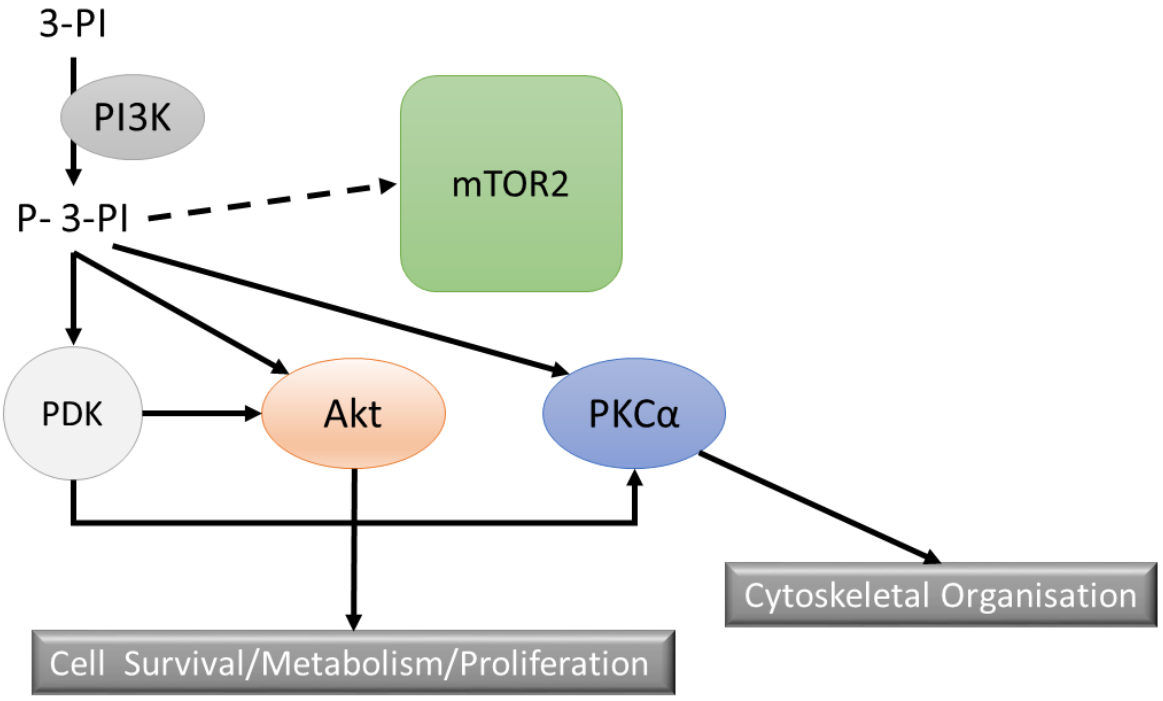

Figure 12 Schematic representation of mTOR2. *It is known that mTOR2 is involved in the mechanisms of Cell Survival, metabolism and proliferation through Akt activation and cytoskeletal organisation through PKCα activation.*

1.4.4 mTOR as a therapeutic target

mTOR is a master regulator of the main cell pathways and thus there is a crescent interest in using it as a therapeutic target. At the moment, drugs are designed to inhibit mTOR. The most common mTOR inhibitor is rapamycin. Rapamycin is a macrolide that was originally found as an antifungal agent but later recognised as having immunosuppressive and anticancer properties (Laplante and Sabatini, 2009; Sabatini, 2006). When rapamycin enters the cell, it binds to FKS06-binding protein of 12 kDa (FKBP12). This complex will bind directly to mTOR in mTOR1, leading to the inhibition of mTOR1-mediated phosphorylation of the substrates S6K1 and 4EBP1. FKBP12-rapamycin cannot bind directly to mTOR in mTOR2, suggesting the effects of rapamycin on cellular signalling are just due to inhibition of mTOR1 (Laplante and Sabatini, 2009; Sabatini, 2006).

Recently a new class of mTOR inhibitors have been developed, which are able to inhibit both mTOR complexes. These are called dual mTOR1/2 inhibitors, and its aim is to have a better effect that the first generation of inhibitors. For example, AZD2014, a dual inhibitor developed by AstraZeneca, demonstrates better inhibitory activity against mTOR1 than rapamycin (Dienstmann *et al.*, 2014). In Table 4 are some mTOR inhibitors, currently in clinical trials.

Table 4 New mTOR inhibitors. (Dienstmann *et al.*, 2014)

Inhibitor	**Manufacturer**	**Target**
Everolimus	Novartis	mTOR1
Temsirolimus	Pfizer	mTOR1
AZD2014	AstraZeneca	mTOR1/2
MLN0128	INK128	mTOR1/2
CC-223	Celgene	mTOR1/2

2. AIMS AND OBJECTIVES

The aim of this PhD project was to investigate a fundamental molecular mechanism underlying the secretion and function of Galectin-9 and soluble Tim-3 in primary human healthy cells and AML cells. This aim will allow to figure out the importance of these proteins in the survival of AML cells.

To achieve this aim, the following objectives were considered.

1. Investigate differential expression and intracellular signalling role of Tim-3 and Galectin-9 in primary human healthy cells.
2. Investigate the role of Tim-3 in trafficking Galectin-9.
3. Investigate and characterise expression of functional neuronal receptor LPHN1 in human AML cells and its involvement in Tim-3/Galectin-9 secretion.
4. Investigate the intracellular pathways transducing the signal from LPHN1 to Tim-3/Galectin-9 autocrine loop.
5. Investigate the effects of Galectin-9 on primary NK cells.

3. MATERIALS AND METHODS

3.1 Materials

All cell culture reagents, were purchased from Sigma (Suffolk, UK). DOPAT transfection reagent, primers and galectin-9 silencing RNA (siRNA) and basic laboratory chemicals were obtained at the same company.

Mouse monoclonal antibodies directed against mTOR, HIF-1α and β-actin, and rabbit polyclonal antibody against phospho-S2448 mTOR, galectin-9, Tim-3, HRP-labelled rabbit anti-mouse secondary antibody were purchased from Abcam (Cambridge, UK). The antibodies against phospho-T389 p70S6 kinase 1 (P70 S6K1), total and phospho-S65 eukaryotic initiation factor 4E binding protein 1 (eIF46E-BP1) antibodies were obtained from Cell Signalling Technology (Danvers, MA, USA). Mouse monoclonal antibody against FLRT-3 was obtained from Santa Cruz Biotechnology (Heidelberg, Germany). Goat anti-mouse and goat anti-rabbit Polyclonal rabbit anti-peptide antibody (clone name: PAL1) against LPHN1 and polyclonal mouse antibody (clone name; dmAb) against Lasso/teneurin-2 were previously described (Silva *et al.*, 2011; Davydov *et al.*, 2009).

Human stem cell factor (SCF) (Wang *et al.*, 2008), anti-Tim-3 monoclonal antibody (Prokhorov *et al.*, 2015) and HMGB1 were a kind gift of Dr Luca Varani.

ELISA-based assay kits were purchased from Bio-Techne (R&D Systems, Abingdon, UK). Maxisorp^{TM} microtitre plates were provided by Nunc (Roskilde, Denmark) or Oxley Hughes Ltd (London, UK).

All other chemicals purchased were of the highest grade of purity and available commercially unless otherwise stated.

3.2 Tissue culture

3.2.1 THP-1, U937, MCF7, Jurkat T cells, K562, LAD2 and RCC-FG1

THP-1 human myeloid leukaemia monocytic macrophages, U937 human leukaemia monocytes, MCF7, Jurkat T cells, K562 chronic myelogenous leukaemia cells, and RCC-FG1 (human renal clear cell line) cells were obtained from the European Collection of Cell Cultures (Salisbury, UK). LAD2 cells (cell line from the bone marrow of a patient with MC sarcoma) were kindly provided by Prof Metcalfe and Dr Kirshenbaum (NAID, NIH, USA; (Kirshenbaum *et al.*, 2003)). Cells were cultured in RPMI 1640 media supplemented with 10% foetal bovine/calf serum, penicillin (50 IV/ml) and streptomycin sulphate (50 µg/ml). They were kept at 37°C and 5% CO_2.

3.2.2 Primary NK cells

Primary NK cells were purified from a buffy coat, prepared from healthy donors. These were purchased from the National Health Blood and transfusion Service (NHSBT, UK) following ethical approval (REC reference: 16-SS-033).

3.2.3 Primary healthy leukocytes obtained from healthy donors

Primary healthy leukocytes were obtained from a buffy coat from human blood, obtained from healthy donors. These were purchased from the national health blood and transfusion service (NHSBT, UK) following ethical approval (REC reference 16-SS-033). Mononuclear-rich leukocytes were obtained by Ficoll-density centrifugation according to the manufacture's (GE Healthcare Life Sciences) protocol and the number of cells was determined using a

haemocytometer and diluted accordingly with HEPES-buffered Tyrode's solution before treatment.

3.2.4 Primary human AML cells

Primary human mononuclear blasts (AML-PB001F, newly diagnosed/untreated) were purchased from All Cells (Alameda, CA, USA) and handled according to manufacturer's instructions following ethical approval (REC reference 16-SS-033).

3.2.5 Primary human CLL cells

Primary human bone marrow derived CLL mononuclear cells (CLL-DM001F, newly diagnosed/untreated) were purchased from All Cells (Alameda, CA, USA) and handled according to manufacturer's instructions following ethical approval (REC reference 16-SS-033).

3.2.6 Primary human blood samples

Blood serum of healthy donors was obtained from buffy coat blood, originated from healthy donors undergoing routine blood donation. It was purchased from the National Health Blood and Transfusion Service (NHSBT, UK) following ethical approval (REC reference: 16-SS-033). Primary human AML serum samples were obtained from the sample bank of University Medical centre Hamburg-Eppendorf (UKE).

3.2.7 Mouse bone narrow extracts

Femur bones of six-week-old C57 BL16 mice (25 ± 2.5 g, kindly provided by Dr. Gurprit Lall, School of Pharmacy, University of Kent) were used for the experiments following approval by the Institutional Animal Welfare an Ethics Review Body. Animals were handled

by authorised personnel in accordance with the Declaration of Helsinki protocols. Bone marrow was isolated from femur bone heads as described before (Swamydas and Lionakis, 2013) and the whole extract (1 mg protein/ml) of it was then obtained.

3.3 Cell lysates

The cells were incubated according to indicate at the results section. After the incubation, the cells were centrifuged 5 min at 3000 rpm and re-suspended in lysis buffer (50 mM Tris-HCl, 5 mM Ethylenediaminetetraacetic acid (EDTA), 150 mM NaCl, 0.5% Nonidet-40, 1 mM phenylmethylsulfonyl fluoride (PMSF), pH8.0). The samples incubated on ice and then were centrifuge 5 min at 13,200 rpm and used straight after or stored at -80°C until future use.

3.4 Protein quantification

This was the method used to quantify the amount of proteins in cell lysates. It was based on the method described by (Bradford, 1976), which allows the quantification of the protein due to a shift in the absorption maximum of the dye (Coomassie Brilliant Blue G-250) from 465 nm to 595 nm, from red to blue, upon binding with protein.

Five µl of cell lysate were mixed with 150 µl of Bradford reagent (0.01% (w/v) Coomassie Brilliant Blue G-250, 4.7% (w/v) ethanol and 8.5% (w/v) phosphoric acid) in a microwell plate. The optical density at 620 nm was read in the plate reader.

3.5 Cell viability assay

The cell viability was perfomed using the Promega (Southampton, UK) MTS (3-(4,5-dimethylthiazol-2-yl)-5(3-carboxymethoxyphenyl)-2-(4-sulfophenyl)-2H-tetrazolium)kit assay.

In this assay, MTS is converted to aqueous formazan by dehydrogenases in the living cells. This conversion is proportional to the amount of living cells and can be by measuring the maximum absorbance of the reaction product at 490 nm (Cory *et al.*, 1991).

To 100 µl of cell and 20 µl of MTS reagent were placed into a microwell plate and mixed. The plate was placed on to the incubator at 37°C for 1-2 hours, and the absorbance at 490 nm was then measured.

3.6 Western-blot analysis[2]

The cell lysates were mixed with 2X or 4X sample buffer (125 mM Tris-HCL, 2% sodium dodecyl sulphate (SDS), 10% glycine, 1 mM dithiothreitol (DTT), 0.002% bromophenol blue, pH6.9) and boiled 5 min at 95°C.

Proteins were resolved on 7.5%, 10% or 12% SDS-polyacrylamide gels, prepared according to Table 5, according to the molecular size of the target protein. The gels run at 150-200 V, with constant voltage, until the dye front was about 1 cm from the bottom of the gel.

Filter paper and/or filter pads, together with nitrocellulose membrane were soaked in blotting buffer and assemble in the transfer cassette according to Figure 13.

[2] Buffers and other solutions used in this section are described in section 7.1 and 7.2, in Appendix.

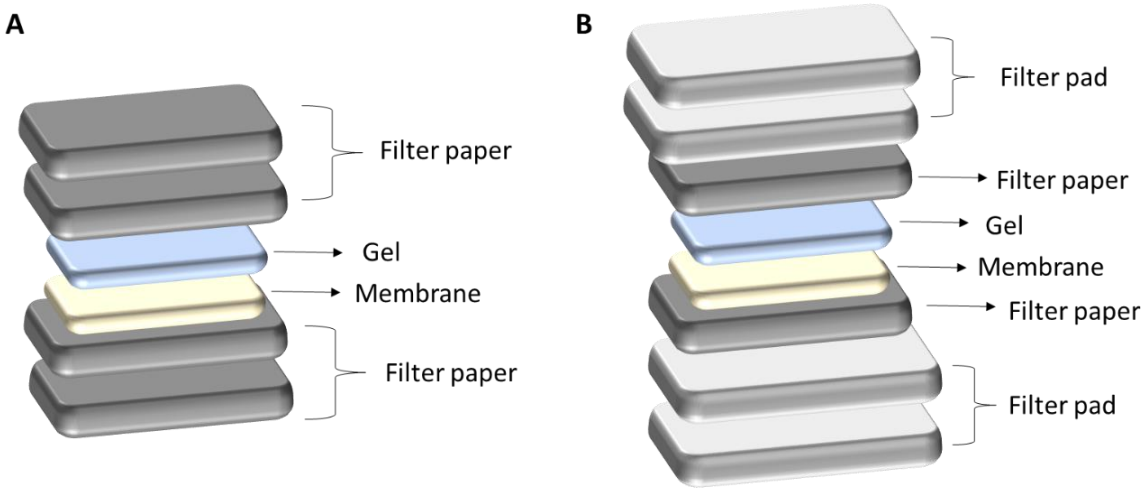

Figure 13 Schematic representation of transfer montage. A. *semi-dry transfer* ***B.*** *wet transfer.*

The transfer was done in a semi-dry (BioRad system) or wet (Invitrogen system) environment at constant voltage and 0.07 Amp (semi-dry transfer) or 0.1 Amp (wet transfer), one to two hours, according to the gel and system used.

The membranes were blocked with blocking buffer (tris-buffered saline, 0.1% Tween 20 (TBST), 2% bovine serum albumin (BSA)) for at least 1 h under constant agitation at room temperature. The antibodies for the target proteins, diluted in blocking buffer, were added to the membrane, and incubated for at least 2 h.

The membranes were washed with TBST for at least 15 min, under constant agitation at room temperature. Li-Cor goat secondary antibodies, conjugated with fluorescent dyes, diluted in TBST, were used according with the manufacturer's protocol in order to visualise the proteins of interest. This was done using a Li-Cor Odyssey imaging system. Western-blot data were subjected to quantitative analysis using Odyssey software and values were normalised against respective β-actin bands.

Some membranes were stripped using a ReBlot^{TM} Plus Kit (Chemicon International) according to the manufacturer's protocol. Membranes were then blocked and scanned using the Li-Cor Odyssey imaging system to make sure that stripping was successfully completed. Then the membranes were re-probed to detect new proteins.

3.7 ELISA

ELISA is an immunoassay were one of the reagents is immobilized on a solid phase and the signal is generated by one enzyme, in this case HRP-Streptavidin.

3.7.1 Detection of phosphor-S2448 mTOR in cell lysates

ELISA plates were coated with mouse anti-mTOR antibody and blocked with 2% BSA.

The cell lysates were added to the plate, and incubated with constant agitation at room temperature for at least 2 h.

The plates were then washed with TBST buffer and anti-phospho-S2448 mTOR antibody was added. The plates were incubated with agitation for at least 2 h and once again, washed with TBST buffer.

1:1000 HRP-labelled goat anti-rabbit IgG (Abcam) in TBST buffer was added to the plates and it reacted for at least 30 min at room temperature. After washing the plates with TBST, bound secondary antibodies were detected by the peroxidase reaction (orthophenylenediamine/H_2O_2).

3.7.2 Detection of exocytosed IL1-β, IL6, TNFα, VEGF, Galectin-9 and soluble Tim-3

Concentrations of the above proteins released into cell culture media were analysed by ELISA (R&D Systems assay kit) according to the manufacturer's protocol.

Tim-3 was also detected using a similar approach, but instead of a kit, mouse anti-Tim-3 (mAnti-Tim-3) was employed as a capture antibody and rabbit anti-Tim-3 (rAnti-Tim-3) as detection antibody. HRP-labelled goat anti-rabbit IgG antibody (Abcam) was used to visualise the reaction.

3.7.3 Detection of soluble Tim-3-Galectin-9 complex

Mouse anti-Tim-3 (mAnti-Tim-3) was added to the ELISA plate and used as capture antibody. The cell lysates were added to the plates and incubated for at least 2 h.

Biotinylated goat anti-galectin-9 (gAnti-Galectin-9, R&D Systems) was used as detection antibody. It was added to the plates and reacted with constant agitation for at least 2 h.

The secondary antibody, HRP-labelled goat anti-rabbit IgG antibody (Abcam), was added to the plates and it reacted for at least 2 h with constant agitation.

The reaction was visualised using HRP-labelled goat anti-rabbit IgG antibody (Abcam). The plates were washed with TBST and bound secondary antibodies were visualised by the peroxidase reaction (orthophenylenediamine/H_2O_2).

3.8 Characterisation of Tim-3 and galectin-9 interactions in cell lysates

An ELISA-based analysis was used. ELISA plates were coated with anti-galectin-9 antibody and then blocked with 2% BSA. Cell lysates were added to the plates and incubated for at least 4 h with constant agitation at room temperature. The plates were washed with TBST and a glycine-HCl pH lowering buffer (pH 2) was then applied to extract the bound proteins.

The extracts were mixed with equal volumes of lysis buffer (50 mM Tris-HCl, 5 mM Ethylenediaminetetraacetic acid (EDTA), 150 mM NaCl, 0.5% Nonidet-40, pH8.0) and with 4X sample buffer (125 mM Tris-HCL, 2% sodium dodecyl sulphate (SDS), 10% glycine, 1 mM dithiothreitol (DTT), 0.002% bromophenol blue, pH6.9) for SDS-PAGE at the ratio of 1:3. The samples were analysed through western-blot.

To confirm that all galectin-9 was extracted, the plate was subjected to analysis with galectin-9 detection antibody followed by standard ELISA steps. Signals obtained were similar to those where PBS was used instead of the sample confirming that all the protein was extracted.

3.9 In cell Western and in cell assay (also known as on cell assay)

To analyse the total amount of Tim-3 and galectin-9, a standard Li-Cor in cell Western assay was used. The in cell assay was also used to detect the amount of these proteins in the cell surface.

3.9.1 In cell Western

In this technique, the cells were centrifuged and re-suspended in cold methanol for 10 min at -20°C. They were then pelleted, by centrifuging and re-suspended in new media (same used in cell culture), at least two times to ensure that no methanol is left.

The cells were re-suspended in fresh medium containing anti-Tim-3 or anti-galectin-9, and they reacted at least 3 h under constant agitation at room temperature. New centrifugation was done and the cells were re-suspended in fresh medium containing Li-Cor goat secondary antibodies. They reacted at least 2 h under constant agitation at room temperature.

The cells were washed and placed in an ELISA plate, where the Li-Cor Odyssey imaging system was used to visualise them and the Odyssey software used for quantitative analysis.

3.9.2 In cell assay

The protocol used for this technique was the same described for in cell Western, but without permeabilisation of the cells with methanol.

Briefly, cells were re-suspended in medium containing anti-Tim-3 or anti-galectin-9, and the reaction was carried out for at least 3 h under constant agitation at room temperature. Cells were centrifuged and re-suspended in fresh medium containing Li-Cor goat secondary antibodies. The biding was done for at least 2 h under constant agitation at room temperature. Cells were then washed and placed in an ELISA plate, where the proteins were visualised using the Li-Cor Odyssey imaging and the Odyssey software was used for the quantitative analysis.

3.10 Transfer of galectin-9/Tim-3 siRNA into U-937 cells and qRT-PCR

For the galectin knock-down, a galectin-9-specific siRNA target sequence (uga ggu gga cga ugu ggu ucc c) which was previously described (Hsu *et al.*, 2015) was used. For Tim-3 knockdown, a commercially available siRNA purchased from Santa Cruz Biotechnology, CA, USA, was employed. As control, it was used a corresponding random siRNA (uac acc guu agc aga cac c dtdt (Wang *et al.*, 2008). Transfection into U-937 cells was performed using DOTAP reagent according to the manufacturer's protocol.

To monitor galectin-9 and Tim-3 mRNA levels we used qRT-PCR (Moritoki *et al.*, 2013)- Total RNA was isolated using a GenElute^{TM} mammalian total RNA preparation kit, followed by a target protein mRNA reverse transcriptase-polymerase chain reaction (RT-PCR) performed in accordance with the manufacturer's protocol (Sigma). This was followed by quantitative real-time PCR. Primer selection was as follows: Galectin-9, 5'-CTTTCATCACCACCATTCTG-3', 5'-ATGTGGAACCTCTGAGCACTG-3' Tim-3, 5'-CATGTTTTCACATCTTCCC-3' actin, 5'-TGACGGGGTCACCCACACTGTGCCCATCTA-3', 5'-CTAGAAGCATTTGCGGTCG-ACGATGGAGGG-3'. Reactions were performed using a LightCycler® 480 real-time PCR system and respective SYBR Green I Master kit (Roche, Burgess Hill, UK). Analysis was performed according to the manufacturer's protocol. Values representing galectin-9 and Tim-3 mRNA levels were normalised against β-actin.

3.11 Characterisation of glycolysis and MGO levels

Glycolytic degradation of glucose was analysed using a colorimetric assay, previously described (Porakishvili *et al.*, 2001). This method relies on the fact that cell lysates can be used as multi-enzyme preparation, to convert glucose into lactate, in the absence of oxygen (Figure 14).

The cell lysates were incubated, in an anaerobic chamber, for 1 h at 37°C with 1% glucose solution, and then proteins were precipitated using a 2% trichloroacetic acid solution. Carbohydrate precipitation was performed using $CuSO_4$ solution in combination with $Ca(OH)_2$, at a final concentration of 60 mg/ml and lactate was converted into acetic aldehyde using concentrated H_2SO_4 at 90°C for 1 min followed by cooling down on ice. The acetaldehyde was then detected using veratrole (1,2-dimethoxybenzene) test.

Methylglyoxal (MGO) was also detected colorimetrically following biochemical modifications (Chaplen *et al.*, 1996a; Chaplen *et al.*, 1996b). It was condensed with reduced glutathione (GSH, 1 mM) for 10 min at 37°C. This was converted into lactate by Glyoxalases I and II at pH 8.0 (Figure 14) (Thornalley, 1993). Lactate was then measured as describe above.

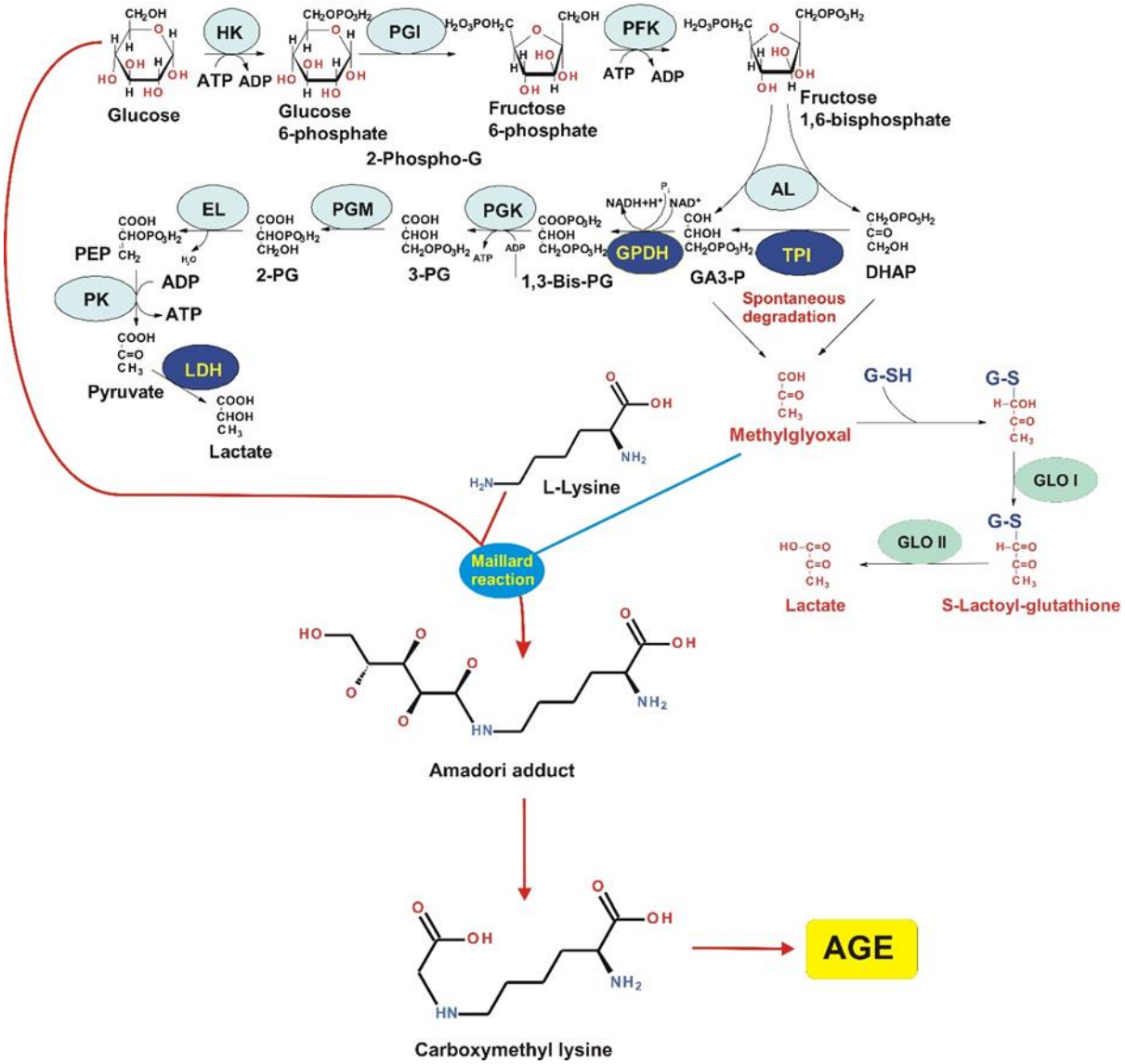

Figure 14 Biochemistry of glycolytic degradation of glucose, generation of methylglyoxal (MGO) and MGO-dependent formation of advanced glycation end (AGE) products. *Additional abbreviations used: HK – hexokinase, PGI – phosphoglucose isomerase, PFK – phosphofructokinase, AL – Aldolase, TPI – Triose-phosphate isomerase, GPDH – glyceraldehyde-3-phosphate dehydrogenase, PGK – phosphoglycerate kinase, PGM – phosphoglycerate mutase, EL – enolase, PK – pyruvate kinase, LDH – lactate dehydrogenase, DHAP – dihydroxyacetone phosphate, GA3-P – glyceraldehyde-3-phosphate, 3-PG – 3-phosphoglycerate, 2-PG – 2-phosphoglycerate, PEP – phosphoenolpyruvate, G-SH – reduced glutathione, GLO (I or II) – glyoxalases I and II* (Gonçalves Silva *et al.*, 2017).

3.12 Analysis of phosphatidylinositol-3 kinase (PI-3K) activity and phosphate groups

Activity of PI-3K was measured using a nonradioactive assay based on the ability of the enzyme to phosphorylate its substrate as previously described (Abooali *et al.*, 2014).

Cell lysates were incubated with 0.1 mg/ml substrate (PI-4,5-diphosphate) in kinase assay buffer (20 mM Tris pH 7.5, 100 mM NaCl, 0.5 mM EDTA, 8 mM $MgCl_2$, 40 µM ATP). The reaction was stopped by adding a mixture of hexane/isopropanol (13:7, v:v) and a mixture of 2 M KCl/HCl_{conc} (8:0.25, v:v). The samples were vortexed and organic phases were washed with HCl (0.1 M). Then the detection of phosphates groups was done using molybdenum reagent containing 2 parts of 25 mM $(MH_4)_6Mo_7O_{24}$, 5 parts of 0.3 M ascorbic acid and 1 part of 2 mM potassium antimonyl-tartrade.

Phosphate groups were characterised using colorimetric assay as mention above.

3.13 Detection of catalytic activity of PKC*α*

Catalytic activity of PKCα was measured as described before based on its ability to phosphorylate specific substrate (Micol *et al.*, 1999).

Briefly, the samples were mixed with 20 mM Tris-HCl pH 7.5, 200 µM $CaCl_2$, 5 mM $MgCl_2$ and added to ELISA plates, previously coated with 0.2 mg/ml Histone_5_III. It reacted 30 min at 37°C. Glycine-HCl pH lowering buffer (pH 2, at 95°C) was added to the plates followed by lysis buffer.

The samples were then mixed with 4X sample buffer (125 mM Tris-HCL, 2% sodium dodecyl sulphate (SDS), 10% glycine, 0.002% bromophenol blue, pH6.9) and resolved using 12%

SDS-polyacrylamide gel. The gel was stained with Coomassie Blue and destained with acetic acid.

3.14 Confocal microscopy

THP-1 cells were cultured in 12 mm cover glasses in 24-well plates. Cells were treated overnight with PMA and fixed/permeabilised during 20 min with ice-cold methanol or a mixture methanol/acetone. Alternatively, cells were fixed in a freshly prepared 2% paraformaldehyde, washed 3 times with PBS and permeabilised with 0.1%TX-100.

Cover glasses were blocked for 1 hr at room temperature with 10% goat serum in PBS. The anti-Tim-3 antibody and anti-galectin-9 antibody both at 1 µg/ml were used as primary antibodies and incubated overnight at 4°C. Goat-anti-mouse Alexa Fluor 488 and goat-anti-rabbit Alexa Fluor 555 were used as secondary antibodies. Cells were incubated with secondary antibodies for 45 min at room temperature. The preparations were examined using the Olympus laser scanning confocal microscope as described previously (Prokhorov *et al.*, 2015; Fasler-Kan *et al.*, 2010). Images were collected and analysed using the proprietary image acquisition software.

3.15 Synchrotron radiation circular dichroism spectroscopy

Human recombinant Tim-3, human recombinant galectin-9 and Tim-3-galectin-9 complex were analysed using SRCD spectroscopy at beam line 23 (Figure 15), Diamond Light Source (Didcot, UK). SRCD measurements were performed using 0.2 µg/ml of samples in 10 cm path length cell, 3 mm aperture diameter and 800 µl capacity using Module B with 1 nm increment, 1s integration time, 1.2 nm bandwidth at 23 °C (Hussain *et al.*, 2012). Results obtained were processed using CDApps (Hussain *et al.*, 2015) and OriginLab™.

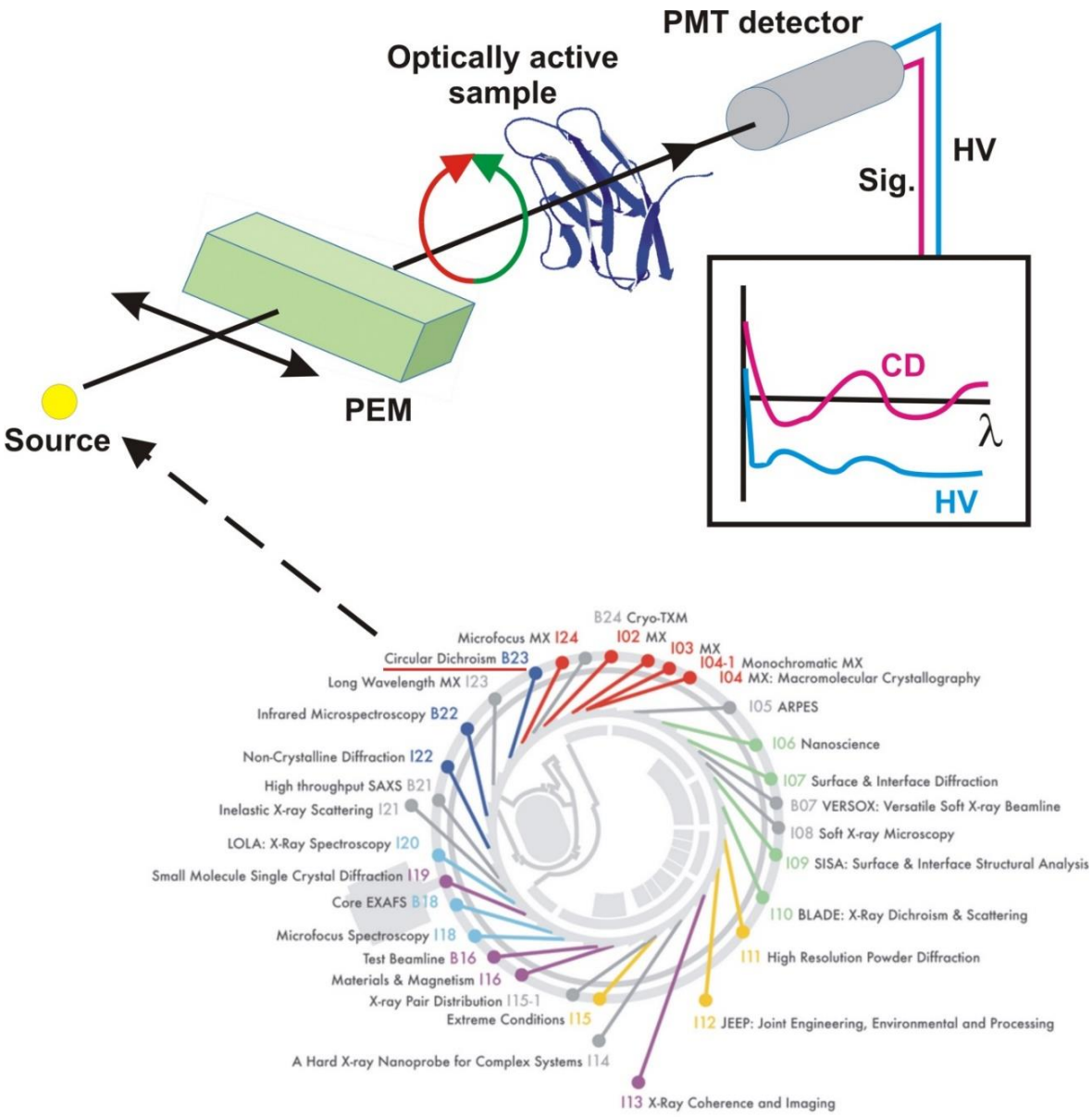

Figure 15 Beam light 23 at Diamond Light Source Synchrotron and scheme of Synchrotron radiation circular dichroism (SRCD) spectroscopy analysis (Gonçalves Silva *et al.*, 2017)**.**

3.16 Leukaemia cell protection assay

K562 and NK cells were cultured separately or as a 1:2 co-culture (K562: NK) for 16 h, at 37°C, in the presence or absence of 0.5 - 5 ng/ml of galectin-9. The unfixed cell cultures were then imaged under an inverted microscope (TE200, Nikon), using phase-contrast lighting, a digital camera and the WinFluor image acquisition software (J. Dempster, University of Strathclyde).

The same camera and microscope settings were used, and images were acquired at several different focal planes. The raw images were analysed using the ImageJ software. Due to the very large difference in the size of K562 and NK cells, it was possible to identify each cell type both in mono-cultures and in co-cultures, by optimising the ranges of particle sizes during automatic particle counting. To correct for artefacts of uneven illumination, background was subtracted, using a 100-μm window and the Sliding paraboloid algorithm. The images were then segmented by automatic thresholding based on manually optimised parameters, which were then applied to all images within each experiment. Any overlapping cells were subsequently split using the Watershed algorithm. The “Analyze Particles” plugin was used to eliminate any artefacts and distorted particles near the edge of the images. The selected areas were then applied to the raw image to determine the actual cell numbers. After the analysis was complete, image contrast was enhanced for some images, to produce illustrations only.

3.17 Statistical analysis

Each experiment was performed at least three times and results were statistically validated by two-tailed Student's t-test (when comparing two events at a time). Multiple comparisons were performed using one-way ANOVA test. Where applicable, a post-hoc Bonferroni correction was used. Statistical probabilities (p) reflecting significant differences between individual events were expressed as *, where $p<0.05$, ** where $p<0.01$ and *** where $p<0.001$.

4. RESULTS AND DISCUSSION

4.1 Differential expression and biochemical activity of the immune receptor Tim-3 in healthy and malignant human myeloid cells

Tim-3, as previous mentioned is a plasma membrane-associated receptor that participates in several biological responses in human immune cells. It is highly expressed in AML cells, which makes it a good possible target for AML therapy, but its biochemical activities are still not well understood. In this chapter, we analyse the total expression and externalization of Tim-3 in primary AML cells compared to primary leukocytes.

4.1.1 Results

4.1.1.1 Tim-3 immune receptor is expressed in AML blasts and healthy leukocytes

The expression and redistribution of Tim-3 in the cells was analysed using in cell Western (ICW) and its presence on the cells' surface using in cell assay (ICA). In this work AML blasts and healthy whole blood leukocytes (PLs) express Tim-3 (Figure 16).

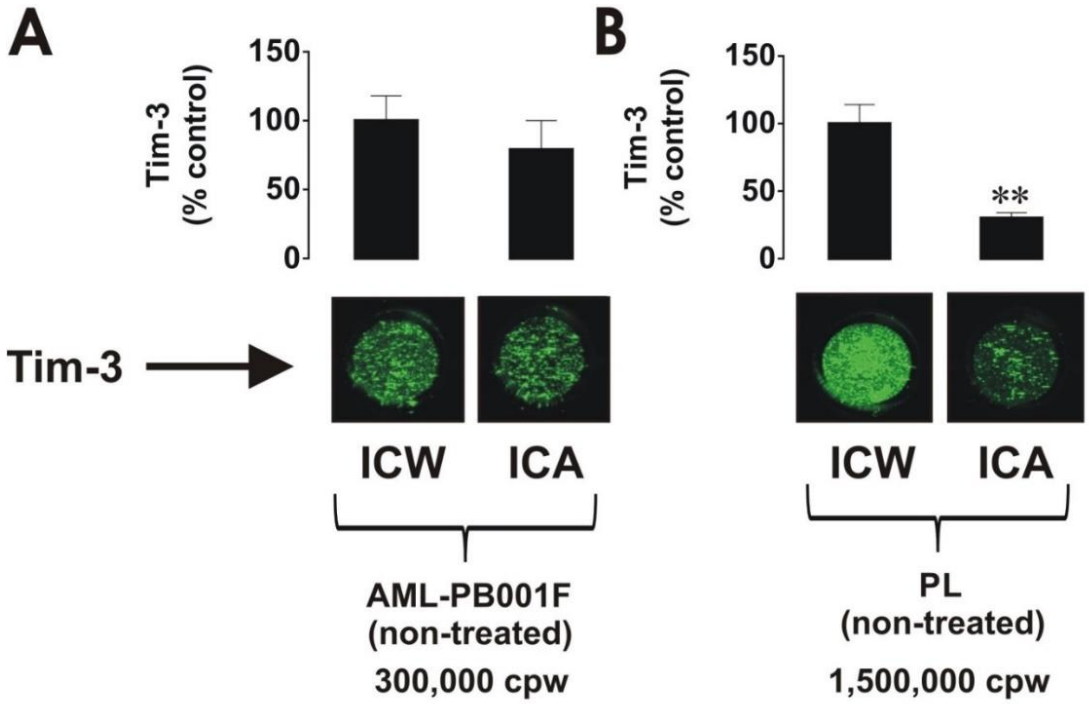

Figure 16 Tim-3 expression and Tim-3 surface presence in AML cells and healthy leukocytes. ***A.*** *$3X10^5$ AML-PB001 primary human AML cells per well* ***B.*** *$1.5X10^6$ healthy PLs per well. Tim-3 expression was done using in cell Western (ICW) and Tim-3 surface presence using in cell assay (ICA). The fluorescence values were normalized to the respective number of cells and use for calculations. Images are from one experiment representatives of three which gave similar results. Quantitative data are shown as means ± SEM of at least three individual experiments; **p < 0.01 vs. control.*

As shown in Figure 16A it is possible to observe that the majority of Tim-3 is externalised in AML cells while in healthy PLs (Figure 16B) this value is approximately 30%. This indicates that most Tim-3 protein was stored inside the cells, where the function of Tim-3 is unknown. Of note that, for the results in Figure 16 it was used 5 times healthier PLs than AML cells, it is likely that AML cells express more Tim-3 than healthy PLs.

4.1.1.2 Tim-3 triggers activation of the mTOR pathway and HIF-1 signalling in primary AML cells and primary healthy human leukocytes (PLs)

In primary AML cells, mTOR S2448 phosphorylation increase after exposure to SCF and anti-Tim-3 antibody stimulation (approximately half of the SCF-induced effect). LPS shown to be a weaker up regulator of the phosphorylation of mTOR S2448. This can be explained by the low TLR4 expression levels indicated by the AML-PB001F primary human AML cells supplier. The PI-3K activity showed the same pattern as mTOR S2448 phosphorylation (Figure 17A).

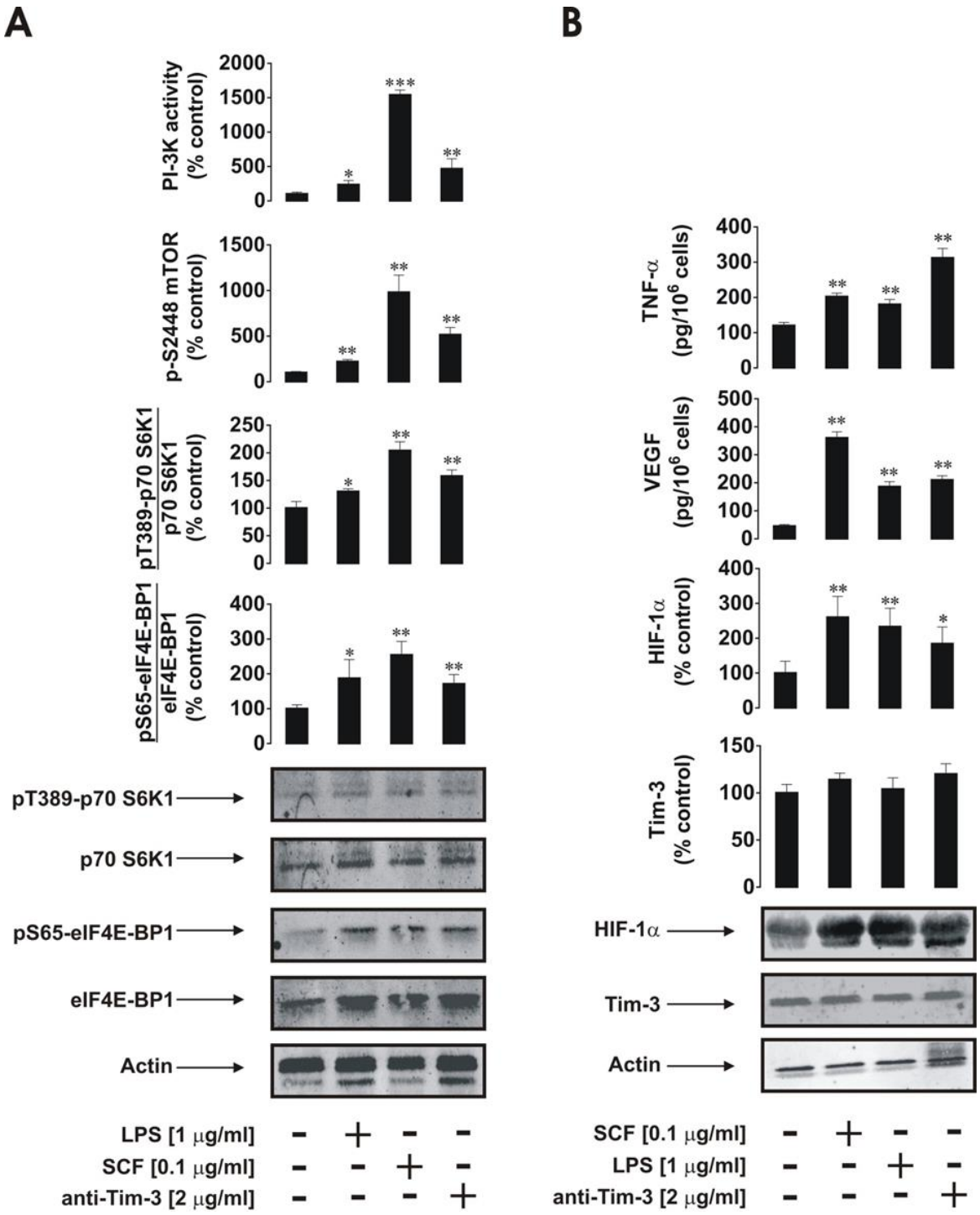

Figure 17 Anti-Tim-3 agonistic[3] antibody induces mTOR activity, HIF-1α accumulation and VEGF and TNFα secretion in primary human AML cells. *AML-PB001F cells were exposed to the indicated concentrations of anti-Tim-3, LPS and SCF for 4 h.* ***A.*** *PI-3K/mTOR pathway activity* ***B.*** *HIF-1α accumulation and VEGF and TNF-α release. Images are from one experiment representatives of four which gave similar results. Quantitative data are shown as means ± SEM of four individual experiments; *p < 0.05; **p < 0.01 vs. control.*

[3] The biding of this antibody triggers the same activity as a ligand (stimulus) would do.

The values obtained for mTOR S2448 phosphorylation and PI-3K activity match the values of mTOR activity monitored by the intracellular amounts of phosphor-T389 p70 S6K1 and phosphor-S65 eIF4E-BP1 (Figure 17A). Both proteins are phosphorylated at the indicated positions by the mTOR kinase complex (Gwinn *et al.*, 2008).

All the tested stimuli showed the ability to upregulate HIF-1α accumulation, being anti-Tim-3 antibody the weakest inducer (Figure 17B).. The effect of LPS in HIF-1α accumulation was stronger than the one observed when anti-Tim-3 antibody was used, which can be explained by the fact that LPS-dependent HIF-1α accumulation trigged by LPS does not depend only on mTOR activation, contrarily to what happen to SCF and anti-Tim-3 antibody HIF-1α accumulation. LPS-induced TLR4-mediated HIF-1α accumulation is known to be triggered through a redox-dependent mechanism, by mTOR and by mitogen-activated protein (MAP) kinase signalling cascades. These three pathways together achieved intensities comparable to mTOR-dependent processes after exposition to SCF (Figure 17A and Figure 17B).

None of the tested stimuli affected the levels of total Tim-3 in primary AML cells (Figure 17B). Anti-Tim-3 antibody upregulated the secretion of TNFα and VEGF. SCF mostly upregulated VEGF secretion but did not had a significant impact in TNFα secretion level (Figure 17B).

Galectin-9 was able to upregulate mTOR kinase activity and HIF-1α accumulation in primary AML cells at levels comparable to the ones observed with anti-Tim-3 antibody. This result suggests that both agonistic ligands have similar activities (Figure 18A and Figure 18B).

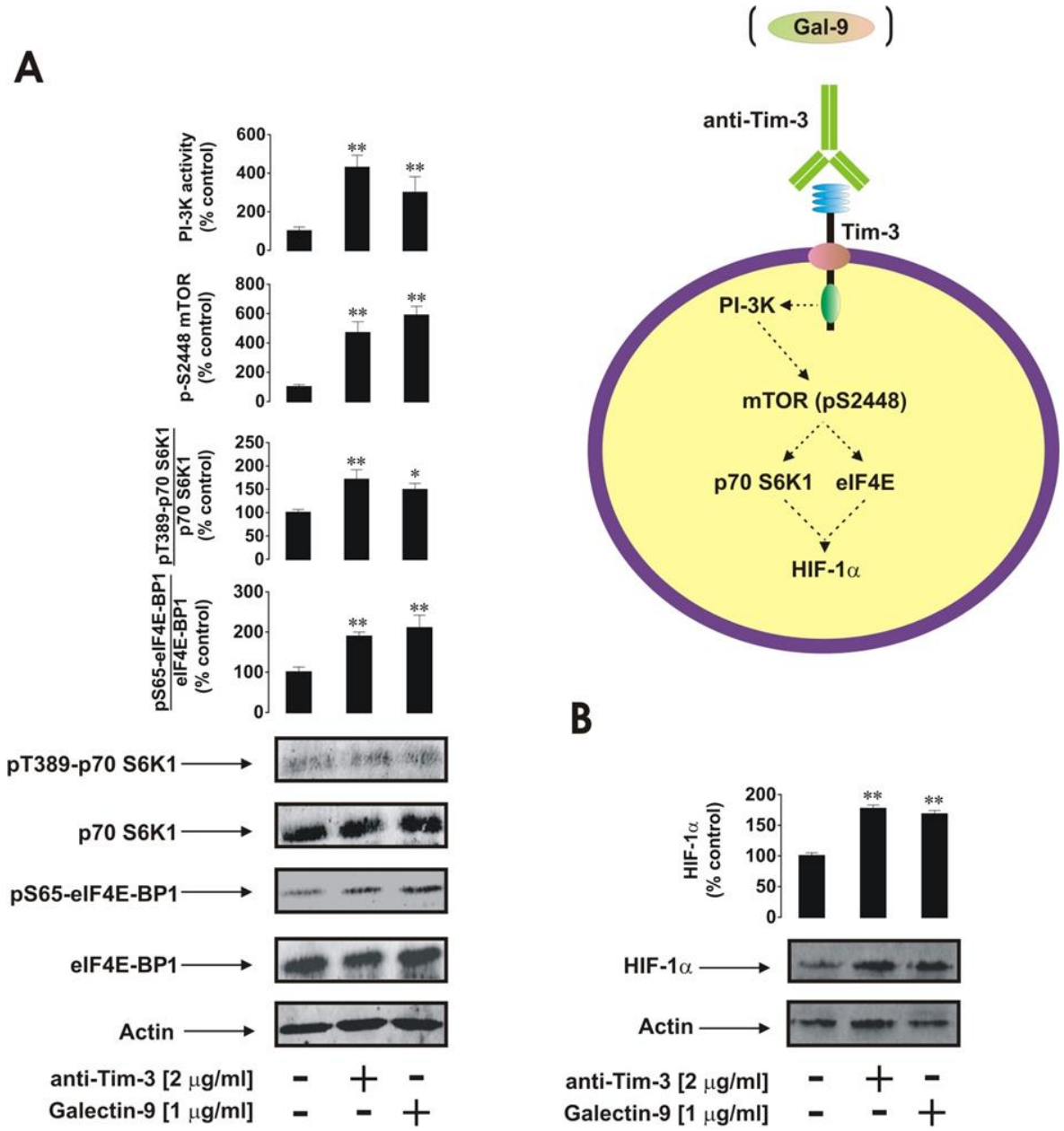

Figure 18 Anti-Tim-3 and galectin-9 induce similar responses in primary human AML cells. *AML-PB001F cells were expose to the indicated concentrations of anti-Tim-3 and galectin-9 for 4 h.* ***A.*** *PI-3K/mTOR pathway activity* ***B.*** *HIF-1α accumulation Images are from one experiment representative of three which gave similar results. Quantitative data are shown as means ± SEM of three individual experiments; *p < 0.05; **p < 0.01 vs. control.*

In primary human healthy leukocytes, the effects of anti-Tim-3 antibody were similar to those in primary AML cells. However, in these cells, LPS, and not SCF, was the most powerful activator (Figure 19A and Figure 19B). This probably happens because the amount of TLR4 express in healthy leukocytes is higher than in AML cells.

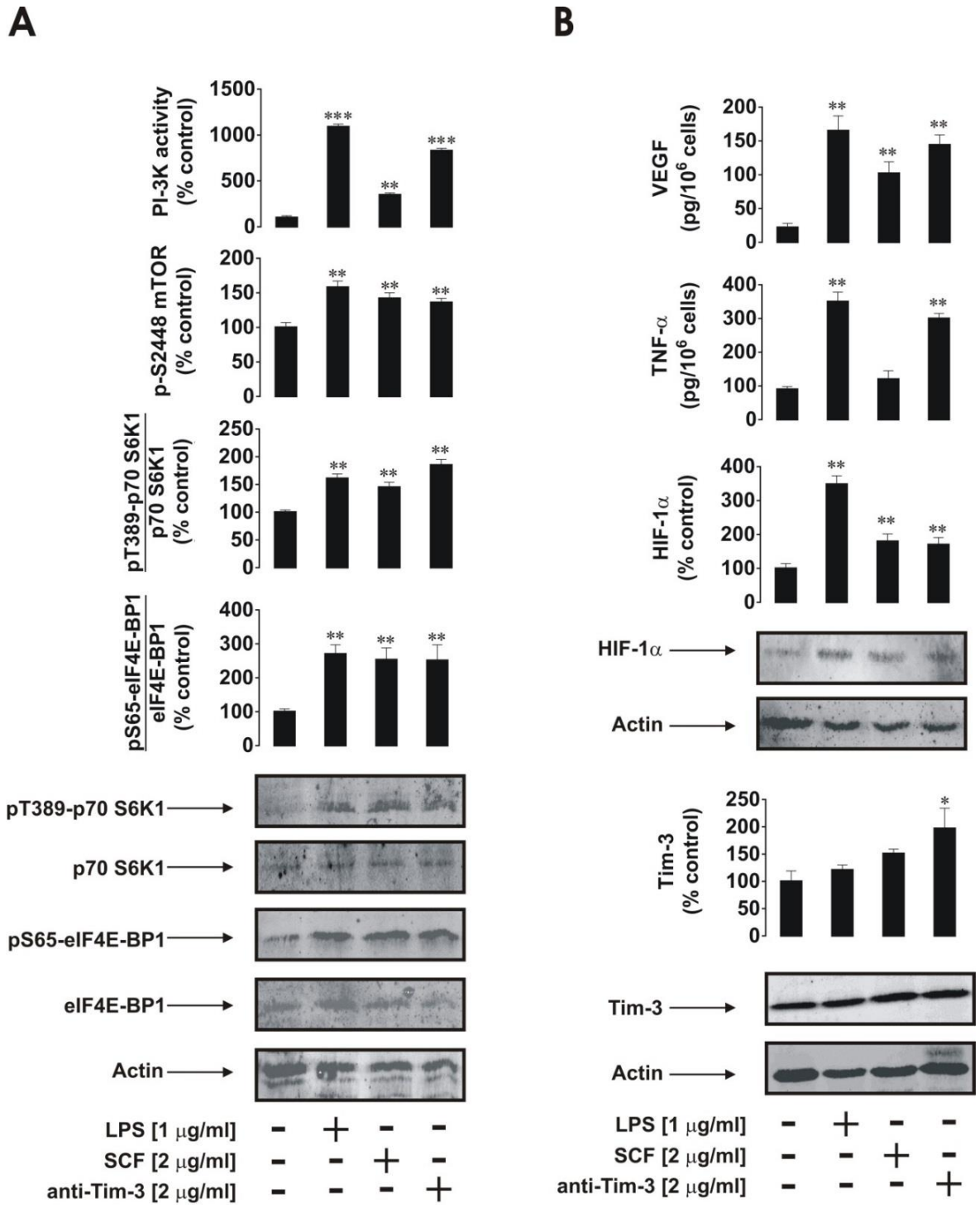

Figure 19 Anti-Tim-3 induces mTOR activity, accumulation of HIF-1α and secretion of VEGF and TNF-α in primary human healthy leukocytes. *PLs were exposed to the indicated concentrations of anti-Tim-3, LPS and SCF for 4 h.* ***A.*** *PI-3K/mTOR pathway activity* ***B.*** *HIP-1α accumulation, VEGF and TNF-α release. Images are from one experiment representative of four which gave similar results. Quantitative data are shown as means ± SEM of four individual experiments; *p < 0.05; **p < 0.01 vs. control.*

The effects of anti-Tim-3 antibody were similar to those of SCF and slightly lower than the effects of anti-Tim-3 antibody detected in primary AML cells (Figure 19A and Figure 19B). The isotype control (IgG 2a) antibody was tested and it did not induce any effect (data not presented).

Levels of intracellular phospho-S2448 mTOR, HIF-1α and Tim-3 and secreted VEGF were significantly higher in AML cells than in healthy PLs, while the secretion level of TNFα was slightly higher in primary AML cells. On the other hand, the levels of PI-3K activity were higher in healthy PLs than in AML cells. These results suggest that these proteins are used by leukaemia cells more than by healthy leukocytes (Figure 20).

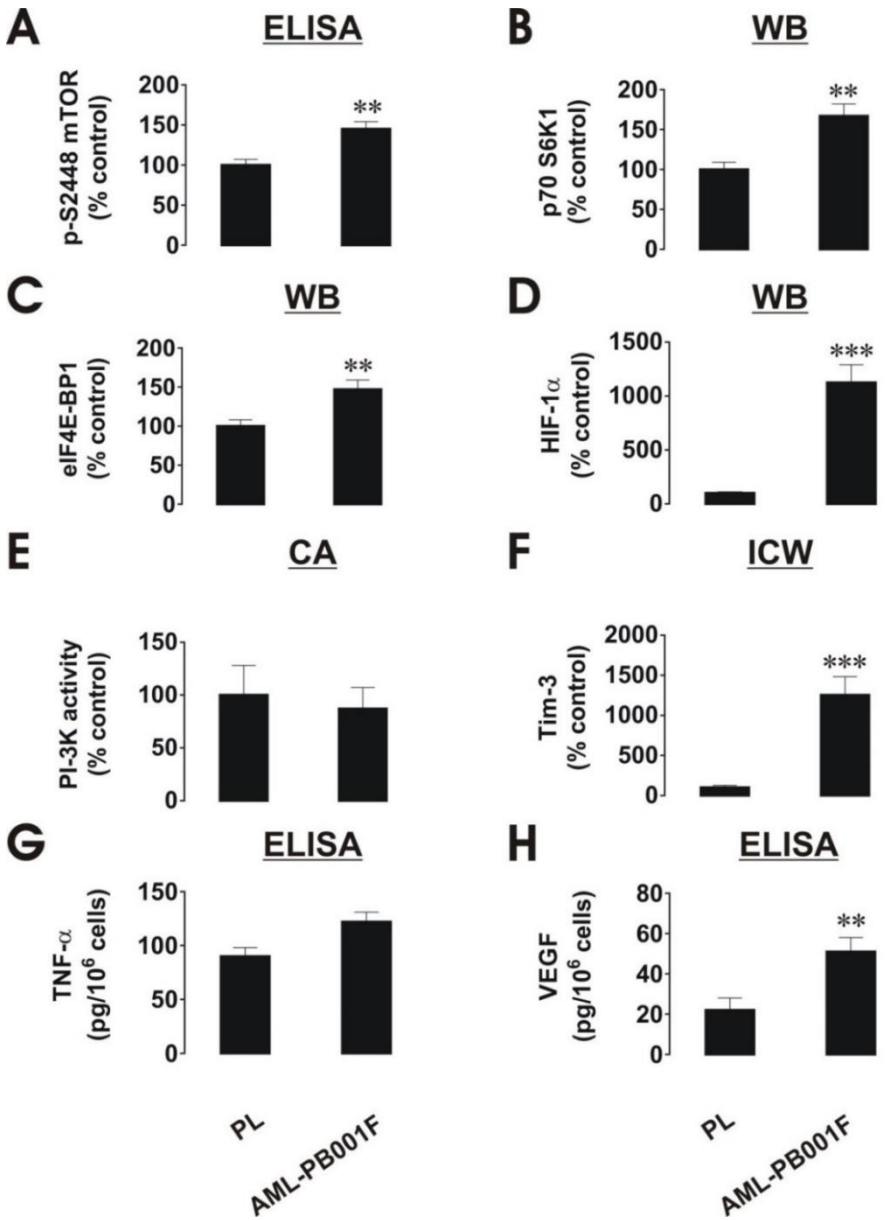

Figure 20 Comparative quantitative analysis of mTOR/HIF-1 pathway components and secretion of VEGF and TNF-α in primary human AML cells and healthy human PLs. *Protein levels were compared based on the indicated type of detection.* ***A.*** *pS2448 mTOR intracellular levels detected by ELISA, normalised against total cellular protein, and compared with the same values.* ***B. C. and D.*** *levels of p70 S6K1, eIF4E-BP1 and HIF-1α protein detected by Western-blot (WB), quantitated, and normalised against respective actin values before comparison and statistical validation of the results.* ***E.*** *PI-3K activity levels measured by colorimetric assay (CA).* ***F.*** *intracellular levels of Tim-3 detected by in cell western (ICW). The fluorescence values obtain for healthy PLs and AML cells were divided by the respective cell number (*Figure 16*) and use for comparison (using PLs value as 100%). Similar results were obtained when comparing Tim-3 values in AML cells and healthy PLs obtain by western blot and normalised against actin.* ***G. and H.*** *TNFα and VEGF measure in the medium by ELISA and amounts per 10^6 cells were compared and statistically validated. Data was obtained from 3 – 6 individual experiments, which gave similar results. Quantitative data are shown as means ± SEM; *p < 0.05; **p < 0.01; ***p < 0.01 vs. control.*

4.1.2 Discussion

It is known that Tim-3 receptor is expressed in healthy human hematopoietic cell but its role is not fully understood (Anderson, 2012). Also, it was recently reported that Tim-3 receptor is highly expressed and externalised in human AML cells (Kikushige and Miyamoto, 2013; Kikushige *et al.*, 2010). In healthy cells, this receptor is not expressed until they reach a mature state and lose the expression of the kit receptor. However, malignant cells can express both receptors. It is known that these cells use kit receptor for growth and proliferation while Tim-3 function is not clear.

Previously, it was reported that Tim-3 mediates activation of the PI-3K/mTOR pathway in human AML cell lines (Prokhorov *et al.*, 2015) and in dendritic cells Tim-3 induces TNFα production (Anderson *et al.*, 2007; Tang and Lotze, 2012) but it is not clear if the same happens in primary human AML cells, since activation of mTOR pathway and TNFα production use growth factors and inflammatory mediator-like responses.

Our results show that primary AML cells express more Tim-3 than primary healthy leukocytes even on the surface. While in PHLs approximately 30% of Tim-3 is expressed on the surface, in AML cells almost all Tim-3 is externalized. This difference probably has impact on Tim-3 activity in its ability to mediate ligand-induced activation of mTOR, HIF-1α accumulation and cytokine release in these cells.

Our results suggest that Tim-3 mediates ligand-induced activation of the mTOR pathway, which involves upregulation of phosphorylation of S2448 mTOR levels, p70 S6K1(T389) and eIF4E-BP-1(S65), accumulation of HIF-1α protein and induced by LPS (classic inflammatory mediator) and SCF (classic hematopoietic growth factor). SCF was the strongest inducer in

AML cells while in PHLs, LPS had the strongest effect. These differences are due to differential expression of TLR4 and kit receptors in healthy and malignant leukocytes.

SCF is known to trigger IL-6 release in primary cells (MacNeil *et al.*, 2014). IL-6 regulates VEGF (Adachi *et al.*, 2006) which is a HIF-1-dependent process (Semenza, 2002). These effects may contribute to both HIF-1α accumulation and VEGF release in addition to SCF (Figure 19).

Background levels of pS2448 mTOR, HIF-1α and Tim-3 as well as p70 S6K1 and eIF4E-BP-1 proteins are much higher in AML cells than in PHLs (Figure 20), especially HIF-1α accumulation that is strong in non-treated AML cells and almost undetectable in primary healthy leukocytes. These results become more interesting knowing that recently it was reported that HIF-1α contributes for Tim-3 expression (Koh *et al.*, 2015). Also, VEGF but not TNFα secretions were significantly higher in non-treated AML cells.

Interestingly, background levels of PI-3K activity were similar in AML cells and PHLs. This suggests that increased background levels of pS2448 mTOR in primary AML cells may be due to high constitutive phosphorylation, previously reported, for example, in LAD2 mast cell lines (Kim *et al.*, 2008; Gibbs *et al.*, 2012). So, mTOR/HIF-1α/VEGF pathway, but not inflammatory TNFα, is permanently used by primary AML cells.

In PHLs and primary AML cells, Tim-3 showed moderate properties as inflammatory receptor that has activity as growth factor (it leads to mTOR activation) and proangiogenic (promotes VEGF release) (Figure 21). Even though mTOR/HIF-1 pathway is triggered by LPS and SCF, a significant increase in TNFα and VEGF secretion was only observed after LPS stimulation. SCF acted mostly in the VEGF release, without triggering TNFα production. The observed high levels of Tim-3 in AML cells compared with PHLs did not result in higher specific biochemical activity of the receptor.

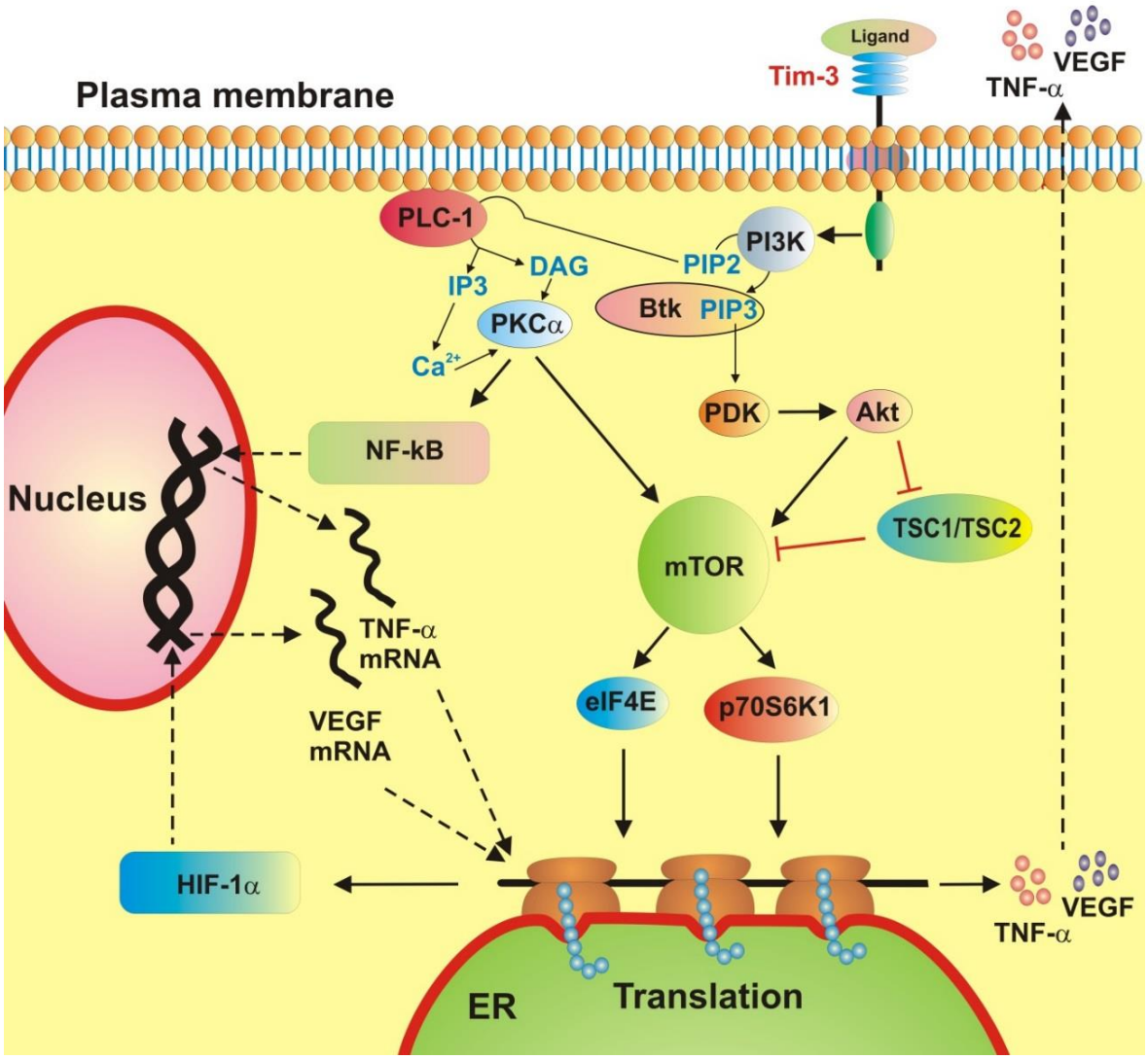

Figure 21 Summary scheme of ligand-induced Tim-3-mediated biological responses in healthy primary human leukocytes and primary AML cells.

4.2 The immune receptor Tim-3 acts as a trafficker in a Tim-3/galectin-9 autocrine loop in human myeloid leukaemia cells

As previous shown, the receptor Tim-3 is highly expressed in primary AML cells, where it seems to act as a growth factor and inflammatory receptor. Recently, it was demonstrated that Tim-3 forms an autocrine loop with galectin-9 (its natural ligand) in human AML cells (Kikushige *et al.*, 2015).

In this section, we analysed the involvement of Tim-3 in the secretion of galectin-9 in AML cells.

4.2.1 Results

4.2.1.1 Galectin-9 is expressed in healthy primary human leukocytes and malignant human myeloid cells and forms a complex with Tim-3 in both cell types

To start, we investigated the expression of galectin-9 by healthy primary human leukocytes (PL) and malignant myeloid cell lines (THP-1). The results showed that THP-1 cells produce more galectin-9 than PLs, but lipopolysaccharide (LPS) and SCF significantly upregulated galectin-9 levels in PLS. The effects of LPS are the strongest while in THP-1 only SCF had a significant impact (Figure 22).

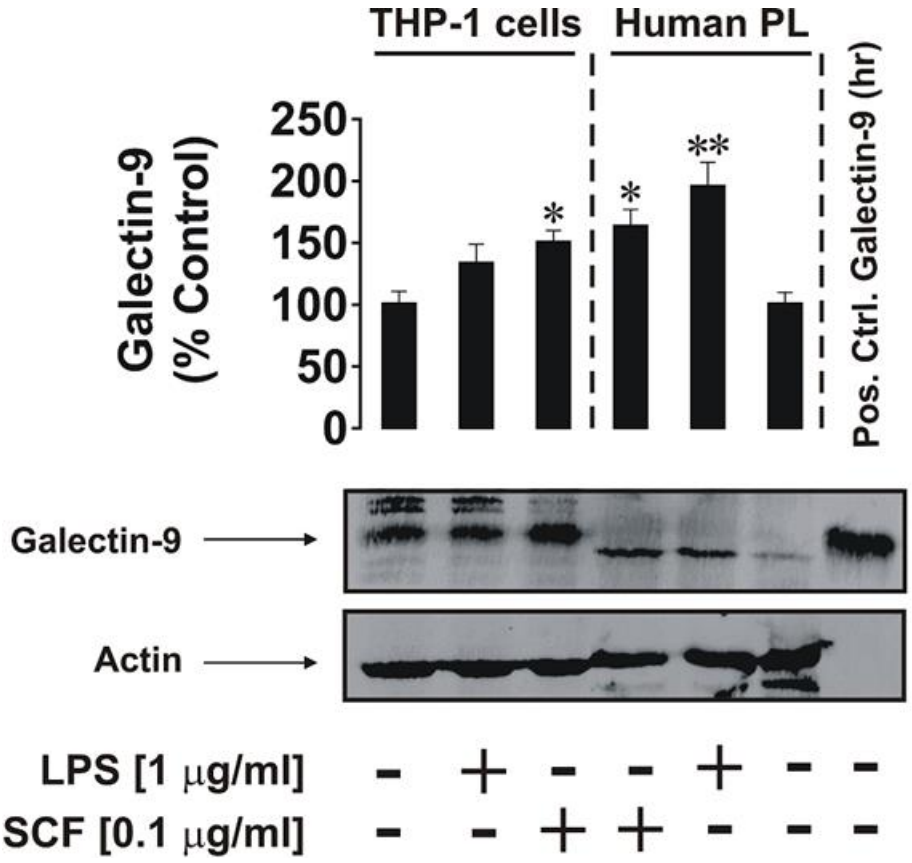

Figure 22 Effects of LPS and SCF on the expression of galectin-9 in THP-1 cells and PLs. *Cells were treated for 4 h with SCF or LPS and then harvested. Western-blot and human recombinant analysed galectin-9 levels galectin-9 (R&D Systems) was used as positive control. Images are from one experiment representative of three which gave similar results. Quantitative data are shown as means ± SEM of three individual experiments; *p < 0.05; **p < 0.01 vs. control.*

In PLs, the band correspondent to galectin-9, appears slightly lower on the gel than the one of THP-1 cells and the positive control (Figure 22). This seems to suggest differences in the post-translational processing of the protein in different cells.

After establishing that these cells produced galectin-9, we proceeded to investigate if galectin-9 and Tim-3 can form a complex. In Figure 23 is a schematic representation of the method used to extract the complex. This method is described in detail in 3.7.3 section of Materials and Methods.

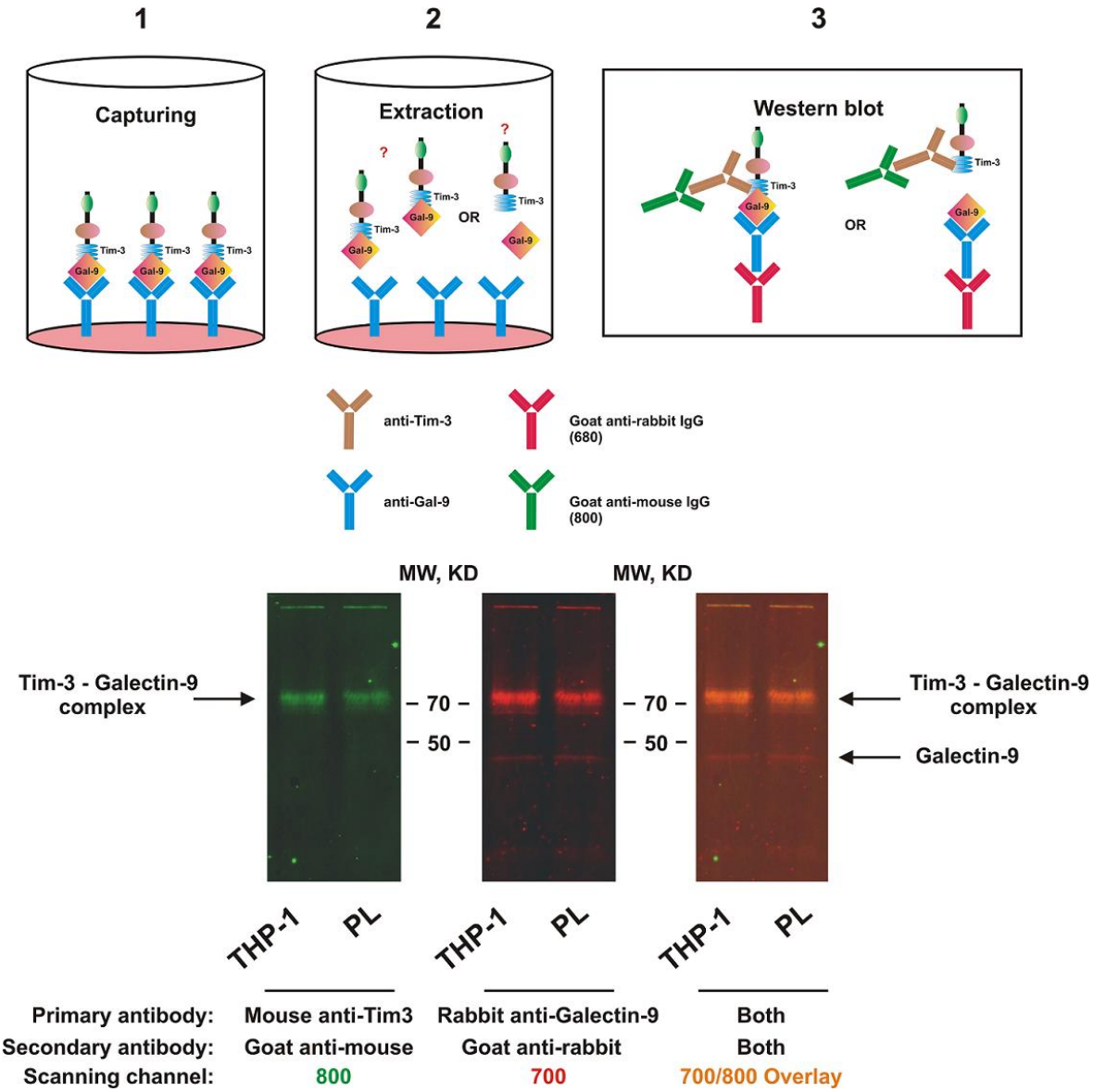

Figure 23 Tim-3 and galectin-9 form a stable complex. *Lysates from 3X10^5 THP-1 cells and 1.5X10^6 PLs were loaded in an ELISA plate, pre-coated with rabbit anti-galectin-9 antibody. After incubation, the capture proteins were extracted using pH lowering buffer and analysed using Western-blot. Images are from one experiment representative of four which gave similar results.*

Both galectin-9 and Tim-3 were detected by Western-blot using anti-galectin-9 rabbit antibody and anti-Tim-3 mouse antibody. Also in both cells was possible to detect galectin-9 and Tim-3 (Figure 23). It is possible to see a band slightly above 70 kDa, which corresponds to the sum of Tim-3 and galectin-9 molecular weights. We also detected traces of free galectin-9, but free

Tim-3 was almost undetectable. Since the complex formed by Tim-3 and galectin-9 was not separated during SDS-PAGE, it indicates that the complex is stable.

The cellular distribution of Tim-3 and galectin-9, comparing the intracellular level with the protein surface presence, was also analysed. In this experiment malignant myeloid cell lines (THP-1 and U937), primary human leukocytes (PLs) and primary AML cells (AML-PB001F) were used (Figure 24).

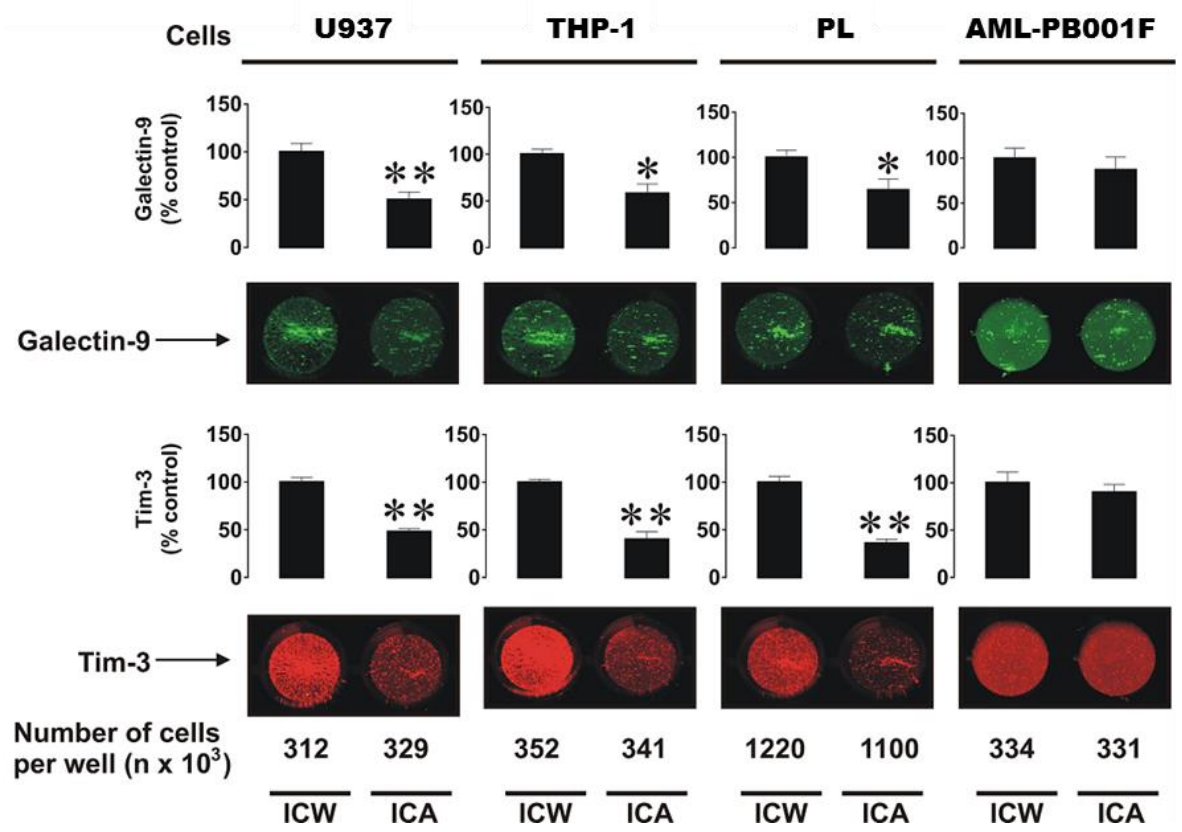

Figure 24 Comparative analysis of Tim-3 and galectin-9 expression and surface presence in human myeloid leukaemia cell lines, PLs and primary human AML cells. *The indicated number of resting U937, THP-1, PLs and primary human AML cells (AML-PB001F) were subjected to ICA or ICW. Images are from one experiment representative of five which gave similar results. Quantitative data are shown as means ± SEM of three individual experiments; *p < 0.05; **p < 0.01 vs. control.*

Resting THP-1, U937 and PLs cells expressed more Tim-3 and galectin-9 intracellular than on the surface, on the other hand primary AML cells expressed more protein on the surface than intracellularly. Interestingly, the ratio Tim-$3_{surface}$/Tim-3_{total} and galectin-$9_{surface}$/galectin-9_{total} was like each other in all studied cell types (Figure 24).

4.2.1.2 Tim-3 is required for galectin release in human myeloid leukaemia cells

After the results above described, we hypothesized that Tim-3 is required for galectin-9 release. To verify this hypothesis, we did knockdown of galectin-9 and Tim-3, using U937 cells, because of their higher siRNA transfection efficiency. Knockdown of galectin-9 expression was done in U937 cells and analysis of these cells, plus analysis of non-treated cells and cells treated for 4 h with 2 µg/ml of anti-Tim-3 stimulatory antibody was done.

It was possible to verify the success of the galectin-9 knockdown using Western-blot (Figure 25A) and quantitative real-time reverse transcription PCR (qRT-PCR; Figure 26).

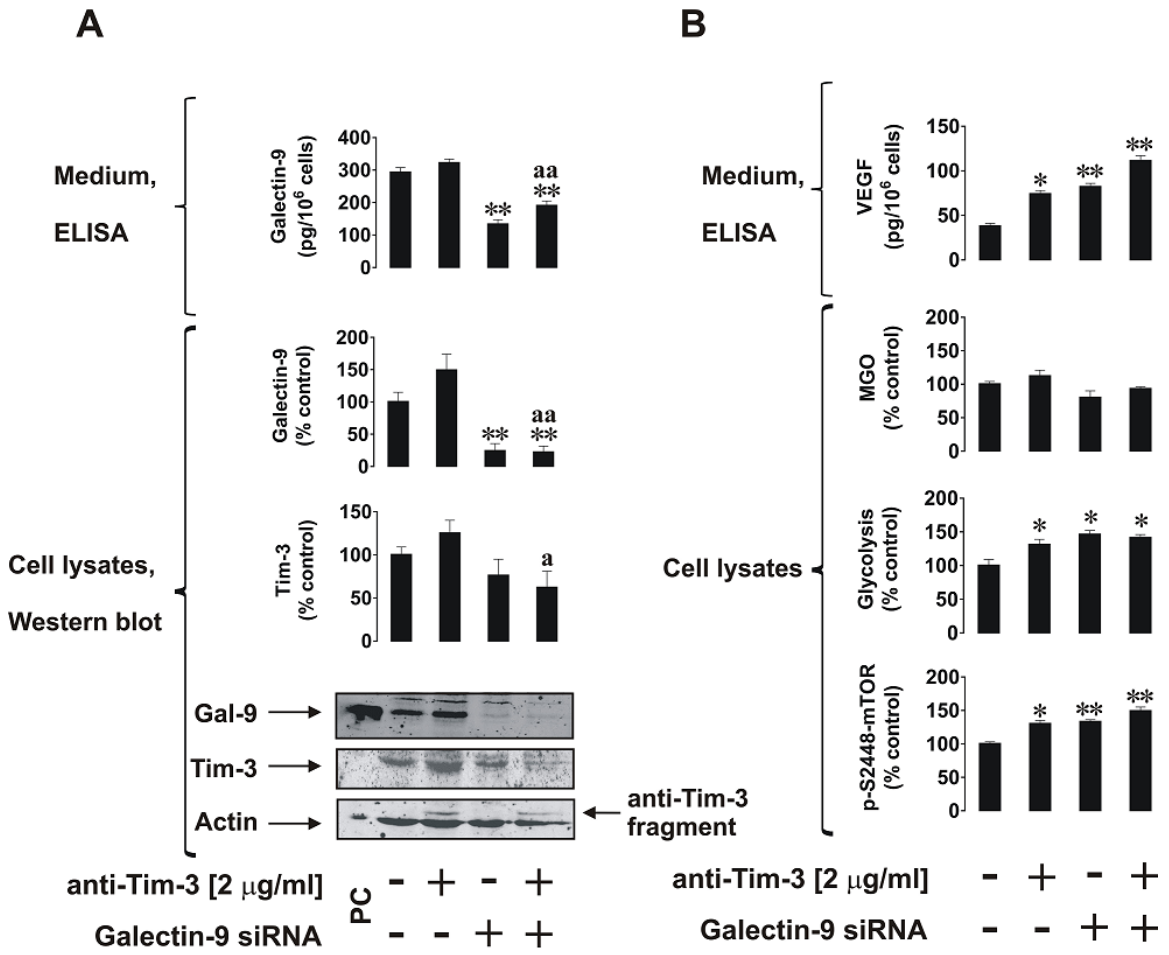

Figure 25 Effects of galectin-9 knockdown on Tim-3 expression and the mTOR pathway. *Non-treated normal (wild-type), galectin-9 knockdown U-937 cells and cells treated for 4 h with 2 μg/ml anti-Tim-3 stimulatory antibody were analysed.* ***A.*** *Tim-3 and galectin-9 levels measured by Western-blot and galectin-9 release measure by ELISA;* ***B.*** *pS2448 mTOR intracellular levels, glycolysis, MGO and VEGF secretion. Images are from one experiment representative of three to five which gave similar results. Quantitative data are shown as means ± SEM of 3-5 individual experiments; *p < 0.05; **p < 0.01 vs. control; [a]p < 0.05; [aa]p < 0.01 vs. anti-Tim-3.*

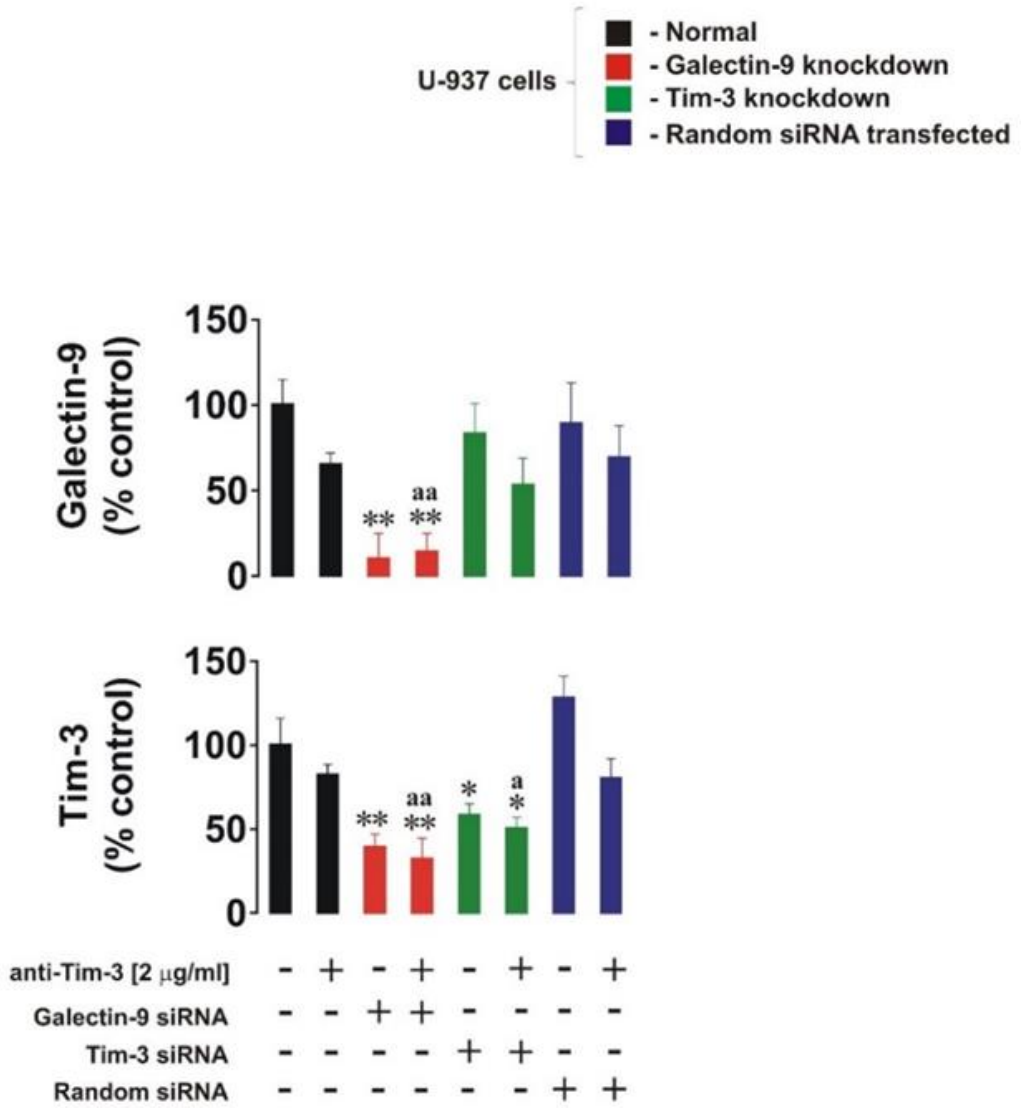

Figure 26 qRT-PCR analysis of galectin-9 and Tim-3 mRNA levels in U937 cells. *Non-treated normal (wild type), galectin-9 knockdown, Tim-3 knockdown and transfected with random siRNA U937 cells, as well as the same cells which underwent 4 h treatment with 2 μg/ml anti-Tim-3, were used. Total RNA was isolated and subjected to qRT-PCR analysis of Tim-3 and galectin-9 mRNA levels as outlined in Materials and Methods. Data are mean values ± SEM of eight independent reactions; * – $p < 0.05$; ** – $p < 0.01$ vs. control; ^{a} – $p < 0.05$; ^{aa} – $p < 0.01$ vs. anti-Tim-3.*

Galectin-9 knockdown reduced the levels of Tim-3 and galectin-9 both intracellularly and on the media (Figure 25A). It also upregulated stimulatory phosphorylation of mTOR at the position S2448. This matches the upregulation of glycolysis and VEGF release, but the levels of methylglyoxal (MGO) did not increase significantly (Figure 25B). This indicates that the efficiency of glycolysis correlates with the activity of glycolytic enzymes, since MGO is spontaneously formed out of dihydroxyacetone phosphate when glycolytic enzymes are oversaturated. MGO catalyses glycation followed by generation of advance glycation end (AGE) products (Figure 14, pp.55). higher amounts of these products could be produced by cancer cells, since they are highly dependent on glycolysis.

The success of Tim-3 knockdown was confirmed by Western-blot (Figure 27) and qRT-PCR (Figure 26), similar to what was done for galectin-9.

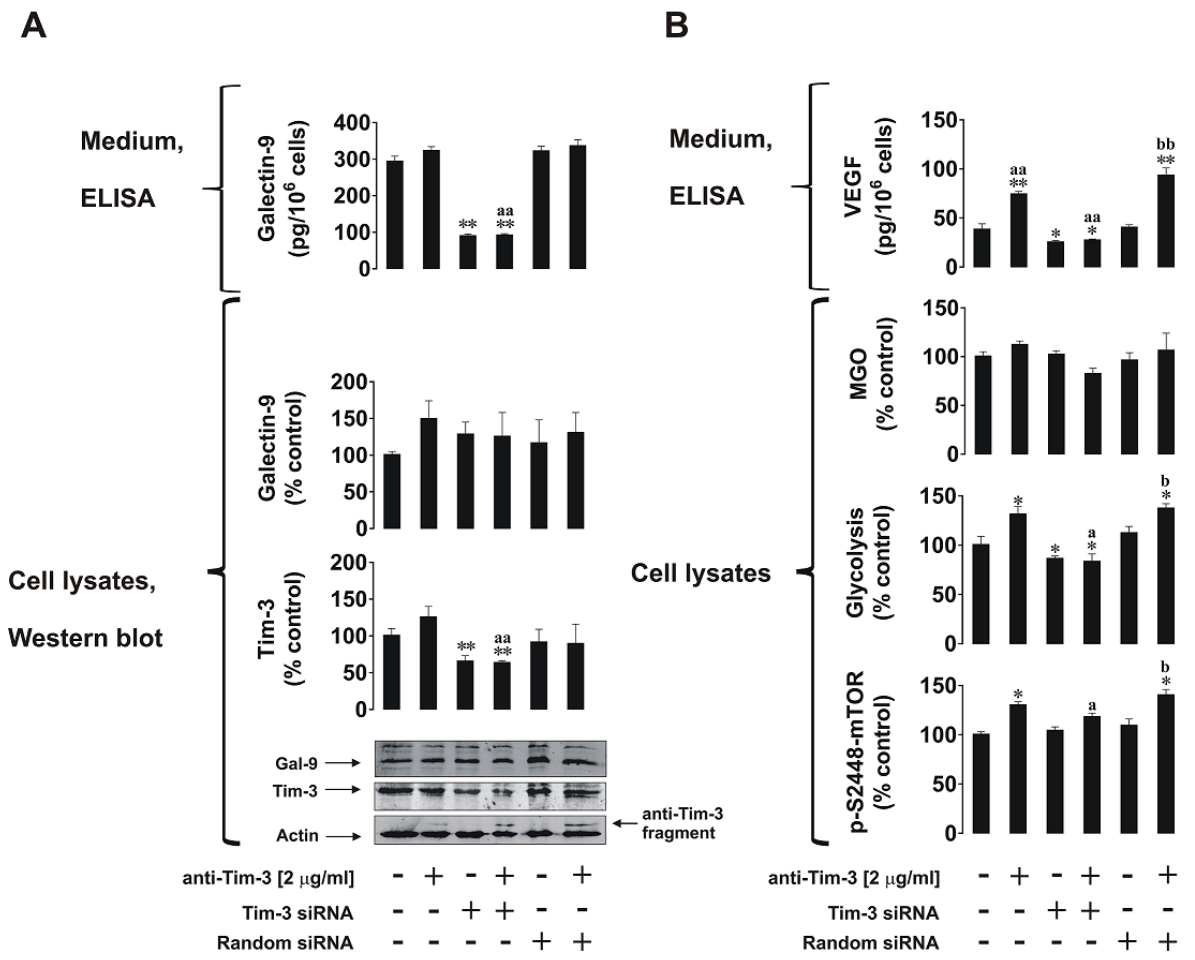

Figure 27 Tim-3 is required for galectin-9 secretion in human myeloid leukaemia cells. *Non-treated normal (wild type), Tim-3 knockdown and transfected with random si-RNA U937, as well as the same cells which underwent 4 h of treatment with 2 μg/ml anti-Tim-3 were used.* ***A.*** *Tim-3 and galectin-9 levels were measured using Western-blot and galectin-9 release was measured by ELISA;* ***B.*** *pS2448 mTOR intracellular levels, glycolysis, MGO and VEGF secretion. Images are from one experiment representative of three to five which gave similar results. Quantitative data are shown as means ± SEM of 3-5 individual experiments; *p < 0.05; **p < 0.01 vs. control; $^{a}p < 0.05$; $^{aa}p < 0.01$ vs. anti-Tim-3; $^{b}p < 0.05$; $^{bb}p < 0.01$ vs. random RNA.*

There was a significant reduction in Tim-3 levels, but levels of Tim-3/galectin-9 complex and intracellular galectin-9 did not became lower. In the meanwhile, levels of galectin-9 secretion suffer a dramatic reduction, suggesting that Tim-3 is required for galectin-9 secretion (Figure 27A).

The level of mTOR phosphorylation in the position S2448 decrease. Also, there was downregulation of glycolysis and VEGF release. The levels of MGO remain about the same, suggesting that glycolytic efficiency was not affected (Figure 27B)

4.2.1.3 Tim-3 is a specific trafficker for galectin-9 in certain cell types

It is known that several cell types are able to produce galectin-9 but not all of these express Tim-3. Therefore, we decided to compare the capability of primary human AML cells and primary human CLL cells to produce galectin-9. Both, AML and CLL cells, secreted detectable amounts of galectin-9. In addition, the amount of secreted galectin-9 significantly increased in AML cells, when these were exposed for 4 h to 2 µg/ml anti-Tim-3. This value remained about the same in CLL cells (Figure 28A).

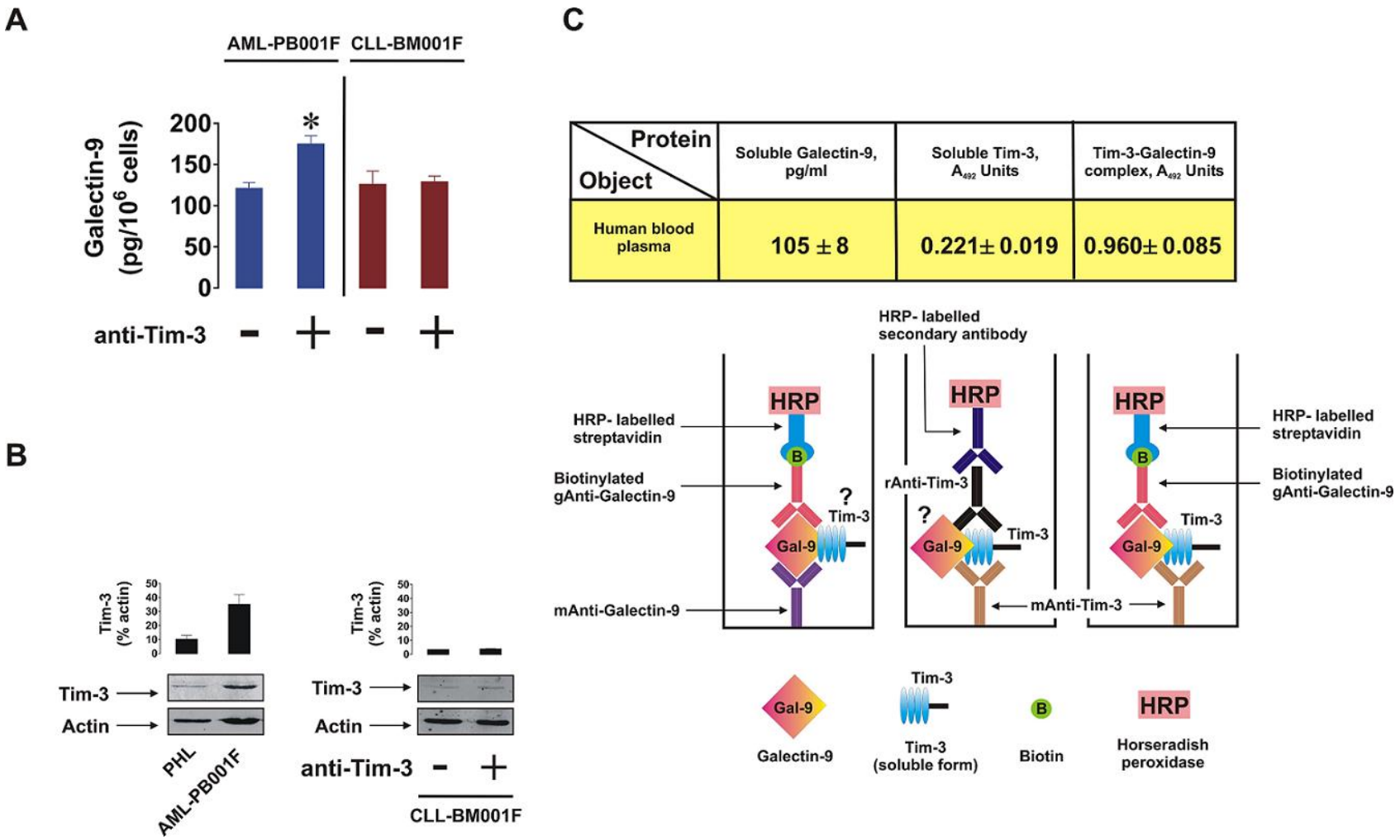

Figure 28 Levels of galectin-9 and Tim-3 in primary AML, CLL and PLs cells and blood plasma. A. *Galectin-9 levels, measured by ELISA, of non-treated and treated for 4 h with anti-Tim-3 primary human AML and CLL cells. Data represent mean values ±SEM of three induvidual experiments; *p < 0.05 vs. control.* ***B.*** *PLs (PHL in the figure), primary human AML and CLL cells analysed by Western-blot for Tim-3. Images are from one experiment representative of four which gave similar results. Data are mean values ±SEM of four individual experiments.* ***C.*** *Levels of galectin-9, soluble Tim-3 and Tim-3/galectin-9 complex from blood plasma of six healthy donors was subjected to ELISA. Data are mean values ±SEM of 3-5 individual experiments.*

Both PLs (showed as PHL in Figure 28B) and AML cells expressed Tim-3, being the amount expressed in AML cells much higher than the one expressed in PLs. On the other hand, CLL cells expressed almost undetectable amounts of Tim-3 (Figure 28B). As mention before, despite the fact that primary CLL cells express almost no Tim-3, they still release gelctin-9, which means that these cells have a different trafficker for galectin-9.

We also analysed by ELISA the amount of Tim-3 and galectin-9 on blood plasma of healthy donors. Both galectin-9 and Tim-3 were detected in these samples (Figure 28C). In these samples was even possible to detected galectin-9 when we capture Tim-3 on the ELISA plate, but when we added intact culture medium or galectin-9 standards instead of the samples no signal was detected. This means that a complex formed by non-cell-associated soluble Tim-3 and galectin-9 is present in blood plasma of healthy donors.

4.2.2 Discussion

It was previously shown that galectin-9 specifically interact with Tim-3, promoting mTOR pathway and forming and autocrine loop with Tim-3 in human AML cells (Kikushige *et al.*, 2015; Prokhorov *et al.*, 2015). Also, galectin-9 specifically interacts with NK and cytotoxic T cells, impairing their ability to attack and kill leukaemia cells (Golden-Mason *et al.*, 2013; Wang *et al.*, 2007; Khaznadar *et al.*, 2014).

The results presented in this chapter show that human myeloid leukaemia cells express and secrete galectin-9 (Figure 22, Figure 24, Figure 26 and Figure 29), being the production of galectin9 upregulated by pro-inflammatory stimulation (LPS) and growth factors (SCF) action.

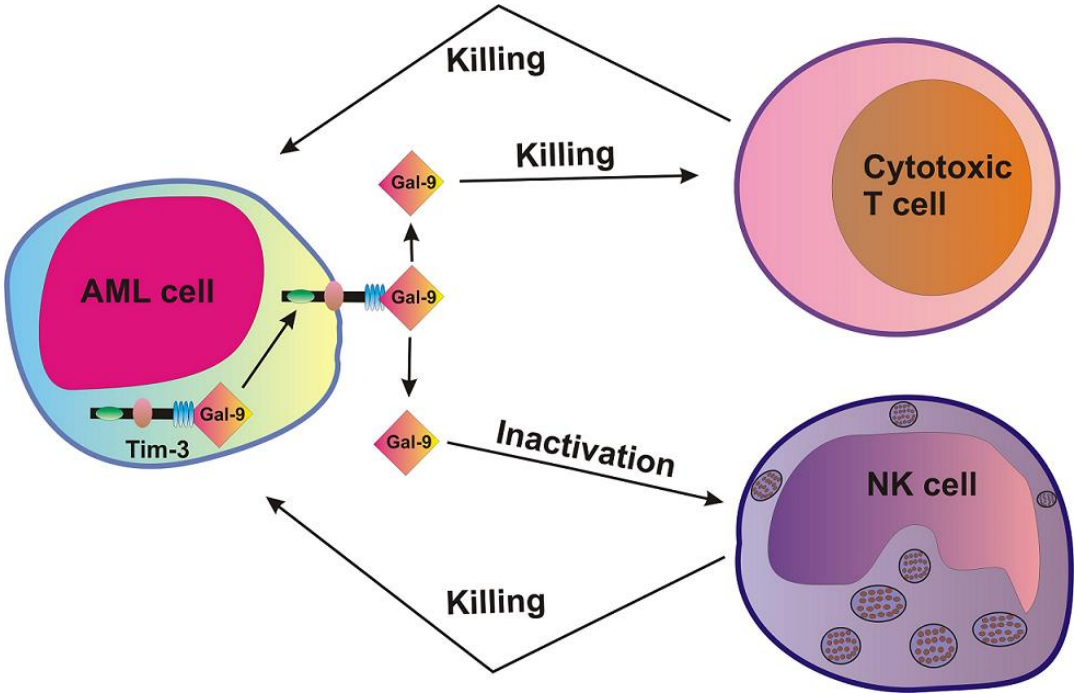

Figure 29 Secretion of galectin-9 in a Tim-3 dependent manner in human AML cells potentially can impair anti-leukaemic activity of cytotoxic T cells and NK cells.

It is possible to see that the secretion of galectin-9 is dependent on Tim-3, since knockdown of this receptor in U937 cells, decrease dramatically this process without affecting galectin-9 intracellular levels (Figure 27A). On the other hand, when we performed galectin-9 knockdown, Tim-3 level had a non-significant decrease (Figure 25A) but levels of Tim-3 mRNA were significantly downregulated (Figure 26). This suggests that transcription of Tim-3 gene depends on intracellular levels of galectin-9. Apparently, galectin-9 levels influence Tim-3 expression in a genomic level while Tim-3 protein controls the secretion of galectin-9.

Recently it was shown that **a** **d**esintegrin **a**nd **m**etaloproteases (ADAM) 10 to 17 controls shedding of Tim-3 from the cell surface in HEK-293 cells and human primary $CD14^+$ monocytes (Moller-Hackbarth *et al.*, 2013a). This suggests that Tim-3 might be shed when it is complexed with galectin-9, being a fragment of Tim-3 shed together with full length galectin-9 from the membrane. This may explain the fact that LPS reduces Tim-3 surface expression (Ma *et al.*, 2013; Moller-Hackbarth *et al.*, 2013a), knowing that our results show LPS-induced

upregulation of galectin-9 levels and the results showed on the previous chapter demonstrated that Tim-3 production is not reduced by LPS but its surface presence is affected. This may be due an increase of intracellular galetin-9 levels leading to increase in galectin-9 secretion together with Tim-3.

The shedding of the complex may be done by ADAM10/17 or other proteolytic enzymes. To support the shedding of Tim-3-galectin-9 complex there is evidence that HIV-1 infection leads to increase of soluble Tim-3 and galectin-9 in blood plasma (Clayton *et al.*, 2015; Tandon *et al.*, 2014) and also PMA upregulates galectin release in Jurkat T cells (Chabot *et al.*, 2002b) and the Tim-3 expression/externalisation (Yoon *et al.*, 2011) and proteolytic shedding (Moller-Hackbarth *et al.*, 2013a). The Matrix metalloproteinase inhibitor BB-94 was able to block the PMA-induced galectin-9 release in Jurkat T cells, suggesting that proteolysis is probably involved in shedding of Tim-3-galectin-9 complex.

Our results also show that CLL bone marrow mononuclear cells secrete galectin-9 but have low amounts of Tim-3 (Figure 28A and B), suggesting that Tim-3 is a cell type-specific trafficker of galectin-9 in AML cells, while other types may use other galectin-9 specific proteins that can be externalised. To support this, there is evidence that galectin-9 may cause Tim-3 independent effects in lymphoid cells (Golden-Mason *et al.*, 2013; Moritoki *et al.*, 2013).

We were able to detect galectin-9and soluble Tim-3 in blood plasma from healthy donors. Also, anti-Tim-3 detection antibody originate a positive signal to visualise that product capture by anti-galetin-9 antibody, indicating that Tim-3-galectin-9 complex is present in human blood plasma (Figure 28C).

Altogether, the results presented in this chapter, indicate that galectin-9 secretion requires Tim-3 in AML cells and this mechanism may be used to impair anticancer activities of cytotoxic T cells and NK cells, allowing malignant blood cells to escape immune attack (Figure 29). The decreased of effects like efficient glycolysis and VEGF production (Figure 25A). As shown on the previous chapter and previous work of our lab (Prokhorov *et al.*, 2015), in myeloid cell lines and PHL, the activity of mTOR pathway is always lower than in primary AML cells. This may be due externalisation of the complex in AML cells (Figure 24).

In this case, the amounts of galectin-9 levels inside that cells are lower, due to the externalisation of the Tim-3-galection-9 complex, which can initiate signalling events before further modification or proteolytic shedding (Figure 30).

Tim-3 and galectin-9 seem to be able to be promising therapeutic targets for a possible cure for AML. Absence of the autocrine loop form by these two proteins and timely capture and inactivation of biological active galectin-9 may decrease the ability of AML cells to escape immune attack by impairing anticancer activities of NK and Cytotoxic T cells. This can lead to the natural eradication of cancer cells.

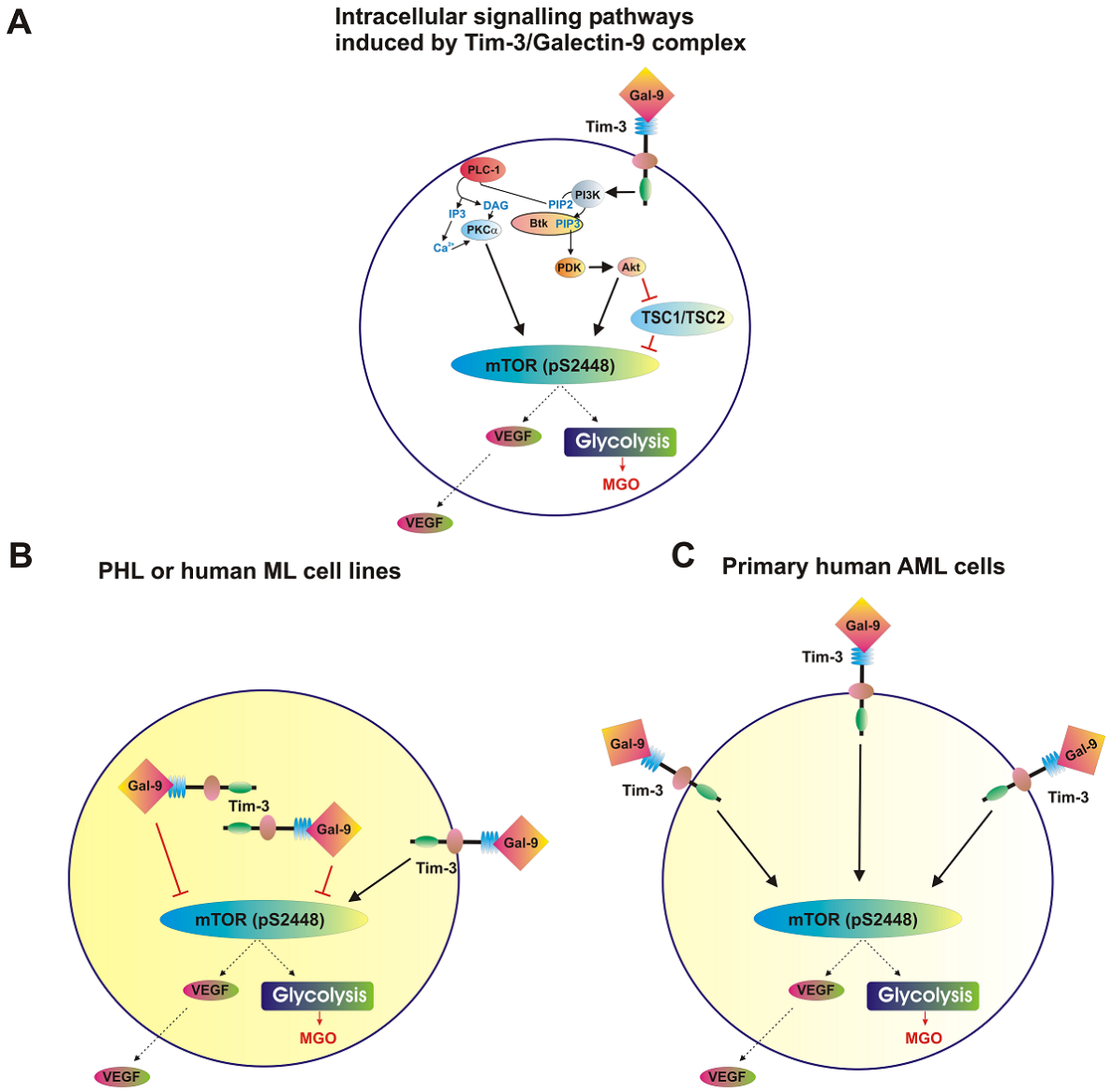

Figure 30 Distribution of Tim-3-galectin-9 complex and its effects in healthy and malignant human leukocytes. A. *intracellular signalling pathways induced by Tim-3-galectin-9 complex* ***B.*** *Tim-3-galectin-9 complex distribution and its effects in PHL and human myeloid leukaemia cell lines (THP-1 and U937).* ***C.*** *Tim-3-galectin-9 complex distribution and its effects in primary human AML cells.*

4.3 Expression of functional neuronal receptor Latrophilin 1 in human acute myeloid leukaemia cells

Recently, latrophilin-1 (LPHN1) was reported to be found in some malignant cells like non-small cell lung cancer and is implicates in its invasive character (Hsu *et al.*, 2009). LPHN1 is an adhesion G-protein-couple receptor that participates in the control of calcium signalling and exocytosis in vertebrate neurons and neuroendocrine cells (Silva and Ushkaryov, 2010) and is reported as absent from blood. This is the main brain receptor for latrotoxin.

Latrotoxin is a black widow (*Latrodectus sp)* spider toxin, which stimulates LPHN responses and thus induces neuronal exocytosis in vertebrates (Silva and Ushkaryov, 2010)

Knowing that exocytosis is an important process in myeloid cell haematopoiesis, especially when they undergo malignant transformation and energy resources are very limited, we decided to investigate if this receptor can be found in myeloid cells.

4.3.1 LPHN1 expression and activity in human myeloid leukaemia cell lines

In order to check the expression of LPHN1 in human myeloid cells, two different cell lines, U937 and THP-1, were used. Both cell lines were stimulated with LPS, LTX or a combination of both.

By using Western-blot analysis it was possible to verify that both cell lines, THP-1 and U937, expressed LPHN1. The levels of LPHN1 expression significantly increased upon treatment with LPS but not with LTX. When a combination of LPS and LTX was used, the same results of LPS alone were obtained (Figure 31 and Figure 32).

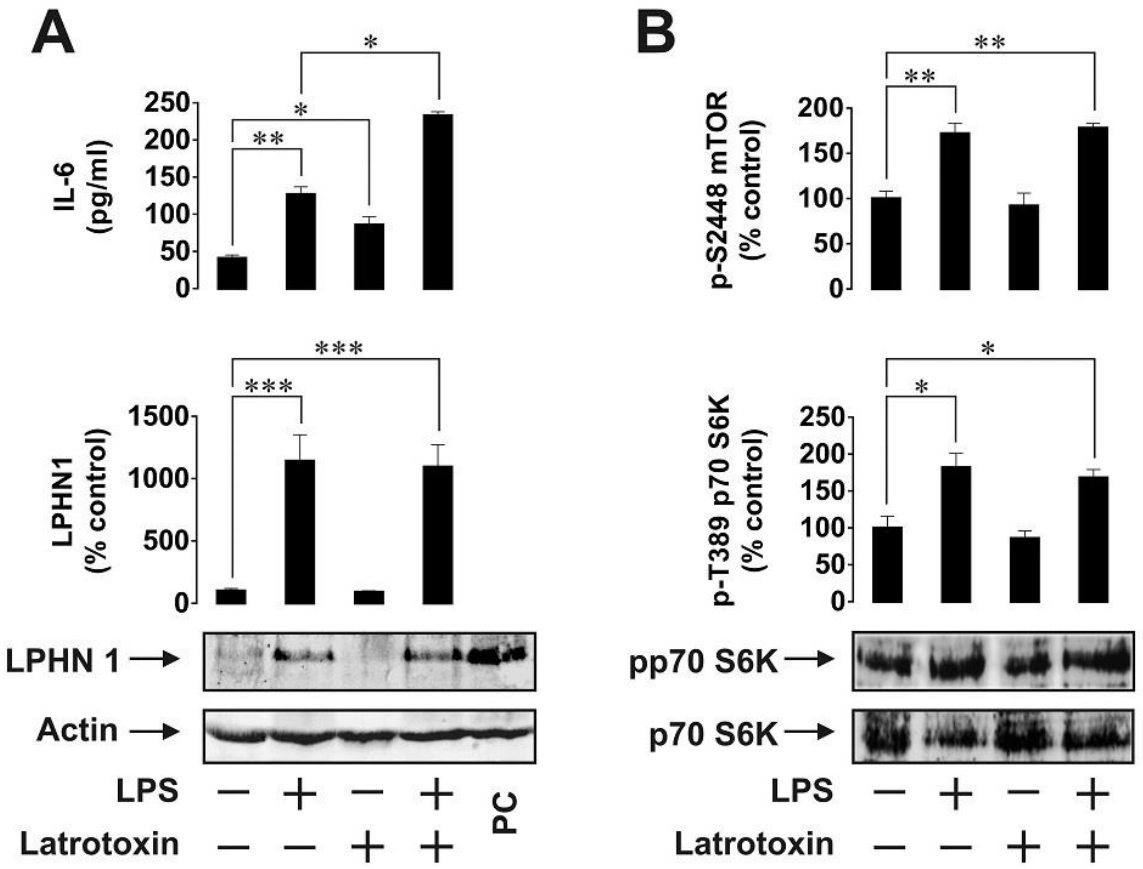

Figure 31 Expression and activity of LPHN1 in U937 cells. *U937 cells were exposed to 1 µg/ml LPS, 500 pM LTX or a combination of both.* ***A.*** *IL-6 release was measured by ELISA and LPHN1 proteins levels were analysed by Western-blot using mouse brain extract as positive control (PC);* ***B.*** *pS2448 mTOR was detected by ELISA and pT389 p70 S6K1 using Western-blot. Western-blot images show one experiment representative of six individual experiments, which gave similar results. Quantitative data are shown as means ± SEM; *p < 0.05; **p < 0.01; ***p < 0.01.*

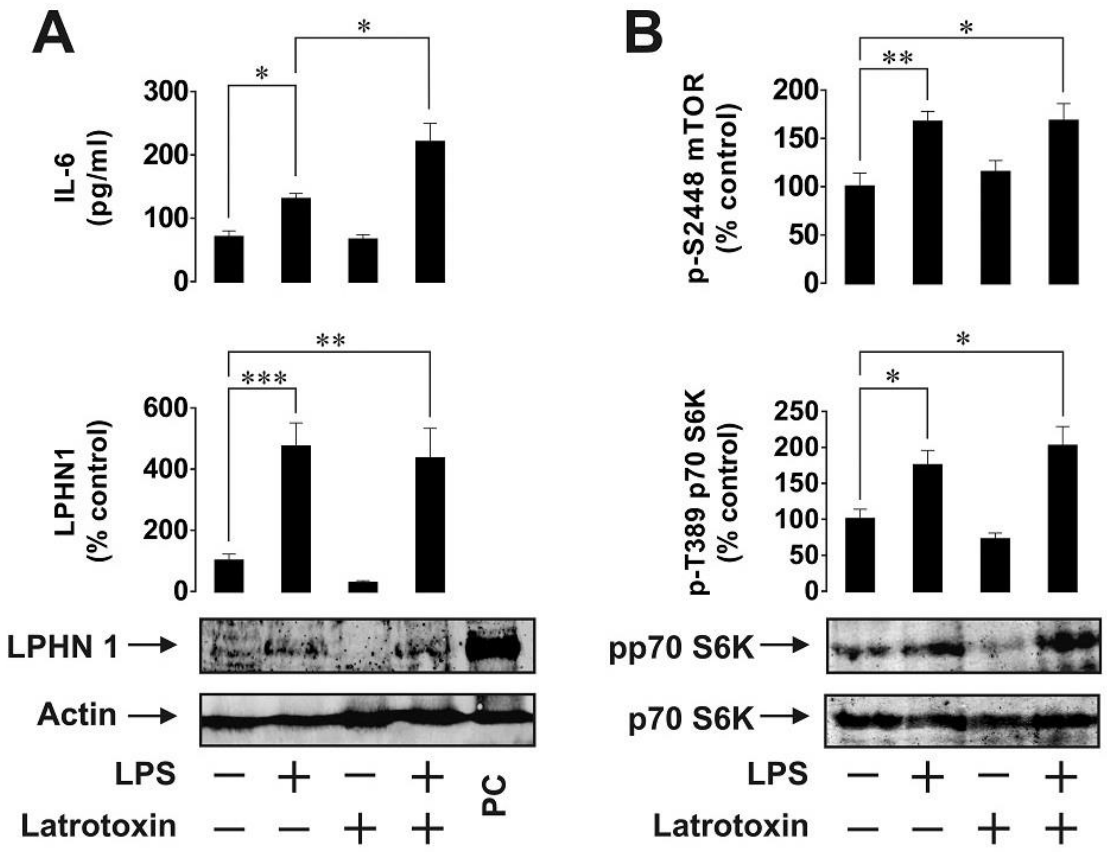

Figure 32 Expression and activity of LPHN1 in THP-1 cells. *THP-1 cells were exposed to 1 µg/ml LPS, 500 pM LTX or a combination of both.* ***A.*** *IL-6 release was measured by ELISA and LPHN1 proteins levels were analysed by Western-blot using mouse brain extract as positive control;* ***B.*** *pS2448 mTOR was detected by ELISA and pT389 p70 S6K1 using Western-blot. Western-blot images show one experiment representative of six individual experiments, which gave similar results. Quantitative data are shown as means ± SEM; *p < 0.05; **p < 0.01; ***p < 0.01.*

Similar to what happened to the level of LPHN1 expression, LTX did not stimulated the release of IL-6 but LPS did. The combination of LTX and LPS increase the release of IL-6 to values two times higher than LPS alone (Figure 31A and Figure 32A). LPS, but not LTX, also activated the mTOR pathway, increasing the value of mTOR phosphorylation at the position S2448 and phosphorylation of its substrate p70 S6K1 at position T389 to values almost two times higher (Figure 31B and Figure 32B).

It is generally known that mTOR regulates many translational pathways, therefore, we hypothesised that this could be responsible for LPS-induced upregulation of LPHN1 expression. To test this hypothesis, we did 1 h of pre-treatment with two mTOR inhibitors, rapamycin and AZD2014, before stimulation with LPS. We also tested different times of stimulation with LPS, concluding that the increase in the expression of LPHN1 was higher after 24 h of stimulation than after 4 h and that this effect is more pronounce in THP-1 than in U937 (Figure 33).

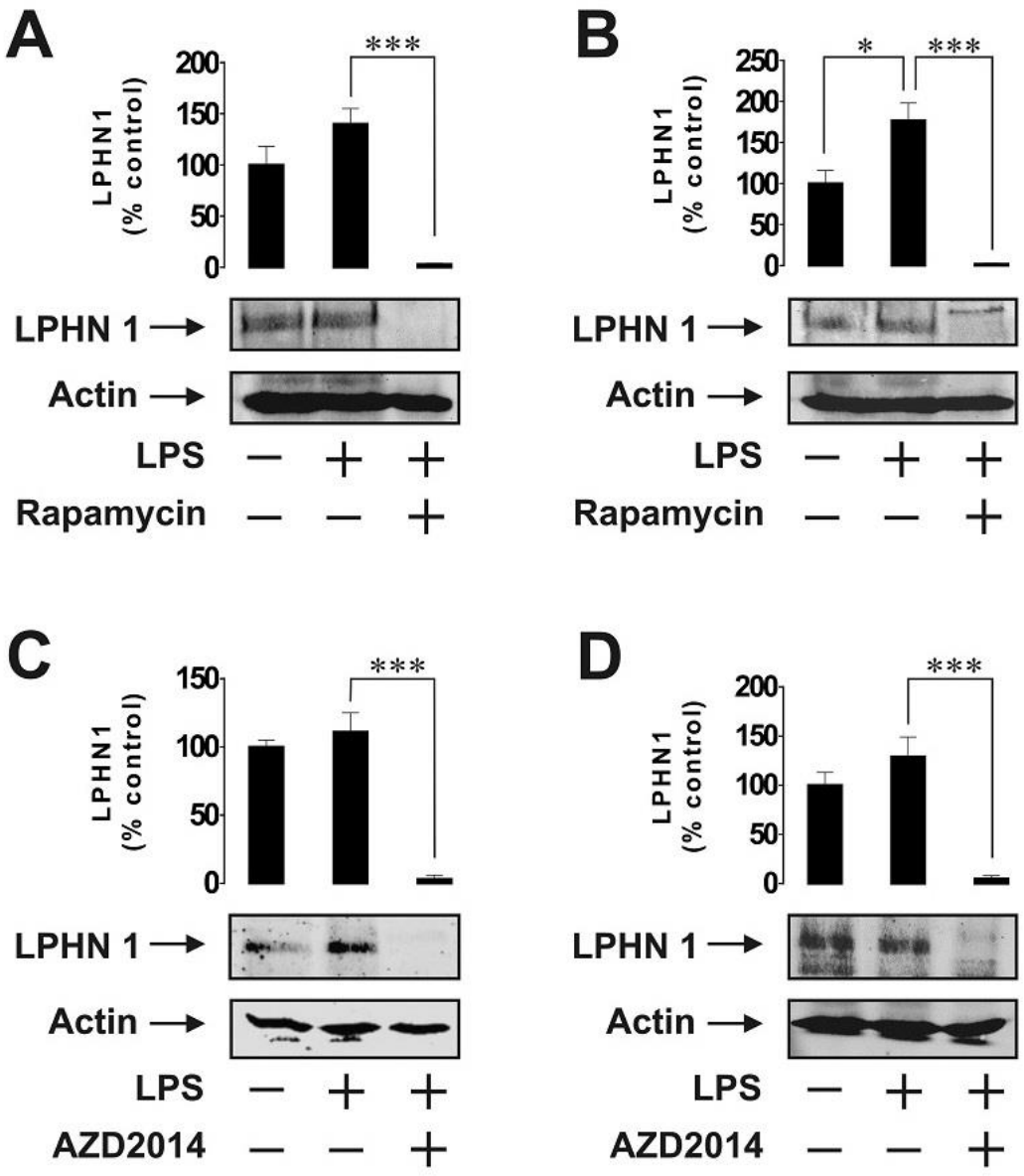

Figure 33 Expression of LPHN1 in U937 and THP-1 cells depends on mTOR. *LPHN1 expression was analysed using Western-blot;* ***A.*** *U937 treated with 1 µg/ml LPS for 4 h with or without 1 h of pre-treatment with 10 µM rapamycin;* ***B.*** *THP-1 treated with 1 µg/ml LPS for 4 h with or without 1 h of pre-treatment with 10 µM rapamycin;* ***C.*** *U937 treated with 1 µg/ml LPS for 4 h with or without 1 h of pre-treatment with 10 µM AZD2014;* ***D.*** *THP-1 treated with 1 µg/ml LPS for 4 h with or without 1 h of pre-treatment with 10 µM AZD2014. Western-blot images show one experiment representative of four individual experiments, which gave similar results. Quantitative data are shown as means ± SEM; *p < 0.05; **p < 0.01; ***p < 0.01.*

In both cell lines, both rapamycin and AZD2014 were able to fully blocked expression of LPHN1 (Figure 33) without affecting viability of the cells. This was verified by MTS cell viability test (data not shown).

4.3.2 Functional LPHN1 is expressed in human primary AML cells, but not in healthy leukocytes

After the obtained results in the AML cell lines, we proceed to test the expression of LPHN1 in primary human AML cells. These cells were exposed to LPS, LTX or a combination of both for 24 h. Similar to what happened in the cell lines, LPS was able to upregulate mTOR activation, by increasing phosphorylation of mTOR at the position S2448. It also upregulated IL-6 release. On the other hand, LTX did not have any effect on both processes (Figure 34). Combination of LPS and LTX was able to increase mTOR activation and IL-6 release more efficiently than LPS on its own (Figure 34).

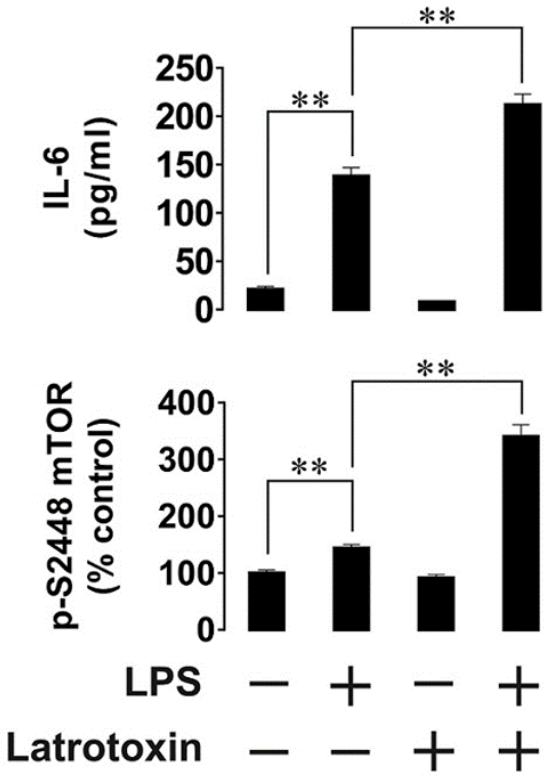

Figure 34 Effects of LPS and LTX on IL-6 exocytosis and mTOR activity in primary human AML cells. *Cells were exposed to 1 µg/ml LPS, 500 pM LTX or combination of both for 24 h. the release IL-6 and the mTOR phosphorylation at position S2448 was measured by ELISA. Data are the mean values ±SEM (n=6), *p < 0.05; **p < 0.01.*

In order to check if LPHN1 expression levels in AML-PB001F cells are control through mTOR pathway, cells were exposed to 4 h of LPS, SCF or anti-Tim-3 antibody. All stimuli were able to upregulate mTOR activation, being SCF the strongest stimuli (Figure 35A). This is due to high expression of kit receptor by these cells, like it was previous mention. Similar to what happen to mTOR activation, the levels of LPHN1 expression were significantly increased by all stimuli (Figure 35A).

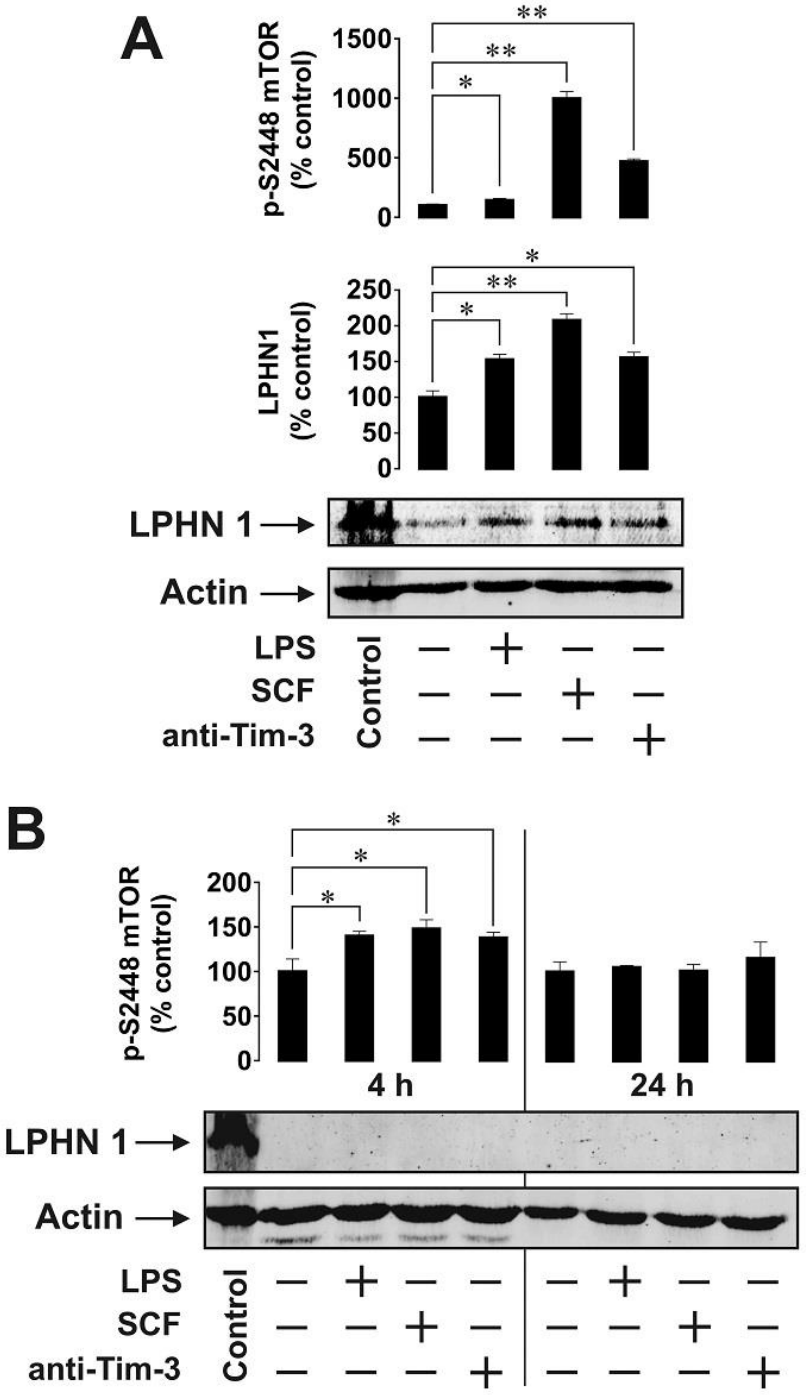

Figure 35 Primary human AML cells but not healthy primary human leukocytes express LPHN1. *LPHN1 protein levels were analysed by Western-blot using mouse brain extract as positive control and pS2448 mTOR was quantitated by ELISA.* ***A.*** *Primary AML-PB001F cells exposed for 4 h to 1 µg/ml LPS, 0.1 µg/ml SCF or 2 ug/ml anti-Tim-3;* ***B.*** *Healthy human primary leukocytes Primary AML-PB001F cells exposed for 4 or 24 h to 1 µg/ml LPS, 0.1 µg/ml SCF or 2 ug/ml anti-Tim-3. Western-blot images show one experiment representative of four individual experiments, which gave similar results. Quantitative data are mean values ±SEM (n=4) *p < 0.05; **p < 0.01.*

The same stimuli were tested in primary healthy leukocytes. After 4 h of incubation, no LPHN1 was detectable. Even increasing the stimuli time for 24 h it was not possible to detect LPHN1 expression (Figure 35B). These results showed the regulation of LPHN1 expression in human AML cells, but not in healthy primary human leukocytes.

4.3.3 Discussion

The results obtained, show that human AML cell lines (U937 and THP-1) express detectable amounts of functional LPHN1 protein, being its expression dependent on the mTOR pathway. LTX, a specific LPHN1 agonist (White *et al.*, 1998), increased LPS-induced exocytosis of IL-6 in both cell lines. The production of IL-6 depends in mTOR (Schreml *et al.*, 2007), but in this case that activity of mTOR was not upregulated by LTX.

Since it is known that the wild type of LTX used in this experiments forms Ca^{2+}-permeable pores in the cell membrane expressing toxin receptors (Volynski *et al.*, 2003), these pores may induce LPHN1-independent exocytosis. But LTX on inserts itself into the membrane after binding the receptor and this will stimulate LPHN1, leading to exocytosis (Volynski *et al.*, 2003; Capogna *et al.*, 2003). Our results showed that LTX only stimulates exocytosis in LPHN1-expressing cells (Figure 31, Figure 32 and Figure 34). A mutant LTX^{N4C}, that does not form pores, was tested and it induced similar results regarding exocytosis of IL-6 in cell lines, confirming that LPHN1 has an active role in its secretion.

Interestingly, when U937 and THP-1 cells were pre-treated with mTOR inhibitors before stimulation by LPS, the expression of LPHN1 was totally abolished (Figure 33). This suggests that LPHN1 expression is fully dependent in the mTOR pathway (Figure 31B and Figure 32B), that is further regulated by LPS. Extra activation of mTOR brings a substantial increase in the amount of expresses LPHN1.

Since it is known that cell lines and primary cells differ in terms of biological activities and protein expression, we checked if the observations made in cell lines can be seen in primary cells. The results obtained did not differ from the previous ones regarding detectable LPHN1 expression and its regulation in response to mTOR stimuli (LPS, SCF and anti-Tim-3).

As previous seen the stimulation with LTX lead to high increase in the release of LPS-induced IL-6. On the other hand, unlike cell lines, LTX upregulates LPS-induce mTOR-activating phosphorylation in primary AML cells. This is probably due to low expression of TLR4, LPS receptor, in primary AML cells as reported by the supplier. In this case, only some mTOR will be activated by LPS while majority will remain phosphorylated creating the possibility of phosphorylation through LPHN1-induced signalling. In cell lines where TLR4 expression levels are higher, probably there is not a sufficient scope for further mTOR activation by LTX. This implies a functional integration of LPHN1 into the AML signalling machinery (Akira and Takeda, 2004; Sumbayev, 2008) (Figure 36).

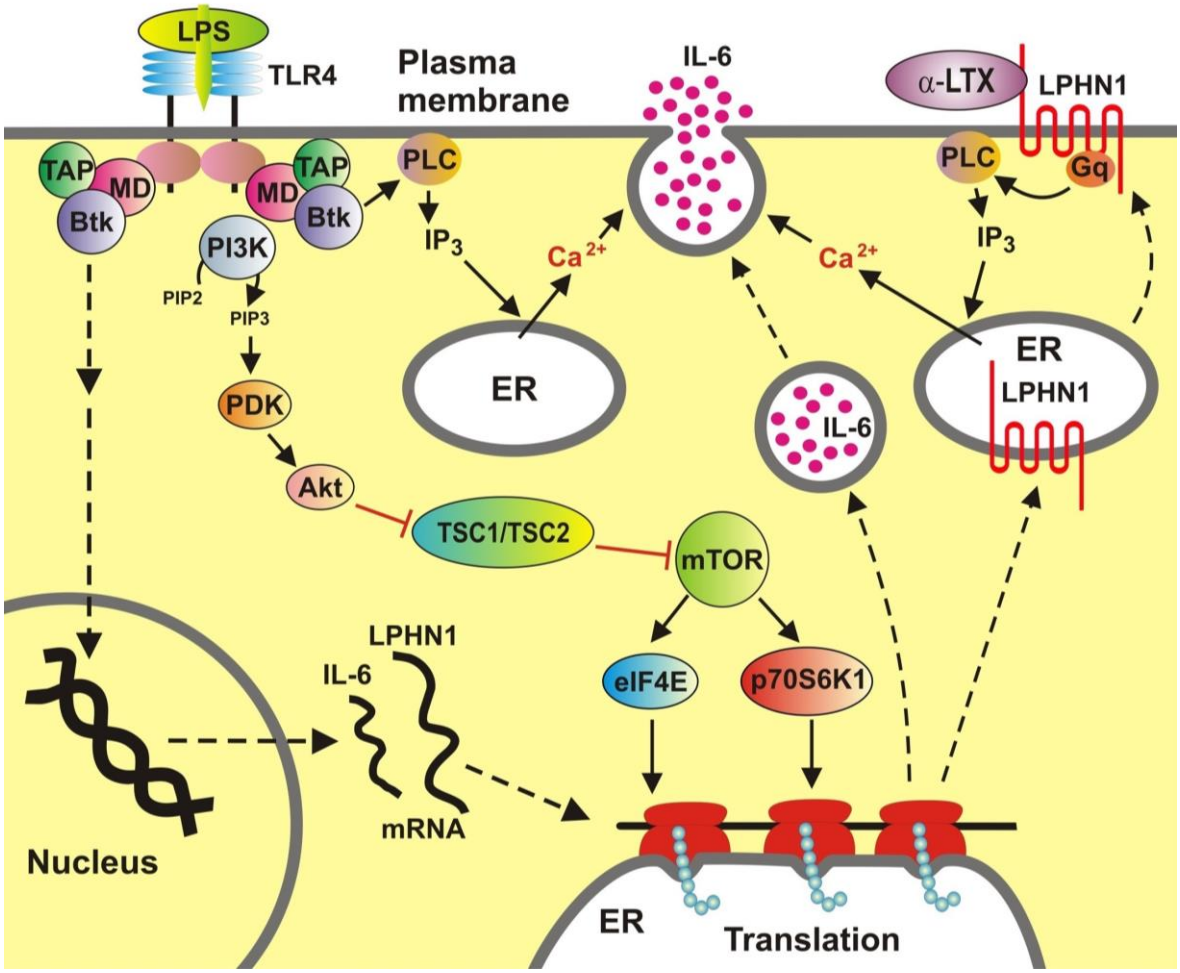

Figure 36 Functional integration of LPHN1 into AML cell signalling machinery. *LPHN1 transcription and translation is induced in AML cells. LPS upregulates LPHN1 transcription and triggers TLR4-mediated activation of the mTOR pathway, which increases translation of LPHN1 and IL-6. In addition, both LPS (through TLR4 and Btk) and LTX (through LPHN1 and Gq) activate PLC, which produces IP_3, leading to release of Ca^{2+} from the ER. Increased cytosolic Ca^{2+} triggers exocytosis of IL-6.* ***Abbreviations:*** *Btk, Bruton's tyrosine kinase; MD, myeloid differentiation factor 88; TAP, Toll-like receptor intracellular TIR domain-associated protein; PI-3K, phosphatidylinositol 3-kinase; PDK, phosphatidylinositol-3-phosphate-dependent kinase; IP_3, inositol trisphosphate; PLC, phospholipase C; Gq, Gαq subunit of a heterotrimeric G protein; TSC1/TSC2, tuberous sclerosis proteins 1 and 2; eIF4E, eukaryotic translation initiation factor 4E; p70S6K1, mTOR-dependent S6 kinase 1; ER, endoplasmic reticulum.* ***Symbols****: ↓activation; ⊥ inactivation; dotted lines, indirect activation involving multiple steps.*

We also used PHL and observed that these cells do not express ay LPHN1, even after stimuli that showed positive effects in AML cells (LPS, SCF and anti-Tim-3). This shows that expression of functional LPHN1 is specific in leukaemia cells.

LPHN1 is important to the survival of malignant leukocytes and also for the release of growth factors and cytokines like VEGF and IL-6. This requires efficient exocytotic machinery and means of controlling and stimulating exocytosis. According to this results LPHN1 can be consider a new biomarker for AML diagnosis, since contrarily to what happens to most existing leukaemia biomarkers, it is only expressed by malignant cells. It could also be explored as new target for anti-leukaemia therapy and drug delivery.

4.4 A fundamental molecular pathway controlling immune escape of human acute leukaemia cells

4.4.1 Tim-3 and Tim-3-galectin-9 complex are differentially shed from the cell surface

It was previously showed that Tim-3 and maybe the complex Tim-3-galectin-9 are shed from cell surface (Moller-Hackbarth *et al.*, 2013a; Chabot *et al.*, 2002b). Also, we previously demonstrated, in this work, that this complex is present in human blood plasma.

We investigated medium used to culture THP-1 cells with or without 16 h of exposure to 100 nM of PMA, that is known to activated proteolytic shedding of Tim-3 (Moller-Hackbarth *et al.*, 2013b), and we immunoprecipitated Tim-3 (as described in Methods and Materials, section 3.7.3). When the galectin-9 specific antibody was used, we detected a band around 32 kDa, a specific galectin-9 band (this is the molecular weight of galectin-9) and another band was detected at 52 kDa (Figure 37A).

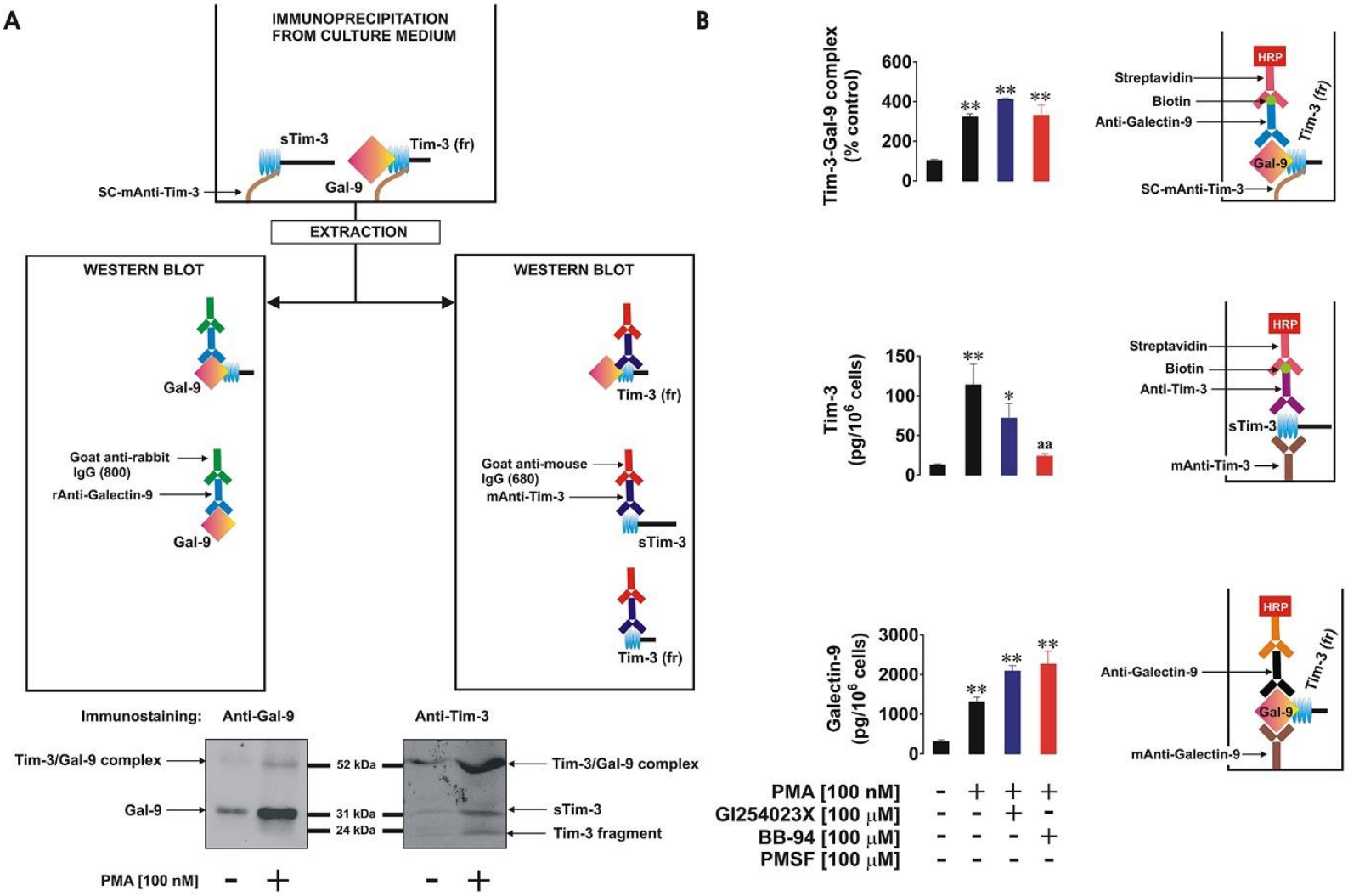

Figure 37 Free galectin-9-bound Tim-3 is shed differentially from the cell surface. *THP-1 cells were pre-treated with 100 mM PMA for 16 h and, after medium exchange, they were exposed to GI254023X (ADAM10/17 inhibitor) and BB-94 (matrix metalloproteinase inhibitor) for 4h.* ***A.*** *Western-blot characterisation of galectin-9 and Tim-3 variants (20 kDa fragment (Tim-3 (fr)) and 33 kDa (soluble Tim-3)) was done using medium from the 4 h of inhibitor treatment.* ***B.*** *Detection of galectin-9, soluble Tim-3 and Tim-3-galectin-9 complex. Images are from one experiment representative of six which gave similar results. Quantitative data are mean values ±SEM (n=6) *p < 0.05; **p < 0.01 vs. control.*

When the anti-Tim-3 antibody was used we detected a specific band at 33 kDa (molecular weight of soluble Tim-3) and other at 20 kDa, that probably corresponds to a Tim-3 fragment shed together with galectin-9 and it was released from the complex during Western-blot procedure and probably is shed at a different cleaved site. With this antibody, a band at 52 kDa was also detected. Since the band at 52 kDa is detectable with both antibodies (Tim-3 and galectin-9 antibody), this probably corresponds to the Tim-3-galectin-9 complex (Figure 37A).

It was reported the Tim-3 may be shed from the cell surface by **a** **d**isintegrin **a**nd **m**etalloproteinase domain-containing proteins (ADAM) 10/17 (Moller-Hackbarth *et al.*, 2013a). So, we decided to investigate if this is associated with release of free Tim-3 and/or Tim-3-galectin-9 complex.

THP-1 cells were exposed to 100 nM PMA, protein expression inductor, for 16 h, after which the medium was replaced with medium containing 100 µM GI254023X (ADAM 10 and 17 inhibitor) or 100 µM BB-94, a matrix metalloproteinase inhibitor and incubated for 4 h. Tim-3 and galectin-9 level in the medium were measure by ELISA and soluble Tim-3-galectin-9 complex was capture with a single chain anti-Tim-3 antibody and detected using a biotinylated anti-gelctin-9 antibody.

The release of Tim-3, galectin-9 and Tim-3-galectin-9 complex was significantly upregulated by PMA (Figure 37B). GI254023X and BB-94 reduced soluble Tim-3 release but had no effect in the release of galectin-9 and Tim-3-galectin-9 complex. This indicates that the shedding of the complex from the cell surface occurs in a different way (Figure 37B).

The lysates from the above described treatment were also analyse by Western-blot. From these results, it is possible to see that despite the increased level of soluble Tim-3, galectin-9 and Tim-3-galectin-9 complex release upon treatment with PMA, the levels of respective cell-associated proteins decreased (Figure 38).

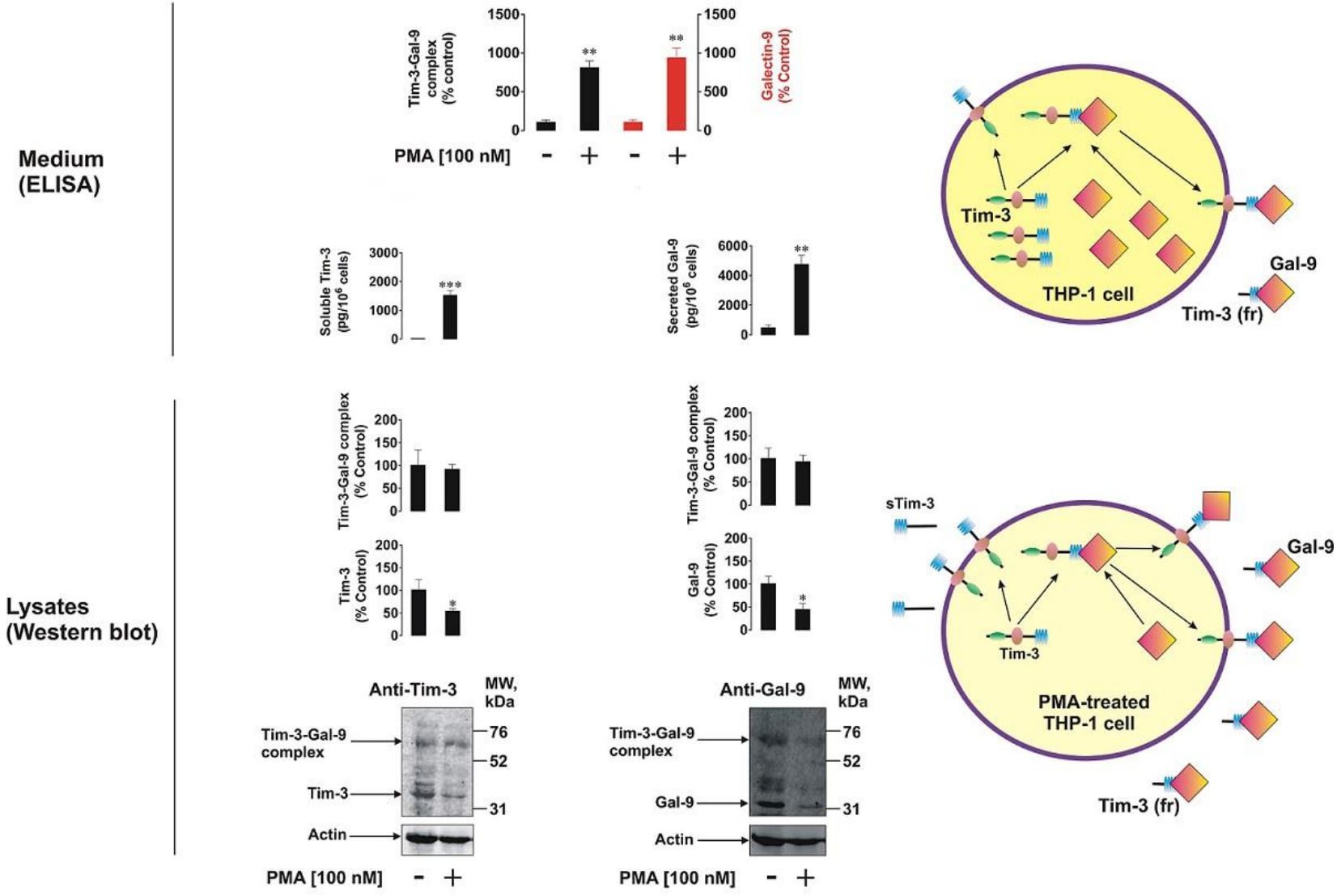

Figure 38 Tim-3, galectin-9 and complex Tim-3-galectin-9's production and/or release is activated by PMA. *THP-1 cells were treated with PMA for 16 h. Levels of Galectin-9 and Tim-3 were analysed by Western-blot and ELISA, levels of complex Tim-3-galectin-9 release by ELISA. The top bar diagram shows comparative analysis (express in % of control) of galectin-9 and complex Tim-3-galectin-9 levels release by PMA-treated and non-treated THP-1 cells. Images are from one experiment representative of three which gave similar results. Quantitative data are mean values ±SEM (n=3) *p < 0.05; **p < 0.01; ***p < 0.001 vs. control.*

A band arround 70 kDa was detectable by both anti-Tim-3 and anti-galectin-9 antibodies in all the assays (Figure 38). 70 kDa corresponds to the sum of the molecular weight of uncleaved Tim-3 and galectin-9, as stated in 4.2.1, and it indicated that a comples between full Tim-3 and galectin-9 is firtst formed, then it undergoes sheding and a soluble form of the complex (with molecular weight of 52 kDa) is released (Figure 38).

These results suggest that PMA induces productions an axocytosis of Tim-3-galectin-9 complex and that the complex and soluble Tim-3 underfo different proteolity sheding. These observations were confirm by co-localisation assays using confocal microscopy (Figure 39).

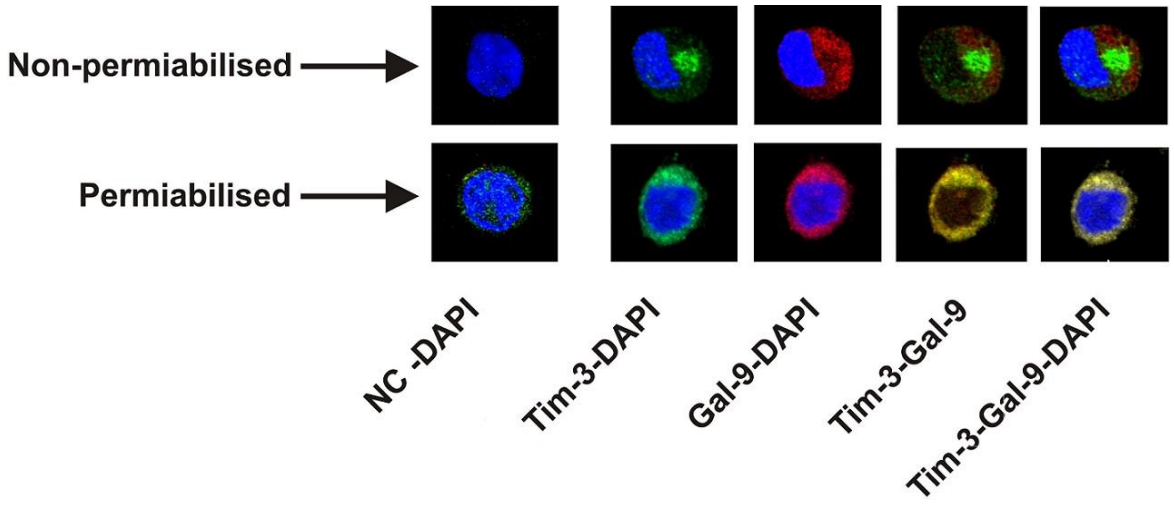

Figure 39 Co-localisation of Tim-3 and galectin-9 in PMA-activated THP-1 cells. *Co-localisation of Tim-3 and galectin 9 was analysed in THP-1 following 24 h of exposure to 100nM PMA using confocal microscopy. Images are from one experiment representative of six which gave similar results.*

The cells for co-localisation were prepared as described in materials and methods. Non permeabilised and methanol-permeabilised THP-1 human AML cells were analysed. Both galectin-9 and Tim-3 were present on the cell surface and in permeabilised cells there was clear evidence of co-localisation of both proteins. In non-permeabilised cells there is sectors full of Tim-3 or galectin-9 and no substantial co-localisation (Figure 39).

Since galectin-9 is soluble, it can only remain on the cell surface it is bound to its receptor, Tim-3. In non-permeabilised cells, no Tim-3 in galectin-9 sectors was detected. This can be explained, since its extracellular part is probably occupied by gal-9 and thus does not react with the antibodies (Figure 39). This indicates that Tim-3 is externalised on its own or acts as a trafficker for galectin-9, that does not have the signal domain required for secretion it requires a trafficker.

To confirm these findings, we analysed blood plasma samples from 98 AML patients and from 12 healthy donors. The levels of galectin-9 and Tim-3 were measure by ELISA and the obtained values were significantly increased in AML patients (Figure 40A, B, E and F).

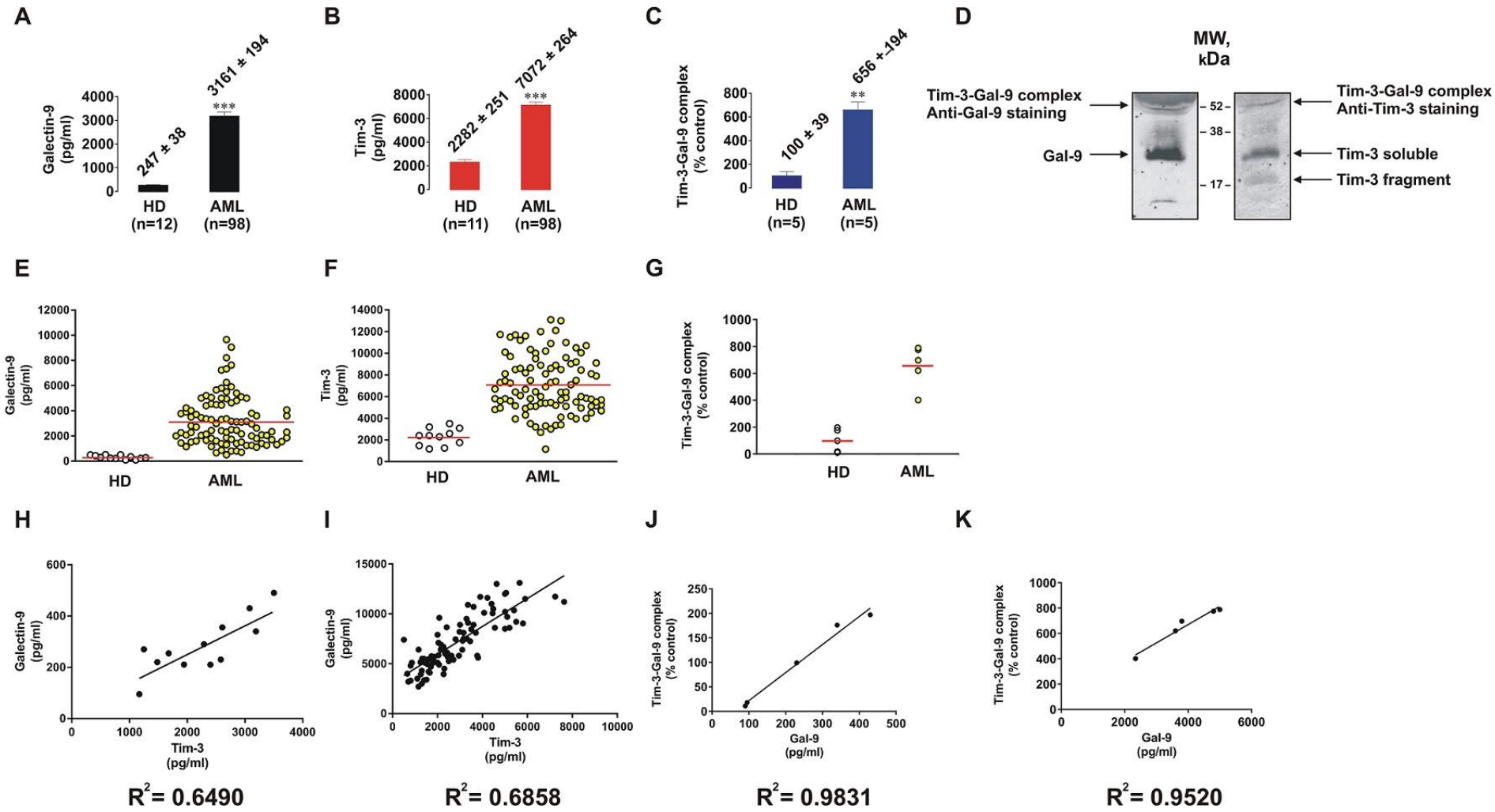

Figure 40 Levels of galectin-9 and soluble Tim-3 are highly increased in blood plasma of AML patients. A., B., E. and F. *Levels of galectin-9 and Tim-3 in blood obtained from healthy donors and AML patients, measured by ELISA.* ***C. and G.*** *Levels of Tim-3-galectin-9 complex in blood plasma of five randomly picked from healthy donors and AML patients measured by ELISA.* ***D.*** *Tim-3 and galectin-9 characterised by Western-blot in five randomly picked AML patients.* ***H. and I.*** *Correlation between Tim-3 and galectin-9.* ***J. and K.*** *Correlation between galectin-9 and Tim-3-galectin-9 complex. Images are from one experiment representative of five which gave similar results. Quantitative data are mean values ±SEM (n=3) *p < 0.05; **p < 0.01; ***p < 0.001 vs. control.*

From the studied groups of samples, we randomly selected five samples from AML patients and five from healthy donors and measured levels of Tim-3-galectin-9 complex by ELISA. As expected, the levels of Tim-3-galectin-9 complex in AML patients was increased, interestingly this increase was similar to the one observed in galectin-9 levels (Figure 40C and G).

Five blood plasma samples of AML patients were analysed by Western-blot to check levels of Tim-3 and galectin-9 (Figure 40D). Both soluble Tim-3 and galectin-9 were detected and also a band around 52 kDa (probably representing the soluble form of Tim-3-galectin-9 complex) was detectable by both anti-Tim-3 and anti-galectin-9 antibodies. A Tim-3 specific band was also detected around 20 kDa (Figure 40D). These results match the ones obtained in THP-1 cells, confirming that soluble Tim-3 and Tim-3-galectin-9 complex are probably shed from plasma membranes of AML cells in a different way.

These results show a clear evidence of a correlation between Tim-3 and galectin-9 level in the plasma of both healthy donors and AML patients and these correlation levels were very similar to each other (Figure 40H and I) suggesting a co-release of both proteins in these groups.

The biophysical properties of Tim-3, galectin-9 and Tim-3-galectin-9 complex were studied using synchrotron radiation circular dichroism (SRCD) spectroscopy at Diamond Light Source (Figure 15, pp58). In Figure 41A, is a schematic representation of the structural organisation of Tim-3 and galectin-9 as well as their interaction.

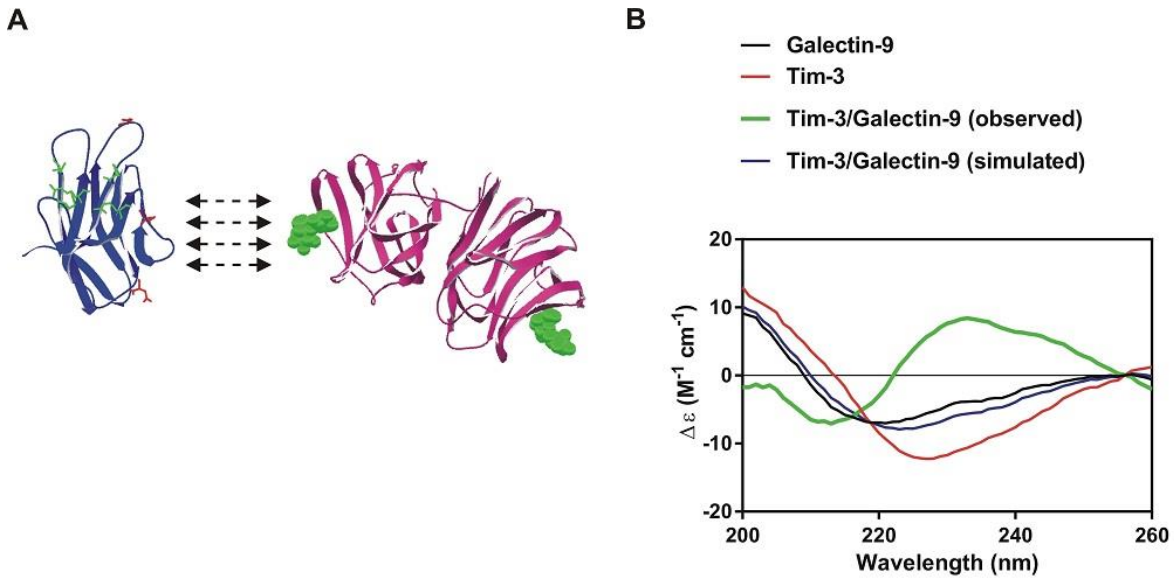

Figure 41 Interaction of Tim-3 with galectin-9 leads to major conformational changes increasing solubility of the protein complex. A. *The schematic structural models of Tim-3 extracellular domain (on the right) and galectin-9 (on the left). In Tim-3 structure, residues involved in galectin-9-independent binding are highlighted in green. Residues, which are potential targets for glycosylation, are highlighted in red. In galectin-9, sugar is located close to a sugar binding site that is shown in green.* ***B.*** *the SRCD spectroscopy of Tim-3, galectin-9 and Tim-3-galectin-9 interaction (both simulated and real curves are presented).*

Galectin-9 interacts with non-glycosylated Tim-3 with nanomolar affinity (Kd=2.8x10^8 M); the binding can be further strengthened by interaction of galectin-9 with glycosylated Tim-3 (Prokhorov *et al.*, 2015). Since the complex is detectable by Western-blot, that means that interaction between a lectin and a sugar is taking place.

SRCD spectroscopy was also done on galectin-9 and Tim-3 mixed at a molar ratio 1:1 (Figure 41B). In this mixture galectin-9 showed a CD spectrum significantly different from the simulated one. This indicates that the interaction of galectin-9 with Tim-3 causes significant conformational change of the proteins with a clear increase in β-strand component. This means that Tim-3 binding may change galectin-9 conformation, resulting in increased ability to interact with receptors in target cells. Since galectin-9 is a tandem protein with two sugar

binding domains, one may bind Tim-3 and the other may stay open for interactions with a receptor molecule associated with the plasma membrane of a target cell.

4.4.2 Latrophilin 1, PKC and mTOR-dependent translation play a crucial role in Tim-3 and galectin-9 production and secretion

We exposed THP-1 cells to 100 mM PMA or 250 pM LTX for 16 h, and the lysates were analysed by Western-blot. Both stimuli, PMA and LTX, downregulated the levels of intracellular Tim-3 and galectin-9, but not on a significant way. In the meanwhile, they significantly increase the level of mTOR phosphorylation at the position S2448, as measure by ELISA (Figure 42A and B).

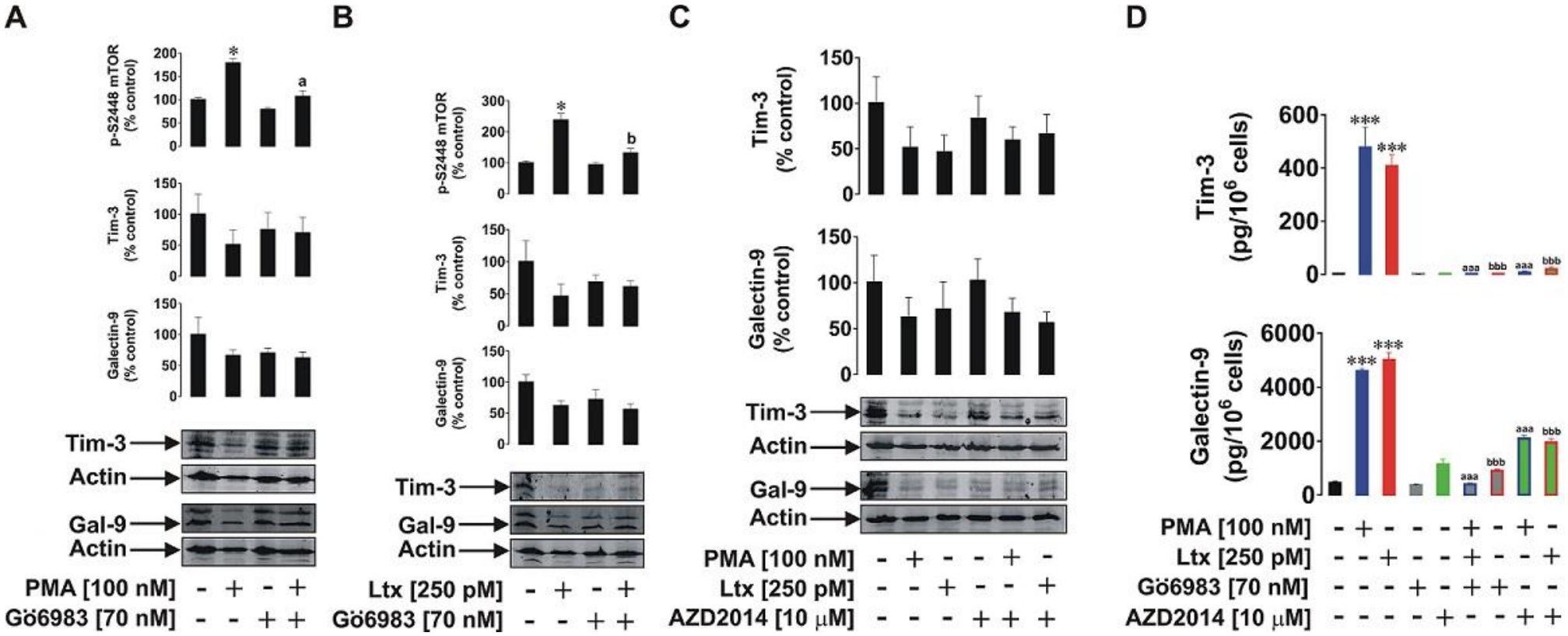

Figure 42 LPHN1, PKCα and mTOR pathways are involved in Tim-3 and galectin-9 production and secretion in AML cells. *THP-1 cells were treated with 100 nM PMA or 250 pM LTX with or without pre-treatment for 1 h Gö6983 (PKCα inhibitor) or AZD2014 (mTOR inhibitor).* ***A., B. and C.*** *Levels of Tim-3 and galectin-9 analysed by Western-blot.* ***D.*** *Levels of Tim-3 and galectin-9 analysed by ELISA. Images are from one experiment representative of three which gave similar results. Quantitative data are mean values ±SEM (n=3) *p < 0.05; **p < 0.01; ***p < 0.001 vs. control; $^{a}p < 0.05$; $^{aa}p < 0.01$; $^{aaa}p < 0.001$ vs. control and $^{b}p < 0.05$; $^{bb}p < 0.01$; $^{bbb}p < 0.001$ vs. control.*

When the cells were pre-treated with 70 mM Gö6983 (PKCα inhibitor), prior to treatment with PMA or LTX, there was attenuation of the stimulus-induced mTOR phosphorylation and downregulation of intracellular levels of Tim-3 and galectin-9. When Gö6983 was used without subsequent stimuli, the levels of mTOR phosphorylation and levels of Tim-3 and galectin-9 intracellular were the same as the control (Figure 42A and B).

The levels of release of soluble Tim-3 and galectin -9 were then analysed by ELISA. PMA and LTX promote release of soluble Tim-3 and galectin-9, but this was attenuated to basic levels by Gö6983. These results suggest that basic release of soluble Tim-3 and galectin-9 does not depend on PKCα and both PMA and LTX induce production of Tim-3 and galectin in THP-1 cells. (Figure 42D).

We also tested the inhibitor AZD2014 (mTOR inhibitor). THP-1 cells were pre-treated with 10 μM AZD2014 before exposure to PMA or LTX. This resulted in a reduction of levels of intracellular Tim-3 and galectin-9 and in the levels of release of the same proteins (Figure 42C and D). These results show that PMA and LTX-induced translation of Tim-3 and galectin-9 depends on the mTOR pathway.

To confirm the physiological role of LPHN1 in galectin-9 and Tim-3 release, we exposed THP-1 cells to FLRT-3 (a physiological LPHN1 ligand (Boucard *et al.*, 2014). 10 nM FLRT-3 induced a significant upregulation of galectin-9 and soluble Tim-3 release (Figure 43A) and PKCα activity in THP-1 cells (Figure 44A).

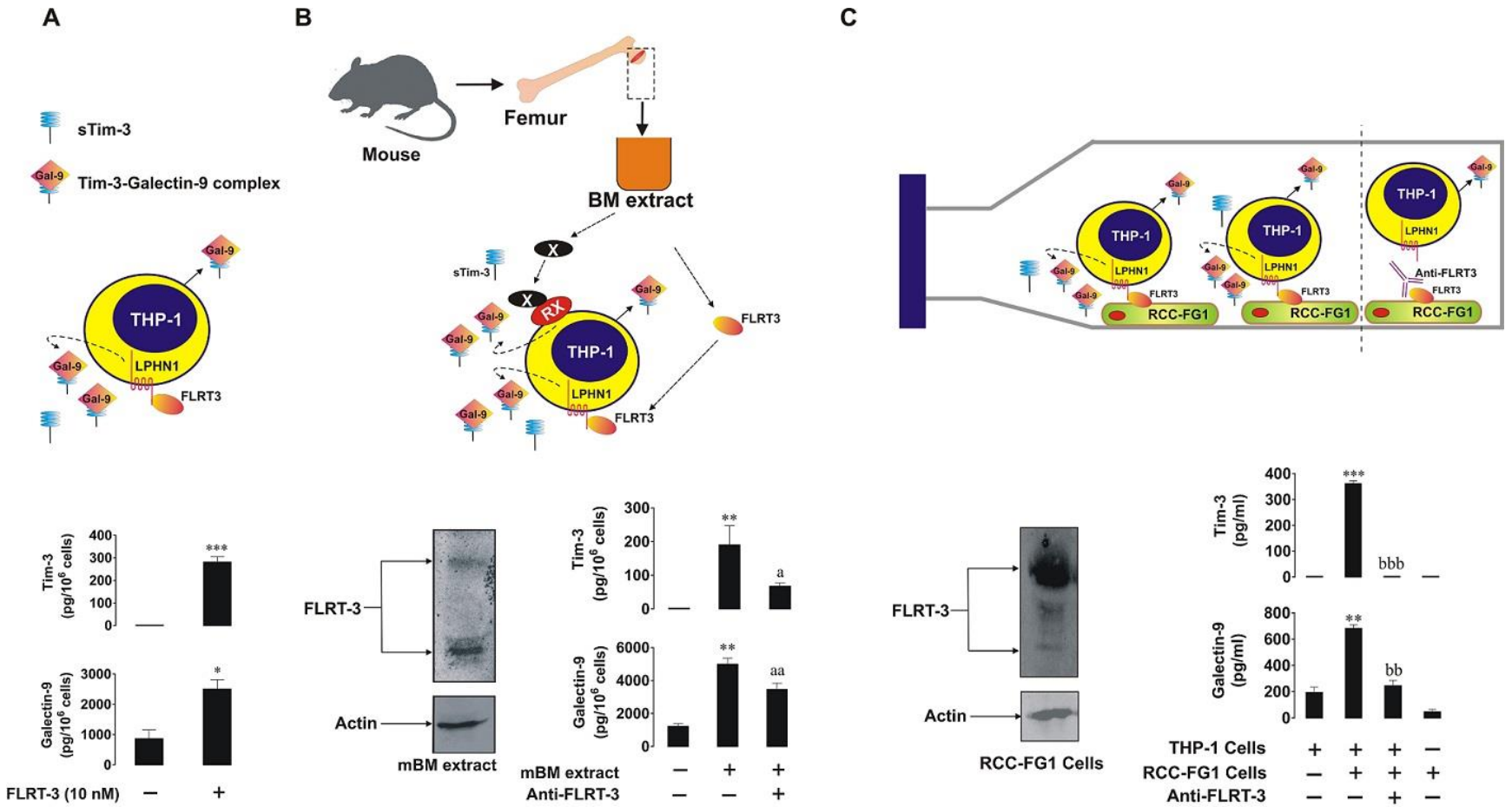

Figure 43 FLRT-3, a physiological ligand of LPHN1, induces galectin-9 and Tim-3 secretion. A. *THP-1 cells were exposed for 16 h to 10 nM human recombinant FLRT-3 followed by measurement of released Tim-3 and galectin-9 by ELISA.* ***B.*** *THP-1 cells were exposed to mouse bone marrow (mBM) extracts for 16 h with or without 1 h pre-treatment with 5 µg/ml anti-FLRT3 antibody. The presence of FLRT-3 in mBM extracts was confirmed by Western blot analysis. Secreted Tim-3 and galectin-9 were measured by ELISA.* ***C.*** *RCC-FG1 cells (FLRT-3 expression was confirmed by Western blot) were co-cultured with THP-1 cells at a ratio of 1 THP-1: 2 RCC-FG1 with or without 1 h pre-treatment with 5 µg/ml FLRT-3 neutralising antibody. Secreted galectin-9 and Tim-3 were measured by ELISA. Images are from one experiment representative of three which gave similar results. Quantitative data depict mean values ± SEM of three independent experiments; *p < 0.05; **p < 0.01; ***p < 0.001 vs. control. Symbols "a" or "b" are used in the way similar to "*" to indicate differences vs. cells treated with mBM extracts or co-cultured with RCC-FG1 cells respectively.*

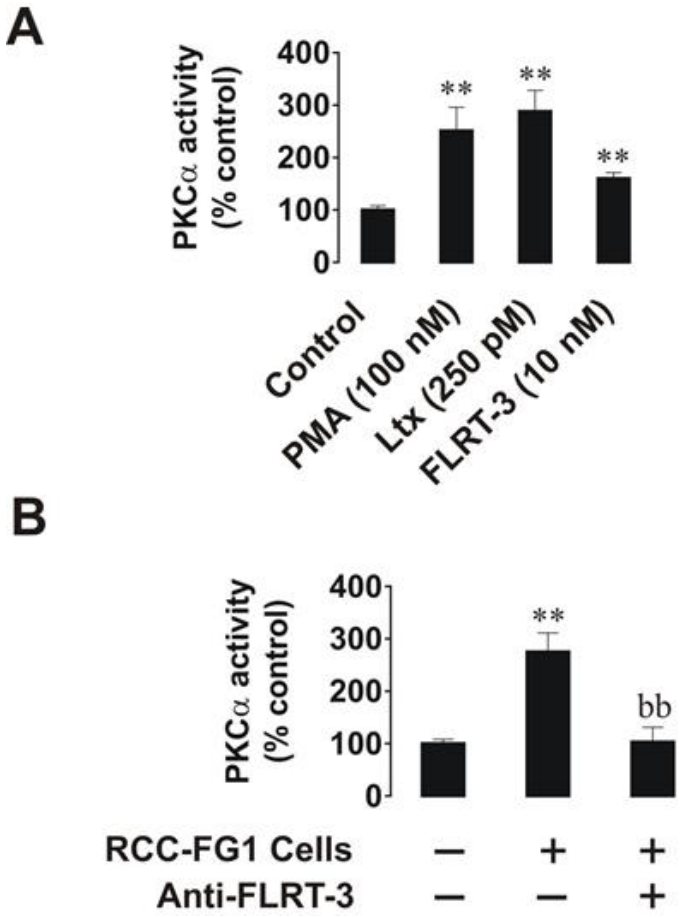

Figure 44 Activity of PKCα in THP-1 human AML cells. A. *Activity of PKCα in resting THP-1 cells and THP-1 cells exposed for 16 h to 100 nM PMA, 250 pM LTX and 10 nM FLRT-3.* ***B.*** *Activity of PKCα analysed in resting THP-1 cells and those co-cultured with RCC-FG1 cells (ratio 1:2) in absence or presence of 5 µg/ml FLRT-3 neutralising antibody. Images are from one experiment representative of three which gave similar results. Quantitative data are the mean values ± SEM of three independent experiments; *p < 0.05; **p < 0.01 vs. control. Symbol "bb" means p<0.01 vs. THP-1/RCC-FG1 co-culture.*

To check if this is physiologically relevant, THP-1 cells were exposed 16 h to mouse bone marrow (mBM) extracts (10 µg protein/ml, which contains FLRT-3, Figure 43B). These treatments were done with or without 1 h of pre-treatment with 5 µg/ml FLRT-3 neutralising mouse antibody. FLRT-3 neutralising mouse ab reduced the effects of mBM extracts but did not attenuate them (Figure 43B). This means that bone marrow contains several activators of galectin-9 secretion in AML cells.

THP-1 cells were then co-cultured with RCC-FG1 renal carcinoma cells, highly adherent cells that express high levels of FLRT-3 and release almost undetectable amounts of galectin-9, in a ratio of 1:2 (Figure 43C). The cells were kept together for 16 h in the absence or presence of 5 µg/ml FLTR-3 neutralising antibody and secretion of galectin-9 and soluble Tim-3 were analysed by ELISA. Presence of RCC-FG1 significantly upregulated PKCα activity, which was attenuated by neutralisation of FLRT-3 (Figure 44B). These results suggest that FLRT-3 (natural ligand of LPHN1) stimulates the release of galectin-9 and soluble Tim-3 from AML cells.

4.4.3 Galectin-9 and soluble Tim-3 attenuate AML cell killing activity of NK cells

Recently, some results seem to show that galectin-9 (soluble or cell surface associated) is able to interact with tim-3 (or maybe other receptors) on cytotoxic lymphoid cells, including NK cell and cytotoxic T cells (Gleason *et al.*, 2012). Given our previous results and this information, we decided to test if Tim-3-galectin-9 interaction is involved in the creation of immunological synapses between target cells and human mast cell sarcoma cells.

LAD2 cells express both Tim-3 and galectin-9, being both mostly on the cell surface as detected by in cell assay and in cell western (Figure 45A). Resting LAD2 cells do not release detectable amounts of galectin-9 and stimulation with IgE increased the release of galectin-9 but did not increase significantly the levels of galectin-9 and Tim-3, checked by Western-blot (Figure 45).

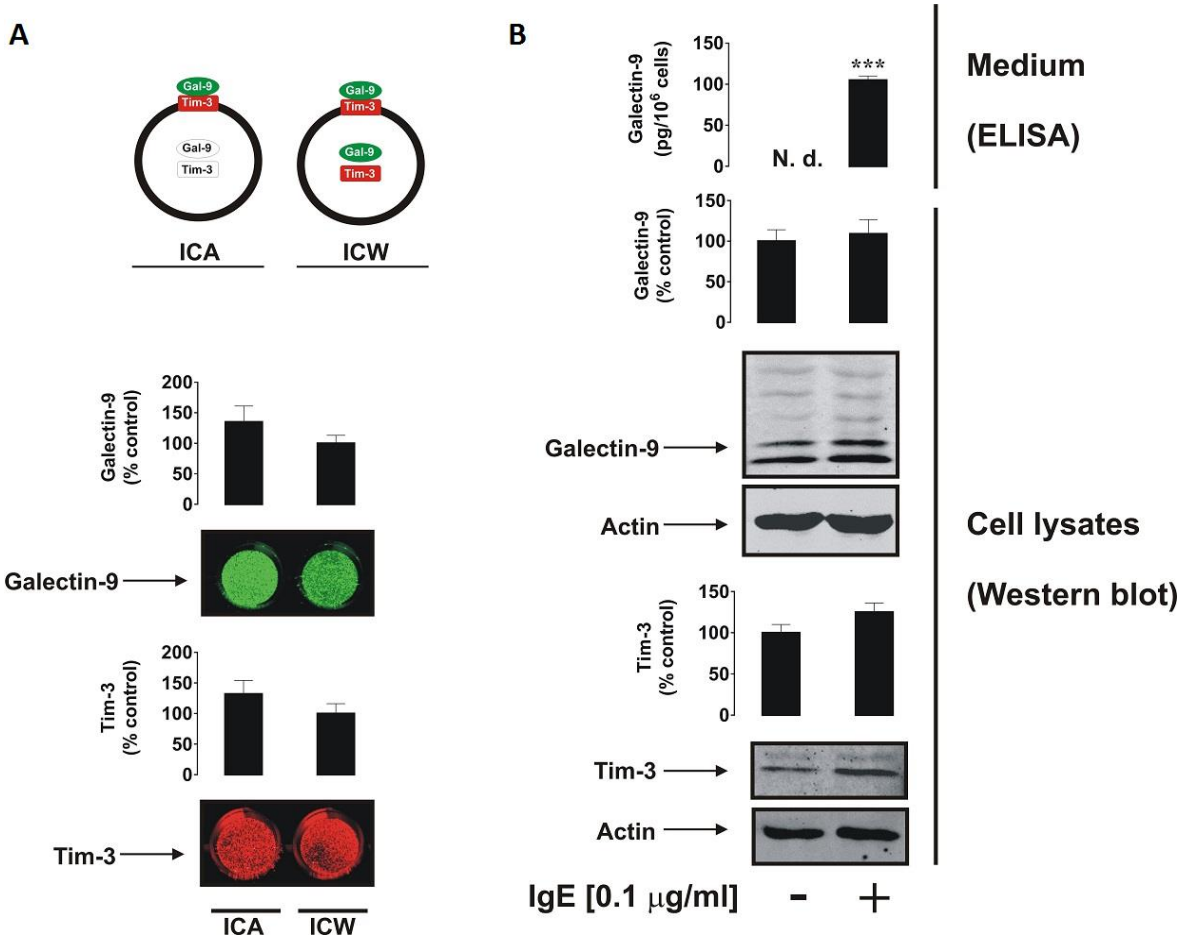

Figure 45 LAD2 cells express and externalise Tim-3 and galectin-9. A. *Surface-based and total Tim-3 and galectin-9 in LAD2 human mast cell sarcoma cells measured by ICA and ICW.* ***B.*** *Protein levels of Tim-3 and galectin-9 were measured in resting and IgE-sensitised LAD2 cells by Western blot. Galectin-9 release was characterised using ELISA. Images are from one experiment representative of three which gave similar results. Quantitative data show mean values ± SEM of three independent experiments; ***p < 0.001 vs. control.*

NK cells isolated from buffy coats of human blood were immobilised in ELISA plates. By Western-blot we verified that these cells express Tim-3 with different glycosylation variants but not detectable galectin-9 (Figure 46).

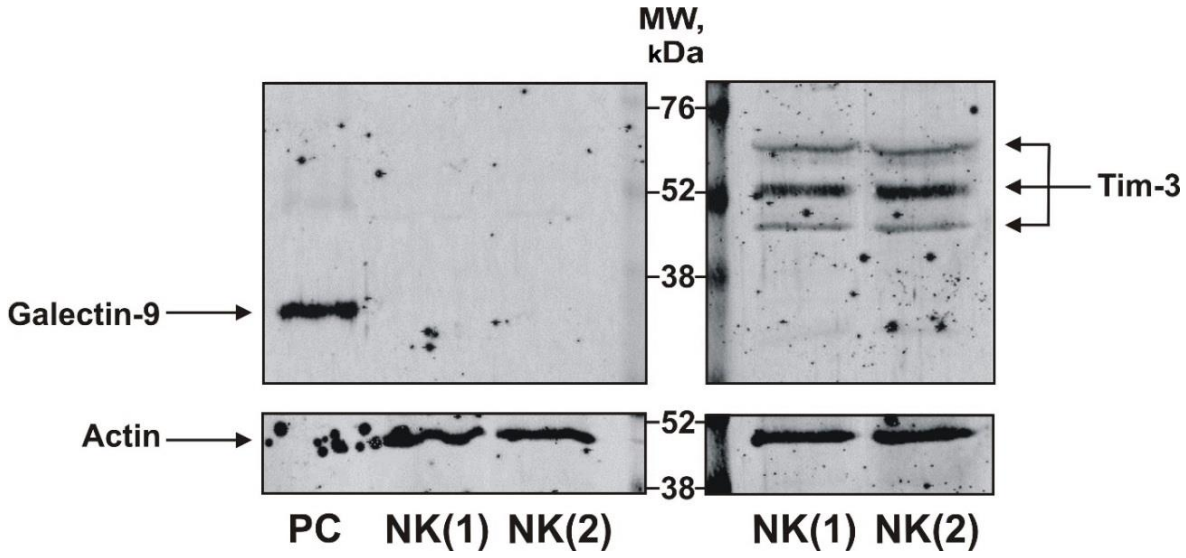

Figure 46 Expression of Tim-3 and galectin-9 in primary human NK cells. *Expressions of both proteins were analysed in whole cell extracts by Western-blot. Human recombinant galectin-9 was used as a positive control. Images are from one experiment representative (two donors in each) of three which gave similar results.*

We applied IgE-sensitised LAD2 cells (Sumbayev *et al.*, 2012) to the NK cells at a ratio of 1:1, with or without 15 min of pre-incubation with galectin-9neutralising antibody or with isotype control antibody to rule out the IgG effect. LAD2 cells were flagged using mouse IgM anti-IgE. The results showed that LAD2 cells bind to NK cells and presence of galectin-9 neutralising antibody decreased this effect (Figure 47). These results confirm that galectin-9 produced by LAD2 cells participates in their interaction with NK cells.

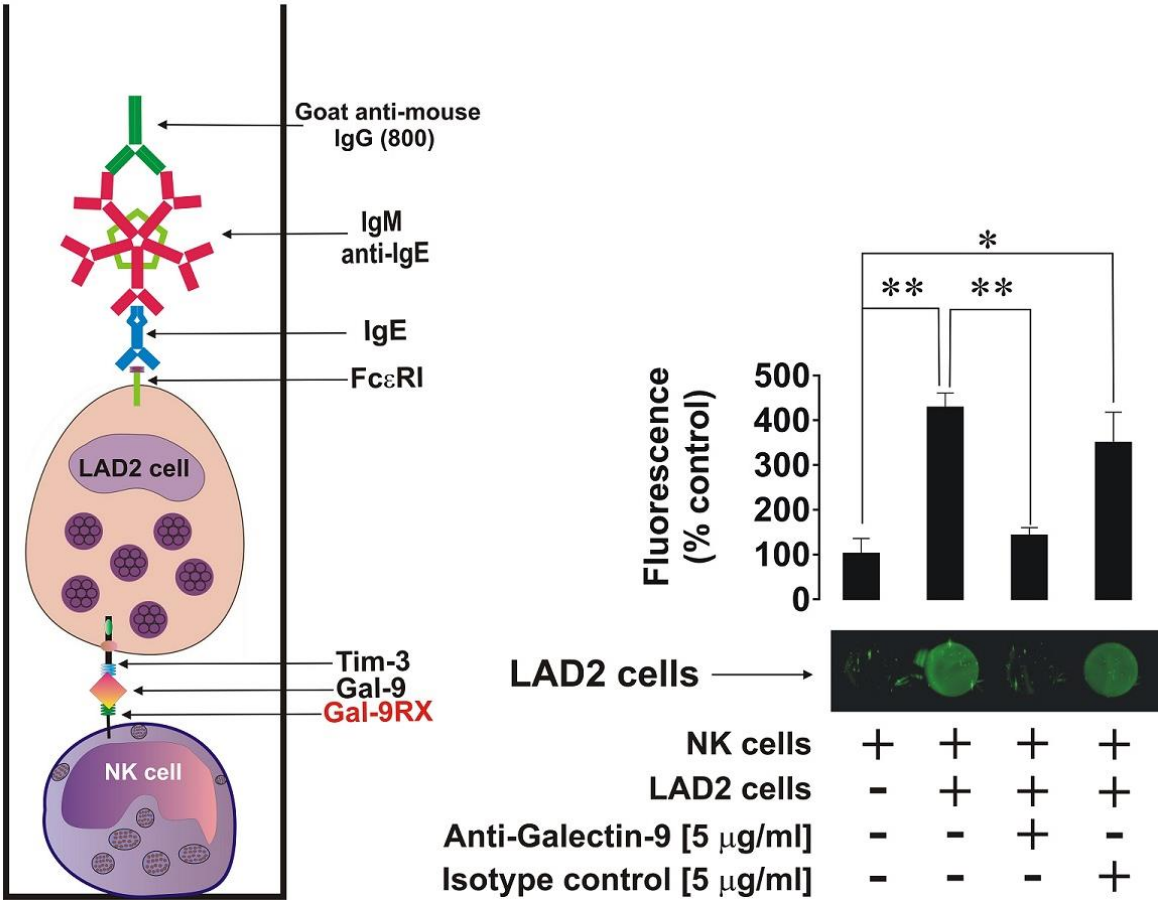

Figure 47 Galectin-9 participates in the formation of an "immunological synapse" between NK cells and LAD2 cells. *Primary human NK cells were immobilised on the surface of MaxiSorp plates and then co-incubated for 30 min with LAD2 cells with or without 30 min pre-treatment of LAD2 cells with 5 μg/ml galectin-9 neutralising antibody (or the same amount of isotype control antibody). LAD2 cells were then visualised by ICA. Images are from one experiment representative of five which gave similar results. Quantitative data represent mean values ± SEM of five independent experiments; *p < 0.05; **p < 0.01.*

We then used K562 chronic myeloid leukaemia cells which do not release detectable amounts of galectin-9 (previously confirm by ELISA). These cells were exposed to PMA for 24 h in maxisorp plates. The medium was replaced with fresh medium containing isolated primary human NK cells at a ratio 1:2 (1 K562 cell for 2 NK cells) in presence or absence of 5 ng/ml human recombinant galectin-9. Cells were co-cultured for 16 h and their viability was tested by MTS assay. The presence of NK cells significantly reduced the viability of K562 cells but presence of galectin-9 attenuated this effect (Figure 48A). During this experiment, the viability of NK cells was not affected (Figure 48A).

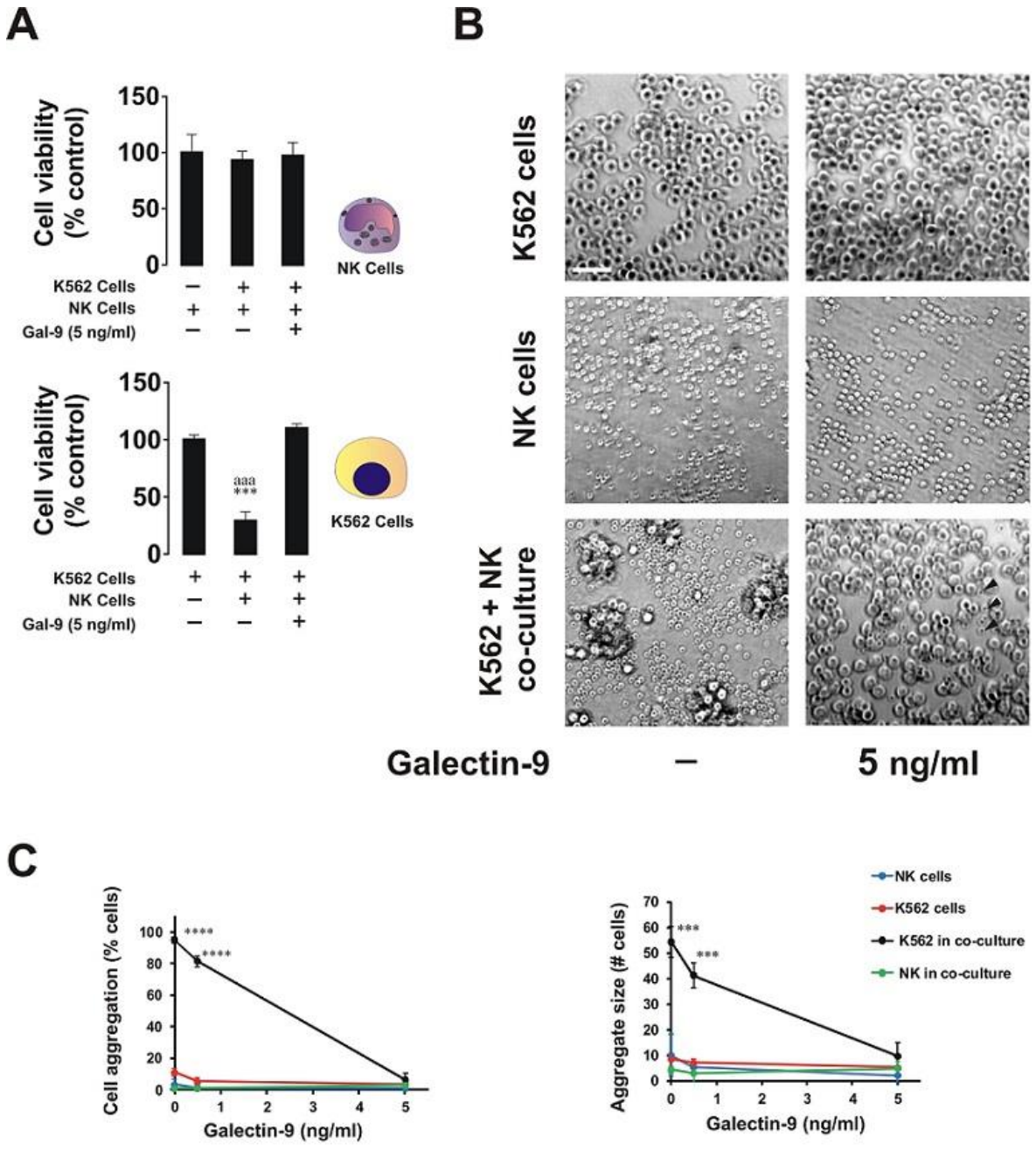

Figure 48 Galectin-9 protects myeloid leukaemia K562 cells from being killed by primary human NK cells. A. *K562 cells co-cultured 16 h with primary human NK cells at a 1:2 ratio, in the absence or presence of 5 ng/ml galectin-9. Viability of K562 and NK cells was measured using MTS test. Images are from one experiment representative of three which gave similar results. Quantitative data represent mean values ± SEM (n=3) independent experiments; ***p < 0.001 vs. control.* ***B.*** *K562 cells co-cultured 16 h with primary human NK cells, at a 1:2 ratio, in presence of different concentrations of galectin-9 (0 – 5 ng/ml). Cells were imaged using phase-contrast microscopy. The images are from one representative experiment of six (n = 6), which gave similar results. Scale bar (the same for all images), 50 μm.* ***C.*** *NK cells-induced aggregation of K562 cells was quantified as a function of galectin-9 concentration. Left, the per cent of cells found in aggregates in individual cultures and in the co-culture. Right, the size of cell aggregates in individual cultures and in the co-culture. The data represent the mean values ± SD of six independent experiments; *, p < 0.05; **, p < 0.01; ****, p < 0.0001.*

Not only the cytotoxic attack by NK cells led to a reduction on K562 viability but also it led to change in the behaviour of these cells causing their massive aggregation, to determine the effect of galectin-9 on K562 cell aggregation in individual or combined K562 and NK cells cultures, we used a phase contrast microscopy.

When there was no galectin-9 present, there was K562 cells aggregation in the presence of NK cells, but when we started increasing the dose of galectin-9 there was a decrease in the K562 cells aggregation by NK cells, in a dose dependent way. When 5 ng/ml galectin-9 were reached no aggregation was detected (Figure 48B and C). This shows that galectin-9 protects myeloid cells from being killed by NK cells. Galectin-9 on its own had no visible effects in both cell types.

We investigated the interactions between AML THP-1 cells and primary human NK cells. These cells were exposed to 100 nM PMA for 16 h and medium was replaced with fresh one containing NK cells at a ratio of 2:1 (2 THP-1 cells to 1 NK cell) And it incubated for 6 h, with or without 5 µg/ml galectin-9 neutralising antibody. We then measure Tim-3-galectin-9 complex and galectin-9 in NK cells by Western-blot analysis and viability of THP-1 cells, activity of granzyme B and caspase-3 and galectin-9 release were monitored. THP-1 viability was reduced when galectin-9 was neutralised (Figure 49A). This is in line with the observed increase in the caspase-3 and granzyme B activities. Galectin-9 levels were not affected (Figure 49A).

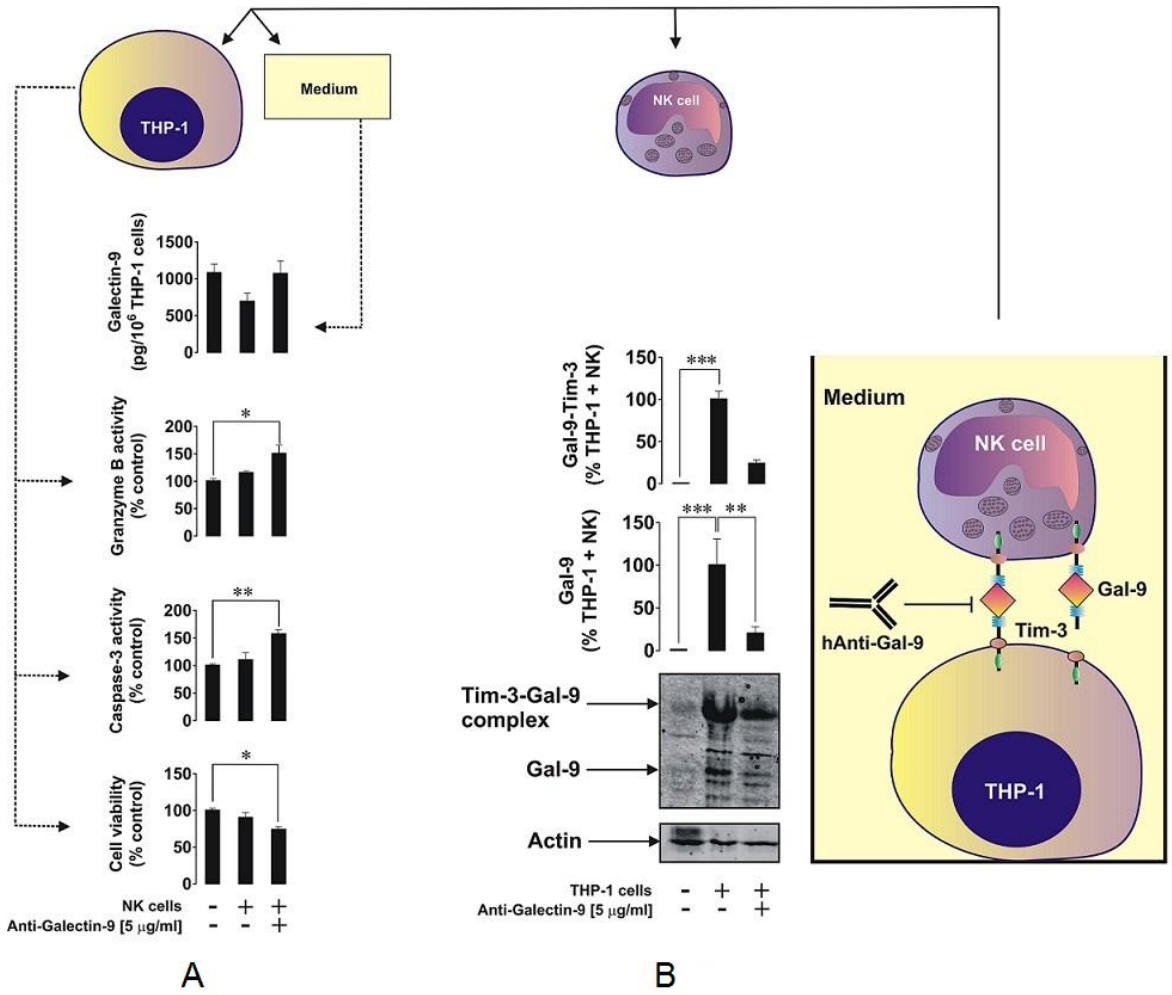

Figure 49 Cell-derived galectin-9 attenuates AML cell killing activity of primary human NK cells. *THP-1 cells were co-incubated with primary human NK cells at 1:2 ratio for 6 h.* ***A.*** *Detection of THP-1 cell viability by MTS test; measurement of activities of granzyme B and caspase 3 in THP-1 cell lysates and released galectin-9.* ***B.*** *Levels of galectin-9 from NK cells measured by Western-blot. Images are from one experiment representative of three which gave similar results. Quantitative data show mean values ± SEM of three independent experiments; *p < 0.05; **p < 0.01; ***p < 0.001 vs control.*

Resting NK cells did not produce detectable amounts of galectin-9, but it was possible to detect galectin-9 and unbroken Tim-3-galectin-9 complex in NK cells co-cultured. The amount of both proteins was reduced when galectin-9 neutralising antibody was used (Figure 49B). These results suggest that THP-1 cells were the source of galectin-9 that probably bound Tim-3 in the surface of NK cells, preventing the delivery of NK cell-derived granzyme B into THP-1 cells, resulting in prevention of the caspase-3-dependent apoptotic pathway.

Previously it was reported that there is a possible reciprocal link between levels of soluble Tim-3 and IL-2, a cytokine that activates NK and T cells cytotoxic activity (Geng *et al.*, 2006). As we previous showed, Tim-3 levels in plasma of healthy donors are significantly lower than AML patients (Figure 40), while IL-2 levels were much higher (Figure 50A and B). We exposed Jurkat T cells (that produce detectable amounts of IL-2) were exposed to increasing concentrations of Tim-3 for 24 h. It is possible to see a clear soluble Tim-3 concentration-dependent and eventually reduction of IL-2 release from Jurkat T cells (Figure 50C).

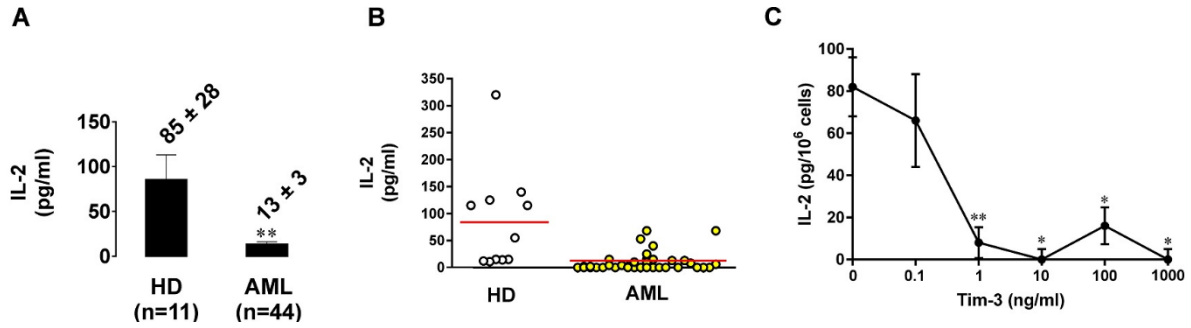

***Figure 50 Soluble Tim-3 attenuates IL-2 release. A. and B**. IL-2 levels measured by ELISA in blood serum of healthy donors and AML patients. **C.** Jurkat T cells were exposed to the increasing concentrations of Tim-3 for 24 h and detection of secreted IL-2 was done by ELISA. Data show mean values ± SEM of three independent experiments; *p < 0.05; **p < 0.01.*

These results show that Tim-3 is able to bind a target protein and reduce the IL-2 production, preventing induction of anti-cancer activity of NK cells and T lymphocytes. All together these results show that there is a pathobiochemical pathway in AML cells. It is related with PKCα activation by LPHN1 leading to expression and exocytosis of soluble Tim-3 and galectin-9, that prevents cytotoxic lymphocytes activation and impair their malignant cell killing activity.

4.4.4 Discussion

As previously mentioned, Tim-3 is shed by ADAM 10/17 proteolytic enzymes, producing soluble Tim-3. Our results showed that this protein can be shed in two different forms, in its free from and complexed with galectin-9. We can see a band at 20 kDa corresponding to a fragment when Tim-3 is in the complex and a band at 33 kDa when there is soluble Tim-3.

The analysis of the complex Tim-3-galectin-9 by Synchrotron radiation circular dichroism (SRCD) suggests that the interaction between Tim-3 and galectin-9 to interact with target proteins. Galectin-9 is a tandem protein that contains two identical covalently fused elements (Delacour *et al.*, 2009). One side of this protein may interact with Tim-3, while the other may bind a receptor molecule, like Tim-3, in the membrane from the target cell. That explains the high efficiency of galectin-9 in triggering Tim-3 on NK cells that do not express galectin-9.

Because it is possible to see Tim-3/galectin-9 complex on the image of the Western-blot in Figure 37, Figure 38 and Figure 40 it is possible that the biding between this proteins is strengthened by the interaction of galectin-9 with Tim-3-associated glycosides,

Previously, it was reported that the release of both Tim-3 and galectin-9 depends on PKCα and proteolysis (Chabot *et al.*, 2002b), our results were able to confirm this. PMA treatment was able to induce PKCα activation, that then activated exocytosis of Tim-3 and galectin-9, and their mTOR-dependent production, in THP-1 AML cells (Figure 42).

Our results, show evidence of co-localisation of Tim-3 and galectin-9 in these cells after PMA exposure (Figure 39). Also, soluble Tim-3 was shown to significantly downregulate IL-2 production, a cytokine required for activation of NK cells and cytotoxic T lymphocytes.

Natural and exogenous LPHN1 ligands activated the PKCα pathway and induced both mTOR-dependent translation of Tim-3-galectin-9 complex and their exocytosis. PKCα provokes agglomeration of SNARE complex, that is responsible for exocytosis (Stöckli *et al.*, 2011; Morgan *et al.*, 2005). Constitutively active PKCα in malignant primary AML cells correlates with poor prognosis and high mortality rate of patients (Kurinna *et al.*, 2006).

When THP-1 cells were exposed to mouse bone marrow extracts, there was a high mortality and an increase in the galectin-9 release levels. When we used FLRT-3 neutralising antibody there was a significant decrease of FLRT-3 induced PKCα-dependent galectin-9 release, this means that galectin-9 and Tim-3 are synthetized and exocytosis by AML cells in a PKCα/mTOR-dependent manner, using available plasma membrane-associated PKCα activating receptors, like LPHN1, to induce the whole pathway.

Galectin-9 prevents the delivery of granzyme B into AML cells, in a perforin and mannose-6-phosphate receptor-dependent process (Figure 51). Inside the cells granzyme B cleaves protein Bid in to tBid, inducing mitochondrial dysfunction and cytochrome c release and activates caspase 3. The proteolytic activation of caspase 3 in addition to the classic pathway may be directly catalysed by granzyme B (Lee *et al.*, 2014). This concept is confirmed by our results in Figure 49.

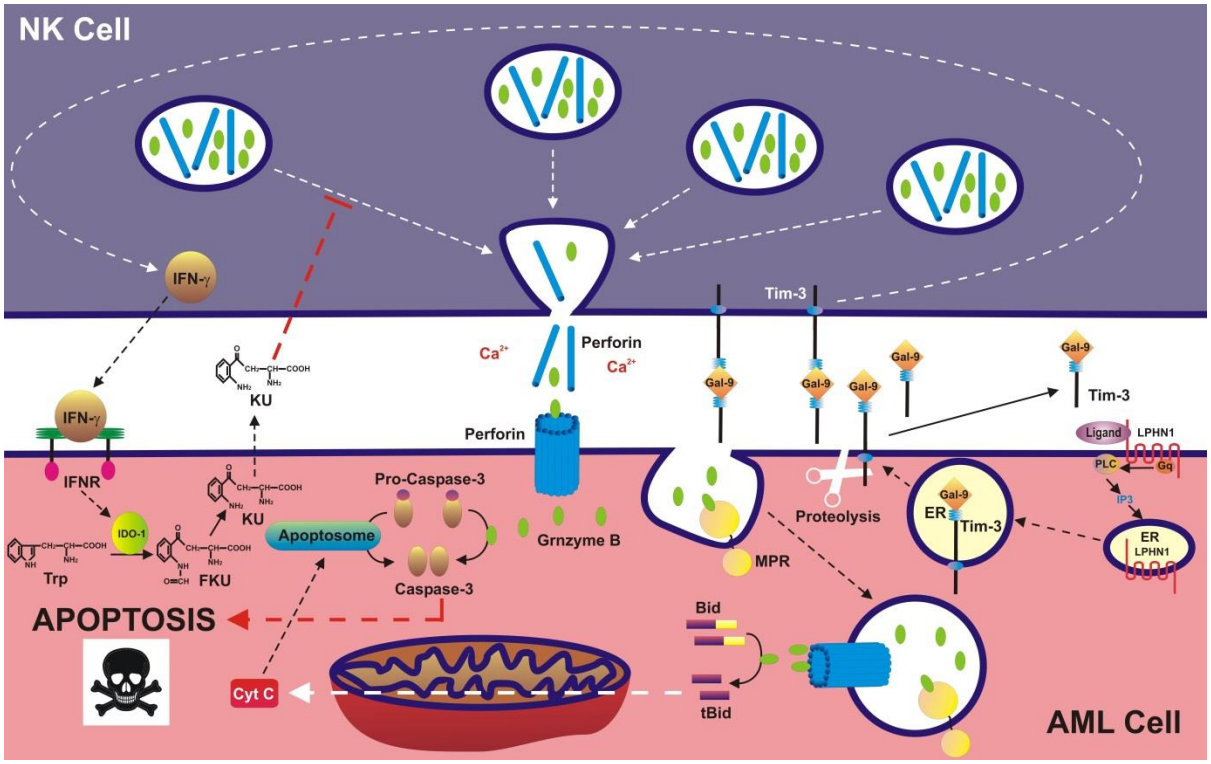

Figure 51 Probable biochemical interactions between AML and NK cells. *LPHN1/Tim-3/galectin-9 pathway leads to externalisation/release of galectin-9, which binds NK cell receptor, probably Tim-3. In response, NK cells release IFN-γ which triggers activation of IDO1 in AML cells. IDO1 converts tryptophan (Trp) into formyl-kynurenine (FKU), which is further degraded into L-kynurenine (KU). KU is released and is capable of attenuating the ability of NK cells to deliver granzyme B into AML cells in perforin/mannose-6-phosphate receptor (MPR)-dependent manner. If successfully delivered, granzyme B catalyse Bid cleavage leading to cytochrome c release from mitochondria. This leads to formation of apoptosome and activation of caspase-3. Furthermore, granzyme B is capable of performing direct proteolytic activation of caspase-3. These effects lead to AML cell apoptosis. However, this process is not taking place due to galectin-9-induced impairing of NK cell activity as previously described.*

It was reported that galectin-9 induces IFN-γ release from NK cells (Gleason *et al.*, 2012), this interacts with AML cells and induced activity of indoleamine 2,3-dioxygenase (IDO1). IDO1 converts L-kynurenine and it is released (Corm *et al.*, 2009; Folgiero *et al.*, 2015; Mabuchi *et al.*, 2016). L-kynurenine affects the ability of NK cells to kill AML cells. Our experiments confirmed this (Figure 51).

Our results show a fundamentally new pathway that leads to production and release of soluble Tim-3 and galectin-9, that prevents activation of NK cells, preventing them to kill malignant cells (Figure 52).

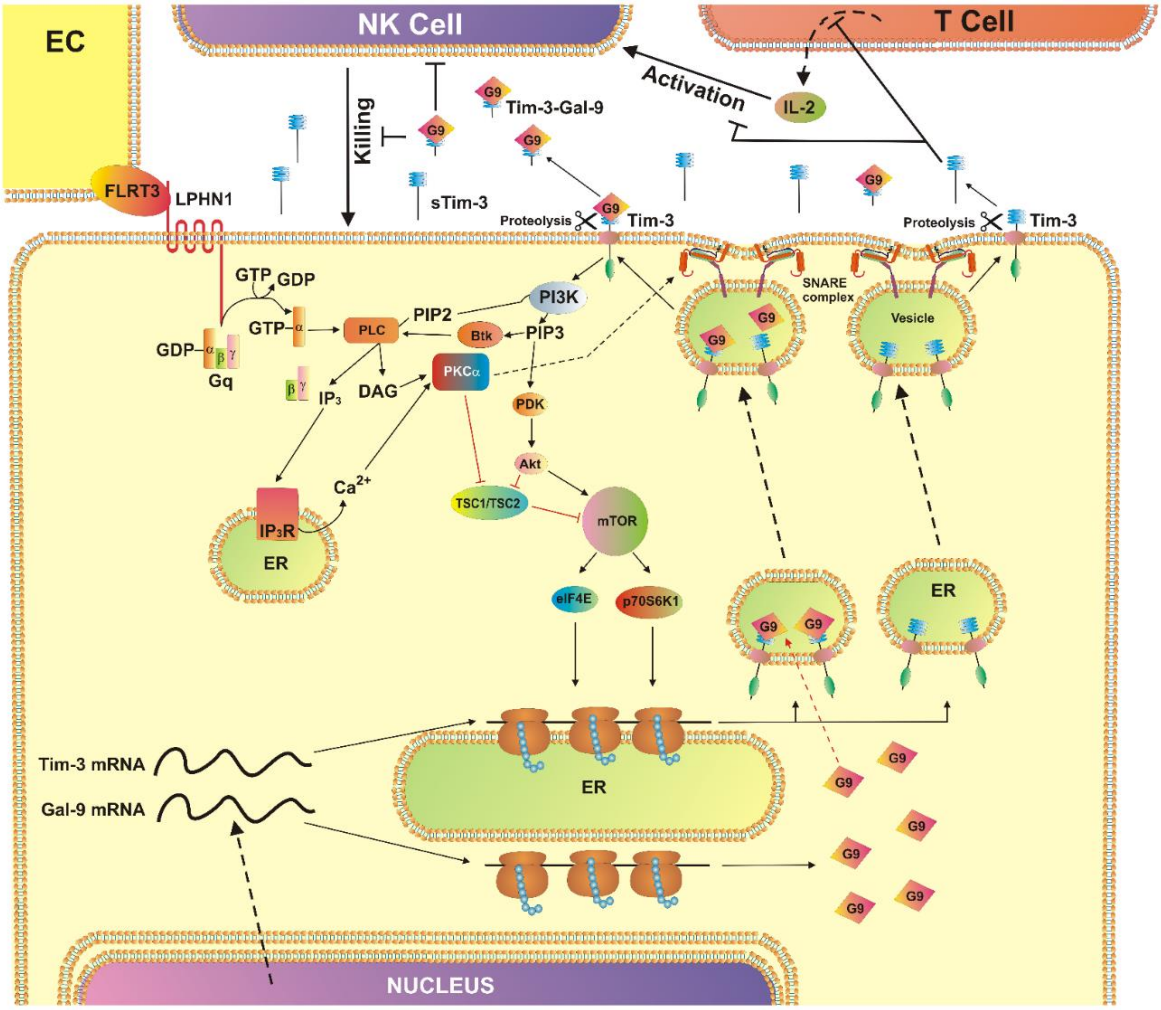

Figure 52 AML cell-based pathobiochemical pathway showing LPHN1-induced classic activation of PKCα, which trigger translation of Tim-3 and galectin-9 as well as their secretion required for immune escape. *FLRT-3 (endothelial cell (EC)-based) – LPHN1 interaction leads to activation of PKCα through classic Gq/PLC/Ca2+ pathway. Ca2+ is mobilised by inositol-3-phospate (IP3) released after PLC-dependent PIP2 degradation. IP3 interacts with ER-associated IP3 receptor (IP3R) leading to Ca2+ mobilisation. PKCα activates mTOR translational pathway through downregulation of TSC1/TSC2. mTOR controls translation of Tim-3 and galectin-9. PKCα also phosphorylates Munc18 exocytosis protein which provokes agglomeration of SNARE complex. This leads to exocytosis of free and galectin-9-complexed Tim-3. Both types of Tim-3 are differentially shed from the cell surface by proteolytic enzymes. Soluble Tim-3 prevents IL-2 secretion required for activation of NK cells and cytotoxic T cells. Galectin-9 impairs AML cell killing activity of NK cells (and other cytotoxic lymphocytes).*

5. CONCLUSIONS

The following conclusions can be made from this work:

1. Tim-3 and Galectin-9 are highly expressed and externalised in primary human AML cells unlike healthy leukocytes, where the expression levels are lower and both proteins are mostly located inside the cell. When externalised, Tim-3/Galectin-9 complex triggers the mTOR translational pathway thus contributing to cell growth and proliferation.
2. Tim-3 acts as a trafficker in Galectin-9 secretion in human AML cells.
3. AML cell lines and primary human AML cells express functional neuronal receptor LPHN1. Its translation is controlled by the mTOR pathway. LPHN1 is involved in induction of Tim-3 and Galectin-9 secretion in human AML cells. It requires stimulation with its ligand, for example, FLRT3 to upregulate exocytosis.
4. Classic Gαq/PLC/PKC pathway is triggering LPHN1-induced exocytosis of Tim-3 and Galectin-9, while translation of both proteins is controlled by the mTOR pathway.
5. Galectin-9 impairs anti-leukaemia activity of primary human NK cells.
6. Taken together, our PhD programme resulted in a discovery of a fundamental biochemical mechanism, which includes ligand-dependent activation of ectopically expressed LPHN1 leading to increased translation and exocytosis of the immune receptor Tim-3 and its ligand Galectin-9. Physiological relevance of these results was validated in ex vivo experiments using primary samples from AML patients. This pathway provides reliable targets for both highly specific diagnosis and immune therapy of AML.

6. BIBLIOGRAPHY

Abooali, M., Lall, G.S., Coughlan, K., Lall, H.S., Gibbs, B.F., Sumbayev, V. V (2014) Crucial involvement of xanthine oxidase in the intracellular signalling networks associated with human myeloid cell function. *Scientific Reports*. **4**, 6307.

Adachi, Y., Aoki, C., Yoshio-Hoshino, N., Takayama, K., Curiel, D.T., Nishimoto, N. (2006) Interleukin-6 induces both cell growth and VEGF production in malignant mesotheliomas. *International Journal of Cancer*. **119**(6), 1303–1311.

Akira, S., Takeda, K. (2004) Toll-like receptor signalling. *Nature Reviews Immunology*. **4**(7), 499–511.

Anderson, A.C. (2012) Tim-3, a negative regulator of anti-tumor immunity. *Current Opinion in Immunology*. **24**(2), 213–216.

Anderson, A.C., Anderson, D.E., Bregoli, L., Hastings, W.D., Kassam, N., Lei, C., Chandwaskar, R., Karman, J., Su, E.W., Hirashima, M., Bruce, J.N., Kane, L.P., Kuchroo, V.K., Hafler, D.A. (2007) Promotion of Tissue Inflammation by the Immune Receptor Tim-3 Expressed on Innate Immune Cells. *Science*. **318**(5853), 1141–1143.

Baron, P. (2005) The Lifesaving Benefits of Annual Blood Screening. *Life Extension Magazine*. [online]. Available from: http://www.lifeextension.com/magazine/2005/5/report_blood/Page-02?p=1 [Accessed March 21, 2017].

Boucard, A.A., Maxeiner, S., Sudhof, T.C. (2014) Latrophilins Function as Heterophilic Cell-adhesion Molecules by Binding to Teneurins: REGULATION BY ALTERNATIVE SPLICING. *Journal of Biological Chemistry*. **289**(1), 387–402.

Bray, F. (2016) The evolving scale and profile of cancer worldwide: Much ado about everything. *Cancer Epidemiology Biomarkers and Prevention*. **25**(1), 3–5.

Broudy, V.C. (1997) Stem cell factor and hematopoiesis. *Blood*. **90**(4), 1345–64.

Cancer Treatment Centers of America (2017) Leukemia information. [online]. Available from: http://www.cancercenter.com/leukemia/learning/ [Accessed March 17, 2017].

Capogna, M., Volynski, K.E., Emptage, N.J., Ushkaryov, Y. a (2003) The alpha-latrotoxin mutant LTXN4C enhances spontaneous and evoked transmitter release in CA3 pyramidal neurons. *The Journal of Neuroscience*. **23**(10), 4044–53.

Chabot, S., Kashio, Y., Seki, M., Shirato, Y., Nakamura, K., Nishi, N., Nakamura, T., Matsumoto, R., Hirashima, M. (2002a) Regulation of galectin-9 expression and release in Jurkat T cell line cells. *Glycobiology*. **12**(2), 111–118.

Chabot, S., Kashio, Y., Seki, M., Shirato, Y., Nakamura, K., Nishi, N., Nakamura, T., Matsumoto, R., Hirashima, M. (2002b) Regulation of galectin-9 expression and release in

Jurkat T cell line cells. *Glycobiology*. **12**(2), 111–118.

Chaplen, F.W.R., Fahl, W.E., Cameron, D.C. (1996a) Detection of Methylglyoxal as a Degradation Product of DNA and Nucleic Acid Components Treated with Strong Acid. *Analytical Biochemistry*. **236**(2), 262–269.

Chaplen, F.W.R., Fahl, W.E., Cameron, D.C. (1996b) Method for Determination of Free Intracellular and Extracellular Methylglyoxal in Animal Cells Grown in Culture. *Analytical Biochemistry*. **238**(2), 171–178.

Chiorazzi, N., Rai, K.R., Ferrarini, M. (2005) Chronic Lymphocytic Leukemia. *New England Journal of Medicine*. **352**(8), 804–815.

Clayton, K.L., Douglas-Vail, M.B., Rahman, A.K.M.N., Medcalf, K.E., Xie, I.Y., Chew, G.M., Tandon, R., Lanteri, M.C., Norris, P.J., Deeks, S.G., Ndhlovu, L.C., Ostrowski, M.A. (2015) Soluble T Cell Immunoglobulin Mucin Domain 3 Is Shed from CD8 + T Cells by the Sheddase ADAM10, Is Increased in Plasma during Untreated HIV Infection, and Correlates with HIV Disease Progression G. Silvestri, ed. *Journal of Virology*. **89**(7), 3723–3736.

Corm, S., Berthon, C., Imbenotte, M., Biggio, V., Lhermitte, M., Dupont, C., Briche, I., Quesnel, B. (2009) Indoleamine 2,3-dioxygenase activity of acute myeloid leukemia cells can be measured from patients' sera by HPLC and is inducible by IFN-γ. *Leukemia Research*. **33**(3), 490–494.

Cory, A.H., Owen, T.C., Barltrop, J.A., Cory, J.G. (1991) Use of an aqueous soluble tetrazolium/formazan assay for cell growth assays in culture. *Cancer communications*. **3**(7), 207–12.

Dana-Farber cancer institute (2014) Myelodysplastic Syndromes Treatment. [online]. Available from: http://www.dana-farber.org/Health-Library/Myelodysplastic-Syndromes-Treatment-(PDQ®).aspx [Accessed February 17, 2017].

Darwish, N.H.E., Sudha, T., Godugu, K., Elbaz, O., Abdelghaffar, H.A., Hassan, E.E.A., Mousa, S.A. (2016) Acute myeloid leukemia stem cell markers in prognosis and targeted therapy: potential impact of BMI-1, TIM-3 and CLL-1. *Oncotarget*. **7**(36).

Das, M., Zhu, C., Kuchroo, V.K. (2017) Tim-3 and its role in regulating anti-tumor immunity. *Immunological Reviews*. **276**(1), 97–111.

Davydov, I.I., Fidalgo, S., Khaustova, S.A., Lelyanova, V.G., Grebenyuk, E.S., Ushkaryov, Y.A., Tonevitsky, A.G. (2009) Prediction of Epitopes in Closely Related Proteins Using a New Algorithm. *Bulletin of Experimental Biology and Medicine*. **148**(6), 869–873.

Delacour, D., Koch, A., Jacob, R. (2009) The Role of Galectins in Protein Trafficking. *Traffic*. **10**(10), 1405–1413.

Deschler, B., Lübbert, M. (2006) Acute myeloid leukemia: Epidemiology and etiology. *Cancer*. **107**(9), 2099–2107.

Dienstmann, R., Rodon, J., Serra, V., Tabernero, J. (2014) Picking the Point of Inhibition: A Comparative Review of PI3K/AKT/mTOR Pathway Inhibitors. *Molecular Cancer*

Therapeutics. **13**(5), 1021–1031.

Estey, E., Döhner, H. (2006) Acute myeloid leukaemia. *Lancet (London, England)*. **368**(9550), 1894–907.

Fasler-Kan, E., Suenderhauf, C., Barteneva, N., Poller, B., Gygax, D., Huwyler, J. (2010) Cytokine signaling in the human brain capillary endothelial cell line hCMEC/D3. *Brain Research*. **1354**, 15–22.

Fitzmaurice, C., Allen, C., Barber, R.M., Barregard, L., Bhutta, Z.A., Brenner, H., Dicker, D.J., Chimed-Orchir, O., Dandona, R., Dandona, L., Fleming, T., Forouzanfar, M.H., Hancock, J., Hay, R.J., Hunter-Merrill, R., Huynh, C., Hosgood, H.D., Johnson, C.O., Jonas, J.B., Khubchandani, J., Kumar, G.A., Kutz, M., Lan, Q., Larson, H.J., Liang, X., Lim, S.S., Lopez, A.D., MacIntyre, M.F., Marczak, L., Marquez, N., Mokdad, A.H., Pinho, C., Pourmalek, F., Salomon, J.A., Sanabria, J.R., Sandar, L., Sartorius, B., Schwartz, S.M., Shackelford, K.A., Shibuya, K., Stanaway, J., Steiner, C., Sun, J., Takahashi, K., Vollset, S.E., Vos, T., Wagner, J.A., Wang, H., Westerman, R., Zeeb, H., Zoeckler, L., Abd-Allah, F., Ahmed, M.B., Alabed, S., Alam, N.K., Aldhahri, S.F., Alem, G., Alemayohu, M.A., Ali, R., Al-Raddadi, R., Amare, A., Amoako, Y., Artaman, A., Asayesh, H., Atnafu, N., Awasthi, A., Saleem, H.B., Barac, A., Bedi, N., Bensenor, I., Berhane, A., Bernabé, E., Betsu, B., Binagwaho, A., Boneya, D., Campos-Nonato, I., Castañeda-Orjuela, C., Catalá-López, F., Chiang, P., Chibueze, C., Chitheer, A., Choi, J.-Y., Cowie, B., Damtew, S., das Neves, J., Dey, S., Dharmaratne, S., Dhillon, P., Ding, E., Driscoll, T., Ekwueme, D., Endries, A.Y., Farvid, M., Farzadfar, F., Fernandes, J., Fischer, F., G/hiwot, T.T., Gebru, A., Gopalani, S., Hailu, A., Horino, M., Horita, N., Husseini, A., Huybrechts, I., Inoue, M., Islami, F., Jakovljevic, M., James, S., Javanbakht, M., Jee, S.H., Kasaeian, A., Kedir, M.S., Khader, Y.S., Khang, Y.-H., Kim, D., Leigh, J., Linn, S., Lunevicius, R., El Razek, H.M.A., Malekzadeh, R., Malta, D.C., Marcenes, W., Markos, D., Melaku, Y.A., Meles, K.G., Mendoza, W., Mengiste, D.T., Meretoja, T.J., Miller, T.R., Mohammad, K.A., Mohammadi, A., Mohammed, S., Moradi-Lakeh, M., Nagel, G., Nand, D., Le Nguyen, Q., Nolte, S., Ogbo, F.A., Oladimeji, K.E., Oren, E., Pa, M., Park, E.-K., Pereira, D.M., Plass, D., Qorbani, M., Radfar, A., Rafay, A., Rahman, M., Rana, S.M., Søreide, K., Satpathy, M., Sawhney, M., Sepanlou, S.G., Shaikh, M.A., She, J., Shiue, I., Shore, H.R., Shrime, M.G., So, S., Soneji, S., Stathopoulou, V., Stroumpoulis, K., Sufiyan, M.B., Sykes, B.L., Tabarés-Seisdedos, R., Tadese, F., Tedla, B.A., Tessema, G.A., Thakur, J.S., Tran, B.X., Ukwaja, K.N., Uzochukwu, B.S.C., Vlassov, V.V., Weiderpass, E., Wubshet Terefe, M., Yebyo, H.G., Yimam, H.H., Yonemoto, N., Younis, M.Z., Yu, C., Zaidi, Z., Zaki, M.E.S., Zenebe, Z.M., Murray, C.J.L., Naghavi, M. (2016) Global, Regional, and National Cancer Incidence, Mortality, Years of Life Lost, Years Lived With Disability, and Disability-Adjusted Life-years for 32 Cancer Groups, 1990 to 2015. *JAMA Oncology*. **98121**.

Folgiero, V., Cifaldi, L., Li Pira, G., Goffredo, B.M., Vinti, L., Locatelli, F. (2015) TIM-3/Gal-9 interaction induces IFNγ-dependent IDO1 expression in acute myeloid leukemia blast cells. *Journal of hematology & oncology*. **8**, 36.

Gao, L., Yu, S., Zhang, X. (2014) Hypothesis: Tim-3/Galectin-9, A New Pathway for Leukemia Stem Cells Survival by Promoting Expansion of Myeloid-Derived Suppressor Cells and Differentiating into Tumor-Associated Macrophages. *Cell Biochemistry and Biophysics*. **70**(1), 273–277.

Geng, H., Zhang, G.-M., Li, D., Zhang, H., Yuan, Y., Zhu, H.-G., Xiao, H., Han, L.-F., Feng,

Z.-H. (2006) Soluble Form of T Cell Ig Mucin 3 Is an Inhibitory Molecule in T Cell-Mediated Immune Response. *The Journal of Immunology*. **176**(3), 1411–1420.

Gibbs, B.F., Silva, I.G., Prokhorov, A., Yasinska, I.M., Casely-hayford, M.A., Berger, S.M., Sumbayev, V. V (2015) Caffeine affects the biological responses of human hematopoietic cells of myeloid lineage *via* downregulation of the mTOR pathway and xanthine oxidase activity. *Oncotarget*. **6**(30).

Gibbs, B.F., Yasinska, I.M., Oniku, A.E., Sumbayev, V. V. (2011) Effects of Stem Cell Factor on Hypoxia-Inducible Factor 1 Alpha Accumulation in Human Acute Myeloid Leukaemia and LAD2 Mast Cells S. Sozzani, ed. *PLoS ONE*. **6**(7), e22502.

Gibbs, B.F., Yasinska, I.M., Pchejetski, D., Wyszynski, R.W., Sumbayev, V. V. (2012) Differential control of hypoxia-inducible factor 1 activity during pro-inflammatory reactions of human haematopoietic cells of myeloid lineage. *The International Journal of Biochemistry & Cell Biology*. **44**(11), 1739–1749.

Giles, F.J. (2002) Acute Myeloid Leukemia. *Hematology*. **2002**(1), 73–110.

Gleason, M.K., Lenvik, T.R., McCullar, V., Felices, M., O'Brien, M.S., Cooley, S. a, Verneris, M.R., Cichocki, F., Holman, C.J., Panoskaltsis-Mortari, A., Niki, T., Hirashima, M., Blazar, B.R., Miller, J.S. (2012) Tim-3 is an inducible human natural killer cell receptor that enhances interferon gamma production in response to galectin-9. *Blood*. **119**(13), 3064–72.

Glick, D., Barth, S., Macleod, K.F. (2010) Autophagy : cellular and molecular mechanisms. *Journal of Pathology The*. **221**(1), 3–12.

Golden-Mason, L., McMahan, R.H., Strong, M., Reisdorph, R., Mahaffey, S., Palmer, B.E., Cheng, L., Kulesza, C., Hirashima, M., Niki, T., Rosen, H.R. (2013) Galectin-9 Functionally Impairs Natural Killer Cells in Humans and Mice. *Journal of Virology*. **87**(9), 4835–4845.

Gonçalves Silva, I., Yasinska, I.M., Sakhnevych, S.S., Fiedler, W., Wellbrock, J., Bardelli, M., Varani, L., Hussain, R., Siligardi, G., Ceccone, G., Berger, S.M., Ushkaryov, Y.A., Gibbs, B.F., Fasler-Kan, E., Sumbayev, V. V. (2017) The Tim-3-galectin-9 Secretory Pathway is Involved in the Immune Escape of Human Acute Myeloid Leukemia Cells. *EBioMedicine*.

Gozuacik, D., Kimchi, A. (2007) Autophagy and Cell Death. In *Autophagy*. pp. 217–245.

Gwinn, D.M., Shackelford, D.B., Egan, D.F., Mihaylova, M.M., Mery, A., Vasquez, D.S., Turk, B.E., Shaw, R.J. (2008) AMPK Phosphorylation of Raptor Mediates a Metabolic Checkpoint. *Molecular Cell*. **30**(2), 214–226.

Hauke, R.J., Tarantolo, S.R. (2000) Hematopoietic Growth Factors. *Laboratory Medicine*. **31**(11), 613–615.

Hehlmann, R., Hochhaus, A., Baccarani, M. (2007) Chronic myeloid leukaemia. *The Lancet*. **370**(9584), 342–350.

Hill, A., Redd, C., Gotham, D., Erbacher, I., Meldrum, J., Harada, R. (2017) Estimated generic prices of cancer medicines deemed cost-ineffective in England: a cost estimation analysis. *BMJ Open*. **7**(1), e011965.

Hsu, Y.-L., Wang, M.-Y., Ho, L.-J., Huang, C.-Y., Lai, J.-H. (2015) Up-regulation of galectin-9 induces cell migration in human dendritic cells infected with dengue virus. *Journal of Cellular and Molecular Medicine*. **19**(5), 1065–1076.

Hsu, Y.C., Yuan, S., Chen, H.Y., Yu, S.L., Liu, C.H., Hsu, P.Y., Wu, G., Lin, C.H., Chang, G.C., Li, K.C., Yang, P.C. (2009) A four-gene signature from NCI-60 cell line for survival prediction in non-small cell lung cancer. *Clinical Cancer Research*. **15**(23), 7309–7315.

Hughes, R.C. (1999) Secretion of the galectin family of mammalian carbohydrate-binding proteins. . **1473**, 172–185.

Hussain, R., Benning, K., Javorfi, T., Longo, E., Rudd, T.R., Pulford, B., Siligardi, G. (2015) CDApps: Integrated software for experimental planning and data processing at beamline B23, Diamond Light Source. *Journal of Synchrotron Radiation*. **22**(2), 465–468.

Hussain, R., Jávorfi, T., Siligardi, G. (2012) Circular dichroism beamline B23 at the Diamond Light Source. *Journal of Synchrotron Radiation*. **19**(1), 132–135.

IARC (2017) Globocan 2012: Estimated Cancer Incidence, Mortality and Prevalence Worldwide in 2012. [online]. Available from: http://globocan.iarc.fr/Pages/fact_sheets_population.aspx [Accessed March 17, 2017].

Jagannathan-Bogdan, M., Zon, L.I. (2013) Hematopoiesis. *Development*. **140**(12), 2463–2467.

Janeway, C.A., Jr, P.T., Walport, M., Shlomchik, M.J. (2001) *Immunobiology*. 5th ed. Garland Science, ed. New York.

Kawai, T., Akira, S. (2007) Signaling to NF-κB by Toll-like receptors. *Trends in Molecular Medicine*. **13**(11), 460–469.

Ke, Q., Costa, M. (2006) Hypoxia-Inducible Factor-1 (HIF-1). *Molecular Pharmacology*. **70**(5), 1469–1480.

Khaznadar, Z., Henry, G., Setterblad, N., Agaugue, S., Raffoux, E., Boissel, N., Dombret, H., Toubert, A., Dulphy, N. (2014) Acute myeloid leukemia impairs natural killer cells through the formation of a deficient cytotoxic immunological synapse. *European Journal of Immunology*. **44**(10), 3068–3080.

Kikushige, Y., Miyamoto, T. (2013) TIM-3 as a novel therapeutic target for eradicating acute myelogenous leukemia stem cells. *International journal of hematology*. **98**(6), 627–33.

Kikushige, Y., Miyamoto, T., Yuda, J., Jabbarzadeh-Tabrizi, S., Shima, T., Takayanagi, S., Niiro, H., Yurino, A., Miyawaki, K., Takenaka, K., Iwasaki, H., Akashi, K. (2015) A TIM-3/Gal-9 Autocrine Stimulatory Loop Drives Self-Renewal of Human Myeloid Leukemia Stem Cells and Leukemic Progression. *Cell Stem Cell*. **17**(3), 341–352.

Kikushige, Y., Shima, T., Takayanagi, S., Urata, S., Miyamoto, T., Iwasaki, H., Takenaka, K., Teshima, T., Tanaka, T., Inagaki, Y., Akashi, K. (2010) TIM-3 is a promising target to selectively kill acute myeloid leukemia stem cells. *Cell stem cell*. **7**(6), 708–17.

Kim, M.-S., Kuehn, H.S., Metcalfe, D.D., Gilfillan, A.M. (2008) Activation and Function of

the mTORC1 Pathway in Mast Cells. *The Journal of Immunology*. **180**(7), 4586–4595.

Kirshenbaum, A.S., Akin, C., Wu, Y., Rottem, M., Goff, J.P., Beaven, M.A., Rao, V.K., Metcalfe, D.D. (2003) Characterization of novel stem cell factor responsive human mast cell lines LAD 1 and 2 established from a patient with mast cell sarcoma/leukemia; activation following aggregation of Fc?RI or Fc?RI. *Leukemia Research*. **27**(8), 677–682.

Kobayashi, T., Kuroda, J., Ashihara, E., Oomizu, S., Terui, Y., Taniyama, A., Adachi, S., Takagi, T., Yamamoto, M., Sasaki, N., Horiike, S., Hatake, K., Yamauchi, A., Hirashima, M., Taniwaki, M. (2010) Galectin-9 exhibits anti-myeloma activity through JNK and p38 MAP kinase pathways. *Leukemia*. **24**(4), 843–850.

Koh, H.S., Chang, C.Y., Jeon, S.-B., Yoon, H.J., Ahn, Y.-H., Kim, H.-S., Kim, I.-H., Jeon, S.H., Johnson, R.S., Park, E.J. (2015) The HIF-1/glial TIM-3 axis controls inflammation-associated brain damage under hypoxia. *Nature Communications*. **6**, 6340.

Kurinna, S., Konopleva, M., Palla, S.L., Chen, W., Kornblau, S., Contractor, R., Deng, X., May, W.S., Andreeff, M., Ruvolo, P.P. (2006) Bcl2 phosphorylation and active PKC α are associated with poor survival in AML. *Leukemia*. **20**(7), 1316–1319.

Laplante, M., Sabatini, D.M. (2009) mTOR signaling at a glance. *Journal of Cell Science*. **122**(20), 3589–3594.

Lee, J., Lee, S.J., Lim, K.T. (2014) ZPDC glycoprotein (24kDa) induces apoptosis and enhances activity of NK cells in N-nitrosodiethylamine-injected Balb/c. *Cellular Immunology*. **289**(1–2), 1–6.

Li, X., He, X., Ma, C., Wang, L., Li, H., Li, F., Hou, M. (2016) Tim-3 as a leukemia stem cell specific marker expressing on bone marrow mononuclear cells is a factor for prognosis evaluation in patients with acute myelogenous leukemia. . **9**(6), 10979–10986.

Liang, J., Wu, Y.-L., Chen, B.-J., Zhang, W., Tanaka, Y., Sugiyama, H. (2013) The C-Kit Receptor-Mediated Signal Transduction and Tumor-Related Diseases. *International Journal of Biological Sciences*. **9**(5), 435–443.

Lu, C., Hassan, H.T. (2006) Human stem cell factor-antibody [anti-SCF] enhances chemotherapy cytotoxicity in human CD34+ resistant myeloid leukaemia cells. *Leukemia Research*. **30**(3), 296–302.

Ma, C.J., Li, G.Y., Cheng, Y.Q., Wang, J.M., Ying, R.S., Shi, L., Wu, X.Y., Niki, T., Hirashima, M., Li, C.F., Moorman, J.P., Yao, Z.Q. (2013) Cis Association of Galectin-9 with Tim-3 Differentially Regulates IL-12/IL-23 Expressions in Monocytes via TLR Signaling Y. Hoshino, ed. *PLoS ONE*. **8**(8), e72488.

Mabuchi, R., Hara, T., Matsumoto, T., Shibata, Y., Nakamura, N., Nakamura, H., Kitagawa, J., Kanemura, N., Goto, N., Shimizu, M., Ito, H., Yamamoto, Y., Saito, K., Moriwaki, H., Tsurumi, H. (2016) High serum concentration of L-kynurenine predicts unfavorable outcomes in patients with acute myeloid leukemia. *Leukemia & Lymphoma*. **57**(1), 92–98.

MacNeil, A.J., Junkins, R.D., Wu, Z., Lin, T.-J. (2014) Stem cell factor induces AP-1-dependent mast cell IL-6 production via MAPK kinase 3 activity. *Journal of Leukocyte*

Biology. **95**(6), 903–915.

Micol, V., Sánchez-Piñera, P., Villalaín, J., de Godos, a, Gómez-Fernández, J.C. (1999) Correlation between protein kinase C alpha activity and membrane phase behavior. *Biophysical journal*. **76**(2), 916–27.

Moller-Hackbarth, K., Dewitz, C., Schweigert, O., Trad, A., Garbers, C., Rose-John, S., Scheller, J. (2013a) A Disintegrin and Metalloprotease (ADAM) 10 and ADAM17 Are Major Sheddases of T Cell Immunoglobulin and Mucin Domain 3 (Tim-3). *Journal of Biological Chemistry*. **288**(48), 34529–34544.

Moller-Hackbarth, K., Dewitz, C., Schweigert, O., Trad, A., Garbers, C., Rose-John, S., Scheller, J. (2013b) A Disintegrin and Metalloprotease (ADAM) 10 and ADAM17 Are Major Sheddases of T Cell Immunoglobulin and Mucin Domain 3 (Tim-3). *Journal of Biological Chemistry*. **288**(48), 34529–34544.

Morgan, A., Burgoyne, R.D., Barclay, J.W., Craig, T.J., Prescott, G.R., Ciufo, L.F., Evans, G.J.O., Graham, M.E. (2005) Regulation of exocytosis by protein kinase C. *Biochemical Society Transactions*. **33**(6), 1341.

Moritoki, M., Kadowaki, T., Niki, T., Nakano, D., Soma, G., Mori, H., Kobara, H., Masaki, T., Kohno, M., Hirashima, M. (2013) Galectin-9 Ameliorates Clinical Severity of MRL/lpr Lupus-Prone Mice by Inducing Plasma Cell Apoptosis Independently of Tim-3 P. Bobé, ed. *PLoS ONE*. **8**(4), e60807.

National Cancer Institute (2013) What You Need To Know About Leukemia. [online]. Available from: https://www.cancer.gov/publications/patient-education/leukemia.pdf [Accessed February 17, 2017].

Orkin, S.H., Zon, L.I. (2008) Hematopoiesis: An Evolving Paradigm for Stem Cell Biology. *Cell*. **132**(4), 631–644.

Passegue, E., Jamieson, C.H.M., Ailles, L.E., Weissman, I.L. (2003) Normal and leukemic hematopoiesis: Are leukemias a stem cell disorder or a reacquisition of stem cell characteristics? *Proceedings of the National Academy of Sciences*. **100**(Supplement 1), 11842–11849.

Pinkel, D., Straume, T., Gray, J.W. (1986) Cytogenetic analysis using quantitative, high-sensitivity, fluorescence hybridization. *Proceedings of the National Academy of Sciences*. **83**(9), 2934–2938.

Pokharel, M. (2012) Leukemia : A Review Article. *International Journal of Advanced Research in Pharmacuetical & Bio Sciences*. **2**(3), 397–407.

Porakishvili, N., Roschupkina, T., Kalber, T., Jewell, A.P., Patterson, K., Yong, K., Lydyard, P.M. (2001) Expansion of CD4+ T cells with a cytotoxic phenotype in patients with B-chronic lymphocytic leukaemia (B-CLL). *Clinical and Experimental Immunology*. **126**(1), 29–36.

Prokhorov, A., Gibbs, B.F., Bardelli, M., Rüegg, L., Fasler-Kan, E., Varani, L., Sumbayev, V. V (2015) The immune receptor Tim-3 mediates activation of PI3 kinase/mTOR and HIF-1 pathways in human myeloid leukaemia cells. *The International Journal of Biochemistry & Cell*

Biology. **59**, 11–20.

Pui, C.-H., Relling, M. V., Downing, J.R. (2004) Acute Lymphoblastic Leukemia. *New England Journal of Medicine*. **350**(15), 1535–1548.

Pui, C.-H., Robison, L.L., Look, A.T. (2008) Acute lymphoblastic leukaemia. *Lancet (London, England)*. **371**(9617), 1030–43.

Roskoski, R. (2005) Structure and regulation of Kit protein-tyrosine kinase—The stem cell factor receptor. *Biochemical and Biophysical Research Communications*. **338**(3), 1307–1315.

Sabatini, D.M. (2006) mTOR and cancer: insights into a complex relationship. *Nature Reviews Cancer*. **6**(9), 729–734.

Sarbassov, D.D., Ali, S.M., Sabatini, D.M. (2005) Growing roles for the mTOR pathway. *Current Opinion in Cell Biology*. **17**(6), 596–603.

Schreml, S., Lehle, K., Birnbaum, D.E., Preuner, J.G. (2007) mTOR-inhibitors simultaneously inhibit proliferation and basal IL-6 synthesis of human coronary artery endothelial cells. *International Immunopharmacology*. **7**(6), 781–790.

Semenza, G.L. (2002) HIF-1 and tumor progression: Pathophysiology and therapeutics. *Trends in Molecular Medicine*. **8**(4 SUPPL.).

Shafat, M.S., Gnaneswaran, B., Bowles, K.M., Rushworth, S.A. (2017) The bone marrow microenvironment – Home of the leukemic blasts. *Blood Reviews*.

Silva, J.-P., Lelianova, V.G., Ermolyuk, Y.S., Vysokov, N., Hitchen, P.G., Berninghausen, O., Rahman, M.A., Zangrandi, A., Fidalgo, S., Tonevitsky, A.G., Dell, A., Volynski, K.E., Ushkaryov, Y.A. (2011) Latrophilin 1 and its endogenous ligand Lasso/teneurin-2 form a high-affinity transsynaptic receptor pair with signaling capabilities. *Proceedings of the National Academy of Sciences*. **108**(29), 12113–12118.

Silva, J.-P., Ushkaryov, Y.A. (2010) The Latrophilins, ?Split-Personality? Receptors. In *Advances in Experimental Medicine and Biology*. pp. 59–75.

Spivak, J.L. (2017) Overview of Leukemia. *Johns Hopkins University School of Medicine*. [online]. Available from: http://www.msdmanuals.com/en-gb/professional/hematology-and-oncology/leukemias/overview-of-leukemia#v974585 [Accessed April 4, 2017].

Stöckli, J., Fazakerley, D.J., James, D.E. (2011) GLUT4 exocytosis. *Journal of Cell Science*. **124**(24), 4147–4159.

Sumbayev, V. V. (2008) LPS-induced Toll-like receptor 4 signalling triggers cross-talk of apoptosis signal-regulating kinase 1 (ASK1) and HIF-1?? protein. *FEBS Letters*. **582**(2), 319–326.

Sumbayev, V. V., Yasinska, I., Oniku, A.E., Streatfield, C.L., Gibbs, B.F. (2012) Involvement of hypoxia-inducible factor-1 in the inflammatory responses of human LAD2 mast cells and basophils. *PLoS ONE*. **7**(3).

Swamydas, M., Lionakis, M.S. (2013) Isolation, Purification and Labeling of Mouse Bone Marrow Neutrophils for Functional Studies and Adoptive Transfer Experiments. *Journal of Visualized Experiments*. (77), 1–7.

Tandon, R., Chew, G.M., Byron, M.M., Borrow, P., Niki, T., Hirashima, M., Barbour, J.D., Norris, P.J., Lanteri, M.C., Martin, J.N., Deeks, S.G., Ndhlovu, L.C. (2014) Galectin-9 Is Rapidly Released During Acute HIV-1 Infection and Remains Sustained at High Levels Despite Viral Suppression Even in Elite Controllers. *AIDS Research and Human Retroviruses*. **30**(7), 654–664.

Tang, D., Lotze, M.T. (2012) Tumor immunity times out: TIM-3 and HMGB1. *Nature Immunology*. **13**(9), 808–810.

Thornalley, P.J. (1993) The glyoxalase system in health and disease. *Molecular Aspects of Medicine*. **14**(4), 287–371.

Volynski, K.E., Capogna, M., Ashton, A.C., Thomson, D., Orlova, E. V., Manser, C.F., Ribchester, R.R., Ushkaryov, Y.A. (2003) Mutant α-latrotoxin (LTXN4C) does not form pores and clauses secretion by receptor stimulation. This action does not require neurexins. *Journal of Biological Chemistry*. **278**(33), 31058–31066.

Wang, C., Liu, J., Wang, L., Geng, X. (2008) Solubilization and Refolding with Simultaneous Purification of Recombinant Human Stem Cell Factor. *Applied Biochemistry and Biotechnology*. **144**(2), 181–189.

Wang, F., He, W., Zhou, H., Yuan, J., Wu, K., Xu, L., Chen, Z.K. (2007) The Tim-3 ligand galectin-9 negatively regulates CD8+ alloreactive T cell and prolongs survival of skin graft. *Cellular Immunology*. **250**(1–2), 68–74.

Wang, H., Naghavi, M., Allen, C., Barber, R.M., Bhutta, Z.A., Carter, A., Casey, D.C., Charlson, F.J., Chen, A.Z., Coates, M.M., Coggeshall, M., Dandona, L., Dicker, D.J., Erskine, H.E., Ferrari, A.J., Fitzmaurice, C., Foreman, K., Forouzanfar, M.H., Fraser, M.S., Fullman, N., Gething, P.W., Goldberg, E.M., Graetz, N., Haagsma, J.A., Hay, S.I., Huynh, C., Johnson, C.O., Kassebaum, N.J., Kinfu, Y., Kulikoff, X.R., Kutz, M., Kyu, H.H., Larson, H.J., Leung, J., Liang, X., Lim, S.S., Lind, M., Lozano, R., Marquez, N., Mensah, G.A., Mikesell, J., Mokdad, A.H., Mooney, M.D., Nguyen, G., Nsoesie, E., Pigott, D.M., Pinho, C., Roth, G.A., Salomon, J.A., Sandar, L., Silpakit, N., Sligar, A., Sorensen, R.J.D., Stanaway, J., Steiner, C., Teeple, S., Thomas, B.A., Troeger, C., VanderZanden, A., Vollset, S.E., Wanga, V., Whiteford, H.A., Wolock, T., Zoeckler, L., Abate, K.H., Abbafati, C., Abbas, K.M., Abd-Allah, F., Abera, S.F., Abreu, D.M.X., Abu-Raddad, L.J., Abyu, G.Y., Achoki, T., Adelekan, A.L., Ademi, Z., Adou, A.K., Adsuar, J.C., Afanvi, K.A., Afshin, A., Agardh, E.E., Agarwal, A., Agrawal, A., Kiadaliri, A.A., Ajala, O.N., Akanda, A.S., Akinyemi, R.O., Akinyemiju, T.F., Akseer, N., Lami, F.H. Al, Alabed, S., Al-Aly, Z., Alam, K., Alam, N.K.M., Alasfoor, D., Aldhahri, S.F., Aldridge, R.W., Alegretti, M.A., Aleman, A. V., Alemu, Z.A., Alexander, L.T., Alhabib, S., Ali, R., Alkerwi, A., Alla, F., Allebeck, P., Al-Raddadi, R., Alsharif, U., Altirkawi, K.A., Martin, E.A., Alvis-Guzman, N., Amare, A.T., Amegah, A.K., Ameh, E.A., Amini, H., Ammar, W., Amrock, S.M., Andersen, H.H., Anderson, B.O., Anderson, G.M., Antonio, C.A.T., Aregay, A.F., Ärnlöv, J., Arsenijevic, V.S.A., Artaman, A., Asayesh, H., Asghar, R.J., Atique, S., Avokpaho, E.F.G.A., Awasthi, A., Azzopardi, P., Bacha, U., Badawi, A., Bahit, M.C., Balakrishnan, K., Banerjee, A., Barac, A., Barker-Collo, S.L., Bärnighausen, T.,

Barregard, L., Barrero, L.H., Basu, A., Basu, S., Bayou, Y.T., Bazargan-Hejazi, S., Beardsley, J., Bedi, N., Beghi, E., Belay, H.A., Bell, B., Bell, M.L., Bello, A.K., Bennett, D.A., Bensenor, I.M., Berhane, A., Bernabé, E., Betsu, B.D., Beyene, A.S., Bhala, N., Bhalla, A., Biadgilign, S., Bikbov, B., Abdulhak, A.A. Bin, Biroscak, B.J., Biryukov, S., Bjertness, E., Blore, J.D., Blosser, C.D., Bohensky, M.A., Borschmann, R., Bose, D., Bourne, R.R.A., Brainin, M., Brayne, C.E.G., Brazinova, A., Breitborde, N.J.K., Brenner, H., Brewer, J.D., Brown, A., Brown, J., Brugha, T.S., Buckle, G.C., Butt, Z.A., Calabria, B., Campos-Nonato, I.R., Campuzano, J.C., Carapetis, J.R., Cárdenas, R., Carpenter, D.O., Carrero, J.J., Castañeda-Orjuela, C.A., Rivas, J.C., Catalá-López, F., Cavalleri, F., Cercy, K., Cerda, J., Chen, W., Chew, A., Chiang, P.P.-C., Chibalabala, M., Chibueze, C.E., Chimed-Ochir, O., Chisumpa, V.H., Choi, J.-Y.J., Chowdhury, R., Christensen, H., Christopher, D.J., Ciobanu, L.G., Cirillo, M., Cohen, A.J., Colistro, V., Colomar, M., Colquhoun, S.M., Cooper, C., Cooper, L.T., Cortinovis, M., Cowie, B.C., Crump, J.A., Damsere-Derry, J., Danawi, H., Dandona, R., Daoud, F., Darby, S.C., Dargan, P.I., das Neves, J., Davey, G., Davis, A.C., Davitoiu, D. V., de Castro, E.F., de Jager, P., Leo, D. De, Degenhardt, L., Dellavalle, R.P., Deribe, K., Deribew, A., Dharmaratne, S.D., Dhillon, P.K., Diaz-Torné, C., Ding, E.L., dos Santos, K.P.B., Dossou, E., Driscoll, T.R., Duan, L., Dubey, M., Duncan, B.B., Ellenbogen, R.G., Ellingsen, C.L., Elyazar, I., Endries, A.Y., Ermakov, S.P., Eshrati, B., Esteghamati, A., Estep, K., Faghmous, I.D.A., Fahimi, S., Faraon, E.J.A., Farid, T.A., Farinha, C.S. e S., Faro, A., Farvid, M.S., Farzadfar, F., Feigin, V.L., Fereshtehnejad, S.-M., Fernandes, J.G., Fernandes, J.C., Fischer, F., Fitchett, J.R.A., Flaxman, A., Foigt, N., Fowkes, F.G.R., Franca, E.B., Franklin, R.C., Friedman, J., Frostad, J., Fürst, T., Futran, N.D., Gall, S.L., Gambashidze, K., Gamkrelidze, A., Ganguly, P., Gankpé, F.G., Gebre, T., Gebrehiwot, T.T., Gebremedhin, A.T., Gebru, A.A., Geleijnse, J.M., Gessner, B.D., Ghoshal, A.G., Gibney, K.B., Gillum, R.F., Gilmour, S., Giref, A.Z., Giroud, M., Gishu, M.D., Giussani, G., Glaser, E., Godwin, W.W., Gomez-Dantes, H., Gona, P., Goodridge, A., Gopalani, S.V., Gosselin, R.A., Gotay, C.C., Goto, A., Gouda, H.N., Greaves, F., Gugnani, H.C., Gupta, R., Gupta, R., Gupta, V., Gutiérrez, R.A., Hafezi-Nejad, N., Haile, D., Hailu, A.D., Hailu, G.B., Halasa, Y.A., Hamadeh, R.R., Hamidi, S., Hancock, J., Handal, A.J., Hankey, G.J., Hao, Y., Harb, H.L., Harikrishnan, S., Haro, J.M., Havmoeller, R., Heckbert, S.R., Heredia-Pi, I.B., Heydarpour, P., Hilderink, H.B.M., Hoek, H.W., Hogg, R.S., Horino, M., Horita, N., Hosgood, H.D., Hotez, P.J., Hoy, D.G., Hsairi, M., Htet, A.S., Htike, M.M.T., Hu, G., Huang, C., Huang, H., Huiart, L., Husseini, A., Huybrechts, I., Huynh, G., Iburg, K.M., Innos, K., Inoue, M., Iyer, V.J., Jacobs, T.A., Jacobsen, K.H., Jahanmehr, N., Jakovljevic, M.B., James, P., Javanbakht, M., Jayaraman, S.P., Jayatilleke, A.U., Jeemon, P., Jensen, P.N., Jha, V., Jiang, G., Jiang, Y., Jibat, T., Jimenez-Corona, A., Jonas, J.B., Joshi, T.K., Kabir, Z., Kamal, R., Kan, H., Kant, S., Karch, A., Karema, C.K., Karimkhani, C., Karletsos, D., Karthikeyan, G., Kasaeian, A., Katibeh, M., Kaul, A., Kawakami, N., Kayibanda, J.F., Keiyoro, P.N., Kemmer, L., Kemp, A.H., Kengne, A.P., Keren, A., Kereselidze, M., Kesavachandran, C.N., Khader, Y.S., Khalil, I.A., Khan, A.R., Khan, E.A., Khang, Y.-H., Khera, S., Khoja, T.A.M., Kieling, C., Kim, D., Kim, Y.J., Kissela, B.M., Kissoon, N., Knibbs, L.D., Knudsen, A.K., Kokubo, Y., Kolte, D., Kopec, J.A., Kosen, S., Koul, P.A., Koyanagi, A., Krog, N.H., Defo, B.K., Bicer, B.K., Kudom, A.A., Kuipers, E.J., Kulkarni, V.S., Kumar, G.A., Kwan, G.F., Lal, A., Lal, D.K., Lalloo, R., Lallukka, T., Lam, H., Lam, J.O., Langan, S.M., Lansingh, V.C., Larsson, A., Laryea, D.O., Latif, A.A., Lawrynowicz, A.E.B., Leigh, J., Levi, M., Li, Y., Lindsay, M.P., Lipshultz, S.E., Liu, P.Y., Liu, S., Liu, Y., Lo, L.-T., Logroscino, G., Lotufo, P.A., Lucas, R.M., Lunevicius, R., Lyons, R.A., Ma, S., Machado, V.M.P., Mackay, M.T., MacLachlan, J.H., Razek, H.M.A. El, Magdy, M., Razek, A. El, Majdan, M., Majeed, A., Malekzadeh, R., Manamo, W.A.A., Mandisarisa, J., Mangalam, S., Mapoma, C.C., Marcenes, W., Margolis, D.J., Martin, G.R., Martinez-Raga,

J., Marzan, M.B., Masiye, F., Mason-Jones, A.J., Massano, J., Matzopoulos, R., Mayosi, B.M., McGarvey, S.T., McGrath, J.J., McKee, M., McMahon, B.J., Meaney, P.A., Mehari, A., Mehndiratta, M.M., Mejia-Rodriguez, F., Mekonnen, A.B., Melaku, Y.A., Memiah, P., Memish, Z.A., Mendoza, W., Meretoja, A., Meretoja, T.J., Mhimbira, F.A., Micha, R., Millear, A., Miller, T.R., Mirarefin, M., Misganaw, A., Mock, C.N., Mohammad, K.A., Mohammadi, A., Mohammed, S., Mohan, V., Mola, G.L.D., Monasta, L., Hernandez, J.C.M., Montero, P., Montico, M., Montine, T.J., Moradi-Lakeh, M., Morawska, L., Morgan, K., Mori, R., Mozaffarian, D., Mueller, U.O., Murthy, G.V.S., Murthy, S., Musa, K.I., Nachega, J.B., Nagel, G., Naidoo, K.S., Naik, N., Naldi, L., Nangia, V., Nash, D., Nejjari, C., Neupane, S., Newton, C.R., Newton, J.N., Ng, M., Ngalesoni, F.N., de Dieu Ngirabega, J., Nguyen, Q. Le, Nisar, M.I., Pete, P.M.N., Nomura, M., Norheim, O.F., Norman, P.E., Norrving, B., Nyakarahuka, L., Ogbo, F.A., Ohkubo, T., Ojelabi, F.A., Olivares, P.R., Olusanya, B.O., Olusanya, J.O., Opio, J.N., Oren, E., Ortiz, A., Osman, M., Ota, E., Ozdemir, R., PA, M., Pain, A., Pandian, J.D., Pant, P.R., Papachristou, C., Park, E.-K., Park, J.-H., Parry, C.D., Parsaeian, M., Caicedo, A.J.P., Patten, S.B., Patton, G.C., Paul, V.K., Pearce, N., Pedro, J.M., Stokic, L.P., Pereira, D.M., Perico, N., Pesudovs, K., Petzold, M., Phillips, M.R., Piel, F.B., Pillay, J.D., Plass, D., Platts-Mills, J.A., Polinder, S., Pope, C.A., Popova, S., Poulton, R.G., Pourmalek, F., Prabhakaran, D., Qorbani, M., Quame-Amaglo, J., Quistberg, D.A., Rafay, A., Rahimi, K., Rahimi-Movaghar, V., Rahman, M., Rahman, M.H.U., Rahman, S.U., Rai, R.K., Rajavi, Z., Rajsic, S., Raju, M., Rakovac, I., Rana, S.M., Ranabhat, C.L., Rangaswamy, T., Rao, P., Rao, S.R., Refaat, A.H., Rehm, J., Reitsma, M.B., Remuzzi, G., Resnikoff, S., Ribeiro, A.L., Ricci, S., Blancas, M.J.R., Roberts, B., Roca, A., Rojas-Rueda, D., Ronfani, L., Roshandel, G., Rothenbacher, D., Roy, A., Roy, N.K., Ruhago, G.M., Sagar, R., Saha, S., Sahathevan, R., Saleh, M.M., Sanabria, J.R., Sanchez-Niño, M.D., Sanchez-Riera, L., Santos, I.S., Sarmiento-Suarez, R., Sartorius, B., Satpathy, M., Savic, M., Sawhney, M., Schaub, M.P., Schmidt, M.I., Schneider, I.J.C., Schöttker, B., Schutte, A.E., Schwebel, D.C., Seedat, S., Sepanlou, S.G., Servan-Mori, E.E., Shackelford, K.A., Shaddick, G., Shaheen, A., Shahraz, S., Shaikh, M.A., Shakh-Nazarova, M., Sharma, R., She, J., Sheikhbahaei, S., Shen, J., Shen, Z., Shepard, D.S., Sheth, K.N., Shetty, B.P., Shi, P., Shibuya, K., Shin, M.-J., Shiri, R., Shiue, I., Shrime, M.G., Sigfusdottir, I.D., Silberberg, D.H., Silva, D.A.S., Silveira, D.G.A., Silverberg, J.I., Simard, E.P., Singh, A., Singh, G.M., Singh, J.A., Singh, O.P., Singh, P.K., Singh, V., Soneji, S., Søreide, K., Soriano, J.B., Sposato, L.A., Sreeramareddy, C.T., Stathopoulou, V., Stein, D.J., Stein, M.B., Stranges, S., Stroumpoulis, K., Sunguya, B.F., Sur, P., Swaminathan, S., Sykes, B.L., Szoeke, C.E.I., Tabarés-Seisdedos, R., Tabb, K.M., Takahashi, K., Takala, J.S., Talongwa, R.T., Tandon, N., Tavakkoli, M., Taye, B., Taylor, H.R., Ao, B.J. Te, Tedla, B.A., Tefera, W.M., Have, M. Ten, Terkawi, A.S., Tesfay, F.H., Tessema, G.A., Thomson, A.J., Thorne-Lyman, A.L., Thrift, A.G., Thurston, G.D., Tillmann, T., Tirschwell, D.L., Tonelli, M., Topor-Madry, R., Topouzis, F., Towbin, J.A., Traebert, J., Tran, B.X., Truelsen, T., Trujillo, U., Tura, A.K., Tuzcu, E.M., Uchendu, U.S., Ukwaja, K.N., Undurraga, E.A., Uthman, O.A., Dingenen, R. Van, van Donkelaar, A., Vasankari, T., Vasconcelos, A.M.N., Venketasubramanian, N., Vidavalur, R., Vijayakumar, L., Villalpando, S., Violante, F.S., Vlassov, V.V., Wagner, J.A., Wagner, G.R., Wallin, M.T., Wang, L., Watkins, D.A., Weichenthal, S., Weiderpass, E., Weintraub, R.G., Werdecker, A., Westerman, R., White, R.A., Wijeratne, T., Wilkinson, J.D., Williams, H.C., Wiysonge, C.S., Woldeyohannes, S.M., Wolfe, C.D.A., Won, S., Wong, J.Q., Woolf, A.D., Xavier, D., Xiao, Q., Xu, G., Yakob, B., Yalew, A.Z., Yan, L.L., Yano, Y., Yaseri, M., Ye, P., Yebyo, H.G., Yip, P., Yirsaw, B.D., Yonemoto, N., Yonga, G., Younis, M.Z., Yu, S., Zaidi, Z., Zaki, M.E.S., Zannad, F., Zavala, D.E., Zeeb, H., Zeleke, B.M., Zhang, H., Zodpey, S., Zonies, D., Zuhlke, L.J., Vos, T., Lopez, A.D., Murray, C.J.L. (2016) Global, regional, and national life expectancy, all-cause mortality,

and cause-specific mortality for 249 causes of death, 1980–2015: a systematic analysis for the Global Burden of Disease Study 2015. *The Lancet*. **388**(10053), 1459–1544.

Wang, X., Proud, C.G. (2006) The mTOR pathway in the control of protein synthesis. *Physiology (Bethesda, Md.)*. **21**, 362–9.

Waugh, D.J.J., Wilson, C. (2008) The interleukin-8 pathway in cancer. *Clinical cancer research : an official journal of the American Association for Cancer Research*. **14**(21), 6735–41.

WebMD, L. (2005) WebMD. [online]. Available from: http://www.webmd.com/cancer/lymphoma/bone-marrow-aspiration-and-biopsy#1 [Accessed March 21, 2017].

White, G.R., Varley, J.M., Heighway, J. (1998) Isolation and characterization of a human homologue of the latrophilin gene from a region of 1p31.1 implicated in breast cancer. *Oncogene*. **17**(26), 3513–3519.

World Cancer Research Fund International Worldwide Data. [online]. Available from: http://www.wcrf.org/int/cancer-facts-figures/worldwide-data [Accessed March 17, 2017].

Wrock, M. (2011) Blood Cell Production. [online]. Available from: https://www.slideshare.net/Firedemon13/hematopoiesis [Accessed April 20, 2017].

Wu, L. (2017) Ophthalmologic Manifestations of Leukemias. *Medscape*. [online]. Available from: http://emedicine.medscape.com/article/1201870-overview?pa=ZLunN8raspTlQlgzMYxxhJN65vObysp9omzo9fFxO0y4EDeiBIx1DyAt3yKYS6IAzqDdiv%2FeyjgmzEx%2FA4qLQON5lPYw%2FtQ7Z8WOOzpssmw%3D#a5 [Accessed April 4, 2017].

Yasinska, I.M., Gibbs, B.F., Lall, G.S., Sumbayev, V. V. (2014) The HIF-1 transcription complex is essential for translational control of myeloid hematopoietic cell function by maintaining mTOR phosphorylation. *Cellular and Molecular Life Sciences*. **71**(4), 699–710.

Yoon, S.-J., Lee, M.J., Shin, D.-C., Kim, J.S., Chwae, Y.-J., Kwon, M.-H., Kim, K., Park, S. (2011) Activation of mitogen activated protein kinase-Erk kinase (MEK) increases T cell immunoglobulin mucin domain-3 (TIM-3) transcription in human T lymphocytes and a human mast cell line. *Molecular Immunology*. **48**(15–16), 1778–1783.

7. APPENDIX

7.1 Electrophoresis solutions

7.1.1 Resolution gel

Table 5 Preparation of SDS-polyacrylamide resolution gels.

	7.5%	**10%**	**12%**
H_2O	5.525 ml	4.9 ml	4.4 ml
1.5 M Tris-HCl (pH 8.8)	2.5 ml	2.5 ml	2.5 ml
40% Acrylamide/Bis-acrylamide	1.875 ml	2.5 ml	3.0 ml
10% (w/v) SDS	100 µl	100 µl	100 µl
10% (w/v) APS	125 µl	125 µl	125 µl
TEMED	25 µl	25 µl	25 µl

7.1.2 Stacking Gel

Table 6 Preparation of SDS-polyacrylamide stacking gels.

	4%
H_2O	3.2 ml
0.5 M Tris-HCl (pH 6.8)	1.25 ml
40% Acrylamide/Bis-acrylamide	0.5 ml
10% (w/v) SDS	50 µl
10% (w/v) APS	100 µl
TEMED	20 µl

7.1.3 1.5 M Tris-HCL pH 8.8

Tris 181.5 g
H_2O 1 l

Adjust pH to 8.8 with HCl.

7.1.4 0.5 M Tris-HCL pH 6.8

Tris 60.5 g
H_2O 1 l

Adjust pH to 6.8 with HCl.

7.1.5 10X Running buffer (8.3)

Tris	30 g
Glycine	144 g
SDS	10 g

Add distilled water until 1 l and check the pH.

7.1.6 Sample buffer

Table 7 Sample buffer preparation.

	2X
0.5 M Tris-HCl pH 6.8	1.25 ml
10% SDS	2 ml
Glycerol	2.5 ml
Bromophenol	10 mg
H_2O	3.75 ml

To this solution, 0.05 ml of mercaptoethanol was added prior to use. For 4X sample buffer the quantity of chemical compounds was double.

7.2 Western-blot buffers

7.2.1 10X Blotting Buffer (pH 8.3)

Tris	30.3 g
Glycine	144 g
H_2O	1 l

Check if the pH is 8.3 but do not adjust it.

7.2.2 1X Blotting Buffer (with 20% Methanol)

10X Blotting buffer	100 ml
Methanol	200 ml
H_2O	700 ml

7.2.3 10X TBS buffer (9% NaCl, 100 mM Tris HCl, pH 7.4)

Tris	12.11 g
NaCl	90 g
H_2O	1 l

Ajust the pH to 7.4, using HCl.

7.2.4 1X TBST buffer (pH 7.4)

10X TBS buffer	100 ml
Tween 20	0.5 ml
H_2O	900 ml

7.3 Publications

Caffeine affects the biological responses of human hematopoietic cells of myeloid lineage *via* downregulation of the mTOR pathway and xanthine oxidase activity

Bernhard F. Gibbs[1,*], Isabel Gonçalves Silva[1,*], Alexandr Prokhorov[1,*], Maryam Abooali[1], Inna M. Yasinska[1], Maxwell A. Casely-Hayford[1], Steffen M. Berger[2], Elizaveta Fasler-Kan[2,3], Vadim V. Sumbayev[1]

[1]School of Pharmacy, University of Kent, Chatham Maritime, ME4 4TB Kent, United Kingdom

[2]Department of Pediatric Surgery and Department of Clinical Research, Inselspital, University Hospital, University of Bern, CH-3010 Bern, Switzerland

[3]Department of Biomedicine, University of Basel and University Hospital Basel, CH-4031 Basel, Switzerland

[*]These authors have contributed equally to this work

Correspondence to:
Vadim Sumbayev, **e-mail:** V.Sumbayev@kent.ac.uk
Elizaveta Fasler-Kan, **e-mail:** elizaveta.fasler@insel.ch

Keywords: myeloid cells, caffeine, Inflammation, allergy

Received: July 06, 2015 Accepted: August 31, 2015 Published: September 11, 2015

ABSTRACT

Correction of human myeloid cell function is crucial for the prevention of inflammatory and allergic reactions as well as leukaemia progression. Caffeine, a naturally occurring food component, is known to display anti-inflammatory effects which have previously been ascribed largely to its inhibitory actions on phosphodiesterase. However, more recent studies suggest an additional role in affecting the activity of the mammalian target of rapamycin (mTOR), a master regulator of myeloid cell translational pathways, although detailed molecular events underlying its mode of action have not been elucidated. Here, we report the cellular uptake of caffeine, without metabolisation, by healthy and malignant hematopoietic myeloid cells including monocytes, basophils and primary acute myeloid leukaemia mononuclear blasts. Unmodified caffeine downregulated mTOR signalling, which affected glycolysis and the release of pro-inflammatory/pro-angiogenic cytokines as well as other inflammatory mediators. In monocytes, the effects of caffeine were potentiated by its ability to inhibit xanthine oxidase, an enzyme which plays a central role in human purine catabolism by generating uric acid. In basophils, caffeine also increased intracellular cyclic adenosine monophosphate (cAMP) levels which further enhanced its inhibitory action on mTOR. These results demonstrate an important mode of pharmacological action of caffeine with potentially wide-ranging therapeutic impact for treating non-infectious disorders of the human immune system, where it could be applied directly to inflammatory cells.

INTRODUCTION

Caffeine (1,3,7-trimethylxanthine) is a purine alkaloid present in the leaves, seeds or nuts of a number of plants and is consumed by many people worldwide on a daily basis due to its presence in tea or coffee. In humans, caffeine is rapidly demethylated by cytochrome P450 isoform 1A2 and then converted mostly into methylated derivatives of uric acid by the enzyme xanthine oxidase (XOD) [1]. For a long time caffeine was recognised as an isosteric inhibitor of cyclic adenosine monophosphate phosphodiesterase (cAMP-PDE) which upregulates intracellular cAMP levels [2]. Caffeine was also found to reduce the role of glycolysis in cell energy metabolism *via* upregulation of lipid degradation (lipolysis) [3, 4].

Recent evidence demonstrated that human hematopoietic cells do not express the cytochrome P450 1A2 isoform and thus should not be able to metabolise caffeine, resulting in the effects of unmodified caffeine [5]. In this case, caffeine could competitively inhibit

XOD [6] rather than act as its substrate (most of the other methylxanthines can be converted by XOD). Moreover, several stable purines including caffeine were recently found to inhibit the activity of the mammalian target of rapamycin (mTOR) in somatic cells [7, 8]. It was also demonstrated that at high concentrations (5 mM), caffeine is capable of inhibiting the mTOR pathway in HOS osteosarcoma cells [7]. In addition, 10 mM caffeine was able to inhibit the PI3K/Akt/mTOR/p70S6K pathway in various cell lines including SH-SY5Y neuroblastoma cells and HeLa cells [9]. 10 mM caffeine was even capable of inhibiting the phosphorylation (Ser473) of Akt in SH-SY5Y cells [9]. In myeloid cells mTOR, a highly conserved serine/threonine kinase, acts as a central regulator of cell growth and metabolism and plays crucial pathophysiological roles in host immune defence, allergic reactions and leukaemia [10]. Importantly, the mTOR pathway plays a pivotal role in non-hypoxic activation of the hypoxia-inducible factor 1 (HIF-1) transcription complex in human myeloid cells. HIF-1 controls the expression of over 40 target genes responsible for glycolysis, angiogenesis and cell adhesion – physiological processes which form a critical part of myeloid cell function in the human immune system. This transcription complex, containing an inducible α and a constitutive β subunit, is a major component of the myeloid cell stress adaptation machinery [11, 12]. Therefore, inhibiting the mTOR/HIF-1 metabolic/signalling axis could be an excellent therapeutic strategy for treating human disorders associated with myeloid cell function – leukaemia, autoimmune disease, and allergy. However, existing mTOR inhibitors are toxic and can cause major side effects and adverse drug reactions. Thus, if the inhibitory activity of caffeine on mTOR has indeed been overlooked for decades, this agent may be an excellent non-toxic drug candidate for the correction of pathophysiological responses of human hematopoietic cells of myeloid lineage.

Here we report for the first time that caffeine inhibits the activation of mTOR in THP-1 human myeloid leukaemia cells, primary human acute myeloid leukaemia (AML) cells and primary human basophils. In THP-1 and primary AML cells caffeine was also found to inhibit XOD. In all cases, the caffeine-mediated attenuation of the mTOR pathway led to the downregulation of ligand-induced glycolysis and cytokine/growth factor/mediator production. Caffeine is known to upregulate lipolysis through activation of hormone sensitive lipase (HSL). This upregulates the Krebs' cycle leading to decreased intracellular levels of 2-oxoglutarate (2-OG), thus preventing degradation of HIF-1α protein (the inducible HIF-1 subunit) by a classical mechanism controlled by HIF-1α prolyl hydroxylases (PHDs). This effect was observed in all of the myeloid cell types studied except for basophils, where HIF-1α accumulation was less PHD-dependent and caffeine completely blocked IgE-induced HIF-1α accumulation. High performance liquid chromatography (HPLC) experiments demonstrated that caffeine entered all of the above cell types and was not metabolised. Taken together, our results reveal novel mechanisms for the downregulatory effects of caffeine on the biological responses of human myeloid cells.

RESULTS

Caffeine inhibits ligand-induced activation of the mTOR pathway and its downstream effects in THP-1 human AML cells

We first investigated the effects of caffeine on ligand-induced mTOR activation through phosphorylation of its S2448 residue in THP-1 cells. Cells were exposed for 4 h to ligands (see below) with or without 1 h pre-treatment with 1 mM caffeine (this concentration corresponds to a therapeutic dose of caffeine and is well below the toxic dose [13]). In line with our previous observations [10], we found that pro-inflammatory ligands of Toll-like receptors (TLRs) 2 (plasma membrane-associated TLR – 1 μg/ml peptidoglycan (PGN) was used as a ligand), 7/8 (endosomal TLRs recognising viral single-stranded RNA – 0.1 μg/ml resiquimod (R848) was employed as a ligand) induce activating S2448 phosphorylation of mTOR. The same effect was observed for stem cell factor (SCF), a major hematopoietic factor which is also known to promote growth of leukaemia cells, where caffeine (1 mM) attenuated its effect in all cases (Figure 1). Intriguingly, caffeine alone did not significantly reduce phospho-S2448 mTOR in non-stimulated cells but significantly reduced background levels of phospho-T389 p70 S6K1 and phospho-S65 eIF4E-BP1 (see Figure 1 for details). This suggests that caffeine is likely to act directly on mTOR as well, which would prevent further phosphorylation but not impact on existing activity. The presence of caffeine close to the catalytic site (in the active site of mTOR) would almost certainly affect its kinase activity. However, it is important to stress that phosphorylation of mTOR at the inhibitory T2446 site was not increased by caffeine. This observation clearly suggests that caffeine is unlikely to enhance the activity of this mTOR downregulatory pathway and is likely to be a potential direct mTOR inhibitor, as some other purine containing compounds (such as cAMP) do [8]. Phosphorylation levels of its substrates (indicators of mTOR kinase activity) – p70 S6 kinase 1 (p70 S6K1 – at position T389) and eukaryotic initiation factor 4E-binding protein 1 (eIF4E-BP1 at position S65) were also significantly upregulated by all the employed ligands as well as phosphorylation of S2448 mTOR. All these processes were attenuated by caffeine (Figure 1).

We next investigated the effects of caffeine on mTOR downstream and associated biochemical pathways induced by PGN, R848 and SCF. We found that caffeine did not downregulate PGN-induced accumulation of HIF-1α protein. This was in line with a significant decrease in HIF-1α PHD activity in cells treated with PGN

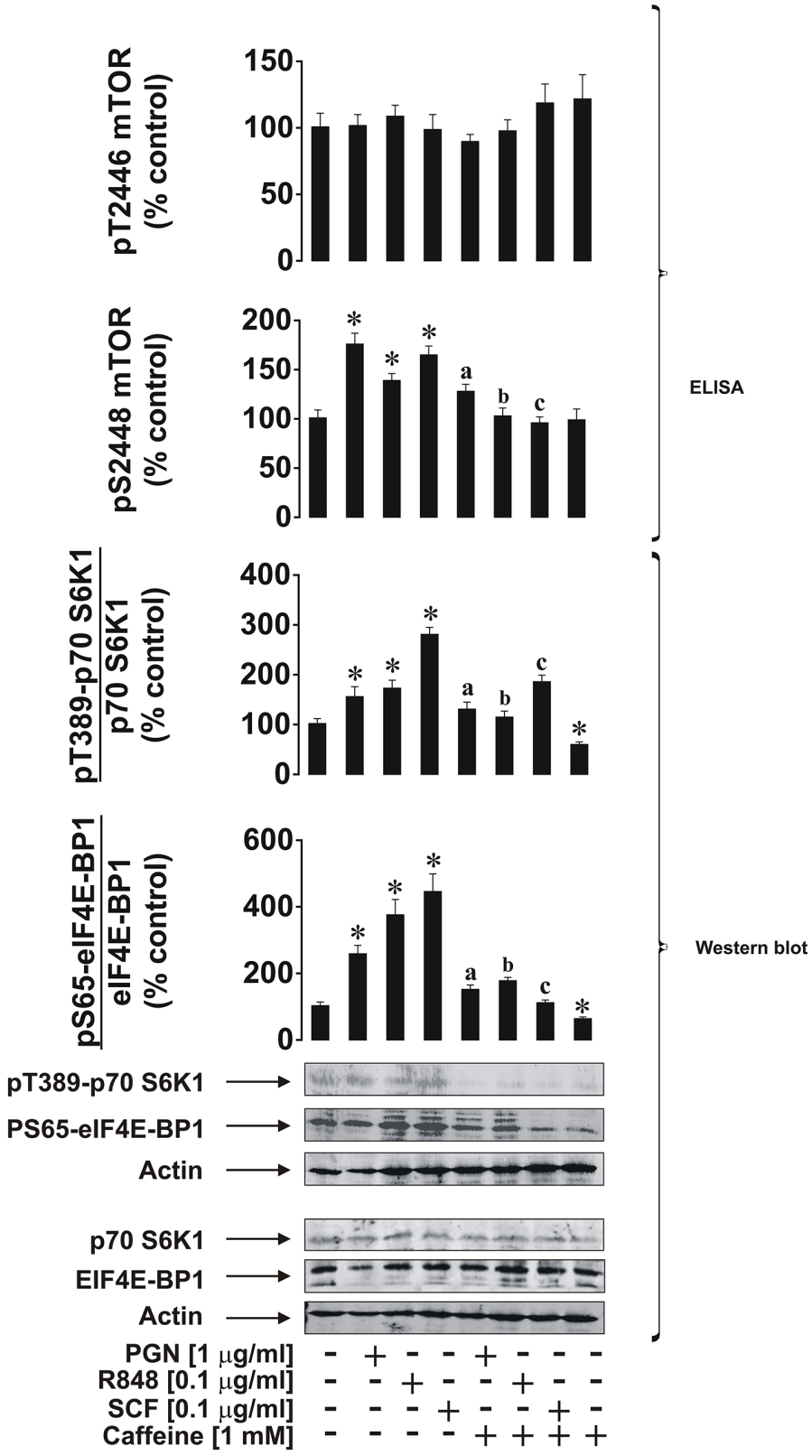

Figure 1: Caffeine inhibits the ligand-induced mTOR signalling pathway in THP-1 human acute myeloid leukaemia cells. Cells were exposed for 4 h to the indicated concentrations of PGN, R848 or SCF with or without 1 h pre-treatment with 1 mM caffeine. Levels of pS2448 and pT2446 phospho-mTOR as well as phosphorylation of its downstream enzymes were analysed as outlined in the Materials and Methods. Western blot data show one representative experiment of four that gave similar results and were quantitatively analysed. Quantitative data are shown as means ± S.D; * – $p < 0.01$ vs. control ($n = 4$), a – $p < 0.01$ vs. PGN alone, b – $p < 0.01$ vs. R848 alone and c – $p < 0.01$ vs. SCF alone.

in the presence of caffeine (Figure 2A). ATP levels, which are often controlled in a HIF-1-dependent manner, were decreased in cells co-stimulated with PGN and caffeine. Levels of cAMP did not undergo significant changes, probably owing to the fact that receptors involved in these events are not G-protein-coupled [14]. They do not provoke adenylate cyclase activation/cAMP production and thus cAMP-PDE-inhibiting activity of caffeine has no effect in this case. AMP levels were also not increased by PGN stimulation, which conforms with our previous observations (Figure 2B). The presence of caffeine did not increase AMP levels despite a significant decrease in PGN-induced XOD activity (Figure 2C). This is likely to be caused by the inhibition of hypoxanthine-guanine phosphoribosyl transferase (HGPRT), an enzyme which converts hypoxanthine (accumulated when XOD was inhibited) into inosine monophosphate (IMP), which is then converted into AMP [15, 16]. However, we could not rule out the possibility of caffeine-dependent effects on other enzymes involved in the conversion of hypoxanthine into AMP. Intracellular reactive oxygen species (ROS) levels upregulated by PGN were also unaffected by caffeine, possibly because XOD is not the main contributor to the intracellular ROS pool (NADPH oxidase plays this role [17]) in this case (Figure 2C). Glycolysis, which was significantly upregulated by PGN, was reduced to its basic level (Figure 2D). This is not surprising, since translation of glycolytic enzymes is likely to be an mTOR-dependent process in human hematopoietic cells [18]. However, intracellular 2-OG levels were almost completely abolished by caffeine (Figure 2D). This may be due to the caffeine-dependent upregulation of lipolysis and, therefore, the Krebs' cycle (which would lead to a reduction of intracellular 2-OG levels and a subsequent decrease in 2-OG-dependent HIF-1α PHD activity, where 2-OG is used as a cofactor [19]; which we observed (Figure 2A)). Furthermore, the pro-inflammatory responses of THP-1 cells induced by PGN (release of TNF-α and IL-6) were attenuated by caffeine (Figure 2E).

The situation with endosomal TLRs 7 and 8 was slightly different, where THP-1 cells were exposed to 0.1 μg/ml R848 with or without 1 h pre-treatment with 1 mM caffeine. We found that, unlike with PGN, R848-induced HIF-1α accumulation was significantly reduced by caffeine. HIF-1α PHD activity was significantly decreased by R848 (as we have reported before [20]), but in the presence of caffeine, PHD activity did not reduce further and was even slightly elevated compared to exposure to R848 alone (Figure 3A). ATP, AMP and cAMP levels in the cells were not affected by caffeine as in the experiments with PGN (Figure 3B). Caffeine inhibited R848-induced XOD activity but also (unlike following the exposure of THP-1 cells to PGN) it reduced intracellular ROS levels upregulated by R848. In the case of endosomal TLRs, XOD contributes to the intracellular ROS pool [17] together with NADPH oxidase (Figure 3C). This result explains the caffeine-dependent decrease in HIF-1α accumulation in THP-1 cells induced by R848, since ROS may play a primary role in the process. Glycolysis was also significantly upregulated in the presence of R848 and this effect was slightly reduced by caffeine. 2-OG levels were significantly reduced (by *ca*. 50%) by caffeine (Figure 3D). R848-induced production of IL-6 and TNF-α were significantly lower in the presence of caffeine (Figure 3E).

SCF-induced biological responses of THP-1 cells were also affected in a way similar to that observed for PGN (see above). THP-1 cells were exposed for 4 h to 0.1 μg/ml SCF with or without 1 h pre-treatment with 1 mM caffeine. We found that SCF-induced HIF-1α accumulation was not decreased in the presence of caffeine which corresponded to a striking decrease in HIF-1α PHD activity in the cells (Figure 4A). ATP, cAMP and AMP levels were not affected at all (Figure 4B). As with TLRs, the Kit receptor, which recognises SCF as a ligand, is not a G-protein coupled receptor (it is a typical receptor tyrosine kinase), and therefore no changes in cAMP levels were observed. SCF-induced XOD activity was reduced by caffeine, however intracellular ROS levels were slightly upregulated by SCF and remained unchanged in the presence of caffeine (Figure 4C). SCF also upregulated glycolysis and caffeine attenuated this process as well as significantly reduced intracellular 2-OG levels (Figure 4D). Finally, SCF-induced vascular endothelial growth factor (VEGF) production was significantly increased upon exposure of the cells to SCF, but this process was attenuated by caffeine (Figure 4D).

In order to confirm that caffeine is able to directly inhibit XOD and, if so, to characterise this process, we studied the kinetics of caffeine effects on purified bovine liver XOD activity using the Lineweaver-Burk approach [21]. We found that caffeine isosterically (in a competitive manner) inhibited XOD (Figure 5). However, the Ki was only 4.022 mM suggesting that caffeine is a weak inhibitor compared to classic XOD inhibitors (for example, allopurinol and sodium tungstate). This confirmed our previous studies showing the ability of caffeine to inhibit XOD *in vitro* but not *in vivo* due to demethylation of the drug.

Caffeine affects SCF-induced responses of primary human AML cells in an mTOR-dependent manner

We sought confirmation of our results using primary human leukocytes. For this purpose we used primary acute myeloid leukaemia cells AML-PB001F purchased from AllCells (Alameda, CA, USA). Cells were exposed to 0.1 μg/ml SCF (these cells express high levels of the Kit receptor) for 4 h with or without 1 h pre-treatment with 1 mM caffeine. We found that SCF induced a significant

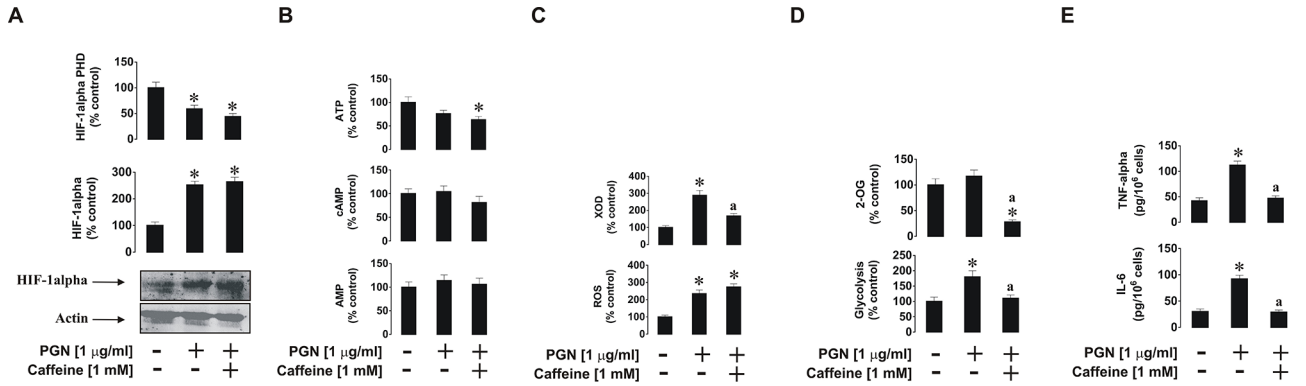

Figure 2: Effects of caffeine on TLR2-mediated biological responses of THP-1 cells. Cells were exposed for 4 h to PGN with or without 1 h pre-treatment with 1 mM caffeine before assessing the indicated biological responses: **A.** HIF-1α accumulation, **B.** ATP/cAMP/AMP levels, **C.** XOD activity and intracellular ROS pool, **D.** glycolysis and 2-OG level as well as **E.** TNF-α/IL-6 release. Western blot data show one representative experiment of three that gave similar results. Quantitative data are shown as means ± S.D; * – $p < 0.01$ vs. control ($n = 3$), a – $p < 0.01$ vs. PGN alone.

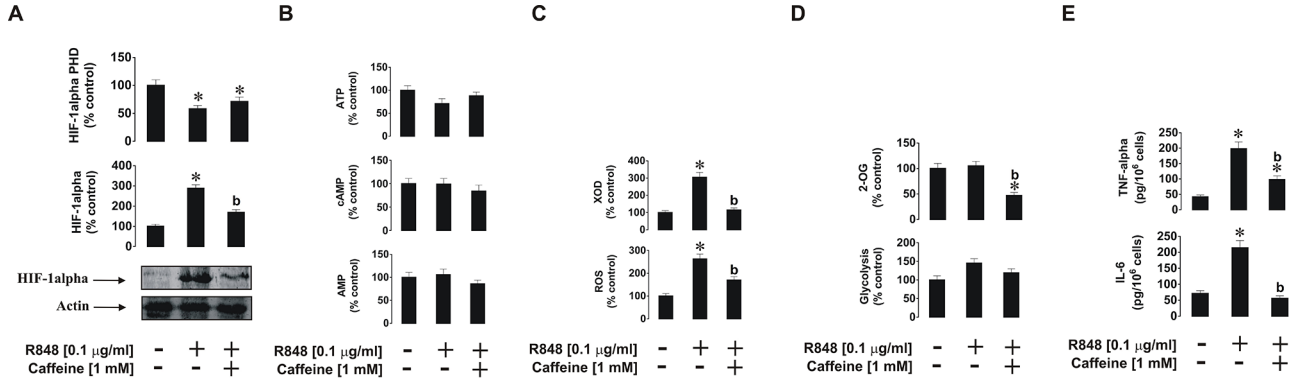

Figure 3: Effects of caffeine on TLR7/8-mediated biological responses of THP-1 cells. Cells were exposed for 4 h to R848 with or without 1 h pre-treatment with 1 mM caffeine before analysing **A.** HIF-1α accumulation, **B.** ATP/cAMP/AMP levels, **C.** XOD activity and intracellular ROS pool, **D.** glycolysis and 2-OG level as well as **E.** TNF-α/IL-6 release. Western blot data show one representative experiment of three that gave similar results. Quantitative data are shown as means ± S.D; * – $p < 0.01$ vs. control ($n = 3$), b – $p < 0.01$ vs. R848 alone.

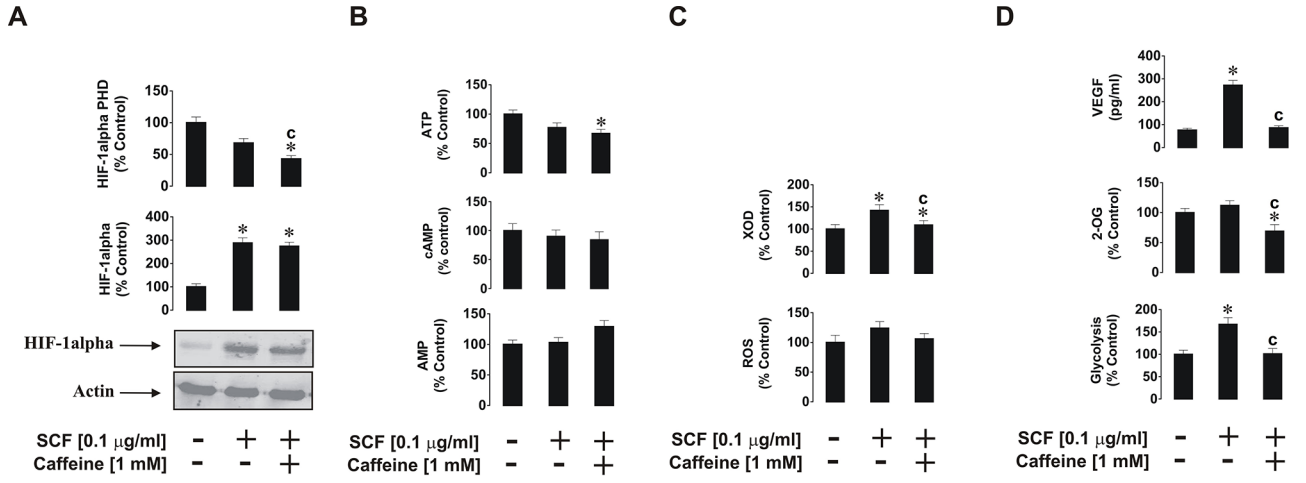

Figure 4: Effects of caffeine on SCF-induced Kit receptor activation in- THP-1 cells. Cells were exposed for 4 h to SCF with or without 1 h pre-treatment with 1 mM caffeine before analysing **A.** HIF-1α accumulation, **B.** ATP/cAMP/AMP levels, **C.** XOD activity and intracellular ROS pool, **D.** glycolysis and 2-OG level as well as VEGF release. Western blot data show one representative experiment of three that gave similar results. Quantitative data are shown as means ± S.D; * – $p < 0.01$ vs. control ($n = 3$), c – $p < 0.01$ vs. SCF alone.

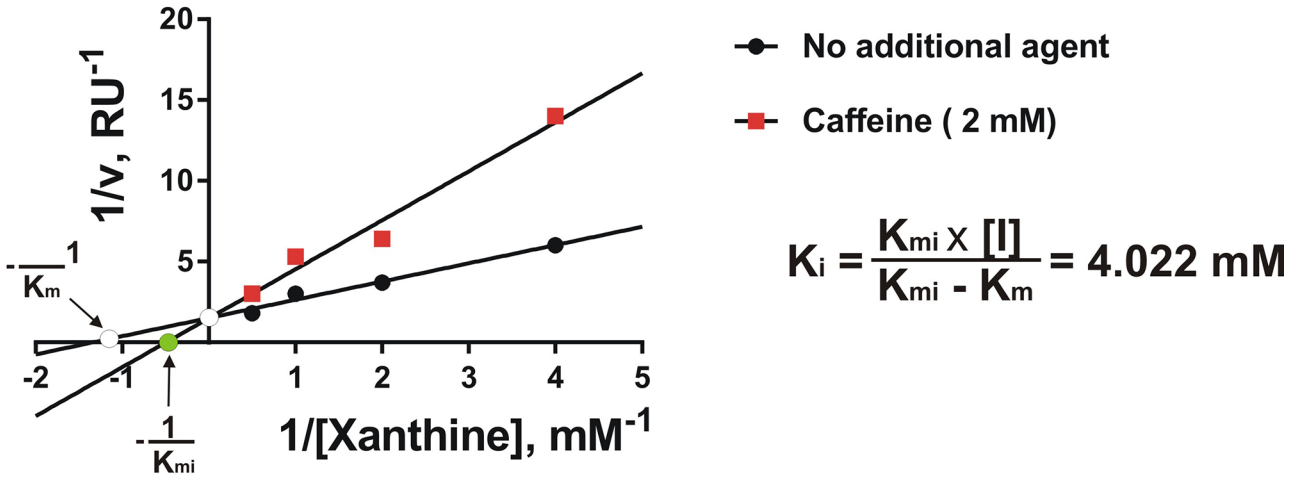

Figure 5: Caffeine is a weak competitive inhibitor of XOD. Kinetics of the effects of caffeine on the activity of purified bovine liver XOD were analysed as described in the Materials and methods. Each point was analysed in quadruplicate.

increase in mTOR phosphorylation at position S2448 and respectively phosphorylation of its substrates – p70 S6K1 and eIF4E-BP1 (Figure 6A). These levels were compared with those in resting primary human leukocytes (PL) obtained from healthy donors (Figure 6A). As in THP-1 cells, SCF induced significant upregulation of HIF-1α accumulation, glycolysis, VEGF release and XOD activity. All these effects were attenuated by caffeine (in the case of HIF-1α – downregulated; the level was still significantly higher than the control) (Figure 6B). Interestingly, background levels of HIF-1α, pS2448 mTOR and XOD activity were significantly higher in primary AML cells compared to primary "healthy" leukocytes (PL) suggesting that these factors/pathways are crucial for AML cell function. Importantly, resting primary human leukocytes obtained from the blood of healthy donors did not accumulate detectable amounts of HIF-1α protein.

Given the effects of caffeine on AML cell function, we next determined the concentration-dependent actions of caffeine on these cells following exposure to 0.1 μg/ml SCF for 4 h with or without 1 h pre-treatment with 0.01, 0.1 and 1 mM caffeine. Levels of pS2448 mTOR were monitored as a biochemical response. We found that SCF-dependent mTOR phosphorylation was significantly affected by 1 and 0.1 but not 0.01 mM caffeine (Figure 7).

Caffeine downregulates anti-IgE-induced activation of human basophils by affecting mTOR signalling

We were next interested in investigating the effects of caffeine on primary human basophils. These terminally differentiated granulocytes display biochemically similar but pathophysiologically different responses compared to THP-1 and primary AML cells. Furthermore, basophils play a crucial role in human allergic reactions since they readily respond to IgE-dependent triggering, although compared to leukaemic myeloid cells they are relatively unresponsive to SCF [22] and TLR2/4 ligands [23]. Stimulation of primary human basophils with 1 μg/ml anti-IgE led to the activation of mTOR phosphorylation at S2448, which was attenuated by caffeine (Figure 8). Similar effects were observed regarding the phosphorylation of mTOR substrates (Figure 8).

As shown previously [24], HIF-1α accumulation was upregulated by anti-IgE. This process was completely blocked by caffeine and the process appeared to be independent of PHD activity, since no significant changes were observed in enzyme activity (Figure 9A). Importantly, we could not detect any XOD activity in basophils, which is supported by our previous observations [21]. Western blot analysis (Figure 9A) demonstrated the absence of XOD protein in basophils. ATP and AMP levels were not affected by any of the treatments; however, cAMP levels were significantly upregulated by anti-IgE and were further increased in the presence of 1 mM caffeine (Figure 9B). This suggests that IgE-induced responses in basophils are indirectly linked to G-protein-coupled receptor signalling, possibly due to the actions of histamine acting through H2 receptors, which may serve as a negative feedback loop limiting further basophil degranulation and histamine release. Intracellular ROS levels were not affected which confirms our previous findings suggesting that IgE-induced basophil responses are orchestrated in a redox-independent manner (Figure 9C). IgE-dependent histamine release was significantly affected by caffeine which is in line with the observed caffeine-dependent downregulation of IgE-induced glycolysis and 2-OG levels (Figure 9D). However, the effect associated with 2-OG levels did not impact HIF-1α accumulation or PHD activity, further confirming our hypothesis that this process is most likely to be PHD-independent in basophils.

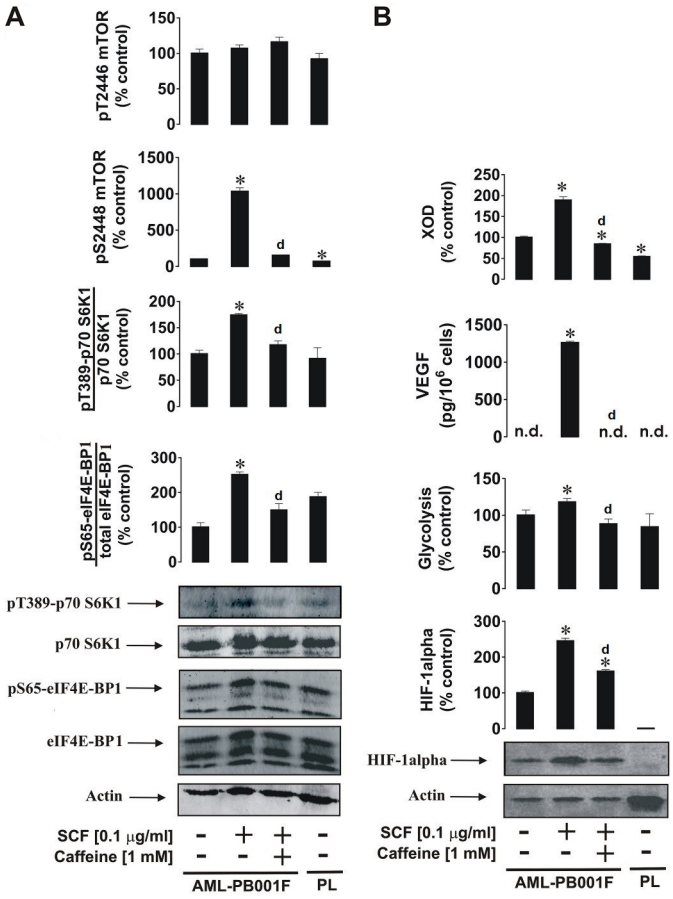

Figure 6: Effects of caffeine on SCF-induced Kit receptor activation in primary human AML cells. AML-PB001F cells were exposed for 4 h to SCF with or without 1 h pre-treatment with 1 mM caffeine before analysis of **A.** mTOR phosphorylation and its biological activity and **B.** HIF-1α accumulation, glycolysis, VEGF release and XOD activity. Western blot data (50,000 cells per well were loaded in each case for AML cells and 90,000 for healthy primary leucocytes) show one representative experiment of three-four (using cells derived from different donors) that gave similar results. In both panels A and B we also show the results obtained from non-treated healthy primary human leukocytes (PL) handled as described in Materials and Methods. Quantitative data are shown as means ± S.D; * – $p < 0.01$ vs. control ($n = 4$ for panel A and $n = 3$ for panel B), d – $p < 0.01$ vs. SCF alone.

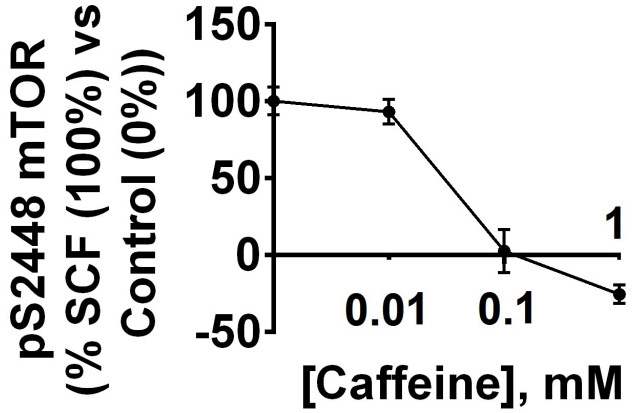

Figure 7: Dose-dependent effects of caffeine on SCF-induced Kit receptor-mediated intracellular pS2448 mTOR levels. AML-PB001F cells were exposed for 4 h to 0.1 μg/ml of SCF with or without 1 h pre-treatment with 0.01, 0.1 or 1 mM caffeine. pS2448 mTOR levels were analysed. Quantitative data are shown as means ± S.D of three individual experiments; * – $p < 0.01$ vs. control.

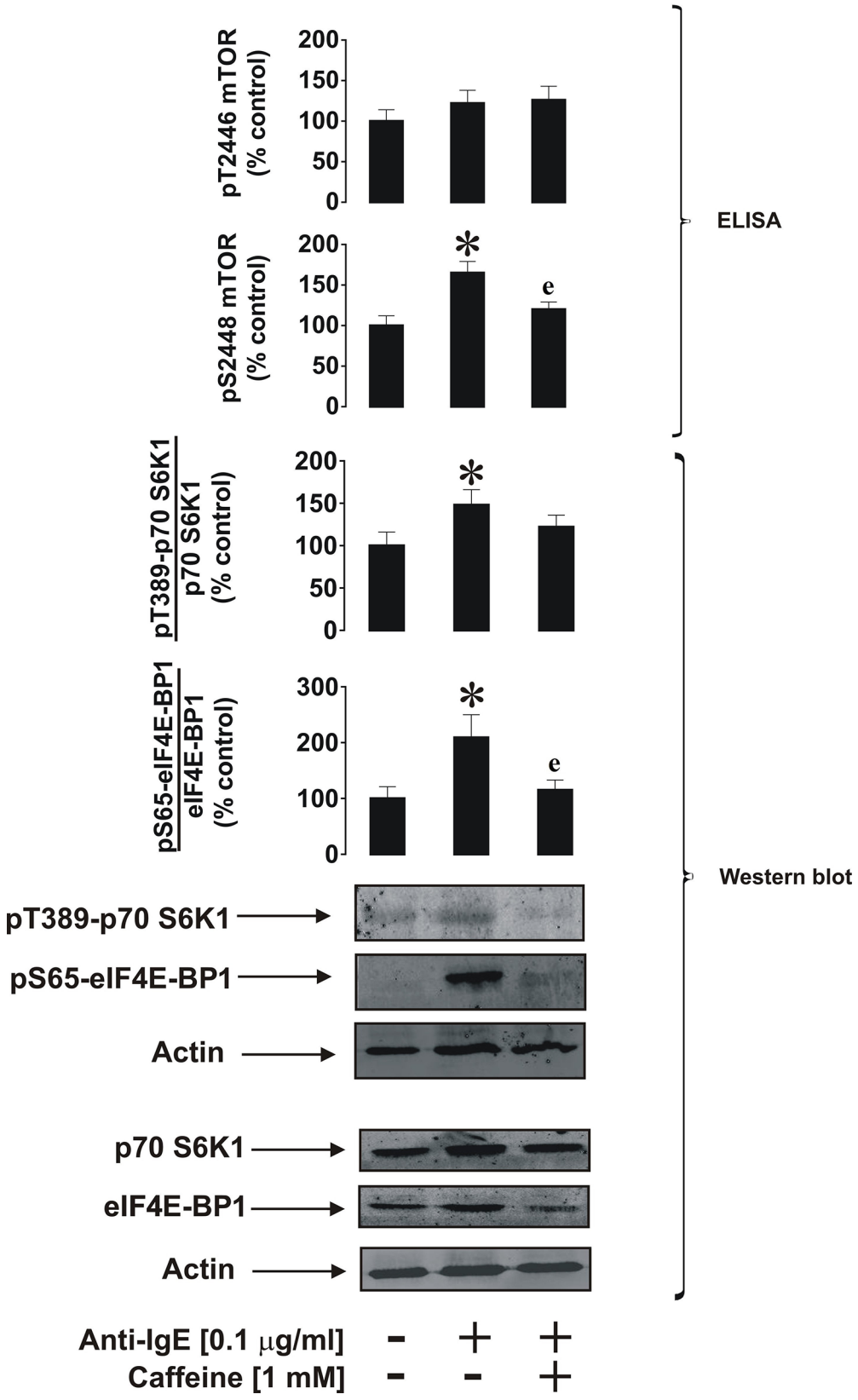

Figure 8: Caffeine inhibits ligand-induced mTOR signalling pathway in primary human basophils. Cells were exposed for 2 h to 0.1 μg/ml anti-IgE with or without 30 min pre-treatment with 1 mM caffeine. pS2448 and pT2446 phospho-mTOR levels as well as phosphorylation of its downstream enzymes were analysed as described in Materials and Methods. Western blot data show one representative experiment of four that gave similar results. Quantitative data are shown as means ± S.D; * – $p < 0.01$ vs. control ($n = 4$), e – $p < 0.01$ vs. anti-IgE alone.

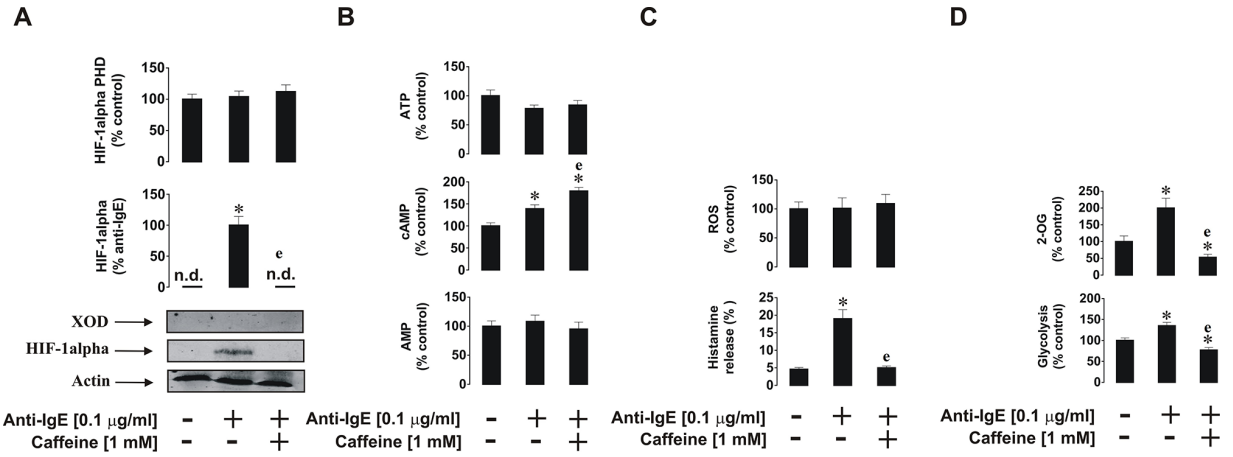

Figure 9: Effects of caffeine on the anti-IgE-induced biological responses of primary human basophils. Cells were exposed for 2 h to 0.1 μg/ml anti-IgE with or without 30 min pre-treatment with 1 mM caffeine before analysis of **A.** HIF-1α accumulation and XOD protein levels, **B.** ATP/cAMP/AMP levels, **C.** intracellular ROS pool and histamine release, **D.** glycolysis and 2-OG level. Western blot data show one representative experiment of three that gave similar results. Quantitative data are shown as means ± S.D ; * – $p < 0.01$ vs. control ($n = 3$), e – $p < 0.01$ vs. anti-IgE alone.

We next further verified the differential involvement of XOD in the biological responses of myeloid cells by assessing whether basophil function could be affected by XOD inhibitors/substrate. We studied the effects of the XOD inhibitor allopurinol, the XOD substrate hypoxanthine (hypoxanthine – chemically is an allopurinol isomer) and the highly specific XOD inhibitor sodium tungstate. Neither of these compounds, however, was able to significantly affect anti-IgE-stimulated basophil histamine release and HIF-1α accumulation (Supplementary Figure S1). We also noticed that, while 0.01 mM caffeine did not significantly inhibit IgE-induced histamine release, HIF-1α accumulation was still markedly reduced at this low caffeine concentration (Supplementary Figure S1). This provides further confirmation of our previous observations [24] suggesting that histamine release and HIF-1 activation are controlled by biochemically independent pathways.

Caffeine is taken up but not metabolised by human myeloid cells

In order to ascertain whether the observed effects described above were due to caffeine or a metabolite we investigated whether the different myeloid cell types employed in the study could metabolised caffeine following cellular uptake. We found that neither THP-1 cells nor primary human leukocytes nor basophils contained the cytochrome P450 1A2 isoform which is primarily responsible for caffeine demethylation (data not shown since they are at zero levels). We then assessed whether caffeine (a) enters the studied cells and (b) is metabolised through other pathways. For this purpose we used high-performance liquid chromatography (HPLC) in order to detect caffeine and its metabolites. As a positive control we used urine of healthy volunteers following consumption of caffeine by them. In the urine we detected six caffeine metabolites as well as unmodified caffeine, suggesting that all the metabolites are detectable by our method and that caffeine is mostly metabolised *in vivo* in humans (Figure 10). In both THP-1 cells and primary human basophils we detected caffeine but none of its metabolites, suggesting that caffeine is endocytosed into these myeloid cells but is not further metabolised. This finding was confirmed by the fact that none of the caffeine metabolites was detected in the culture medium; only unmodified caffeine was detected (Figure 10). These data suggest that the effects of caffeine observed in the study were solely caused by unmodified caffeine.

Taken together, our results demonstrate for the first time that caffeine affects the biological responses of human myeloid cells, including leukaemia cell lines, primary AML cells and primary human basophils by downregulating the mTOR pathway and differentially inhibiting XOD.

DISCUSSION

Caffeine, a plant-derived purine alkaloid, was chemically identified over 100 years ago and its effects were observed even before Biochemistry developed into an independent field of science [1]. However, due to its metabolism and labile properties, the effects of caffeine in human hematopoietic cells (where it remains unmetabolised) were completely overlooked. Given the fact that some purine compounds were found to directly inhibit mTOR, we were interested to see whether caffeine displays such an activity too. Alternatively, unmodified caffeine was found to inhibit XOD, which we recently showed to play a major role in myeloid cell responses. We were therefore interested in discovering whether caffeine plays a major role

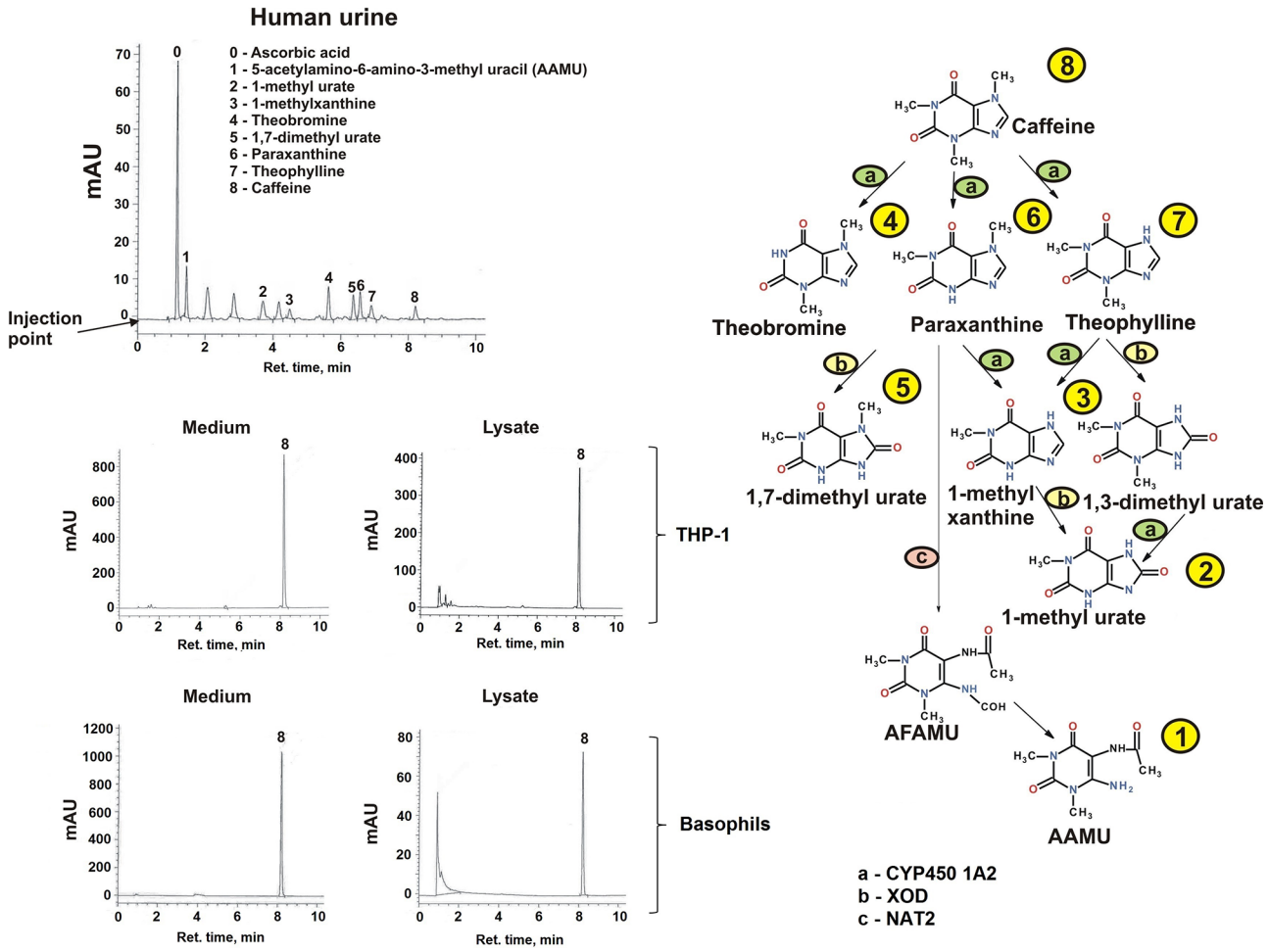

Figure 10: Determination of caffeine and its metabolites in human urine and myeloid cells. Caffeine and its metabolites in human urine (coffee drinkers) and medium/lysates of THP-1 cells (exposed for 4 h to 1 mM caffeine) and human basophils (exposed for 2 h to 1 mM caffeine) were detected by HPLC. The caffeine metabolic pathway in humans is also presented indicating how each metabolite is obtained biochemically. CYP4501A – cytochrome P450 A2; XOD – xanthine oxidase; NAT2 – N-acetyltransferase 2; AAMU – 5 Acetylamino-6-amino-3-methyluracil; AFMU – 5 Acetylamino-6-formylamino-3-methyluracil.

in the biological responses of human hematopoietic cells of myeloid lineage based on its potential actions on XOD and mTOR. These leukocytes determine human innate immune responses and are affected during severe human disorders such as AML and allergy. Thus, elucidating a potentially overlooked mechanism of caffeine may result in additional therapeutic uses for this methylxanthine which was rapidly taken up by these myeloid cells but not metabolised.

We analysed the effects of caffeine on the pro-inflammatory and pro-leukaemic responses of human AML cells using THP-1 cell line and primary AML cells as well as on the pro-allergic reactions of primary human basophils. Caffeine was found to downregulate activating phosphorylation (S2448 position) of the mTOR protein thus affecting its kinase activity. This occurred in both THP-1 cells (upon exposure to PGN, R848 and SCF) as well as in primary AML cells stimulated with SCF (TLR expression levels are quite low in these cells). Importantly, caffeine did not increase phosphorylation of the T2446 residue of mTOR. This shows that caffeine does not activate specific mTOR downregulatory cascades, for example the AMPK pathway [10]. Intracellular AMP (specific AMP kinase activator) levels were also not affected by caffeine. However, caffeine inhibited XOD activity in both THP-1 and primary AML cells. Our previous studies showed that inhibition of XOD by allopurinol or sodium tungstate led to a significant increase in intracellular AMP levels and therefore induced AMPK-dependent downregulatory phosphorylation of mTOR at position T2446 [21]. Here, we also observed inhibition of XOD but without increases in intracellular AMP levels. Recently, it was reported that caffeine is capable of inhibiting Akt phosphorylation thus preventing mTOR activation (presumably through phosphorylation of its S2448 residue). However, other studies demonstrated that, in tissues expressing high levels of XOD (for example skeletal muscles), high concentrations of caffeine (10 mM) activate AMPK [7]. These tissues, however, can metabolise caffeine. XOD expression in leukocytes (even in AML cells)

is relatively low compared to other tissues and in basophils where the presence of XOD was even undetectable [21].

Although caffeine is a weak inhibitor of XOD compared to allopurinol and especially sodium tungstate, it might affect the re-use of purines in myeloid cells (this system is quite robust in leukocytes and is not affected by allopurinol or tungastates, which are specific XOD inhibitors only – especially tungstates, where tungsten replaces molybdenum in the catalytic site of the enzyme causing its irreversible inhibition). Caffeine is known to inhibit HGPRT, however, in myeloid cells its inhibitory effects are more striking since it is not metabolised in these cells [25]. This means that, upon inhibition of XOD by caffeine, levels of hypoxanthine are increased. However, hypoxanthine can't be converted into IMP and further down to AMP [21] (for more details, see Supplementary Figure S2). This lack of increase in AMP levels prevents the activation of AMP kinase and subsequent phosphorylation of mTOR at T2446.

Inhibition of mTOR and XOD by caffeine did not lead to the attenuation of HIF-1α accumulation in THP-1 and primary AML cells. This was due to a significant decrease in HIF-1α PHD activity (resulting from the decrease in intracellular 2-OG levels required for this reaction in form of a co-factor). Caffeine activates lipolysis by upregulating the activity of hormone-sensitive lipase (HSL), which is well expressed in myeloid cells [4, 25]. This leads to a decrease in glycolysis, which is further supported by a decrease in mTOR kinase activity which is required for translation of glycolytic enzymes [18, 26]. Such an effect results in the upregulation of the Krebs' cycle and thus in a decrease in intracellular 2-OG levels that affect HIF-1α PHD activity, thus preventing physiological degradation of HIF-1α protein. The effects described above are summarised in the scheme presented in the Figure 11.

Caffeine was revealed to inhibit mTOR, thus downregulating glycolysis. Previous reports suggested a possible influence of caffeine on NF-kB activity and calcium-dependent signalling [7, 27]. All these effects are likely to be responsible for the decreases in cytokine production observed in the present study (e.g. TNF-α and IL-6 in the case of TLR ligand stimulation and VEGF when the cells were exposed to SCF). These effects took place in both THP-1 and primary AML cells.

Despite the well-known fact that caffeine is an effective inhibitor of cAMP-PDE [2], no significant changes in intracellular cAMP levels were observed in THP-1 or AML cells. This could be explained by the fact that neither TLRs nor the SCF receptor (Kit) are G-protein coupled receptors. Therefore, they do not activate adenylate cyclase, the enzyme, which converts ATP into cAMP.

A different picture was observed in primary human basophils which did not express detectable amounts of XOD. Here, we also observed inhibition of IgE-induced mTOR kinase activity and abrogation of the mediator (histamine) release. However, HIF-1α accumulation did not seem to be PHD dependent in these cells and therefore, upon inhibition of mTOR kinase activity, IgE-induced HIF-1α accumulation was attenuated by caffeine. However, in contrast to AML and THP-1 cells, we observed a significant increase in intracellular cAMP levels in basophils which were further upregulated by caffeine. Basophils release histamine and also express H2-type histamine receptors which are G-protein-coupled and thus activate adenylate cyclase [15]. The cAMP levels induced by the autocrine actions of histamine are therefore preserved by caffeine as an inhibitor of cAMP-PDE. In this case, it is likely that we observed additional inhibition of mTOR activation due to the indirect actions of caffeine by increasing cAMP. All the effects reported were studied at 1 mM caffeine. However, dose-response investigations demonstrated that it displays its activities in primary AML cells and basophils at 0.1 mM though not at 0.01 mM.

Taken together, our results demonstrate, for the first time, that unmodified caffeine inhibits mTOR function by targeting its kinase activity during the biological responses of various human myeloid cells. These findings support observations made by other groups regarding caffeine effects on the mTOR pathway in non-blood cells [7, 8]. Furthermore, caffeine inhibits XOD activity but, unlike XOD-specific inhibitors, it does not upregulate the re-use of purines in AML cells. In contrast, basophils do not express detectable amounts of XOD. Since caffeine is a non-toxic drug with relatively few side effects at therapeutic concentrations, and easily metabolised in non-blood cells, our findings may lead to new avenues for therapy of human disorders affecting myeloid hematopoietic cells. However, it is obvious that high concentrations of caffeine would need to be maintained in order to achieve either its anti-inflammatory/anti-allergic effects or to affect SCF-induced biological responses. Because of this, the therapeutic actions of caffeine would more likely be achieved following external applications of this drug. For example, caffeine could be applied as a cream supplement or through other forms of direct application of unmodified caffeine on target myeloid cells with the purpose of their inactivation or elimination (previous studies have shown the ability of caffeine to induce programmed cell death [7, 8]). Alternatively, for internal applications, one might consider the recently discovered advantages of Nanobiotechnology or other highly specific forms of drug delivery in order to supply caffeine directly to myeloid cells.

MATERIALS AND METHODS

Materials

RPMI-1640 medium, foetal calf serum and supplements, caffeine, bovine liver XOD, PGN, goat anti-human-IgE, caffeine metabolites and an ATP luminometric detection kit were purchased from Sigma (Suffolk, UK). AMP/cAMP detection kits were purchased from Promega (Southampton, UK). Maxisorp™ microtitre plates were obtained from Nunc (Roskilde, Denmark) as well as from

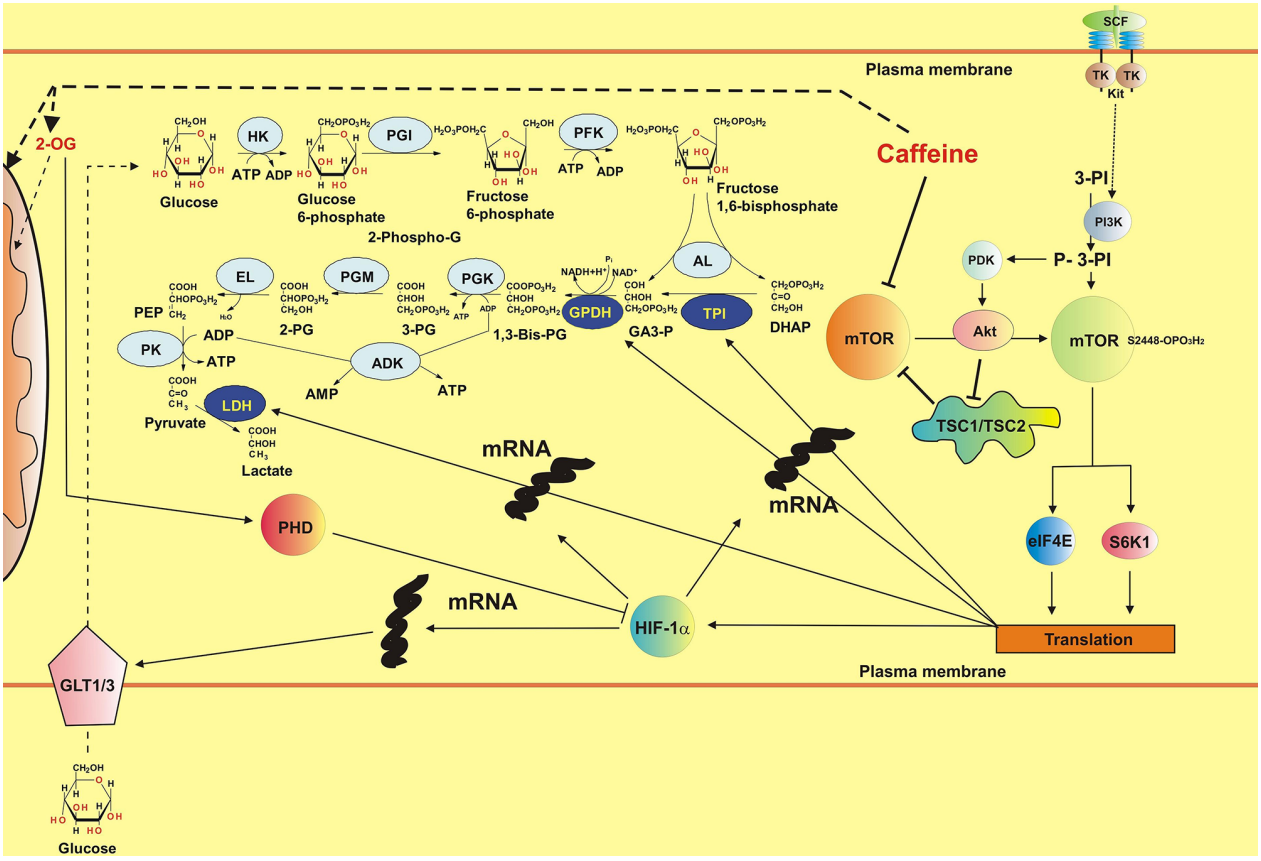

Figure 11: Possible biochemical mechanisms of the effects of caffeine on the mTOR pathway, HIF-1 activity and energy metabolism in human myeloid cells (SCF-induced responses are used as the example). Additional abbreviations used: HK – hexokinase, PGI – phosphoglucose isomerase, PFK – phosphofructokinase, AL – Aldolase, TPI – Triose-phosphate isomerase, GPDH – glyceraldehyde-3-phosphate dehydrogenase, PGK – phosphoglycerate kinase, PGM – phosphoglycerate mutase, EL – enolase, PK – pyruvate kinase, LDH – lactate dehydrogenase, DHAP – dihydroxyacetone phosphate, GA3-P – glyceraldehyde-3-phosphate, 3-PG – 3-phosphoglycerate, 2-PG – 2-phosphoglycerate, PEP – phosphoenolpyruvate, GLT1/3 – glucose transporters 1/3, TSC1/TSC2 – Tuberous sclerosis proteins 1 and 2, PDK – P-3-PI-dependent kinase, ADK – adenylate kinase, TK – tyrosine kinase.

Oxley Hughes Ltd (London, UK). Mouse monoclonal antibodies to HIF-1α, mTOR and β-actin as well as rabbit polyclonal antibodies against phospho-S2448 mTOR and phospho-T2446 mTOR were from Abcam (Cambridge, UK). Antibodies against phospho-T389 p70 S6 kinase 1 (p70 S6K1), total and phospho-S65 eukaryotic initiation factor 4E binding protein 1 (eIF4E-BP1) antibodies were obtained from Cell Signalling Technology (Danvers, MA USA). Goat anti-mouse and goat anti-rabbit fluorescence dye-labelled antibodies were obtained from Li-Cor (Lincoln, Nebraska USA). ELISA-based assay kits for the detection of IL-6, TNF-α and VEGF were purchased from R&D Systems (Abingdon, UK). All other chemicals were of the highest grade of purity that were commercially available (from either Sigma or Fisher Scientific).

THP-1 human myeloid cells

THP-1 human leukaemia monocytic macrophages were obtained from the European collection of Cell Cultures (Salisbury, UK). Cells were cultured in RPMI 1640 media supplemented with 10% foetal calf serum, penicillin (50 IU/ml) and streptomycin sulfate (50 μg/ml). Cells used in the experiments were from the 5–35th passage.

Primary human AML cells

Primary human AML mononuclear cells (AML-PB001F, newly diagnosed/untreated) were purchased from AllCells (Alameda, CA, USA) and handled in accordance with manufacturer's instructions. Cells derived from two different patients were used in the experiments.

Primary human leukocytes obtained from healthy donors

Primary human leukocytes were obtained from buffy coat blood (prepared from healthy donors) purchased from the National Health Blood and Transfusion Service (NHSBT, UK) following ethical approval (REC reference: 12/WM/0319). Mononuclear-rich leukocytes were obtained by Ficoll-density centrifugation according to the manufacturer's

protocol. Cell numbers were determined using a haemocytometer and diluted accordingly with HEPES-buffered Tyrode's solution before treatment as indicated.

Primary human basophils

Primary human basophils were obtained from buffy coats and isolated from the leukocyte-rich fraction obtained by Ficoll density centrifugation as described above. Basophils were then purified by a negative selection procedure to 90–100% purity (as judged by alcian blue staining) using a commercially available kit, as previously described [28]. Basophils were pre-incubated for 15 min at 37°C in HEPES-buffered Tyrode's solution and then treated as indicated.

Stem cell factor

Human SCF protein was produced in *E.Coli* and purified in accordance with published protocols [29].

Western blot analysis

Expressions of HIF-1α, total and phospho-T389 p70 S6K1, total and phospho-S65 eIF4E-BP1 as well as XOD protein levels were determined by Western blot analysis and compared to β-actin in order to determine equal protein loading, as previously described [10]. Li-Cor goat secondary antibodies, conjugated with fluorescent dyes, were used according to the manufacturer's protocol in order to visualise the proteins of interest using a Li-Cor Odyssey imaging system. Western blot data were subjected to quantitative analysis using Odyssey software and values were normalised against respective β-actin bands.

Detection of phospho-S2448 and phospho-T2446 mTOR in cell lysates by ELISA

Phosphorylation of mTOR was monitored using ELISA assays as recently described [10, 21, 30]. Briefly, the ELISA plates were coated with mouse anti-mTOR antibodies and blocked with 2% BSA. Cell lysates were then added to the wells and kept at room temperature for at least 2 h (under constant agitation). After extensive washing with TBST buffer, anti-phospho-S2448 (or anti-phospho-T2446) mTOR antibody was added and plates were incubated for at least 2 h at room temperature with constant agitation. Plates were then washed with TBST buffer and incubated with 1:1000 HRP-labelled goat anti-rabbit IgG in TBST buffer. After extensive washing with TBST, bound secondary antibodies were then detected by the peroxidase reaction (ortho-phenylenediamine/H_2O_2).

HIF-1α PHD assay

To detect HIF-1α PHD activity we employed a peptide-based assay [31]. HIF-1α-free cell lysates were used to avoid the impact of intracellular HIF-1α hydroxylation. Lysates of non-treated and treated THP-1 cells were incubated for one hour in 96-well ELISA plates which were coated with HIF-1α capture antibodies and blocked with BSA as described previously. Lysates were then subjected PHD assay following this incubation period.

Detection of intracellular ATP, cAMP, AMP, ROS and 2-OG levels, xanthine oxidase activity as well as glycolysis intensity

ATP was detected using a commercial luminometric kit (Sigma) according to the manufacturer's protocol. AMP and cAMP levels were detected using luminometric assay kits in accordance with manufacturer's protocols. Intracellular ROS levels were also monitored by luminometric assay as previously described [32]. 2-OG levels were analysed using a glutamate dehydrogenase spectrophotometric assay [33]. Xanthine oxidase activity was measured as described before [21]. The intensity of glycolysis was determined based on the ability cell lysate enzymes, used as a multienzyme preparation, to convert glucose into lactate under anaerobic conditions, which was achieved by employing an anaerobic chamber [10].

Detection of IL-6, TNF-α and VEGF release

Concentrations of these cytokines released into the cell culture media were analysed by ELISA (R&D Systems assay kit) according to the manufacturer's protocol.

Measurement of histamine release

Histamine releases were assessed using spectrofluorometic autoanalysis as previously described [34]. Histamine releases were calculated from the histamine contents released into the supernatants as a percentage of total histamine content present in lysed cell pellets.

High performance liquid chromatography

Caffeine and its metabolites were analysed in urine according to a previously described protocol [35, 36] with minor modifications. Healthy subjects were asked to refrain from all caffeine containing beverages and chocolate for 1 day. At 8 a.m. on the test day subjects were asked to consume 2 cups of very strong espresso (approximately 200 mg of caffeine) and 6 hours later urine was collected for analysis.

10 ml of urine were mixed with 200 mg of ascorbic acid. The pH was adjusted to 3.5 with 30% acetic acid. 200 µl of urine were mixed with 140 mg of ammonium sulfate, 25 µl of internal standard (137 MU) and vortexed at full speed for 1 min. The metabolites were extracted with chloroform:isopropanol (95:5) and centrifuged. The organic phase was evaporated to dryness using nitrogen or Speedvac and the pellet was dissolved in 750 µl of diluent

containing MeOH : acetic acid : water (20:0.5:979.5 vol:vol:vol) and 5 µl of the sample was analysed by Agilent HPLC system (the flow rate was 0.5 ml/min) with a UV detector using a gradient elution profile. Caffeine, caffeine metabolites and the internal standard were separated on an Agilent XBD C18 reverse phase column (1.8 µm, 4.6 × 50 mm). The solvents used for the elution were mobile phase A containing MeOH : acetic acid : water (20:0.5:979.5 vol:vol:vol) and mobile phase B (MeOH : acetic acid : water 700:0.5:229.5 vol:vol:vol). The gradient program was 0% B (0 min), 100% (0.1 to 15 min) and 0% (15.1 to 18 min). The analytes were detected by UV absorbance at 280 nm. Calibration curves were developed using known amounts of metabolites.

Analysis of total cytochrome P450 and activity of CYP450 1A2

Total CYP450 was analysed by a classic spectrophotometric method initially proposed by Omura and Sato [37]. CYP450 1A2 activity was analysed based on its ability to oxidise caffeine using NADPH as a donor. Mouse liver homogenates obtained from commercial sources were used as positive control.

Statistical analysis

Each experiment was performed at least three times and statistical analysis was conducted using a two-tailed Student's *t* test. Statistical probabilities (p) were expressed as *, where $p < 0.01$.

ACKNOWLEDGMENTS

Alexandr Prokhorov was a fellow of the European Academy of Allergy and Clinical Immunology (EAACI). Regretfully, he has tragically died in an accident in recent past. The work was partially supported by the University of Kent Faculty of Sciences Research Fund. We are also grateful to Dr. Simon Stafford (Oxley Hughes Ltd, London, UK) for the gift of ELISA plates and to Ms Irene Wegner (University of Applied Sciences Northwestern Switzerland, Institute of Chemistry and Bioanalytics) for her assistance with HPLC experiments. We are most grateful to Dr. Luca Varani from Institute for Research in Biomedicine, Universita' della Svizzera Italiana (USI) via Vela 6, 6500 Bellinzona, Switzerland for his generous help with SCF purification.

CONFLICTS OF INTEREST

There is no conflict of interest that the authors should disclose.

REFERENCES

1. Miners JO, Birkett DJ. The use of caffeine as a metabolic probe for human drug metabolizing enzymes. Gen Pharmacol. 1996; 27:245–249.
2. Stefanovich V. Cyclic 3′,5′-adenosine monophosphate phosphodiesterase (cAMP PDE) and cyclic 3′,5′-guanosine monophosphate phosphodiesterase (cGMP PDE) in microvessels isolated from bovine cortex. Neurochem Res. 1997; 4:681–687.
3. Spriet LL, MacLean DA, Dyck DJ, Hultman E, Cederblad G, Graham TE. Caffeine ingestion and muscle metabolism during prolonged exercise in humans. Am J Physiol. 1992; 262:E891–898.
4. Donsmark M, Langfort J, Holm C, Ploug T, Galbo H. Contractions activate hormone-sensitive lipase in rat muscle by protein kinase C and mitogen-activated protein kinase. J Physiol. 2003; 550:845–854.
5. Krovat BC, Tracy JH, Omiecinski CJ. Fingerprinting of cytochrome P450 and microsomal epoxide hydrolase gene expression in human blood cells. Toxicol Sci. 2000; 55:352–360.
6. Sumbaev VV, Rozanov AY. Effect of caffeine on xanthine oxidase activity. Ukr Biokhim Zh. 1997; 69:196–200.
7. Miwa S, Sugimoto N, Yamamoto N, Shirai T, Nishida H, Hayashi K, Kimura H, Takeuchi A, Igarashi K, Yachie A, Tsuchiya H. Caffeine induces apoptosis of osteosarcoma cells by inhibiting AKT/mTOR/S6K, NF-kappaB and MAPK pathways. Anticancer Res. 2012; 32:3643–3649.
8. Saiki S, Sasazawa Y, Imamichi Y, Kawajiri S, Fujimaki T, Tanida I, Kobayashi H, Sato F, Sato S, Ishikawa K-I, Imoto M, Hattori N. Caffeine induces apoptosis by enhancement of autophagy via PI3K/Akt/mTOR/p70S6K inhibition. Autophagy. 2011; 7:176–187.
9. Xie J, Ponuwei GA, Moore CE, Willars GB, Tee AR, Herbert TP. cAMP inhibits mammalian target of rapamycin complex-1 and -2 (mTORC1 and 2) by promoting complex dissociation and inhibiting mTOR kinase activity. Cell Signal. 2011; 23:1927–1935.
10. Yasinska IM, Gibbs BF, Lall GS, Sumbayev VV. The HIF-1 transcription complex is essential for translational control of myeloid hematopoietic cell function by maintaining mTOR phosphorylation. Cell Mol Life Sci. 2014; 71:699–710.
11. Semenza GL. HIF-1 and tumor progression: pathophysiology and therapeutics. Trends Mol Med. 2002; 8:S62–67.
12. Walmsley SR, Cadwallader KA, Chilvers ER. The role of HIF-1alpha in myeloid cell inflammation. Trends Immunol. 2005; 26:434–439.
13. Natarajan G, Lulic-Botica M, Aranda JV. Clinical pharmacology of caffeine in the newborn. NeoReviews. 2007; 8:e214–e221.

14. Akira S, Takeda K. Toll-like receptor signalling. Nat Rev Immunol. 2004; 4:499–511.
15. Nolan LL, Kidder GW. Caffeine: its action on purine metabolizing enzymes. Biochem Biophys Res Commun. 1979; 91:253–262.
16. Ferrer I, Costell M, Grisolia S. Lesch-Nyhan syndrome-like behavior in rats from caffeine ingestion: changes in HGPRTase activity, urea and some nitrogen metabolism enzymes. FEBS Lett. 1982; 141:275–278.
17. Nicholas SA, Bubnov VV, Yasinska IM, Sumbayev VV. Involvement of xanthine oxidase and hypoxia-inducible factor 1 in Toll-like receptor 7/8-mediated activation of caspase 1 and interleukin-1beta. Cell Mol Life Sci. 2011; 68:151–158.
18. Pollizzi KN, Powell JD. Integrating canonical and metabolic signalling programmes in the regulation of T cell responses. Nat Rev Immunol. 2014; 14:435–446.
19. Sumbayev VV, Nicholas SA. Hypoxia-inducible factor 1 as one of the "signaling drivers" of Toll-like receptor-dependent and allergic inflammation. Arch Immunol Ther Exp (Warsz). 2010; 58:287–294.
20. Nicholas SA, Sumbayev VV. The role of redox-dependent mechanisms in the downregulation of ligand-induced Toll-like receptors 7, 8 and 4-mediated HIF-1 alpha prolyl hydroxylation. Immunol Cell Biol. 2010; 88:180–186.
21. Abooali M, Lall GS, Coughlan K, Lall HS, Gibbs BF, Sumbayev VV. Crucial involvement of xanthine oxidase in the intracellular signalling networks associated with human myeloid cell function. Sci Rep. 2014; 4:6307.
22. Frenz AM, Gibbs BF, Pearce FL. The effect of recombinant stem cell factor on human skin and lung mast cells and basophil leukocytes. Inflamm Res. 1997; 46:35–39.
23. Sumbayev VV, Yasinska IM, Oniku AE, Streatfield CL, Gibbs BF. Involvement of hypoxia-inducible factor-1 in the inflammatory responses of human LAD2 mast cells and basophils. PLoS One. 2012; 7:e34259.
24. Sumbayev VV, Nicholas SA, Streatfield CL, Gibbs BF. Involvement of hypoxia-inducible factor-1 HIF(1alpha) in IgE-mediated primary human basophil responses. Eur J Immunol. 2009; 39:3511–3519.
25. Degang Y, Akama T, Hara T, Tanigawa K, Ishido Y, Gidoh M, Makino M, Ishii N, Suzuki K. Clofazimine modulates the expression of lipid metabolism proteins in Mycobacterium leprae-infected macrophages. PLoS Negl Trop Dis. 2012; 6:e1936.
26. Cheng SC, Quintin J, Cramer RA, Shepardson KM, Saeed S, Kumar V, Giamarellos-Bourboulis EJ, Martens JH, Rao NA, Aghajanirefah A, Manjeri GR, Li Y, Ifrim DC, Arts RJ, van der Veer BM, Deen PM, Logie C, O'Neill LA, Willems P, van de Veerdonk FL, van der Meer JW, Ng A, Joosten LA, Wijmenga C, Stunnenberg HG, Xavier RJ, Netea MG. mTOR- and HIF-1alpha-mediated aerobic glycolysis as metabolic basis for trained immunity. Science. 2014; 345:1250684.
27. Ren H, Teng Y, Tan B, Zhang X, Jiang W, Liu M, Du B, Qian M. Toll-like receptor-triggered calcium mobilization protects mice against bacterial infection through extracellular ATP release. Infect Immun. 2014; 82:5076–5085.
28. Gibbs BF, Papenfuss K, Falcone FH. A rapid two-step procedure for the purification of human peripheral blood basophils to near homogeneity. Clin Exp Allergy. 2008; 38:480–485.
29. Wang C, Liu J, Wang L, Geng X. Solubilization and refolding with simultaneous purification of recombinant human stem cell factor. Appl Biochem Biotechnol. 2008; 144:181–189.
30. Prokhorov A, Gibbs BF, Bardelli M, Ruegg L, Fasler-Kan E, Varani L, Sumbayev VV. The immune receptor Tim-3 mediates activation of PI3 kinase/mTOR and HIF-1 pathways in human myeloid leukaemia cells. Int J Biochem Cell Biol. 2015; 59:11–20.
31. Gibbs BF, Yasinska IM, Oniku AE, Sumbayev VV. Effects of stem cell factor on hypoxia-inducible factor 1 alpha accumulation in human acute myeloid leukaemia and LAD2 mast cells. PLoS One. 2011; 6:e22502.
32. Kapiszewska M, Cierniak A, Elas M, Lankoff A. Lifespan of etoposide-treated human neutrophils is affected by antioxidant ability of quercetin. Toxicol *In Vitro*. 2007; 21:1020–1030.
33. Kozhukhar AV, Yasinska IM, Sumbayev VV. Nitric oxide inhibits HIF-1alpha protein accumulation under hypoxic conditions: implication of 2-oxoglutarate and iron. Biochimie. 2006; 88:411–418.
34. Shore PA, Burkhalter A, Cohn VH Jr. A method for the fluorometric assay of histamine in tissues. J Pharmacol Exp Ther. 1959; 127:182–186.
35. Butler MA, Lang NP, Young JF, Caporaso NE, Vineis P, Hayes RB, Teitel CH, Massengill JP, Lawsen MF, Kadlubar FF. Determination of CYP1A2 and NAT2 phenotypes in human populations by analysis of caffeine urinary metabolites. Pharmacogenetics. 1992; 2:116–127.
36. Sarkar M, Stabbert R, Kinser RD, Oey J, Rustemeier K, von Holt K, Schepers G, Walk RA, Roethig HJ. CYP1A2 and NAT2 phenotyping and 3-aminobiphenyl and 4-aminobiphenyl hemoglobin adduct levels in smokers and non-smokers. Toxicol Appl Pharmacol. 2006; 213:198–206.
37. Omura T, Sato R. The Carbon Monoxide-Binding Pigment of Liver Microsomes. I. Evidence for Its Hemoprotein Nature. J Biol Chem. 1964; 239:2370–2378.

SUPPLEMENTARY FIGURES

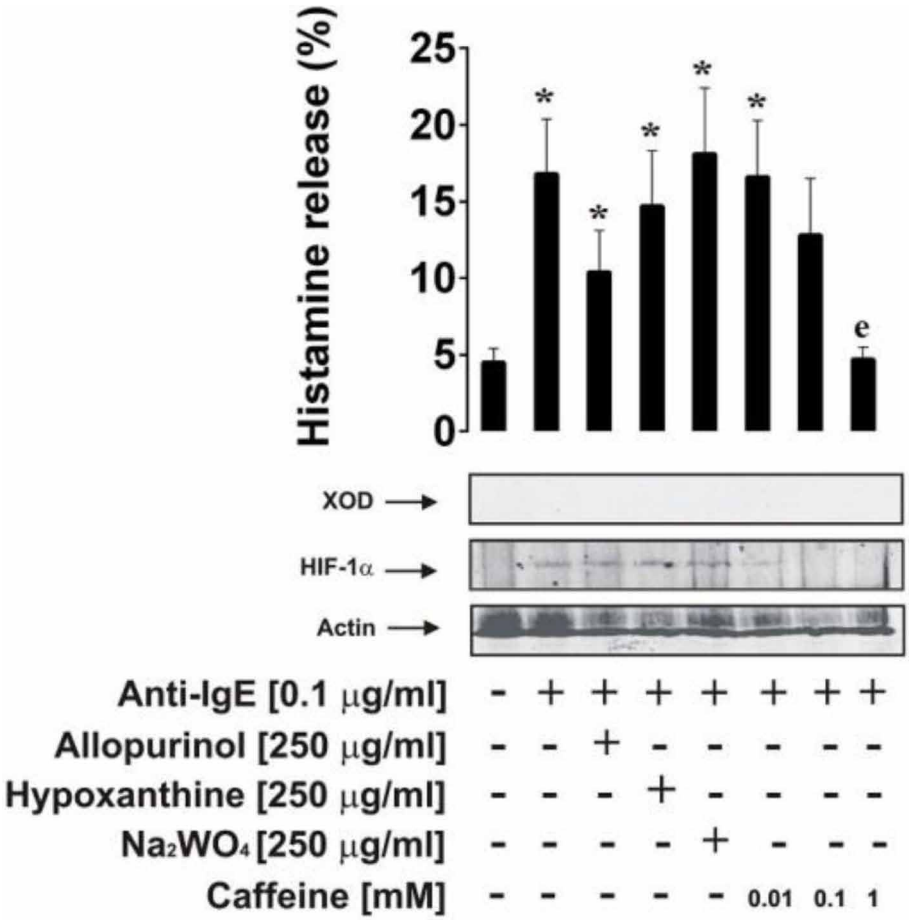

Supplementary Figure S1: Effects of allopurinol, hypoxanthine, sodium tungstate and caffeine on anti-IgE-induced histamine release and HIF-1α accumulation in primary human basophils. Basophils were exposed for 2 h to 0.1 μg/ml anti-IgE with or without 30 min pre-treatment with indicated concentrations of inhibitors or hypoxanthine. Western blot data show one representative experiment of three that gave similar results. Quantitative data are shown as means ± S.D ; * – $p < 0.01$ vs. control ($n = 3$), e – $p < 0.01$ vs. anti-IgE alone.

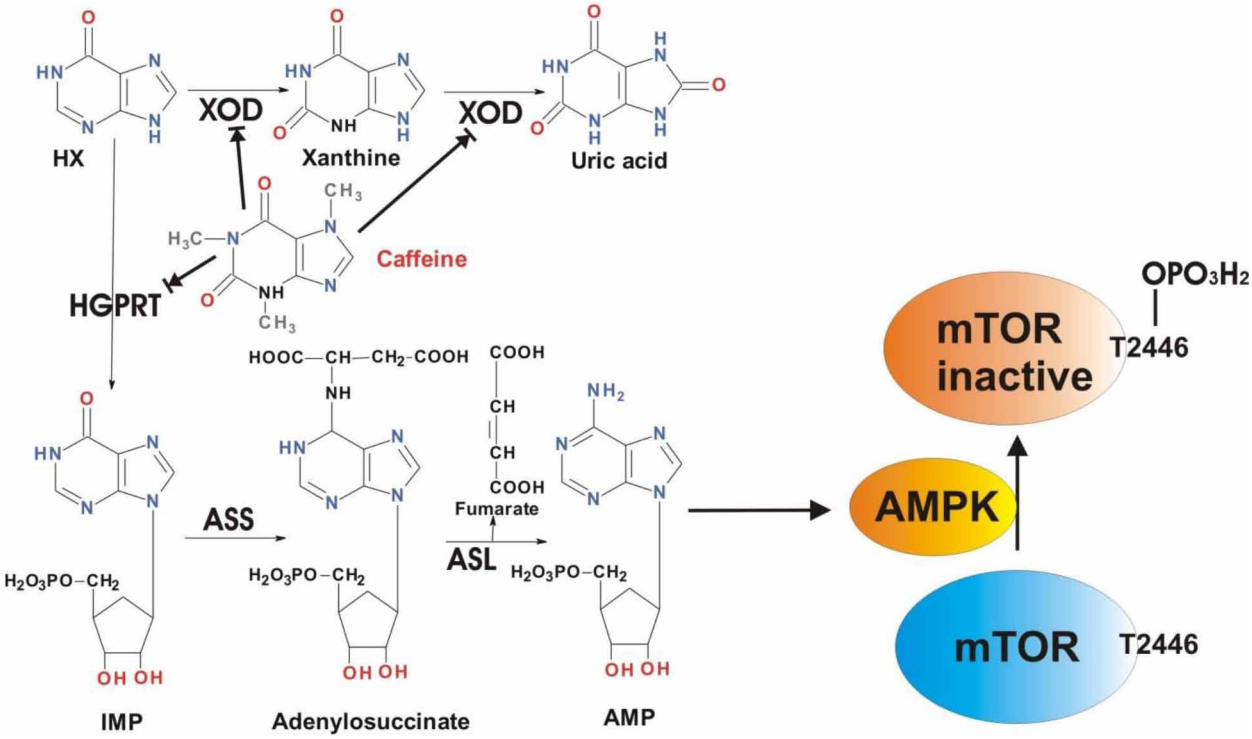

Supplementary Figure S2: Possible biochemical mechanisms of the actions of caffeine on hypoxanthine degradation and re-use. Additional abbreviations used: ASS – adenylosuccinate synthase; ASL – adenylosuccinate lyase.

Differential expression and biochemical activity of the immune receptor Tim-3 in healthy and malignant human myeloid cells

Isabel Gonçalves Silva[1], Bernhard F. Gibbs[1], Marco Bardelli[2], Luca Varani[2], Vadim V. Sumbayev[1]

[1]School of Pharmacy, University of Kent, Anson Building, Kent, ME4 4TB, United Kingdom

[2]Institute for Research in Biomedicine, Universita' della Svizzera italiana (USI) 6500 Bellinzona, Switzerland

Correspondence to:
Vadim V. Sumbayev, **e-mail:** V.Sumbayev@kent.ac.uk
Bernhard F. Gibbs, **e-mail:** B.F.Gibbs@kent.ac.uk
Luca Varani, **e-mail:** luca.varani@irb.usi.ch

Keywords: *Tim-3, acute myeloid leukaemia, myeloid cells*

Received: *July 01, 2015* ***Accepted:*** *September 04, 2015* ***Published:*** *September 16, 2015*

ABSTRACT

The T cell immunoglobulin and mucin domain 3 (Tim-3) is a plasma membrane-associated receptor which is involved in a variety of biological responses in human immune cells. It is highly expressed in most acute myeloid leukaemia (AML) cells and therefore may serve as a possible target for AML therapy. However, its biochemical activities in primary human AML cells remain unclear. We therefore analysed the total expression and surface presence of the Tim-3 receptor in primary human AML blasts and healthy primary human leukocytes isolated from human blood. We found that Tim-3 expression was significantly higher in primary AML cells compared to primary healthy leukocytes. Tim-3 receptor molecules were distributed largely on the surface of primary AML cells, whereas in healthy leukocytes Tim-3 protein was mainly expressed intracellularly. In primary human AML blasts, both Tim-3 agonistic antibody and galectin-9 (a Tim-3 natural ligand) significantly upregulated mTOR pathway activity. This was in line with increased accumulation of hypoxia-inducible factor 1 alpha (HIF-1`) and secretion of VEGF and TNF-`. Similar results were obtained in primary human healthy leukocytes. Importantly, in both types of primary cells, Tim-3-mediated effects were compared with those induced by lipopolysaccharide (LPS) and stem cell factor (SCF). Tim-3 induced comparatively moderate responses in both AML cells and healthy leukocytes. However, Tim-3, like LPS, mediated the release of both TNF-` and VEGF, while SCF induced mostly VEGF secretion and did not upregulate TNF-` release.

INTRODUCTION

The immune receptor T-cell immunoglobulin and mucin domain 3 (Tim-3) is involved in a variety of leukocyte biological responses [1]. In T cells it mainly mediates the inhibition of Th1 responses, while in dendritic cells it has a pro-inflammatory effect. In monocytes and macrophages Tim-3 is involved in phagocytosis [1]. However, in myeloid leukaemia cell lines Tim-3 was shown to induce a moderate growth factor/pro-inflammatory responses, similar to those observed by myeloid cell growth factors (for example stem cell factor – SCF) [2, 3].

Interestingly, Tim-3 is highly expressed in leukaemia cells, especially in T-cell lymphocytic leukaemia cells as well as acute myeloid leukaemia (AML) cells [4–6]. In leukaemic T cells Tim-3 agonists induce programmed cell death pathways, while in AML cells this does not seem to be the case [1, 6]. However, the biochemical mechanisms involved in the activation of human myeloid cells and, especially, in AML cells, are largely unknown.

Tim-3 is considered as one of the possible AML antigens, since malignant AML cells preserve the ability to express the SCF receptor (Kit or CD117) as well as Tim-3 [5, 7]. In contrast, myeloid stem cells only express Kit receptors but not Tim-3 [5]. Conversely, in most cases,

mature myeloid cells express Tim-3 but not Kit receptors [5, 8]. Despite these differences in cell surface presence, total expression levels of Tim-3 in AML cells are also significantly increased compared to healthy leukocytes [5].

In myeloid cell lines and primary myeloid hematopoietic cells Tim-3 is known to mediate the activation of NF-kB transcription factor and TNF-α secretion [3]. Furthermore, in AML cell lines, Tim-3 moderately activates the mammalian target of rapamycin (mTOR, a master regulator of myeloid cell translational pathways). This results in activation of the hypoxia-inducible factor 1 (HIF-1) transcription complex, which upregulates glycolysis and expression/secretion of the pro-angiogenic vascular endothelial growth factor (VEGF) [2]. However, the differential effects of Tim-3 in *ex vivo* systems such as primary human AML cells versus healthy human leukocytes have not yet been elucidated.

In the present study, we therefore analysed both the total and cell surface expressions of the Tim-3 receptor in primary human AML blasts and healthy primary human leukocytes obtained from peripheral blood (buffy coats). We found that, in primary AML cells, Tim-3 expression is much higher compared to primary healthy leukocytes. We also observed that Tim-3 receptor molecules were mostly expressed on the surface of primary AML cells, while the majority of Tim-3 protein remained inside primary human healthy leukocytes. In primary human AML blasts (AML-PB001F), Tim-3 agonistic antibody as well as galectin-9 (one of the natural ligands of Tim-3) induced activation of the mTOR pathway (by mTOR-dependent phosphorylation of p70 S6 kinase 1 (p70 S6K1) and eIF4E-binding protein-1 (eIF4E-BP1)). This was in line with HIF-1 activation and increased secretion of VEGF and TNF-α. Similar results were obtained in primary human leukocytes isolated from buffy coats obtained from the blood of healthy donors. Importantly, in both types of primary cells, the effects were compared with those induced by lipopolysaccharide (LPS, a Gram-negative bacteria-derived toll-like receptor 4 (TLR4) ligand) and SCF (Kit ligand). In primary AML cells SCF induced the strongest biological response, whereas LPS displayed comparatively greater effects on primary human leukocytes. Tim-3 in both cases induced moderate cellular responses. However, although Tim-3, like LPS, triggered the release of both TNF-α and VEGF, SCF induced mostly VEGF secretion and did not significantly impact the TNF-α release.

RESULTS

Primary human AML blasts and healthy leukocytes express the Tim-3 immune receptor

Our recent work demonstrated that Tim-3 mediates the activation of mTOR *via* phosphorylation of its S2448 residue and HIF-1 signalling in human AML cell lines [2]. We therefore sought to understand the expression and behaviour of this receptor in primary human AML cells (AML-PB001F primary mononuclear blasts were used) in comparison with healthy whole blood primary human leukocytes (PLs).

In order to compare the expression and, more importantly, re-distribution of Tim-3 in the cells we analysed its total amount and cell surface presence using in-cell Western and in-cell assay respectively. We found that both primary AML blasts and healthy whole blood leukocytes expressed Tim-3 as detected by in-cell Western and in-cell assay (Figure 1A and 1B). However, in AML cells most of the receptor molecules were externalised, whereas in healthy PLs only around 30% were present on the surface, clearly indicating that the vast majority of Tim-3 protein was stored inside the cell (Figure 1A and 1B), where Tim-3 function is unknown. These findings confirm that AML cells express more Tim-3 protein compared to healthy leukocytes and, importantly, AML cells retain almost all Tim-3 receptor molecules on their cell surface.

Tim-3 triggers activation of the mTOR pathway and HIF-1 signalling in primary AML cells and primary healthy human leukocytes (PLs)

Given the high expression/externalisation levels of Tim-3 protein in primary human AML cells compared to PLs we sought to obtain evidence on differences in receptor downstream activities. We found that, in primary AML cells, mTOR S2448 phosphorylation was substantially increased upon exposure to SCF as well as to anti-Tim-3 antibody stimulation (about 50% of SCF-induced effect), while LPS displayed a weaker ability to upregulate the intracellular levels of phospho-S2448 mTOR. The same pattern was observed for PI-3K activity (Figure 2A). Activity of LPS can be explained by the low TLR4 expression levels reported by the supplier for AML-PB001F primary human AML cells. These results were in line with mTOR activity levels monitored based on intracellular amounts of phospho-T389 p70 S6 K1 and phospho-S65 eIF4E-BP1 (Figure 2A).

Both proteins are phosphorylated at the indicated positions by the mTOR kinase complex [9]. All the stimuli demonstrated the ability to upregulate HIF-1α accumulation; anti-Tim-3 was the weakest inducer (Figure 2B) which is consistent with the observations made in cell lines. Stronger LPS-induced effects in this case were due to the fact that LPS-dependent HIF-1α accumulation, unlike the one triggered by both SCF and anti-Tim-3, did not solely depend on mTOR activation. LPS-induced TLR4-mediated HIF-1α accumulation is known to be jointly triggered through a redox-dependent mechanism, as well as mTOR and mitogen-activated protein (MAP) kinase signalling cascades [10, 11]. Therefore, the observed effects were achieved jointly *via* activation of all three pathways, the intensities of

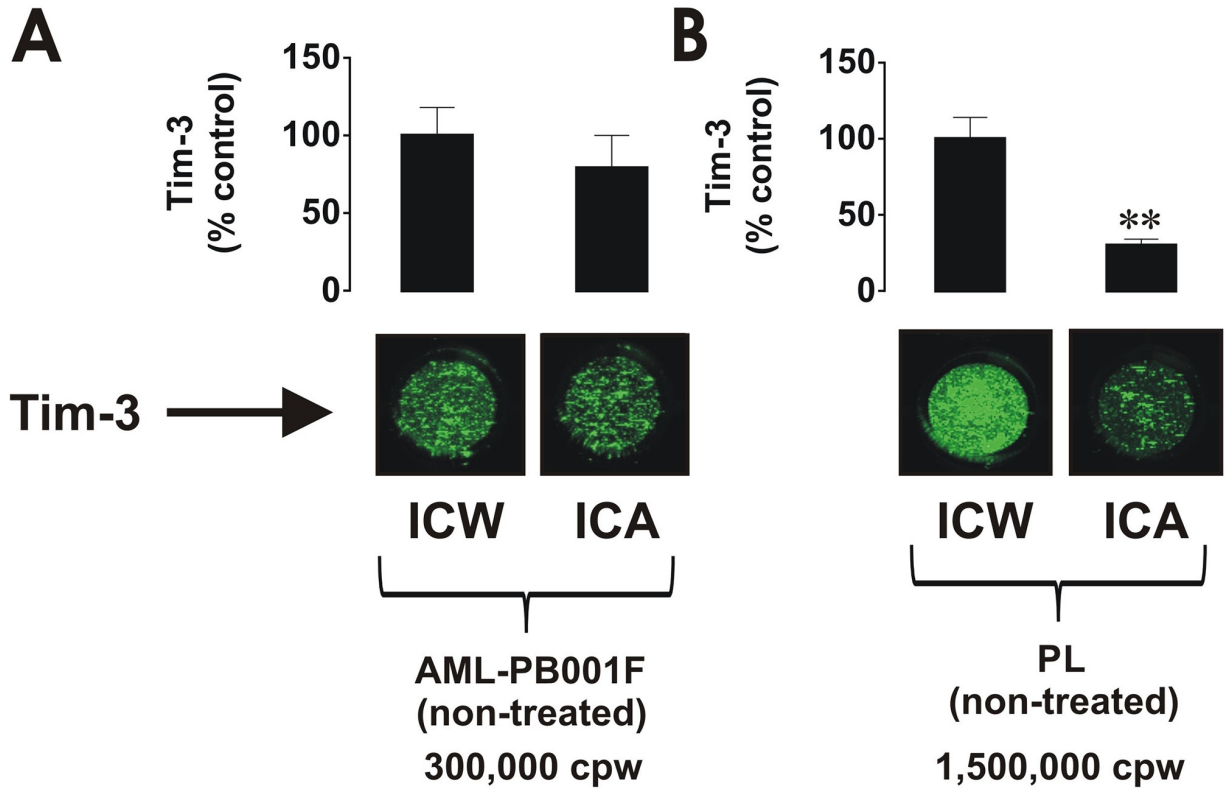

Figure 1: Comparative analysis of Tim-3 expression and surface presence in primary human AML cells and healthy leukocytes. 300,000 per well of AML-PB001F primary human AML cells **A.** and 1,500,000 per well of healthy PLs **B.** were subjected to in-cell Western (ICW) in order to detect total Tim-3 expression. The Tim-3 surface presence was analysed by in-cell assay (ICA). For healthy PLs, 1,500,000 cells per well were necessary to properly visualise Tim-3 receptor on the cell surface. Fluorescence values obtained for AML cells and healthy PLs were divided by respective cell number (300,000 or 1,500,000) and used for calculations. Images are from one experiment representative of three which gave similar results. Quantitative data are shown as means ± SEM of at least three individual experiments; $^{**}p < 0.01$ vs. control.

which were comparable with mTOR-dependent processes following exposure to SCF (Figure 2A and 2B). Total Tim-3 levels were not affected by any of the above stimuli, while in AML cell lines SCF and Tim-3 receptor activation upregulated total Tim-3 expression (Figure 2B). Importantly, as with LPS, anti-Tim-3 antibody was able to upregulate secretion of both TNF-α and VEGF, while SCF mostly upregulated VEGF production and did not dramatically change TNF-α secretion level (Figure 2B).

Galectin-9, a natural Tim-3 ligand [2, 5], demonstrated the ability to upregulate both mTOR kinase activity and HIF-1α accumulation in primary AML-PB001F blasts at levels comparable to those seen with anti-Tim-3. This suggests similar activities of both agonistic ligands (Figure 3A and 3B).

In primary human healthy leukocytes the effects of anti-Tim-3 antibody were similar to those observed in AML cells. However, in healthy PLs LPS (and not SCF) was the most powerful cell activator (Figure 4A and 4B). This is probably due to the fact that healthy leukocytes contain more cells which express TLR4 than those that express Kit receptors. The effects of anti-Tim-3 antibody in this case were similar to those of SCF and slightly lower than the effects of anti-Tim-3 detected in primary human AML blasts (Figure 4A and 4B). Isotype control (IgG 2a) antibody [2] was also incubated with all the cell types studied and did not induce any effect in cell lines or primary leukocytes (data not shown).

Interestingly, background intracellular levels of phospho-S2448 mTOR, HIF-1α and Tim-3 proteins as well as VEGF, but not PI-3K activity and secreted TNF-α, were significantly higher in AML blasts compared to healthy PLs (a quantitative breakdown is shown in Figure 5A–5H). These findings confirm that the proteins discussed above are used by leukaemia cells on a permanent basis more than by healthy leukocytes.

DISCUSSION

The immune receptor Tim-3 is expressed in healthy human hematopoietic cells and, despite numerous studies, its functional role is still a subject for intensive research [6]. Recent evidence demonstrated that the Tim-3 receptor is highly expressed and externalised in human AML cells [5, 7]. Importantly, progenitor hematopoietic cells do not express Tim-3 receptors while they produce substantial

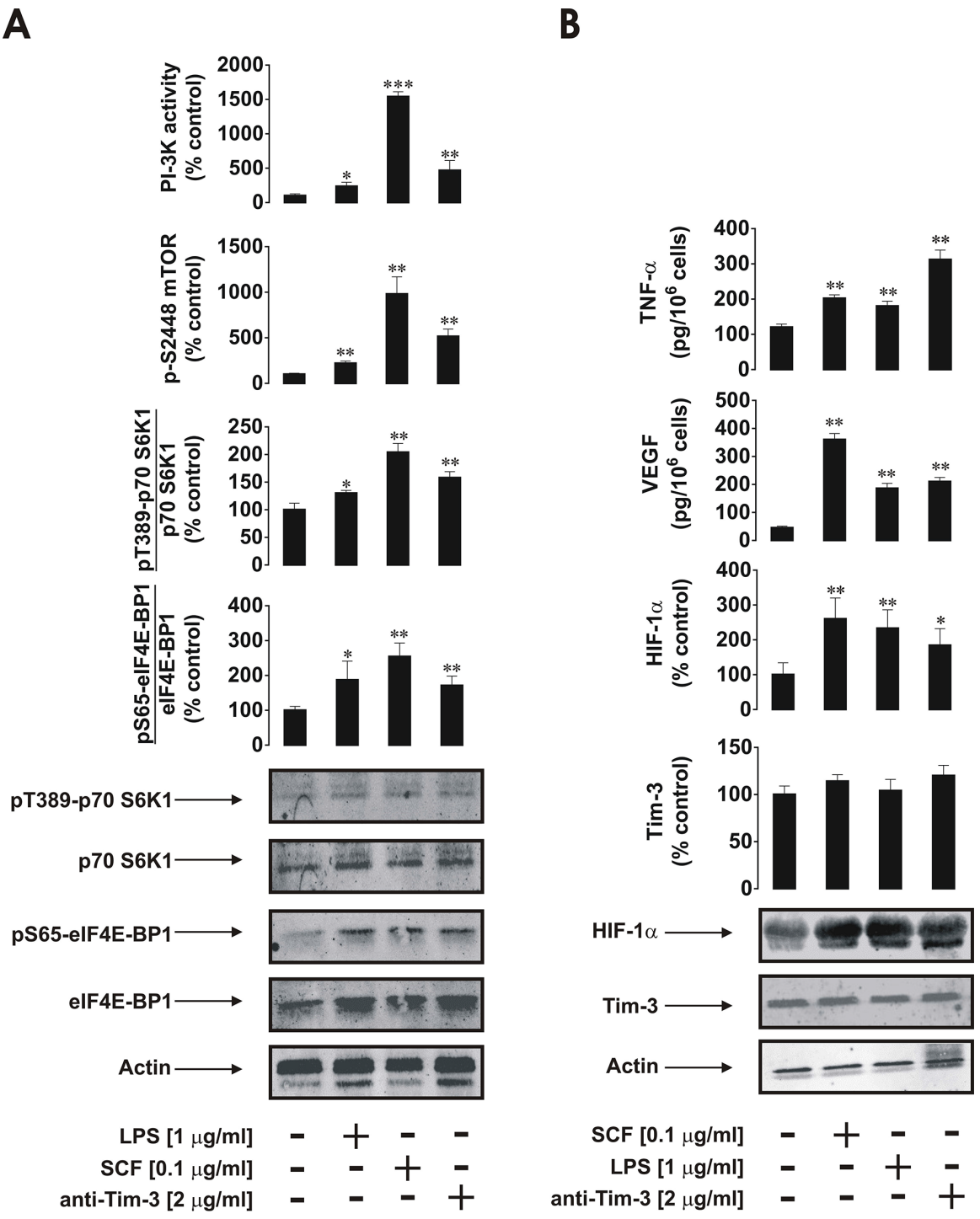

Figure 2: Anti-Tim-3 agonistic antibody induces mTOR activity, HIF-1α accumulation as well secretion of VEGF and TNF-α in primary human AML cells. AML-PB001F cells were exposed for 4 h for the indicated concentrations of anti-Tim-3, LPS and SCF, followed by analysis of PI-3K/mTOR pathway activity **A.** HIF-1α accumulation and release of VEGF and TNF-α **B.** Images are from one experiment representative of four which gave similar results. Quantitative data are shown as means ± SEM of four individual experiments; *$p < 0.05$; **$p < 0.01$ vs. control.

amounts of Kit (SCF) receptors. Mature healthy leukocytes generally lose their ability to express the Kit receptor but start expressing Tim-3 protein. Malignant AML cells express both receptors and thus their growth and proliferation depend on SCF while the biological activity of Tim-3 remains unclear [5]. It was reported that, in primary dendritic cells, Tim-3 induces TNF-α production through the NF-kB transcription factor [1, 3]. Our recent studies demonstrated that Tim-3 mediates activation of the PI3K/mTOR pathway in human AML cell lines [2].

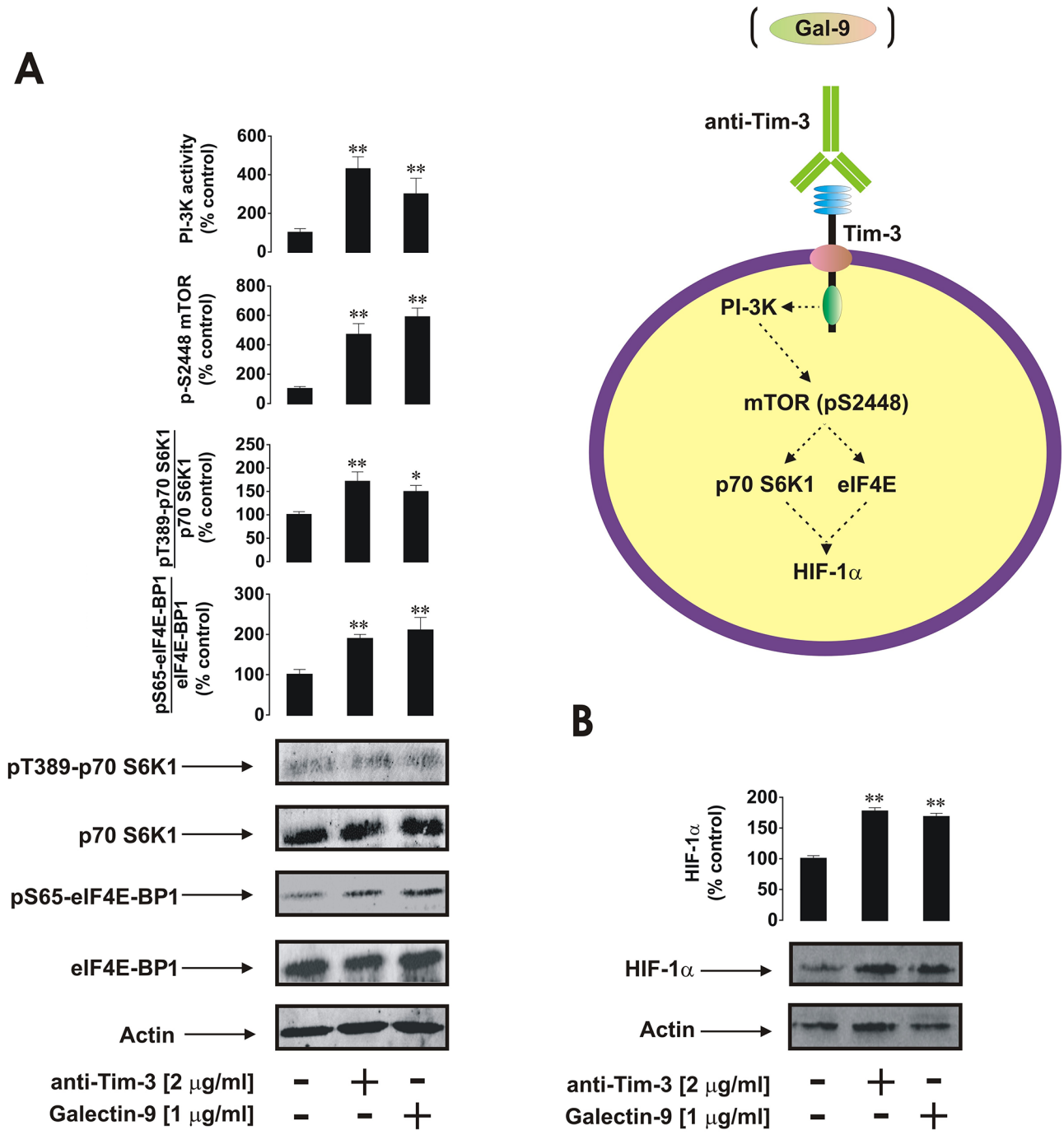

Figure 3: Anti-Tim-3 and galectin-9 induce similar responses in primary human AML cells. AML-PB001F cells were exposed for 4 h for the indicated concentrations of anti-Tim-3 and galectin-9 followed by analysis of PI-3K/mTOR pathway activity **A.** and HIF-1α accumulation **B.** Images are from one experiment representative of three which gave similar results. Quantitative data are shown as means ± SEM of three individual experiments; *$p < 0.05$; **$p < 0.01$ vs. control.

However, it was not clear whether similar effects take place in primary human AML cells in comparison with healthy primary leukocytes, since activating both mTOR pathways and TNF-α production utilize both growth factor and inflammatory mediator-like responses.

We observed that primary AML cells generate more Tim-3 protein compared to healthy leukocytes, including cell surface protein expression. Only about 30% of Tim-3 molecules were externalised in primary healthy leukocytes, while almost all Tim-3 protein was present on the cell surface of primary AML cells. This could have impact on differences in activity of the protein in terms of its ability to mediate ligand-induced activation of mTOR, HIF-1α accumulation and cytokine releases. Our results suggest that Tim-3 mediates ligand-induced activation of the mTOR pathway, which involves upregulation of

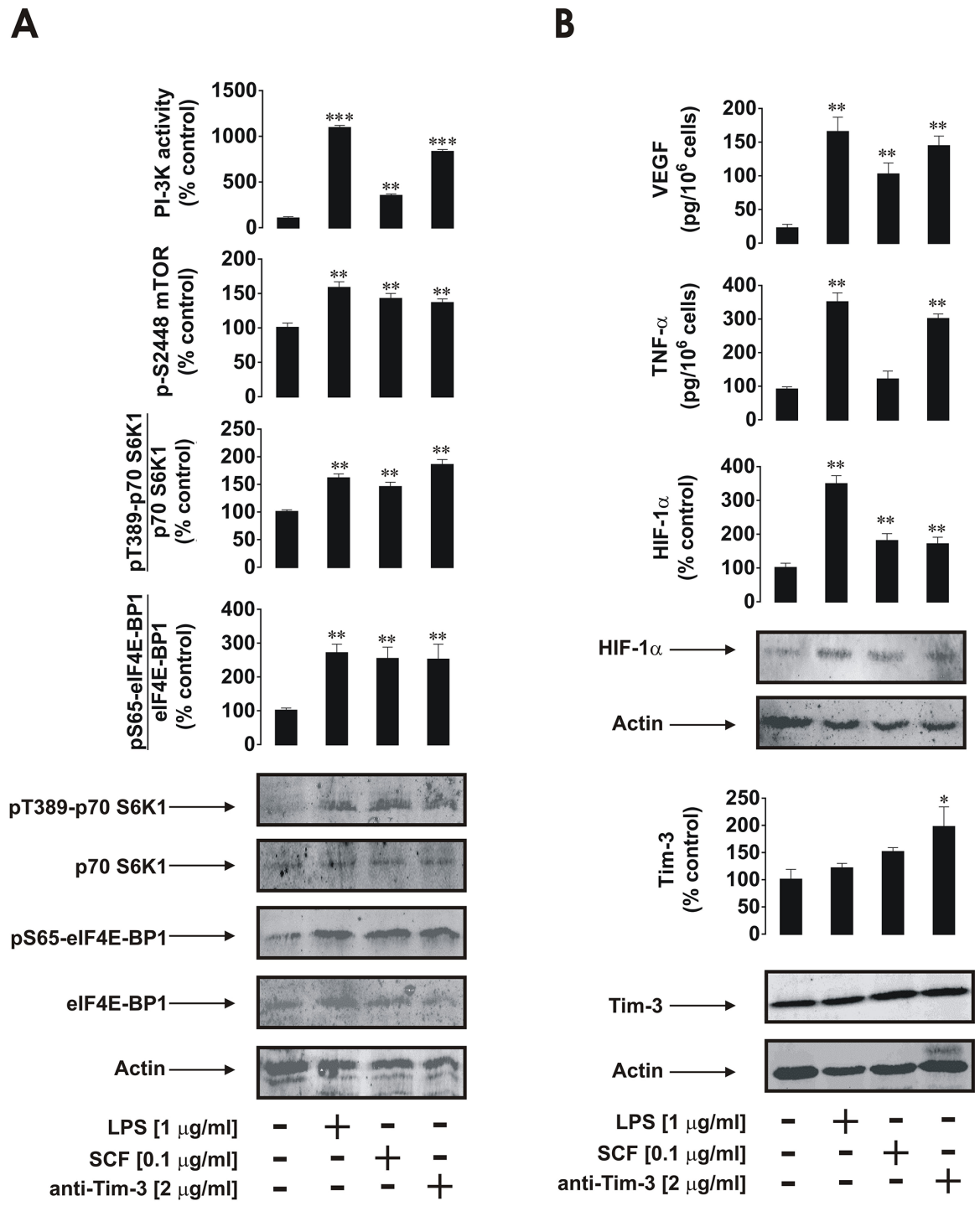

Figure 4: Anti-Tim-3 induces mTOR activity, HIF-1α accumulation as well secretion of VEGF and TNF-α in primary human healthy leukocytes. PLs were exposed for 4 h for the indicated concentrations of anti-Tim-3, LPS and SCF followed by analysis of PI-3K/mTOR pathway activity **A.** HIF-1α accumulation and release of VEGF and TNF-α **B.** Images are from one experiment representative of four which gave similar results. Quantitative data are shown as means ± SEM of four individual experiments; *$p < 0.05$; **$p < 0.01$ vs. control.

phospho-S2448 mTOR levels, phosphorylation of p70 S6K1(T389) and eIF4E-BP1 (S65), accumulation of HIF-1α protein and secretion of TNF-α and VEGF. It is however, clear that the effects are moderate and are weaker than those induced by LPS or SCF, a classic inflammatory mediator and hematopoietic growth factor, respectively.

In AML cells, SCF displayed the highest biological activity while LPS effects were stronger in healthy whole blood PLs. These differences are due to differential expression of TLR4 and Kit receptors in healthy and malignant leukocytes. SCF-induced responses in healthy PLs are likely to involve both direct and indirect effects.

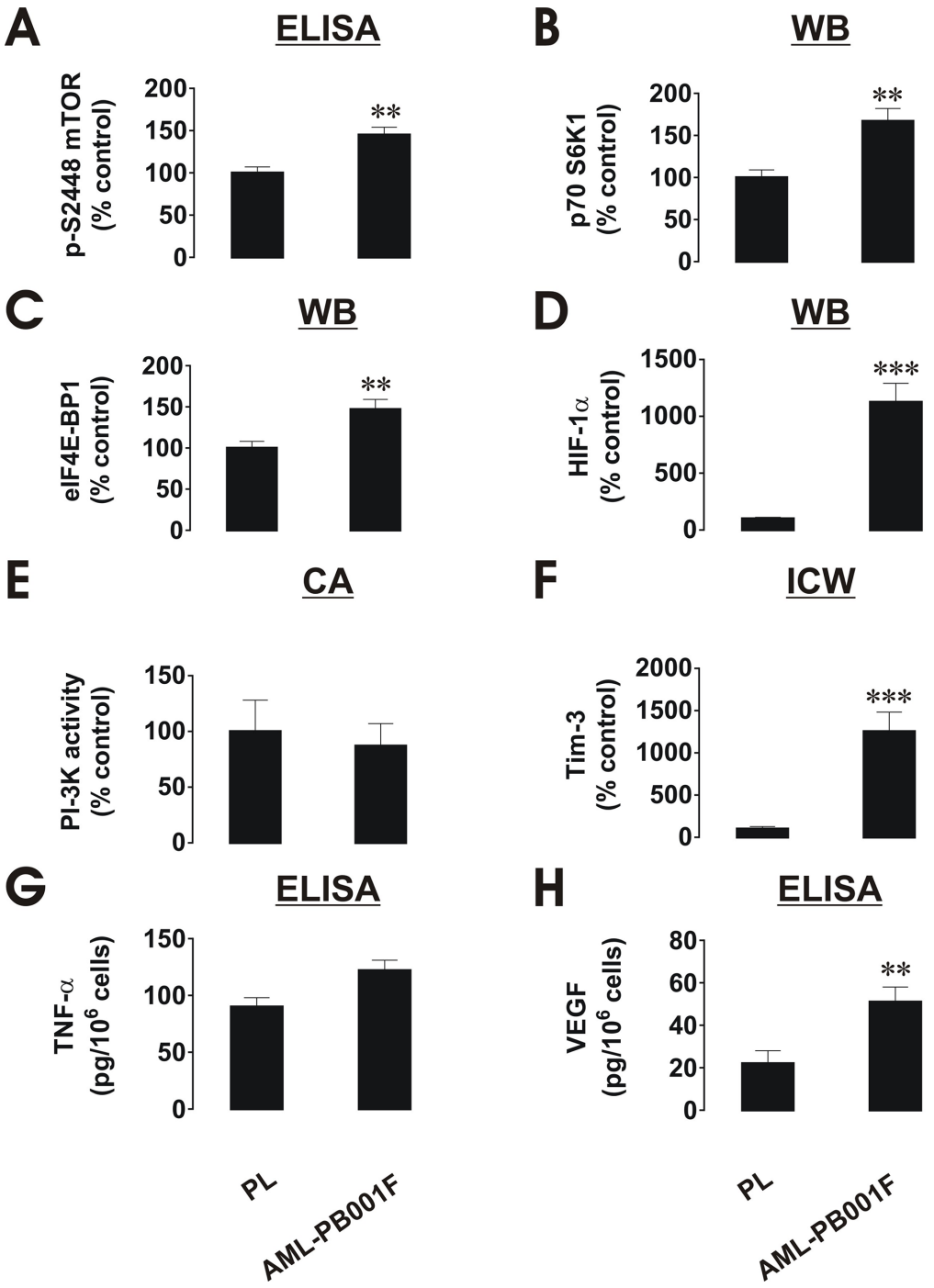

Figure 5: Comparative quantitative analysis of mTOR/HIF-1 pathway components as well as VEGF/TNF-α secretion in primary human AML cells and healthy human PLs. Protein levels were compared based on the indicated type of detection. **A.** pS2448 mTOR intracellular levels were detected by ELISA, normalised against total cellular protein and compared (results were statistically validated). **B, C.** and **D.** – Levels of p70 S6K1, eIF4E-BP1 and HIF-1α protein were detected by Western blot (WB), quantitated and normalised against respective actin values before comparison and statistical validation of the results. **E.** PI-3K activity levels were measured by colorimetric assay (CA), **F.** – Intracellular levels of Tim-3 were detected by in-cell Westerns (ICW). Fluorescence values obtained for healthy PLs and AML cells and were divided by respective cell number (1,500,000 or 300,000, see Figure 1) and used for comparison (the value in PLs was considered as 100%). Similar results were obtained when comparing Tim-3 values in AML cells and healthy PLs obtained by Western blot and normalised against actin **G.** TNF-α and **H.** VEGF levels were measured in the medium by ELISA and the amounts per 10^6 cells were compared and statistically validated. Data was obtained from 3–6 individual experiments, which gave similar results. Quantitative data are shown as means ± SEM; *$p < 0.05$; **$p < 0.01$; ***$p < 0.01$ vs. control.

Several types of leukocytes express Kit receptors. This includes hematopoietic stem cells, multipotent progenitors, common myeloid progenitors, common lymphoid progenitors, megakaryocytes, myeloblasts, small lymphocytes, eosinophils, NK cells and dendritic cells [8, 12, 13]. Altogether, this amounts to more than 5–10% of blood leukocytes. SCF is known to trigger IL-6 release in primary cells [14] and we have also observed a clear increase in IL-6 secretion in healthy PLs exposed to 100 ng/ml SCF for 4 h (data not shown). IL-6 is known to upregulate VEGF release [15], which is a HIF-1-dependent process [16]. These effects could contribute to both HIF-1α accumulation and VEGF release in addition to SCF (primary stimulus, see Figure 4 for more details).

Although Tim-3 ligands are known to trigger programmed death of T cells and demonstrate downregulatory properties (especially malignant types, [1], 55–86% of all leukocytes are myeloid cells. Therefore, phenotypically, we observed the response of the vast majority of the total cell pool, indicating that the observed effects were likely to be derived from myeloid cells.

Intriguingly, the background levels of phospho-S2448 mTOR, HIF-1α, Tim-3 as well as p70 S6K1/eIF4E-BP-1 proteins are significantly higher in non-treated AML cells compared to resting healthy PLs (see Figure 5 for details). This phenomenon is especially applicable to the HIF-1α accumulation which is strong in non-treated AML cells and almost undetectable (detectable only upon loading around 140,000 cell per well) in healthy PLs. This observation becomes more intriguing in light of recently reported contribution of HIF-1 to Tim-3 expression [17]. Respectively, VEGF but not TNF-α secretions were significantly higher in non-treated AML cells compared to healthy PLs. Importantly, background levels of the PI-3K activity were very similar in AML cells and healthy PLs. This suggests that the increased background levels of pS2448 mTOR in primary AML cells could be due to increased constitutive phosphorylation as reported, for example, for the LAD2 mast cell line [18, 19]. LAD2 mast cells are also derived from the myeloid lineage, and were obtained from a 44-year-old male patient suffering from mastocytosis. Analysis of bone marrow biopsies/aspirates showed results consistent with an aggressive form of mast cell leukemia/sarcoma [20]. This suggests that the mTOR/HIF-1/VEGF pathway, but not inflammatory TNF-α, is used permanently by AML cells compared to healthy PLs.

Taken together, our findings indicate that Tim-3 in primary leukocytes, both healthy and malignant AML cells, displays moderate properties of an inflammatory receptor with additional growth factor (mTOR activation) and pro-angiogenic (VEGF release) activities (a summary of the biochemical activities of Tim-3 in AML cells is provided in Figure 6). Although the mTOR/HIF-1 pathway is triggered by both LPS and SCF, we only observed a significant increase in TNF-α/VEGF secretion (production of both factors is regulated by mTOR [21, 22]) following LPS stimulation. SCF induced mostly VEGF release and did not trigger the production of pro-inflammatory TNF-α. However, highly increased levels of Tim-3 protein in AML cells compared to those in healthy PLs did not result in higher specific biochemical activity of the receptor.

Currently, Tim-3 is being considered as a target antigen for anti-leukaemia therapy including T-cell leukaemia and AML [5] as well as to reverse T cell exhaustion and restore anti-tumour immunity [23]. In addition to the current knowledge, our findings suggest that Tim-3 is more abundant on the surface of AML cells compared to healthy leukocytes. This, together with the moderate biochemical activities associated with Tim-3 activation, is encouraging since it highlights a relatively easy way of recognition and selective targeting of human AML cells.

MATERIALS AND METHODS

Materials

RPMI-1640 medium, foetal calf serum and supplements, *P. aeruginosa* LPS, were purchased from Sigma (Suffolk, UK). Maxisorp™ microtitre plates were obtained either from Nunc (Roskilde, Denmark) or kindly provided by Oxley Hughes Ltd (London, UK). Mouse monoclonal antibodies to HIF-1α, mTOR and β-actin as well as rabbit polyclonal antibodies against phospho-S2448 mTOR were purchased from Abcam (Cambridge, UK). Antibodies against phospho-T389 p70 S6 kinase 1 (p70 S6K1), total and phospho-S65 eukaryotic initiation factor 4E binding protein 1 (eIF4E-BP1) antibodies were obtained from Cell Signaling Technology (Danvers, MA USA). Goat anti-mouse and goat anti-rabbit fluorescence dye-labelled antibodies were obtained from Li-Cor (Lincoln, Nebraska USA). ELISA-based assay kits for the detection of VEGF, TNF-α and IL-6 were purchased from Bio-Techne (R&D Systems, Abingdon, UK). All other chemicals were of the highest grade of purity and available commercially unless otherwise stated.

Primary human AML cells

Primary human AML mononuclear blasts (AML-PB001F, newly diagnosed/untreated) were purchased from AllCells (Alameda, CA, USA) and handled in accordance with manufacturer's instructions. Cells from two different patients were analysed.

Primary human leukocytes obtained from healthy donors (buffy coats)

Primary human leukocytes were obtained from buffy coat blood (which originated from healthy donors undergoing routine blood donation). The buffy coat

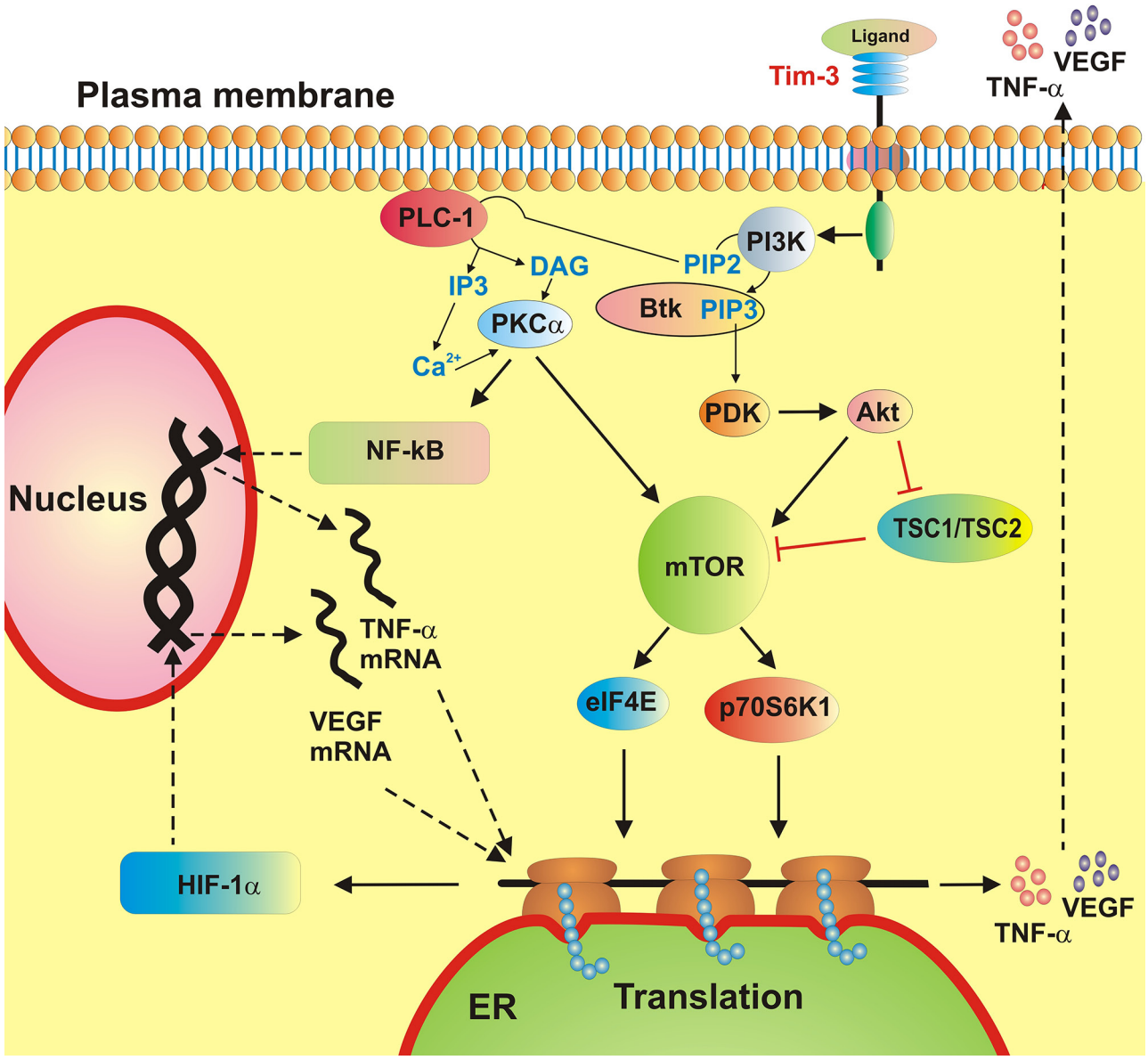

Figure 6: A schematic summary of ligand-induced Tim-3-mediated biological responses in healthy primary human leukocytes and primary human AML cells.

blood was purchased from the National Health Blood and Transfusion Service (NHSBT, UK) following ethical approval (REC reference: 12/WM/0319). Mononuclear-rich leukocytes were obtained by Ficoll-density centrifugation according to the manufacturer's protocol. Cell numbers were determined using a haemocytometer and diluted accordingly with HEPES-buffered Tyrode's solution before treatment as indicated below.

Stem cell factor

Human SCF protein was produced in *E.Coli* and purified in accordance with published protocols [24].

Western blot analysis

Expressions of HIF-1α, total and phospho-T389 p70 S6K1, as well as total and phospho-S65 eIF4E-BP1 were determined by Western blot analysis and compared to β-actin in order to determine equal protein loading, as previously described [25]. Li-Cor goat secondary antibodies, conjugated with fluorescent dyes, were employed according to the manufacturer's protocol in order to visualise detected proteins (using a Li-Cor Odyssey imaging system). Following Western blot detection of phospho-T389 p70S6K1 and phospho-S65-eIF4E-BP1, membranes were stripped using a ReBlot™ Plus Kit (Chemicon International) according to the

manufacturer's protocol. Membranes were then blocked and scanned using a Li-Cor Odyssey imaging system to make sure that stripping was successfully completed. Then membranes were re-probed with antibodies in order to detect the total amounts of p70S6K1 and eIF4E-BP1. Western blot data were quantitatively analysed using Odyssey software and values were normalised against respective β-actin bands.

Detection of phospho-S2448 mTOR in cell lysates by ELISA

Phosphorylation of mTOR was analysed by ELISA as recently described [25]. Briefly, 96-well ELISA plates were coated with mouse anti-mTOR antibodies and then blocked with 2% BSA. Cell lysates were then added to the wells and incubated at room temperature for 2 h under constant agitation. After extensive washing with Tris-Buffered Saline and Tween 20 (TBST) buffer, anti-phospho-S2448 mTOR antibodies were added and plates incubated for 2 h at room temperature with constant agitation. After washing with TBST buffer plates were incubated with HRP-labelled goat anti-rabbit IgG (1:1000 dilution in TBST buffer). After 1 h incubation, plates were extensively washed using TBST and bound secondary antibodies were detected by the peroxidase reaction (ortho-phenylenediamine/H_2O_2).

In-cell western and in-cell assay

We employed a standard Li-Cor in-cell Western assay to analyse total Tim-3 expressions in primary human AML cells and healthy primary leukocytes (PLs). The in-cell assay was also applied to detect Tim-3 protein surface presence in the studied cells [2].

Detection of VEGF, TNF-α and IL-6 release

Concentrations of these cytokines released into the medium were analysed by ELISA (R&D Systems assay kits) according to the manufacturer's instructions.

Analysis of phosphatidylinositol-3 kinase (PI-3K) activity

The activity of PI-3K was measured using a non-radioactive assay based on the ability of the enzyme to phosphorylate its substrate as previously described [26].

Statistical analysis

Each experiment was performed at least three times and statistical analysis was conducted using a two-tailed Student's *t* test. Statistical probabilities (p) were expressed as *, where $p < 0.05$, **, where $p < 0.01$ and *** when $p < 0.001$.

CONFLICTS OF INTEREST

There is no conflict of interest that the authors should disclose.

REFERENCES

1. Tang D, Lotze MT. Tumor immunity times out: TIM-3 and HMGB1. Nat Immunol. 2012; 13:808–810.
2. Prokhorov A, Gibbs BF, Bardelli M, Ruegg L, Fasler-Kan E, Varani L, Sumbayev VV. The immune receptor Tim-3 mediates activation of PI3 kinase/mTOR and HIF-1 pathways in human myeloid leukaemia cells. Int J Biochem Cell Biol. 2015; 59:11–20.
3. Anderson AC, Anderson DE, Bregoli L, Hastings WD, Kassam N, Lei C, Chandwaskar R, Karman J, Su EW, Hirashima M, Bruce JN, Kane LP, Kuchroo VK, Hafler DA. Promotion of tissue inflammation by the immune receptor Tim-3 expressed on innate immune cells. Science. 2007; 318:1141–1143.
4. Ngiow SF, von Scheidt B, Akiba H, Yagita H, Teng MW, Smyth MJ. Anti-TIM3 antibody promotes T cell IFN-gamma-mediated antitumor immunity and suppresses established tumors. Cancer Res. 2011; 71:3540–3551.
5. Kikushige Y, Miyamoto T. TIM-3 as a novel therapeutic target for eradicating acute myelogenous leukemia stem cells. Int J Hematol. 2013; 98:627–633.
6. Anderson AC. Tim-3, a negative regulator of anti-tumor immunity. Curr Opin Immunol. 2012; 24:213–216.
7. Kikushige Y, Shima T, Takayanagi S, Urata S, Miyamoto T, Iwasaki H, Takenaka K, Teshima T, Tanaka T, Inagaki Y, Akashi K. TIM-3 is a promising target to selectively kill acute myeloid leukemia stem cells. Cell Stem Cell. 2010; 7:708–717.
8. Broudy VC. Stem cell factor and hematopoiesis. Blood. 1997; 90:1345–1364.
9. Gwinn DM, Shackelford DB, Egan DF, Mihaylova MM, Mery A, Vasquez DS, Turk BE, Shaw RJ. AMPK phosphorylation of raptor mediates a metabolic checkpoint. Mol Cell. 2008; 30:214–226.
10. Frede S, Stockmann C, Freitag P, Fandrey J. Bacterial lipopolysaccharide induces HIF-1 activation in human monocytes via p44/42 MAPK and NF-kappaB. Biochem J. 2006; 396:517–527.
11. Sumbayev VV. LPS-induced Toll-like receptor 4 signalling triggers cross-talk of apoptosis signal-regulating kinase 1 (ASK1) and HIF-1alpha protein. FEBS Lett. 2008; 582:319–326.
12. Oriss TB, Krishnamoorthy N, Ray P, Ray A. Dendritic cell c-kit signaling and adaptive immunity: implications for the upper airways. Curr Opin Allergy Clin Immunol. 2014; 14:7–12.
13. Yuan Q, Austen KF, Friend DS, Heidtman M, Boyce JA. Human peripheral blood eosinophils express a functional

c-kit receptor for stem cell factor that stimulates very late antigen 4 (VLA-4)-mediated cell adhesion to fibronectin and vascular cell adhesion molecule 1 (VCAM-1). J Exp Med. 1997; 186:313–323.

14. MacNeil AJ, Junkins RD, Wu Z, Lin TJ. Stem cell factor induces AP-1-dependent mast cell IL-6 production via MAPK kinase 3 activity. J Leukoc Biol. 2014; 95:903–915.
15. Adachi Y, Aoki C, Yoshio-Hoshino N, Takayama K, Curiel DT, Nishimoto N. Interleukin-6 induces both cell growth and VEGF production in malignant mesotheliomas. Int J Cancer. 2006; 119:1303–1311.
16. Semenza GL. HIF-1 and tumor progression: pathophysiology and therapeutics. Trends Mol Med. 2002; 8:S62–67.
17. Koh HS, Chang CY, Jeon SB, Yoon HJ, Ahn YH, Kim HS, Kim IH, Jeon SH, Johnson RS, Park EJ. The HIF-1/glial TIM-3 axis controls inflammation-associated brain damage under hypoxia. Nat Commun. 2015; 6:6340.
18. Kim MS, Kuehn HS, Metcalfe DD, Gilfillan AM. Activation and function of the mTORC1 pathway in mast cells. J Immunol. 2008; 180:4586–4595.
19. Gibbs BF, Yasinska IM, Pchejetski D, Wyszynski RW, Sumbayev VV. Differential control of hypoxia-inducible factor 1 activity during pro-inflammatory reactions of human haematopoietic cells of myeloid lineage. Int J Biochem Cell Biol. 2012; 44:1739–1749.
20. Kirshenbaum AS, Akin C, Wu Y, Rottem M, Goff JP, Beaven MA, Rao VK, Metcalfe DD. Characterization of novel stem cell factor responsive human mast cell lines LAD 1 and 2 established from a patient with mast cell sarcoma/leukemia; activation following aggregation of FcepsilonRI or FcgammaRI. Leuk Res. 2003; 27:677–682.
21. Choi YK, Kim CK, Lee H, Jeoung D, Ha KS, Kwon YG, Kim KW, Kim YM. Carbon monoxide promotes VEGF expression by increasing HIF-1alpha protein level via two distinct mechanisms, translational activation and stabilization of HIF-1alpha protein. J Biol Chem. 2010; 285:32116–32125.
22. Li CY, Li X, Liu SF, Qu WS, Wang W, Tian DS. Inhibition of mTOR pathway restrains astrocyte proliferation, migration and production of inflammatory mediators after oxygen-glucose deprivation and reoxygenation. Neurochem Int. 2015; 83–84:9–18.
23. Sakuishi K, Apetoh L, Sullivan JM, Blazar BR, Kuchroo VK, Anderson AC. Targeting Tim-3 and PD-1 pathways to reverse T cell exhaustion and restore anti-tumor immunity. J Exp Med. 2010; 207:2187–2194.
24. Wang C, Liu J, Wang L, Geng X. Solubilization and refolding with simultaneous purification of recombinant human stem cell factor. Appl Biochem Biotechnol. 2008; 144:181–189.
25. Yasinska IM, Gibbs BF, Lall GS, Sumbayev VV. The HIF-1 transcription complex is essential for translational control of myeloid hematopoietic cell function by maintaining mTOR phosphorylation. Cell Mol Life Sci. 2014; 71:699–710.
26. Abooali M, Lall GS, Coughlan K, Lall HS, Gibbs BF, Sumbayev VV. Crucial involvement of xanthine oxidase in the intracellular signalling networks associated with human myeloid cell function. Sci Rep. 2014; 4:6307.

Research Paper

Expression of functional neuronal receptor latrophilin 1 in human acute myeloid leukaemia cells

Vadim V. Sumbayev[1], Isabel Gonçalves Silva[1], Jennifer Blackburn[1], Bernhard F. Gibbs[1], Inna M. Yasinska[1], Michelle D. Garrett[2], Alexander G. Tonevitsky[3], Yuri A. Ushkaryov[1]

[1]School of Pharmacy, University of Kent, Chatham, Kent, ME4 4TB, United Kingdom

[2]School of Biosciences, University of Kent, Canterbury, Kent, CT2 7NJ, United Kingdom

[3]Hertsen Moscow Oncology Research Institute, Branch of The National Medical Research Radiological Center, Ministry of Health of The Russian Federation, 125284, Moscow, Russian Federation

Correspondence to: Vadim V. Sumbayev, **email:** V.Sumbayev@kent.ac.uk
Yuri A. Ushkaryov, **email:** Y.Ushkaryov@kent.ac.uk

Keywords: *latrophilin, myeloid leukaemia, mammalian target of rapamycin*

Received: *March 17, 2016* ***Accepted:*** *May 29, 2016* ***Published:*** *June 14, 2016*

ABSTRACT

Acute myeloid leukaemia (AML) is a blood cancer affecting cells of myeloid lineage. It is characterised by rapid growth of malignant leukocytes that accumulate in the bone marrow and suppress normal haematopoiesis. This systemic disease remains a serious medical burden worldwide. Characterisation of protein antigens specifically expressed by malignant cells, but not by healthy leukocytes, is vital for the diagnostics and targeted treatment of AML. Here we report, for the first time, that the neuronal receptor latrophilin-1 is expressed in human monocytic leukaemia cell lines and in primary human AML cells. However, it is absent in healthy leukocytes. Latrophilin-1 is functional in leukaemia cells tested, and its biosynthesis is controlled through the mammalian target of rapamycin (mTOR), a master regulator of myeloid cell translational pathways. Our findings demonstrate that latrophilin-1 could be considered as a novel biomarker of human AML, which offers potential new avenues for AML diagnosis and treatment.

INTRODUCTION

Latrophilin-1 (LPHN1) is an adhesion G-protein-coupled receptor, which participates in control of calcium signalling and exocytosis in vertebrate neurons and neuroendocrine cells. LPHN1 is highly expressed in the brain, detected at low levels in some other tissues, and reported as absent from blood [1]. Interestingly, this protein and its homologues appear to be upregulated in malignant cells: LPHN1 is found in non-small cell lung cancer and is implicated in its invasive character [2], while LPHN2 and 3 are upregulated or mutated in several types of metastatic cancer [3–5]. Stimulation of LPHN1 induces intracellular Ca^{2+} mobilisation and thus triggers significant exocytosis of neurotransmitters, which is crucial for normal neuronal function [6–7]. LPHN1 also plays an important role in cell surface interactions (reviewed in [1]). Exocytotic activity is also required for cytokine/growth factor release during myeloid cell haematopoiesis [8–11], especially when myeloid leukocytes undergo malignant transformation. Firstly, the energy resources of leukaemia cells are normally very limited [8–12] and lead to oxygen starvation. Therefore, the bone marrow vasculature plays a pivotal role in the survival of leukaemia cells, which induce angiogenesis by releasing vascular endothelial growth factor (VEGF) and other pro-angiogenic factors. Secondly, leukaemic cells produce and release interleukin 6 (IL-6), which is necessary to support their own survival and proliferation [13]. These processes require efficient exocytosis. We therefore hypothesised that myeloid leukaemia cells may express LPHN1, a receptor that is able to convert cell-surface interactions into intracellular signals leading to activation of exocytosis.

Here we report, for the first time, that LPHN1 expression is clearly detectable at both RNA and protein level in human monocytic leukaemia (ML)

cell lines (U937 and THP-1) and in primary human acute myeloid leukaemia (AML) cells. Treatment of all these leukaemia cells with the inflammatory mediator lipopolysaccharide (LPS) further upregulates LPHN1 translation *via* mammalian target of rapamycin (mTOR, a master regulator of myeloid cell translation and growth [14]). When LPHN1 is stimulated by its high-affinity ligand [7], α-latrotoxin (LTX), this significantly increases LPS-induced IL-6 release from leukaemia cell lines and primary cells. In contrast, in healthy primary human leukocytes, LPHN1 expression is not detectable and is not induced by the mTOR activators LPS, SCF or anti-Tim-3. We therefore conclude that LPHN1 is a novel pharmacoproteomic biomarker of human AML that offers new approaches to therapeutic targeting of this disease.

RESULTS

LPHN1 expression and activity in human ML cell lines

In order to investigate the possibility of LPHN1 expression in human AML cells, we first used human ML cell lines, U937 and THP-1. Cells were stimulated for 24 h with LPS, LTX or a combination of these ligands. LPS is a pathogen-associated molecular pattern shared by Gram-negative bacteria and is recognised by the Toll-like receptor 4 (TLR4), which is expressed by human myeloid cells [13]. LPS was chosen to avoid TLR4 activation by endogenous ligands (such as proteins released after dysfunctionalisation of mitochondria), which themselves induce the expression and release of IL-6 and other important factors required for leukaemia cell survival [15]. Using Western blot analysis, we found that U937 cells constitutively expressed LPHN1 (Figure 1A) and the same pattern was observed in THP-1 cells (Figure 2A). In both U937 and THP-1 cells, LPHN1 expression levels were significantly increased (4-12-fold) by LPS, but not by LTX; when used in combination with LPS, LTX also did not significantly change LPHN1 levels compared to LPS alone (Figures 1A and 2A). However, whilst LTX alone did not stimulate IL-6 release, LTX combined with LPS induced the release of IL-6 that was 2 times greater than for LPS alone in both U937 and THP-1 human ML cells (Figures 1A and 2A).

We also found that LPS, but not LTX, significantly activated the mTOR pathway: LPS augmented by 2-fold the activating phosphorylation of mTOR at S2448 and increased the phosphorylation of its substrate, p70 S6 kinase 1 (p70 S6K1) at position T389. This was clearly observed in both cell lines (Figures 1B and 2B).

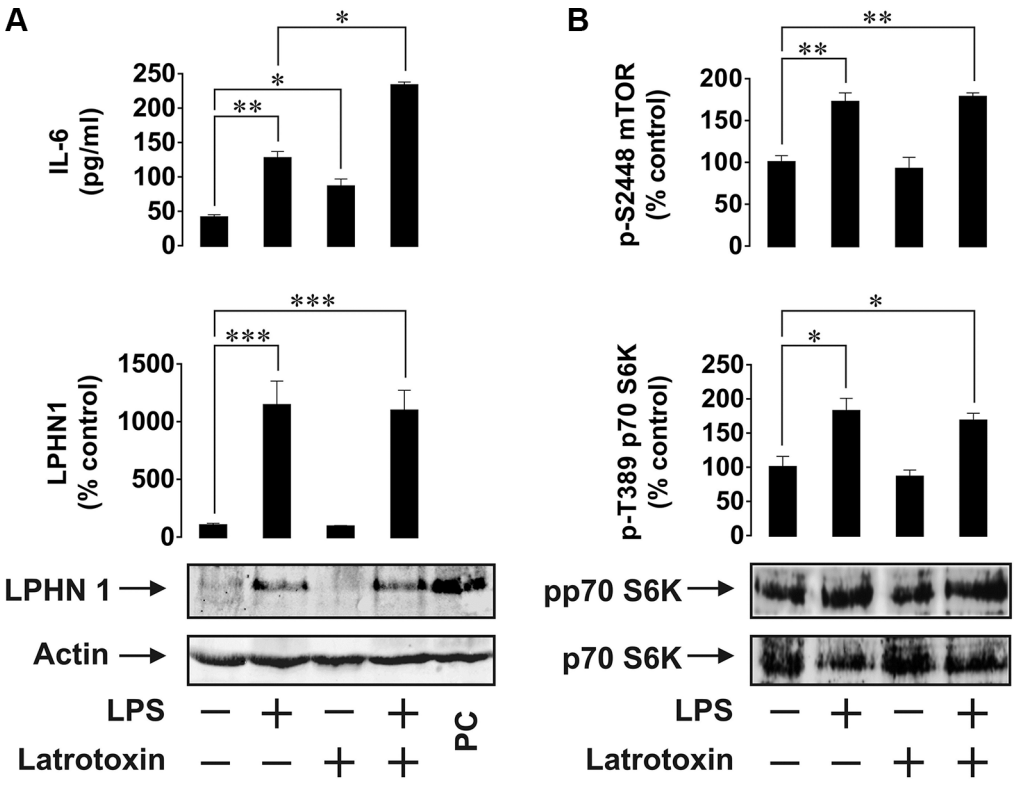

Figure 1: Expression and activity of LPHN1 in U937 human ML cells. (**A**) U937 cells were exposed to 1 μg/ml LPS, 500 pM LTX or a combination of these two ligands for 24 h. Following cell lysis, IL-6 release was measured by ELISA, whilst LPHN1 protein levels were analysed by Western blotting. PC; positive control for LPHN1 (mouse brain extract). (**B**) Phospho-S2448 mTOR and phospho-T389 p70 S6K1 were detected using ELISA and Western blotting, respectively. Western blot images show one experiment representative of six, all of which gave similar results. Data are the mean values ± SEM ($n = 6$). *$p < 0.05$; **$p < 0.01$; ***$p < 0.001$.

Since mTOR is a master regulator of myeloid cell translational pathways [14], it could be hypothesised that the mTOR pathway is responsible for LPS-induced upregulation of LPHN1 protein levels. We therefore exposed both U937 and THP-1 cells for 4 h to 1 μg/ml LPS with or without 1h pre-treatment with rapamycin (a highly specific mTOR inhibitor). We observed that 4-h exposure to LPS led to a moderate increase in LPHN1 expression in both U937 and THP-1 cells, which was less than the increase induced by 24 h stimulation and more pronounced in THP-1 versus U937 cells. In both cell lines, rapamycin fully blocked the expression of LPHN1 (Figure 3A and 3B). Importantly, rapamycin did not affect the viability of the cells, as verified using MTS cell viability test (data not shown). In order to confirm the role of mTOR signalling in upregulation of LPHN1, we performed a similar experiment using another mTOR inhibitor, AZD2014 [16]. AZD2014 did not affect cell viability as measured by cell viability assay (data not shown); however, in both U937 and THP-1 cells, AZD2014 obliterated expression of LPHN1 protein (Figure 3C and 3D).

Functional LPHN1 is expressed in human primary AML cells, but not in healthy leukocytes

Next, we asked whether functional LPHN1 is expressed in primary human AML cells. We exposed AML-PB001F primary human mononuclear blasts for 24 h to LPS, LTX or a combination of these ligands. We found that LPS upregulated both mTOR activation and IL-6 release by these cells. LTX alone was ineffective, but in combination with LPS it significantly increased both mTOR activation and IL-6 exocytosis (Figure 4). In order to determine whether LPHN1 expression levels in AML-PB001F cells were also controlled through the mTOR pathway, we exposed these cells for 4 h to different mTOR activators: LPS, SCF or anti-Tim-3 antibody. We found that each stimulus led to a significant increase in the activating phosphorylation of mTOR (on S2448, Figure 5A), while the SCF-induced effect was stronger due to high levels of Kit receptor expression by these cells [17]. The magnitude of mTOR-dependent effects provoked by LPS, SCF and anti-Tim-3 in human AML cells observed here agrees well with previously published data [17]. Interestingly, all stimuli significantly induced LPHN1 expression, as shown by Western blot analysis (Figure 5A).

Most importantly, when we tested healthy primary human leukocytes, they did not show any LPHN1 expression (even after overexposure of Western blots). Furthermore, LPHN1 was also undetectable following 4 or 24 h exposures of healthy leukocytes to LPS, SCF or anti-Tim-3 antibody (Figure 5B).

To confirm the results based on protein expression, we then conducted quantitative real-time PCR (RT-PCR) to detect and quantify LPHN1 mRNA. These experiments demonstrated that LPHN1 mRNA is detected in THP-1 cells and primary AML cells, but not in healthy primary human leukocytes (Figure 5C). Furthermore, we noted that LPS significantly increased the already high level of

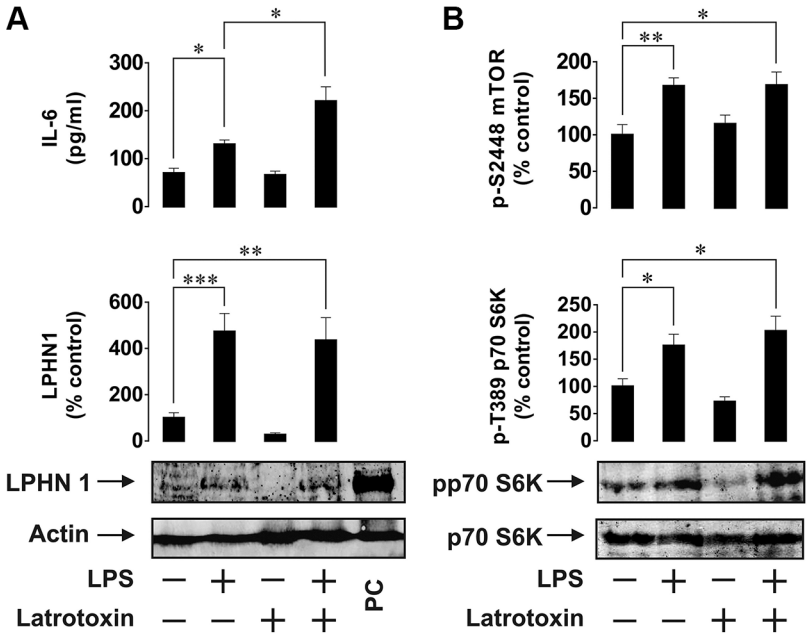

Figure 2: Effects of LPS and LTX on LPHN1 expression, IL-6 exocytosis and mTOR activity in THP-1 human ML cells. (**A**) THP-1 cells were exposed to 1 μg/ml LPS, 500 pM LTX or a combination of these two ligands for 24 h. Following cell lysis, LPHN1 protein levels were analysed by Western blot. IL-6 release was measured by ELISA. (**B**) Phospho-S2448 mTOR and phospho-T389 p70 S6K1 were detected using ELISA and Western blot, respectively. Western blot images show one experiment representative of six, which gave similar results. Data are mean values ± SEM ($n = 6$). *$p < 0.05$; **$p < 0.01$; ***$p < 0.001$.

LPHN1 mRNA in THP-1 cells and primary AML cells. In contrast, even a 24 h exposure to LPS did not induce LPHN1 mRNA expression in primary healthy human leukocytes (Figure 5C).

Taken together, our findings demonstrate the regulated expression of the functional neuronal receptor LPHN1 in human AML cells, but not in healthy primary human leukocytes. This opens a new direction in research of malignant transformation and survival of cancerous white blood cells and the role of LPHN1 in these processes.

DISCUSSION

LPHN1 functions as an exocytosis promoter acting through calcium mobilisation/signalling machinery [1, 6, 7]. The presence of regulated exocytosis is one of the main features of neurons and neuroendocrine cells, where this receptor is highly abundant. However, the requirement of exocytosis in malignant cells, in particular myeloid leukocytes, has not yet been investigated and there are no reports regarding a possible role of LPHN1 in leukaemia and pro-leukaemic haematopoiesis.

We therefore considered the possibility of LPHN1 protein expression in human leukaemia cells. Our studies demonstrate that resting ML cells from U937 and THP-1 human cell lines clearly express LPHN1 mRNA and possess detectable amounts of functional LPHN1 protein. We also show that expression of functional LPHN1 is dependent on the mTOR pathway. LTX, a specific LPHN1 agonist [3], significantly increased LPS-induced exocytosis of IL-6 in both cell lines. Since the production of IL-6 protein depends on mTOR [18], and the activity of the mTOR pathway was not upregulated by LTX in either cell line employed, it is evident that LTX triggers IL-6 exocytosis rather than its biosynthesis. Wild type LTX used in our experiments is known to form Ca^{2+}-permeable pores in the membrane of cells expressing toxin receptors [6], and such pores could potentially induce LPHN1-independent exocytosis. However, LTX only inserts itself into the membrane after binding the receptor [6], and this interaction always stimulates LPHN1, leading to exocytosis [6, 7]. Indeed, in our experiments, the toxin stimulated secretion in LPHN1-expressing cells only (Figures 1, 2, 4). Furthermore, mutant LTX^{N4C}, which does not form pores [7], induced similar exocytosis of

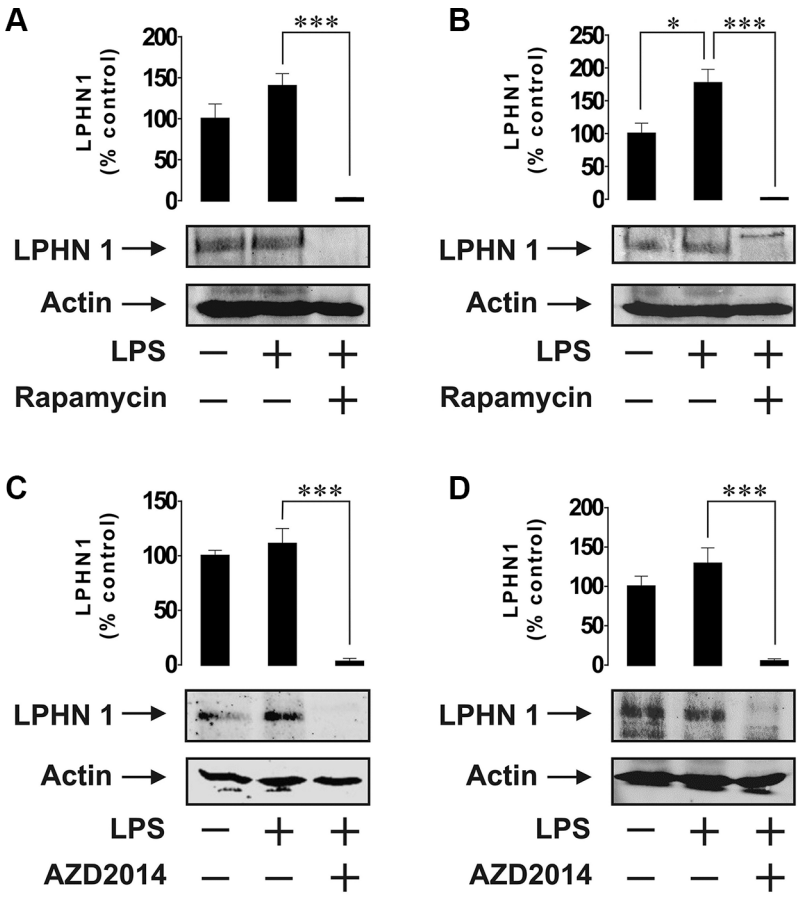

Figure 3: Expression of LPHN1 in U-937 and THP-1 cells depends on mTOR. U-937 (**A**, **C**) and THP-1 (**B**, **D**) cells were exposed to 1 μg/ml LPS for 4 h with or without 1 h pre-treatment with 10 μM rapamycin (A, B) or AZD2014 (C, D). LPHN1 expression was then measured using Western blot analysis. Western blot images show one experiment representative of four, which gave similar results. Data are mean values ± SEM ($n = 4$). *$p < 0.05$; **$p < 0.01$; ***$p < 0.001$.

IL-6 in THP-1/U-937 cells (data not shown), confirming the active role of LPHN1 in this secretion. Interestingly, LPHN1 expression is completely abolished when the cells are pre-treated with the mTOR inhibitors (rapamycin or AZD2014) before stimulation of U937 or THP-1 cells by LPS (Figure 3). This suggests that the process of LPHN1 expression fully depends on the mTOR pathway. As shown in Figures 1B and 2B, both cell lines demonstrate a background activity of the mTOR pathway, which is further upregulated by LPS, and it is this additional activation of mTOR that brings about the substantial increase in the amount of expressed LPHN1 at 24 h.

Clearly, ML cell lines differ from malignant leukocytes *in vivo* both in terms of biological activities and protein expression profiles. However, patient-derived primary human AML cells (we used primary AML-PB001F mononuclear blasts obtained from leukaemia patients) do not differ from the two ML cell lines in respect of the easily detectable LPHN1 expression and its upregulation in response to mTOR stimuli (LPS, SCF and anti-Tim-3). Similarly, stimulation of the primary leukaemia cells with LTX leads to a substantial increase in the release of LPS-induced IL-6. On the other hand, unlike in the cell lines, LTX also upregulates LPS-induced mTOR-activating phosphorylation in the primary AML cells. Our observed effect is likely to be the result of low expression of the LPS receptor, TLR4, in the primary AML cells, as reported by their supplier. As a result of the lower TLR4 signalling, only some mTOR will be activated by LPS, while the majority of mTOR will still remain unphosphorylated and therefore subject to further phosphorylation through LPHN1-induced signalling. In cell lines, where the TLR4 expression levels are higher, there may not be sufficient scope for further activation of mTOR by LTX. This finding implies a functional integration of LPHN1 into the AML signalling machinery [13, 19]. Its possible functions are summarised in Figure 6.

One very important finding of this work is that primary healthy human leukocytes do not express any LPHN1. Furthermore, LPHN1 expression is not inducible by exposure of the healthy cells to any of the stimuli that show positive effects in AML cells: LPS, SCF or anti-Tim-3. This clearly demonstrates that the expression of functional LPHN1 occurs specifically in leukaemia cells only. Quantitative RT-PCR experiments further confirm that healthy primary leukocytes do not possess detectable LPHN1 mRNA. This indicates that the change in the expression profile of this important receptor only takes place in leukocytes during or as a result of malignant transformation. The importance of LPHN1 to malignant leukocytes is evident: for their survival, these cells release certain growth factors and cytokines (for example, VEGF

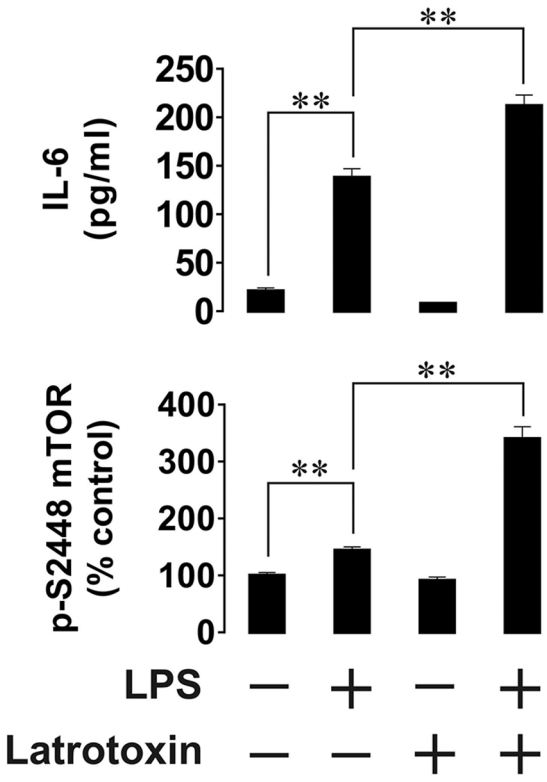

Figure 4: Effects of LPS and LTX on IL-6 exocytosis and mTOR activity in primary human AML cells. Primary human AML-PB001F cells were exposed to 1 µg/ml LPS, 500 pM LTX or a combination of these two ligands for 24 h. Following cell lysis, IL-6 release into the medium and mTOR S2448-phosphorylation in cell lysates were measured by ELISA. Data are the mean values ± SEM ($n = 6$). *$p < 0.05$; **$p < 0.01$.

and IL-6). This requires not only the presence of efficient exocytotic machinery, but also the means of controlling and stimulating exocytosis, for example, in response to leukocyte cell-surface interactions.

LPNH1 can, therefore, be further considered as a novel biomarker for AML diagnostics. Most existing leukaemia biomarkers are relative: they are expressed in both healthy and malignant cells, but their levels are higher in malignant cells; in contrast, LPHN1 is totally absent from healthy leukocytes and is thus an absolute biomarker of leukaemic cells. Furthermore, LPHN1 could now be explored as a potential novel target for anti-leukaemia therapy and drug delivery. For this purpose, it would be essential to identify a ligand that could bind and activate LPHN1 in leukaemia cells. Such a ligand would not only allow a full characterisation of the malignant transformation pathway, but would also provide a potential therapeutic target(s) to prevent LPHN1-induced exocytosis in leukaemia cells. The ligand of leukaemia LPHN1 could be a soluble factor circulating in blood plasma or it could be expressed on the surface of certain blood, endothelial or bone marrow cells. We previously characterised the natural LPHN1 ligand of nervous tissue (Lasso/teneurin-2) [20]. However, in the current work we were unable to detect Lasso by Western blot in ML cell lines (THP-1 and U-937), primary healthy leukocytes or blood plasma obtained from healthy donors (data not shown). Future research will concentrate on the identification and isolation of peripheral ligand/s of leukaemic LPHN1.

MATERIALS AND METHODS

Materials

All cell culture reagents were from Sigma (Suffolk, UK). Microtitre plates were obtained from Nunc (Roskilde, Denmark). LTX and LTX^{N4C} were purified as previously described [6]. Mouse monoclonal antibodies to mTOR and β-actin and rabbit polyclonal antibodies against phospho-S2448 mTOR were from Abcam (Cambridge,

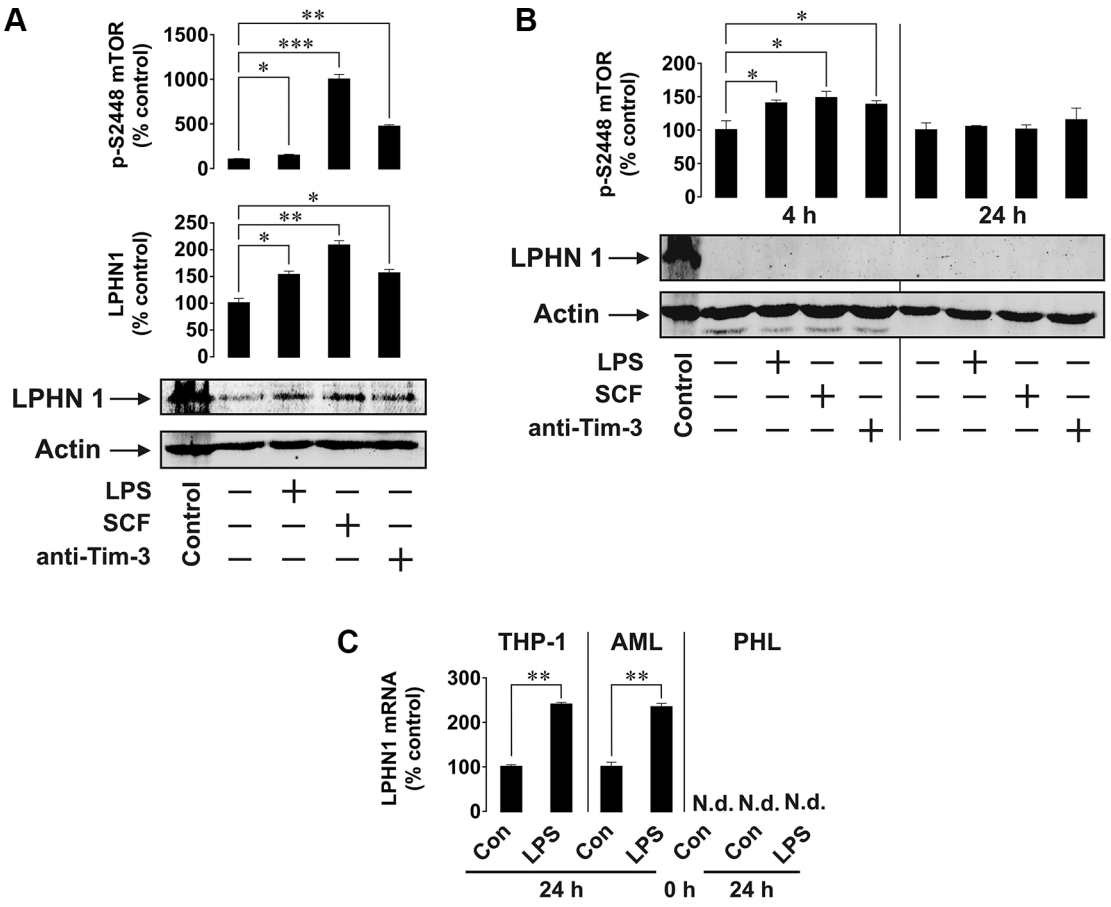

Figure 5: Primary human AML cells but not healthy primary human leukocytes express LPHN1. (**A**, **B**) Primary AML-PB001F cells (A) were exposed for 4 h and healthy human leukocytes (B) for 4 h or 24 h to 1 μg/ml LPS, 0.1 μg/ml SCF or 2 μg/ml anti-Tim-3. Following cell lysis, LPHN1 protein levels were analysed by Western blotting and phospho-S2448 mTOR was quantitated by ELISA. Control, mouse brain extract. (**C**) Quantitative RT-PCR was used to determine the levels of LPHN1 mRNA in THP-1 cells, primary human AML cells and primary healthy human leukocytes (PHL) prior to any treatment (0 h Con), after a 24 h incubation without stimulation (24 h Con), or after a 24 h stimulation with 1 μg/ml LPS (24 h LPS). Data are the mean values ± SEM (n = 4). N.d., not detectable; *$p < 0.05$; **$p < 0.01$.

UK). Antibodies against phospho-T389 and total p70 S6 kinase 1 (p70 S6K1) were obtained from Cell Signalling Technology (Danvers, MA USA). Goat anti-mouse and goat anti-rabbit fluorescent dye-labelled antibodies were from Li-Cor (Lincoln, Nebraska USA). ELISA-based assay kits for the detection of IL-6, was from R&D Systems (Abingdon, UK). The polyclonal rabbit anti-peptide antibody PAL1 against LPHN1 and polyclonal mouse antibody dmAb against Lasso/teneurin-2 were previously described [20, 21]. Human SCF [22] and anti-Tim-3 monoclonal antibody [23] were a kind gift of Dr. Luca Varani.

THP-1 and U937 human myeloid cells

THP-1 human myeloid leukaemia monocytic macrophages and U937 human leukaemia monocytes were obtained from the European Collection of Cell Cultures (Salisbury, UK). Cells were cultured in RPMI 1640 media supplemented with 10% foetal calf serum, penicillin (50 IU/ml) and streptomycin sulphate (50 µg/ml).

Primary human AML cells

Primary human AML mononuclear cells (AML-PB001F, newly diagnosed/untreated) were purchased from AllCells (Alameda, CA, USA) and handled in accordance with manufacturer's instructions. Cells from four different patients were used in reported experiments.

Primary human leukocytes from healthy donors

Primary human leukocytes were obtained from blood buffy coat (prepared from healthy donors) purchased from the National Health Blood and Transfusion Service (NHSBT, UK) following ethical approval (REC reference: 12/WM/0319) [17, 24]. Mononuclear-rich leukocytes were obtained by Ficoll-density centrifugation according to the manufacturer's (GE Healthcare Life Sciences) protocol. Cell numbers were determined using a haemocytometer and diluted accordingly with HEPES-buffered Tyrode's solution before treatment, as indicated.

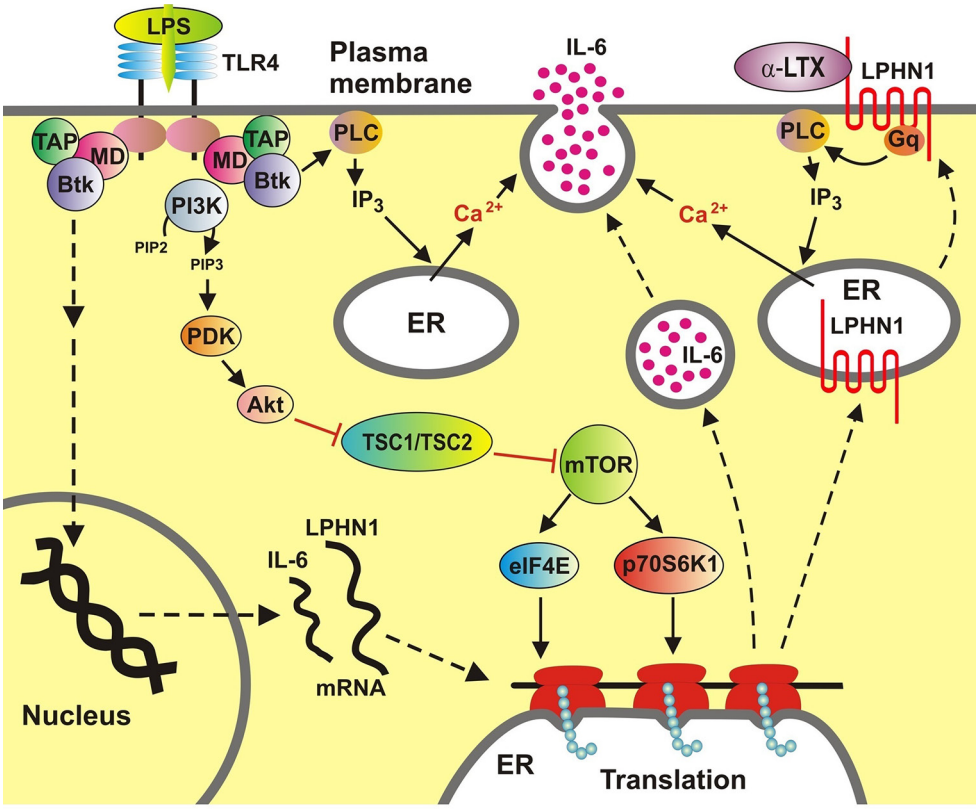

Figure 6: Functional integration of LPHN1 into AML cell signalling machinery. LPHN1 transcription and translation is induced in AML cells. LPS upregulates LPHN1 transcription and triggers TLR4-mediated activation of the mTOR pathway, which increases translation of LPHN1 and IL-6. In addition, both LPS (through TLR4 and Btk) and LTX (through LPHN1 and Gq) activate PLC, which produces IP_3, leading to release of Ca^{2+} from the ER. Increased cytosolic Ca^{2+} triggers exocytosis of IL-6. Abbreviations: Btk, Bruton's tyrosine kinase; MD, myeloid differentiation factor 88; TAP, Toll-like receptor intracellular TIR domain-associated protein; PI-3K, phosphatidylinositol 3-kinase; PDK, phosphatidylinositol-3-phosphate-dependent kinase; IP_3, inositol trisphosphate; PLC, phospholipase C; Gq, Gαq subunit of a heterotrimeric G protein; TSC1/TSC2, tuberous sclerosis proteins 1 and 2; eIF4E, eukaryotic translation initiation factor 4E; p70S6K1, mTOR-dependent S6 kinase 1; ER, endoplasmic reticulum. Symbols: ←activation; ├ inactivation; dotted lines, indirect process involving multiple steps.

Western blot analysis

The levels of LPHN1, total and phospho-T389 p70 S6K1 as well as Lasso/teneurin 2 were determined by Western blot analysis, as previously described [17, 23]. Fluorescently labelled antibodies (Li-Cor) were used according to the manufacturer's protocol to visualise the proteins of interest using an Odyssey imaging system (Li-Cor). Western blot data were subjected to quantitative analysis using the Odyssey software and values were normalised against respective β-actin bands.

Quantitative real-time reverse transcription PCR (qRT-PCR)

Total RNA was extracted using the Illustra RNAspin Midi RNA isolation kit (GE Healthcare) and quantified spectroscopically with a Nanodrop 2000® (Thermo Scientific). cDNA was synthesised using Transcriptor First Strand cDNA Synthesis Kit (Roche), which was performed in accordance with the manufacturer's protocol. Relative quantification of LPHN1 mRNA was performed using SYBR Green I Master reaction mix (Roche) and a LightCycler 480 (Roche). The house-keeping gene β-actin was used as a reference gene. The following primers were used at a final concentration of 0.5 μM: LPHN1, 5′-AGCCGCCCCGAGGCCGGAACCTA-3′ and 5′-AGG TTGGCCCCGCTGGCATAGAGGGAGTC-3′; Actin, 5′-T TCGCGGGCGACGATGC-3′ and 5′-GGGGCCACACGC AGCTCATT-3′.

PCR reactions began with incubation at 95ºC for 3 min 30 s, then proceeded for 45 cycles of 95ºC for 10 s, 60ºC for 20 s and 72°C for 10 s. Fluorescence level was detected at 80°C in each cycle. A final elongation step was held at 72°C for 5 min. Raw fluorescence data were analysed using LinRegPCR quantitative PCR data analysis programme [25]. Amplified products were examined on 1.5% agarose gel containing ethidium bromide.

Detection of phospho-S2448 mTOR in cell lysates by ELISA

Phosphorylation of mTOR was monitored using ELISA assays as recently described [15]. Briefly, ELISA plates were coated with mouse anti-mTOR antibodies and blocked with 2% BSA. Cell lysates were then added to the wells and incubated with agitation at room temperature for 2 h. After washing with TBST buffer, anti-phospho-S2448 mTOR antibody was added and plates were incubated with agitation for 2 h at room temperature. Plates were then washed with TBST buffer and incubated with 1:1000 HRP-labelled goat anti-rabbit IgG in TBST buffer. After washing with TBST, bound secondary antibodies were detected by the peroxidase reaction (ortho-phenylenediamine/H_2O_2).

Detection of exocytosed IL-6

Concentrations of IL-6 released into cell culture media were analysed by ELISA (R&D Systems assay kit) according to the manufacturer's protocol.

Cell viability assay

Cell viability was analysed using the Promega (Southampton, UK) MTS (3-(4,5-dimethylthiazol-2-yl)-5-(3-carboxymethoxyphenyl)-2-(4-sulfophenyl)-2H-tetrazolium) assay kit according to the manufacturer's protocol.

Statistical analysis

Each experiment was performed 3–6 times and statistical analysis was conducted using ANOVA test with Bonferroni correction.

ACKNOWLEDGMENTS

We are grateful to Luca Varani (Institute for Research in Biomedicine, Bellinzona, Switzerland) for providing SCF and anti-Tim-3 monoclonal antibody. The proteins were produced in accordance with the protocols outlined in Materials and Methods.

The work was supported in part by the University of Kent Faculty of Sciences Research Fund and School of Pharmacy research funding (to VVS and YAU), by The Russian Scientific Foundation (Grant 16-15-00290 to AGT), and by a Daphne Jackson Trust postdoctoral fellowship (to IMY).

CONFLICTS OF INTREST

None.

REFERENCES

1. Silva JP, Ushkaryov YA. The latrophilins, "split-personality" receptors. Adv Exp Med Biol. 2010; 706:59–75.
2. Hsu YC, Yuan S, Chen HY, Yu SL, Liu CH, Hsu PY, Wu G, Lin CH, Chang GC, Li KC, Yang PC. A four-gene signature from NCI-60 cell line for survival prediction in non-small cell lung cancer. Clin Cancer Res. 2009; 15:7309–7315.
3. White GR, Varley JM, Heighway J. Isolation and characterization of a human homologue of the latrophilin gene from a region of 1p31.1 implicated in breast cancer. Oncogene. 1998; 17:3513–3519.
4. Zhang S, Liu Y, Liu Z, Zhang C, Cao H, Ye Y, Wang S, Zhang Y, Xiao S, Yang P, Li J, Bai Z. Transcriptome profiling of a multiple recurrent muscle-invasive urothelial carcinoma of the bladder by deep sequencing. PLoS One. 2014; 9:e91466.

5. Kan Z, Jaiswal BS, Stinson J, Janakiraman V, Bhatt D, Stern HM, Yue P, Haverty PM, Bourgon R, Zheng J, Moorhead M, Chaudhuri S, Tomsho LP, et al. Diverse somatic mutation patterns and pathway alterations in human cancers. Nature. 2010; 466:869–873.

6. Volynski KE, Capogna M, Ashton AC, Thomson D, Orlova EV, Manser CF, Ribchester RR, Ushkaryov YA. Mutant α-latrotoxin (LTX^{N4C}) does not form pores and causes secretion by receptor stimulation:This action does not require neurexins. J Biol Chem. 2003; 278:31058–31066.

7. Capogna M, Volynski KE, Emptage NJ, Ushkaryov YA. The α-latrotoxin mutant LTX^{N4C} enhances spontaneous and evoked transmitter release in CA3 pyramidal neurons. J Neurosci. 2003; 23:4044–4053.

8. Broudy VC. Stem cell factor and hematopoiesis. Blood. 1997; 90:1345–1364.

9. Song Y, Tan Y, Liu L, Wang Q, Zhu J, Liu M. Levels of bone marrow microvessel density are crucial for evaluating the status of acute myeloid leukemia. Oncol Lett. 2015; 10:211–215.

10. Padro T, Ruiz S, Bieker R, Burger H, Steins M, Kienast J, Buchner T, Berdel WE, Mesters RM. Increased angiogenesis in the bone marrow of patients with acute myeloid leukemia. Blood. 2000; 95:2637–2644.

11. Civini S, Jin P, Ren J, Sabatino M, Castiello L, Jin J, Wang H, Zhao Y, Marincola F, Stroncek D. Leukemia cells induce changes in human bone marrow stromal cells. J Transl Med. 2013; 11:298.

12. Reynaud D, Pietras E, Barry-Holson K, Mir A, Binnewies M, Jeanne M, Sala-Torra O, Radich JP, Passegue E. IL-6 controls leukemic multipotent progenitor cell fate and contributes to chronic myelogenous leukemia development. Cancer Cell. 2011; 20:661–673.

13. Akira S, Takeda K. Toll-like receptor signalling. Nat Rev Immunol. 2004; 4:499–511.

14. Yasinska IM, Gibbs BF, Lall GS, Sumbayev VV. The HIF-1 transcription complex is essential for translational control of myeloid hematopoietic cell function by maintaining mTOR phosphorylation. Cell Mol Life Sci. 2014; 71:699–710.

15. Nicholas SA, Coughlan K, Yasinska I, Lall GS, Gibbs BF, Calzolai L, Sumbayev VV. Dysfunctional mitochondria contain endogenous high-affinity human Toll-like receptor 4 (TLR4) ligands and induce TLR4-mediated inflammatory reactions. Int J Biochem Cell Biol. 2011; 43:674–681.

16. Zheng B, Mao JH, Qian L, Zhu H, Gu DH, Pan XD, Yi F, Ji DM. Pre-clinical evaluation of AZD-2014, a novel mTORC1/2 dual inhibitor, against renal cell carcinoma. Cancer Lett. 2015; 357:468–475.

17. Gonçalves Silva I, Gibbs BF, Bardelli M, Varani L, Sumbayev VV. Differential expression and biochemical activity of the immune receptor Tim-3 in healthy and malignant human myeloid cells. Oncotarget. 2015; 6:33823–33833. doi: 10.18632/oncotarget.5257.

18. Schreml S, Lehle K, Birnbaum DE, Preuner JG. mTOR-inhibitors simultaneously inhibit proliferation and basal IL-6 synthesis of human coronary artery endothelial cells. Int Immunopharmacol. 2007; 7:781–790.

19. Sumbayev VV. LPS-induced Toll-like receptor 4 signalling triggers cross-talk of apoptosis signal-regulating kinase 1 (ASK1) and HIF-1alpha protein. FEBS Lett. 2008; 582:319–326.

20. Silva JP, Lelianova VG, Ermolyuk YS, Vysokov N, Hitchen PG, Berninghausen O, Rahman MA, Zangrandi A, Fidalgo S, Tonevitsky AG, Dell A, Volynski KE, Ushkaryov YA. Latrophilin 1 and its endogenous ligand Lasso/teneurin-2 form a high-affinity transsynaptic receptor pair with signaling capabilities. Proc Natl Acad Sci U S A. 2011; 108:12113–12118.

21. Davydov, II, Fidalgo S, Khaustova SA, Lelyanova VG, Grebenyuk ES, Ushkaryov YA, Tonevitsky AG. Prediction of epitopes in closely related proteins using a new algorithm. Bull Exp Biol Med. 2009; 148:869–873.

22. Wang C, Liu J, Wang L, Geng X. Solubilization and refolding with simultaneous purification of recombinant human stem cell factor. Appl Biochem Biotechnol. 2008; 144:181–189.

23. Prokhorov A, Gibbs BF, Bardelli M, Rüegg L, Fasler-Kan E, Varani L, Sumbayev VV. The immune receptor Tim-3 mediates activation of PI3 kinase/mTOR and HIF-1 pathways in human myeloid leukaemia cells. Int J Biochem Cell Biol. 2015; 59:11–20.

24. Gibbs BF, Gonçalves Silva I, Prokhorov A, Abooali M, Yasinska IM, Casely-Hayford MA, Berger SM, Fasler-Kan E, Sumbayev VV. Caffeine affects the biological responses of human hematopoietic cells of myeloid lineage via downregulation of the mTOR pathway and xanthine oxidase activity. Oncotarget. 2015; 6:28678–28692. doi: 10.18632/oncotarget.5212.

25. Ruijter JM, Ramakers C, Hoogaars WM, Karlen Y, Bakker O, van den Hoff MJ, Moorman AF. Amplification efficiency: linking baseline and bias in the analysis of quantitative PCR data. Nucleic Acids Res. 2009; 37:e45.

OncoImmunology

ISSN: (Print) 2162-402X (Online) Journal homepage: http://www.tandfonline.com/loi/koni20

The immune receptor Tim-3 acts as a trafficker in a Tim-3/galectin-9 autocrine loop in human myeloid leukemia cells

Isabel Gonçalves Silva, Laura Rüegg, Bernhard F. Gibbs, Marco Bardelli, Alexander Fruehwirth, Luca Varani, Steffen M. Berger, Elizaveta Fasler-Kan & Vadim V. Sumbayev

To cite this article: Isabel Gonçalves Silva, Laura Rüegg, Bernhard F. Gibbs, Marco Bardelli, Alexander Fruehwirth, Luca Varani, Steffen M. Berger, Elizaveta Fasler-Kan & Vadim V. Sumbayev (2016) The immune receptor Tim-3 acts as a trafficker in a Tim-3/galectin-9 autocrine loop in human myeloid leukemia cells, OncoImmunology, 5:7, e1195535, DOI: 10.1080/2162402X.2016.1195535

To link to this article: http://dx.doi.org/10.1080/2162402X.2016.1195535

ONCOIMMUNOLOGY
2016, VOL. 5, NO. 7, e1195535 (11 pages)
http://dx.doi.org/10.1080/2162402X.2016.1195535

Taylor & Francis
Taylor & Francis Group

ORIGINAL RESEARCH

OPEN ACCESS

The immune receptor Tim-3 acts as a trafficker in a Tim-3/galectin-9 autocrine loop in human myeloid leukemia cells

Isabel Gonçalves Silva[a], Laura Rüegg[a], Bernhard F. Gibbs[a], Marco Bardelli[b], Alexander Fruehwirth[b], Luca Varani[b], Steffen M. Berger[c], Elizaveta Fasler-Kan[c,d], and Vadim V. Sumbayev[a]

[a]School of Pharmacy, University of Kent, Canterbury, United Kingdom; [b]Institute for Research in Biomedicine, Universita' della Svizzera italiana (USI), Bellinzona, Switzerland; [c]Department of Pediatric Surgery and Department of Clinical Research, Children's Hospital, Inselspital, University of Bern, Bern, Switzerland; [d]Department of Biomedicine, University of Basel and University Hospital Basel, Basel, Switzerland

ABSTRACT

The immune receptor Tim-3 is often highly expressed in human acute myeloid leukemia (AML) cells where it acts as a growth factor and inflammatory receptor. Recently, it has been demonstrated that Tim-3 forms an autocrine loop with its natural ligand galectin-9 in human AML cells. However, the pathophysiological functions of Tim-3 in human AML cells remain unclear. Here, we report for the first time that Tim-3 is required for galectin-9 secretion in human AML cells. However, this effect is cell-type specific and was found so far to be applicable only to myeloid (and not, for example, lymphoid) leukemia cells. We concluded that AML cells might use Tim-3 as a trafficker for the secretion of galectin-9 which can then be possibly used to impair the anticancer activities of cytotoxic T cells and natural killer (NK) cells.

ARTICLE HISTORY
Received 15 April 2016
Revised 19 May 2016
Accepted 19 May 2016

KEYWORDS
Acute myeloid leukemia; galectin-9; Tim-3

Introduction

The T cell immunoglobulin and mucin domain 3 (Tim-3) is a plasma membrane-associated protein which is highly expressed in acute myeloid leukemia (AML) cells and is therefore considered as a potential target for anti-AML therapy.[1,2] Although the biochemical activities of Tim-3 have recently been elucidated,[3-7] the functional role of this protein/receptor in AML cells remains unclear and the reasons for striking increases in Tim-3 levels in these cells are also not yet understood. Galectin-9, which was found to be a natural Tim-3 ligand,[3,5] was recently suggested to form an autocrine loop, where newly released galectin-9 interacts with Tim-3 expressed on the cell surface.[3] Furthermore, in leukocytes Tim-3 is known to be shed by proteolytic enzymes including metalloproteinases.[8] This leads to the dissociation of Tim-3 from the plasma membrane as a soluble protein, which then can be detectable in human blood plasma.[8,9] The physiological role of this shedding remains unclear as well as the functions of soluble Tim-3. However, it is known that galectin-9 is capable of impairing the immunological activities of cytotoxic T cells as well as natural killer (NK) cells[1,10,11] In cytotoxic T cells galectin-9 was found to induce apoptotic death,[11] while in NK cells it mainly affected cytokine production thus impairing their cytotoxicity function.[10] These effects might therefore help AML cells to escape immune attack by both cytotoxic T cells and NK cells.[1,10,11]

Given the above, we hypothesized that Tim-3 might act as a trafficker for galectin-9 in AML cells. We found that galectin-9 is expressed in the AML cell line THP-1, in primary human AML cells, and in primary healthy human leukocytes (although in this case the expression was considerably lower). Galectin-9 is capable of forming a stable complex with Tim-3 in cell lysates. We also detected that in THP-1 and U-937 cell lines as well as in primary healthy leukocytes the surface presence of Tim-3 is much lower compared to primary human AML cells. The same effect was observed for galectin-9. Galectin-9 knockdown in U-937 cells reduced their total Tim-3 levels. Furthermore, Tim-3 knockdown in U-937 cells did not show reductions in intracellular galectin-9 levels but galectin-9 secretion was dramatically reduced. We therefore suggested that Tim-3 is required for galectin-9 secretion in AML cells. Primary human chronic lymphoid leukemia (CLL) cells were also capable of secreting galectin-9 but expressed very low amounts of Tim-3. These results suggest that Tim-3 might be required for galectin-9 secretion in AML cells. Using ELISA, we were able to detect galectin-9 and soluble Tim-3 in human blood plasma obtained from healthy donors. Furthermore, capturing soluble Tim-3 on ELISA plates also led to detection of galectin-9. These results suggest the presence of Tim-3-galectin-9 complexes in human blood plasma but do not indicate whether they are formed inside secreting cells, on their surface, or constitutively present in blood plasma.

CONTACT Bernhard F. Gibbs B.F.Gibbs@kent.ac.uk; Elizaveta Fasler-Kan elizaveta.fasler@insel.ch; Vadim V. Sumbayev V.Sumbayev@kent.ac.uk
Supplemental data for this article can be accessed on the publisher's website.

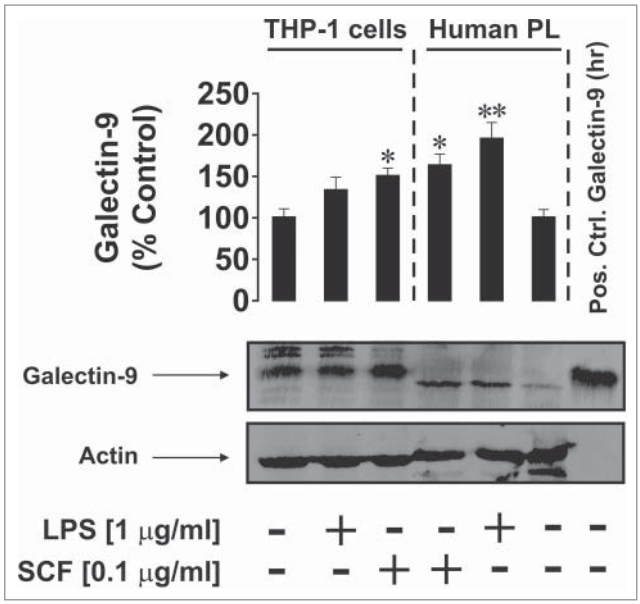

Figure 1. Effects of LPS and SCF on galectin-9 protein expression in THP-1 cells and PHL (abbreviated as PL in the figure). Cells were treated for 4 h with the indicated concentrations of LPS and SCF, then harvested and galectin-9 protein expression levels were analyzed by Western blot as outlined in Materials and Methods. Images are from one experiment representatives of three which gave similar results. Human recombinant galectin-9 (R&D Systems) was used as a positive control. Data are mean values ± SEM of three independent experiments; $^{*}p < 0.05$; $^{**}p < 0.01$ vs. control.

Results

Galectin-9 is expressed in healthy primary human leukocytes and malignant human myeloid cells and forms a complex with Tim-3 in both cell types

We first assessed whether healthy primary human leukocytes (PHL) and malignant human myeloid cell lines express galectin-9 and if its expression could be affected by pro-inflammatory stimulation as well as growth factor-induced biological responses. For this purpose, we used PHL which were isolated from buffy coat blood obtained from healthy donors and THP-1 human myeloid leukemia cells which were reported to express galectin-9.[6]

We found that THP-1 cells produced more galectin-9 compared to PHL, however, lipopolysaccharide (LPS, ligand of pro-inflammatory Toll-like receptor (TLR) 4[12]) and stem cell growth factor (SCF—a major haematopoietic cytokine responsible for the promotion of leukemia progression[13]) significantly upregulated galectin-9 levels in PHL (LPS was however shown, to be a stronger activator). Interestingly, galectin-9 bands in PHL cells appeared slightly lower on the gel compared to THP-1 cells and the positive control (Fig. 1), suggesting potential differences in post-translational processing. Only SCF was able to significantly increase galectin-9 levels in THP-1 cells (Fig. 1).

We then asked whether galectin-9 is capable of forming a complex with Tim-3 in cell lysates. For this purpose, we coated MaxiSorp ELISA plates with rabbit capture antibody directed against galectin-9 followed by the addition of cell lysates (see Materials and Methods). After incubation, galectin-9 was extracted and detected by Western blot analysis using anti-galectin-9 rabbit antibody. Tim-3 was also detected using highly specific mouse antibody. We found that in both THP-1 and PHL cells Tim-3 and galectin-9 gave positive staining at above 70 KDa which corresponds to the sum of Tim-3 and galectin-9 molecular weights detected in these cells by Western blot analysis (Fig. 2). Traces of free galectin-9 were still detectable, while Tim-3 was almost undetectable. The fact that SDS-PAGE electrophoresis did not separate these proteins indicates the formation of a stable complex. Since this did not occur with recombinant proteins expressed in *E. Coli* (which lack glycosylation), it is reasonable to surmise that the lectin (galectin-9) binds to sugar moieties on Tim-3 protein. The fact that both un-complexed proteins were detected by Western blot in fresh cell lysates suggests the requirement of both time and the presence of a surface (a solid phase—ELISA plate bottom in our case) to form such a steady complex.

Next, we analyzed the cellular distribution of Tim-3 and galectin-9 comparing intracellular levels with cell-surface expressions. We used THP-1 and U-937 human myeloid cell lines, primary human AML cells (AML-PB001F) as well as PHL. We measured the total amounts of both proteins using in-cell Western assay in comparison to the amounts present on the cell surface using in-cell assay (also called on-cell assay; as described in the Materials and Methods). We observed that resting THP-1, U-937, and PHL cells expressed substantially more Tim-3 and galectin-9 intracellularly than on the surface. In contrast, primary AML cells had comparatively greater surface presence of both proteins (Fig. 3). Interestingly the ratios of $\text{Tim-3}_{\text{surface}}/\text{Tim-3}_{\text{total}}$ and $\text{galectin-9}_{\text{surface}}/\text{galectin-9}_{\text{total}}$ were quite similar to each other in all studied cell types (Fig. 3).

Tim-3 is required for galectin-9 release in human myeloid leukemia cells

We next asked whether Tim-3 is required for galectin-9 release and used U-937 cells (higher siRNA transfection efficiency could be reached with this cell line using our DOTAP transfection method) to investigate our hypothesis. We also studied if galectin-9 is required for Tim-3 production. First, we knocked down galectin-9 expression in U-937 cells as outlined in Materials and Methods. Non-treated normal and galectin-9 knockdown U-937 cells as well as those treated for 4 h with 2 μg/mL anti-Tim-3 stimulatory antibody[5] were analyzed. Successful knockdown of galectin-9 was confirmed by Western blot analysis (Fig. 4A) as well as quantitative real-time reverse transcription PCR (qRT-PCR; Fig. S1). We found that galectin-9 knockdown reduced cellular Tim-3 levels as well as affecting galectin-9 levels (both intracellular and released (Fig. 4A)). Previously, we reported that Tim-3 activates the mTOR pathway resulting in upregulation of glycolysis and release of pro-angiogenic vascular endothelial growth factor (VEGF). We found that galectin-9 knockdown upregulated stimulatory phosphorylation of mTOR (position S2448, Fig. 4B). This result was in line with the upregulation of glycolysis and VEGF release (Fig. 4B). Interestingly, we could not observe a significant increase in intracellular levels of methylglyoxal (MGO, Fig. 4B) in either case, indicating that the efficiency of glycolysis correlates with the activity of glycolytic enzymes, since MGO is spontaneously formed out of dihydroxyacetone phosphate when glycolytic enzymes are oversaturated. MGO catalyzes

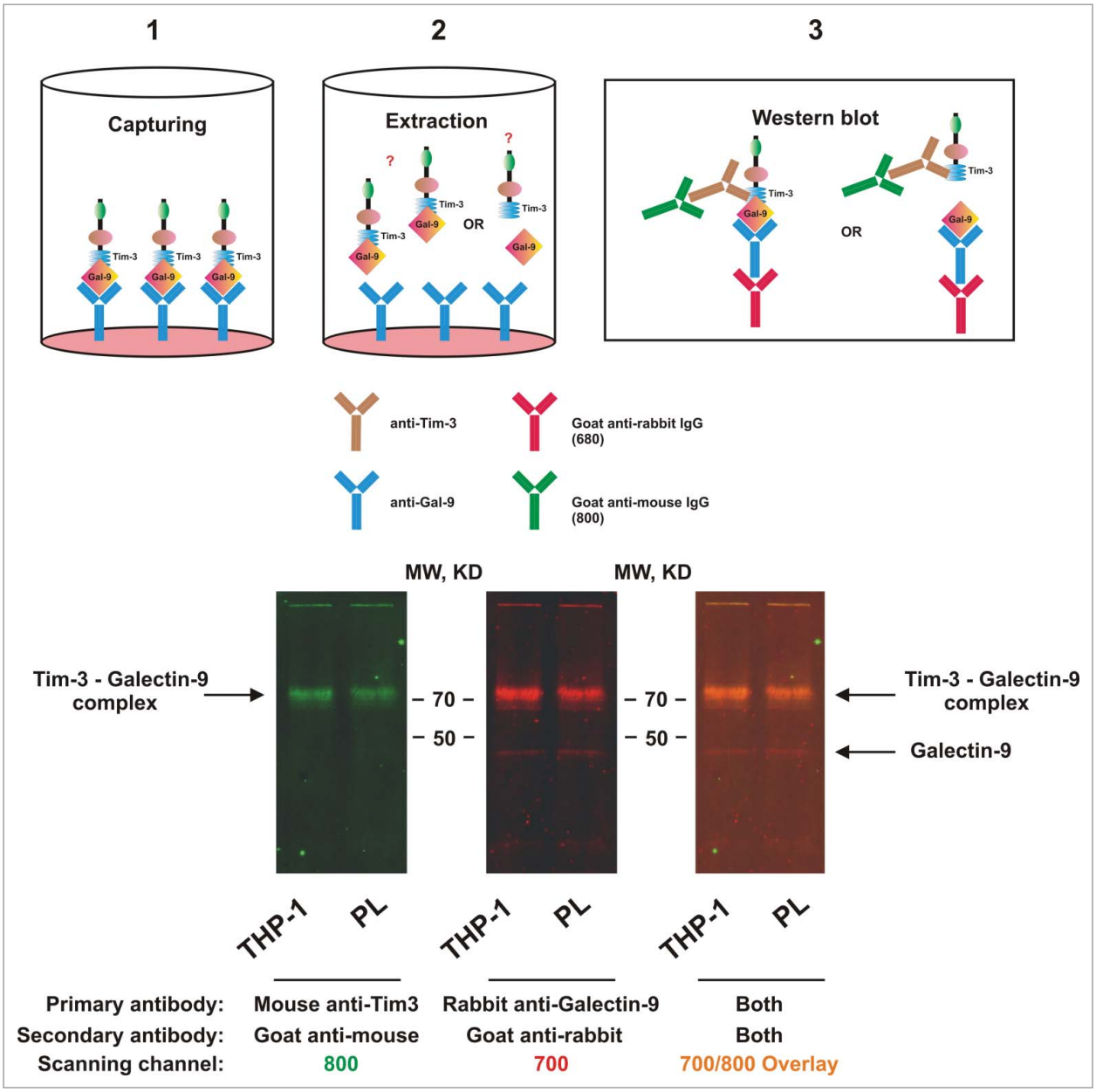

Figure 2. Galectin-9 and Tim-3 form a stable complex. Lysates obtained from 300,000 THP-1 cells or 1,500,000 PHL (abbreviated as PL in the figure; expression levels of both proteins were *ca.* 5 times lower in PHL compared to THP-1) were loaded onto an ELISA plate pre-coated with rabbit anti-galectin-9 antibody as described in Materials and Methods). Following incubation, captured proteins were extracted and subjected to Western blot analysis (see Materials and Methods for details). Both Tim-3 (using mouse anti-Tim-3 antibody) and galectin-9 (using rabbit anti-galectin-9 antibody) were stained. Images are from one experiment representative of four which gave similar results.

glycation followed by generation of advanced glycation end products (Fig. S2). Higher amounts of these products could be produced by cancer cells given their dependence on glycolysis.

In Tim-3 knockdown U-937 cells (successful knockdown was confirmed by Western blot, Fig. 5A, and qRT-PCR, Fig. S1), we saw a significant reduction in Tim-3 levels. No reduction in Tim-3/galectin-9 levels and no other effects were observed when using negative control random siRNA (Fig. 5, Fig. S1) which confirmed the specificity of the events observed. Tim-3 knockdown did not lead to changes in intracellular galectin-9 levels but dramatically reduced galectin-9 secretion, suggesting that Tim-3 is required for the release of galectin-9 (Fig. 5A). Reduction in Tim-3-mediated mTOR phosphorylation at S2448 and respectively downregulation of glycolysis/VEGF release was also observed in Tim-3 knockdown U-937 cells. No significant changes in MGO levels were observed suggesting that glycolytic efficiency—a key energy pathway in leukemia cells—was not affected (Fig. 5B).

Tim-3 is a specific trafficker for galectin-9 in certain cell types

It is generally known that many cell types, including lymphoid cells, are capable of producing galectin-9 but not all of them express Tim-3. We therefore compared the capability of primary human AML cells and primary human CLL cells to produce galectin-9. Both cell types secreted detectable amounts of

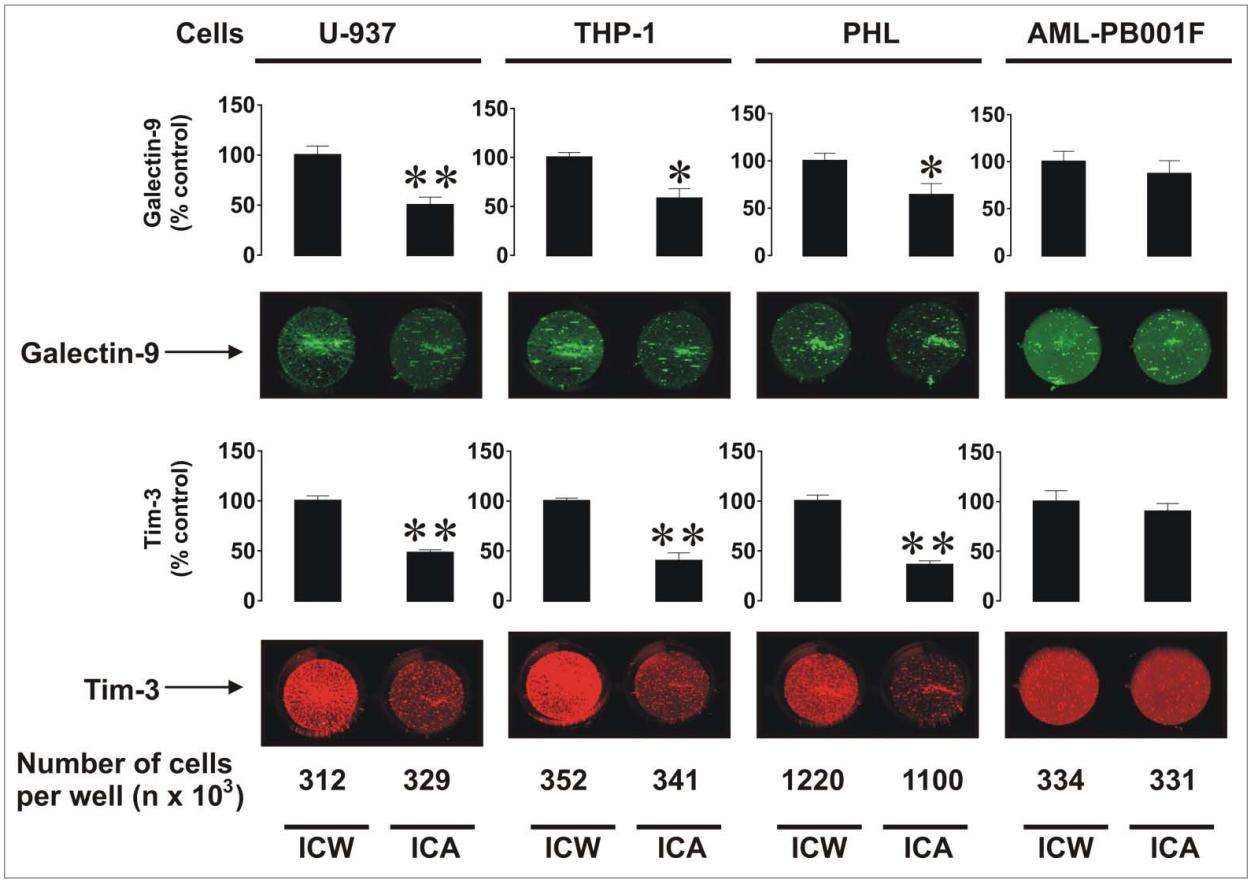

Figure 3. Comparative analysis of total and surface-based Tim-3 and galectin-9 proteins in human myeloid leukemia cell lines, PHL, and primary human AML cells. The indicated numbers of resting U-937 and THP-1 cells, PHL and primary human AML cells (AML-PB001F) were subjected to in-cell assay (ICA, detecting surface proteins) or in-cell Western (ICW, total protein detection) analysis as described in Materials and Methods. Images are from one experiment representative of five which gave similar results. Data are mean values ± SEM of five independent experiments; $^{*}p < 0.05$; $^{**}p < 0.01$ vs. control.

galectin-9. In AML cells, but not in CLL cells, the amount of secreted galectin-9 was significantly increased by 4 h of exposure to 2 μg/mL anti-Tim-3 (Fig. 6A). Both PHL and AML cells expressed Tim-3 but this expression was much higher in AML cells compared to PHLs (Tim-3/actin ratios were analyzed, Fig. 6B). CLL cells expressed almost undetectable amounts of Tim-3 but still they were capable of releasing galectin-9, indicating that they probably use a different trafficker for this protein.

Finally, we observed that blood plasma of healthy donors contained both galectin-9 and soluble Tim-3 as measured by ELISA. Intriguingly, when capturing Tim-3 on the ELISA plate and applying detection antibody directed against galectin-9 we were able to detect a clear signal (Fig. 6C) which was not applicable when intact cell culture medium or galectin-9 standards were used. This means that a complex formed by non-cell-associated soluble Tim-3 and galectin-9 is present in the blood plasma of healthy donors. Our previous experiments demonstrated that anti-Tim-3 antibody does not compete with galectin-9.[5]

Discussion

Galectin-9 is a typical galectin family member which has a tandem structure.[10,14] It has been reported to specifically interact with the immune receptor Tim-3 inducing mTOR pathway activation as well as forming an autocrine loop with Tim-3 in human AML cells.[3,5] Due to very high expression levels of Tim-3 in AML cells this protein is currently considered as a target for anti-AML therapy. Furthermore, galectin-9 was reported to specifically target cytotoxic T cells and NK cells and impair their ability to attack and kill leukemia cells.[10,11,15]

Our present study clearly shows that human myeloid leukemia cells express and secret galectin-9 (Figs. 1, 3, and 7 and Fig. S1). Importantly, galectin-9 production is upregulated by pro-inflammatory stimulation (LPS) and growth factor (SCF) action in both healthy human leukocytes and AML cells (THP-1 cell line). Release of galectin-9 was clearly dependent on the Tim-3. Tim-3 knockdown in U-937 cells led to significant reductions in galectin-9 secretion compared to normal (wild type) U-937 cells (Fig. 5A). Tim-3 protein levels were also reduced (but not significantly) in galectin-9 knockdown U-937 cells compared to wild type cells (Fig. 4A). However, Tim-3 mRNA levels were significantly downregulated in galectin-9 knockdown U-937 cells (Fig. S1) suggesting that transcription of the Tim-3 gene depends on intracellular levels of galectin-9. Interestingly, Tim-3 knockdown did not affect intracellular galectin-9 levels in U-937 cells, as measured by Western blot analysis, but dramatically reduced the capability of these cells to secrete galectin-9. These results suggest that galectin-9 levels influence Tim-3 expression at a genomic level, whereas Tim-3

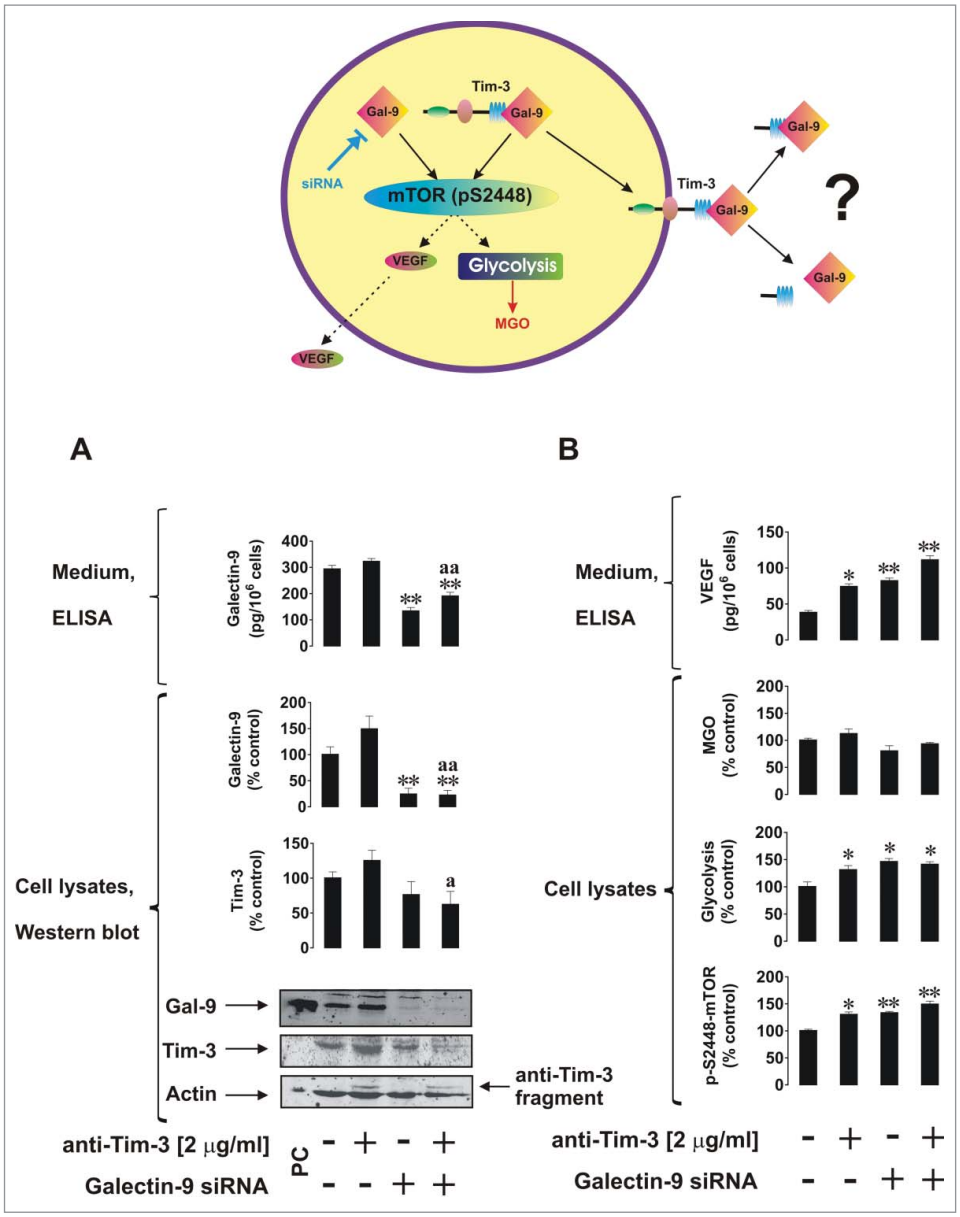

Figure 4. The effects of galectin-9 knockdown on Tim-3 expression and the mTOR pathway. Non-treated normal (wild type) and galectin-9 knockdown U-937 cells, as well as those which underwent 4 h treatment with 2 μg/mL anti-Tim-3 stimulatory antibodies, were analyzed for Tim-3 and galectin-9 levels, galectin-9 release (A), pS2448 mTOR intracellular levels, glycolysis, MGO, and VEGF secretion (B). Images are from one experiment representative of three which gave similar results. Data are mean values ± SEM of 3–5 independent experiments; $^{*}p < 0.05$; $^{**}p < 0.01$ vs. control; $^{a}p < 0.05$; $^{aa}p < 0.01$ vs. anti-Tim-3.

protein controls the capability of myeloid leukemia cells to secrete galectin-9.

Recent evidence demonstrated that **A** disintegrin **a**nd **m**etalloproteases (ADAM) 10 and 17 control shedding of Tim-3 from the cell surface in HEK-293 cells and human primary $CD14^{+}$ monocytes.[8] This suggests that Tim-3 might undergo shedding when it is in complex with galectin-9, which allows dissociation of the Tim-3 fragment together with the full-length galectin-9 protein. This hypothesis might explain why LPS reduces cellular Tim-3 surface expression[6,8] taking into account our results demonstrating LPS-induced upregulation of galectin-9 levels. Our previous study demonstrated that Tim-3 protein production is not reduced by LPS[5] while surface presence is affected.[6,8] This might be the result of increased intracellular galectin-9 levels leading to enhanced galectin-9 secretion which, as we have described above, requires Tim-3. ADAM10/17 or other proteolytic enzymes can then possibly shed the Tim-3/galectin-9 complex. Further evidence also supports the rapid shedding process such as *via* ligand-induced Tim-3-mediated activation of the mTOR pathway.

Although Tim-3 is a weaker signal transducer compared to Kit (SCF receptor) or TLR4, a moderate level of mTOR activation could be the result of swift removal of the extracellular domain which terminates the signal prematurely compared to those observed for non-cleaved receptors (as TLR4 or Kit). Furthermore, in support of a Tim-3/galectin-9 complex shedding scenario, other factors, such as HIV-1 infection, lead to increases in both soluble Tim-3 and galectin-9 levels in blood plasma.[9,16] Also, phorbol 12-myriastate 13-acetate (PMA) was found to upregulate galectin release in Jurkat T cells,[17] where

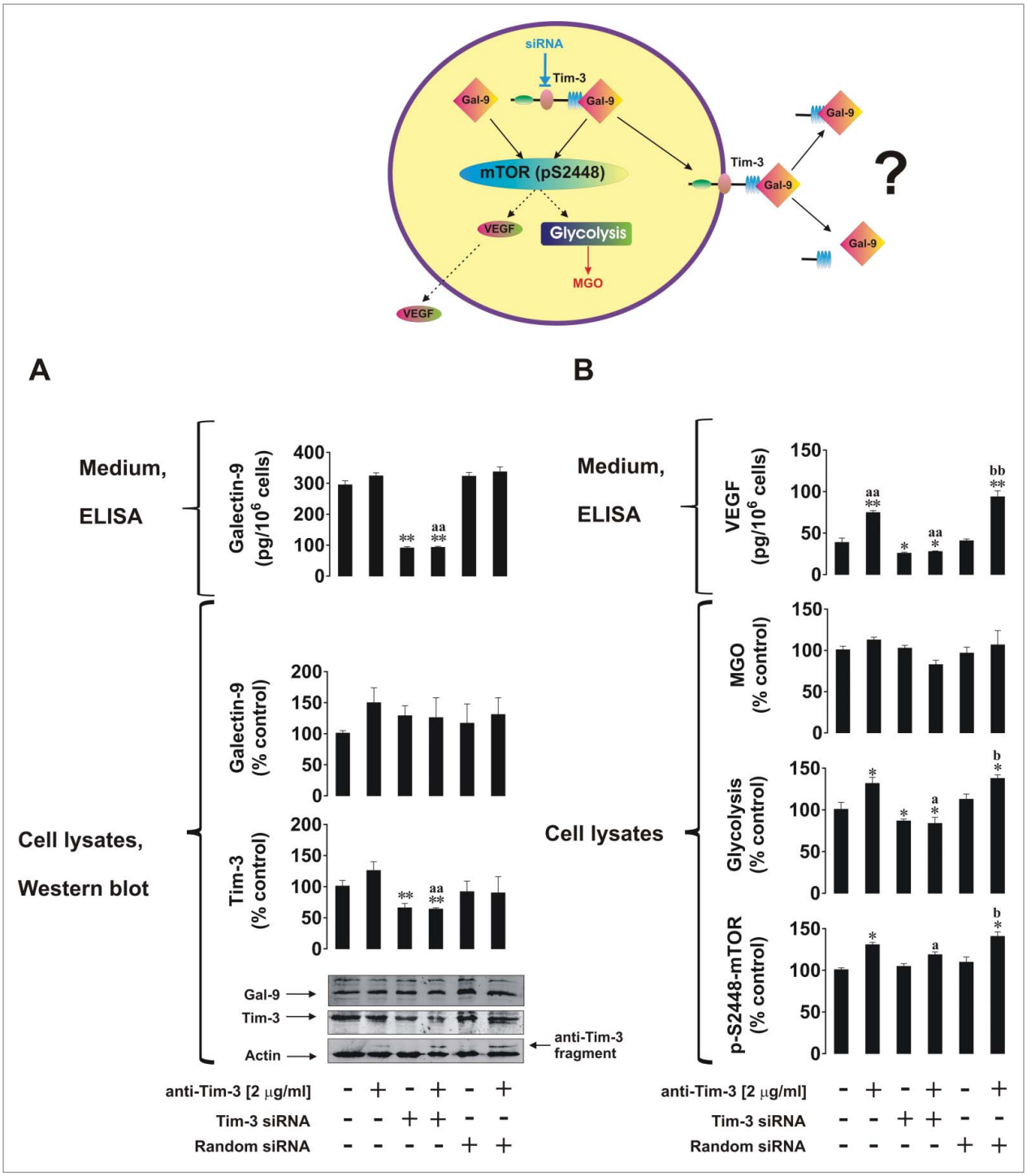

Figure 5. Tim-3 is required for galectin-9 secretion in human myeloid leukemia cells. Non-treated normal (wild type), Tim-3 knockdown and transfected with random siRNA U-937 cells, as well as the same cells which underwent 4 h treatment with 2 μg/mL anti-Tim-3, were subjected to analysis for Tim-3 and galectin-9 levels, galectin-9 release (A), pS2448 mTOR intracellular levels, glycolysis, MGO, and VEGF secretion (B). Images are from one experiment representative of three which gave similar results. Data are mean values ± SEM of 3–5 independent experiments; $^{*}p < 0.05$; $^{**}p < 0.01$ vs. control; $^{a}p < 0.05$; $^{aa}p < 0.01$ vs. anti-Tim-3; $^{b}p < 0.05$; $^{bb}p < 0.01$ vs. random siRNA.

it also upregulates Tim-3 expression/externalisation.[18] PMA is also known to promote Tim-3 proteolytic shedding.[8] Matrix metalloproteinase inhibitor BB-94 (ADAM10 was also found to be sensitive to it[19]) was able to abolish PMA-induced galectin-9 release in Jurkat T cells (immortalised T lymphocytic cell line derived from T cell leukemia[17]), suggesting that proteolysis is probably involved in shedding Tim-3 complexed with galectin-9.

Our results also demonstrated that CLL bone marrow mononuclear cells (containing elevated levels of $CD4^{+}$ T cells with a cytotoxic phenotype[20]) are capable of secreting galectin-9 but they only produce very low amounts of Tim-3 (Figs. 6A and B). This suggests that Tim-3 is a cell type-specific trafficker of galectin-9 in AML cells, while other cell types (such as CLL bone marrow mononuclear cells) might use other galectin-9-specific proteins, which can be externalized. In support of this,

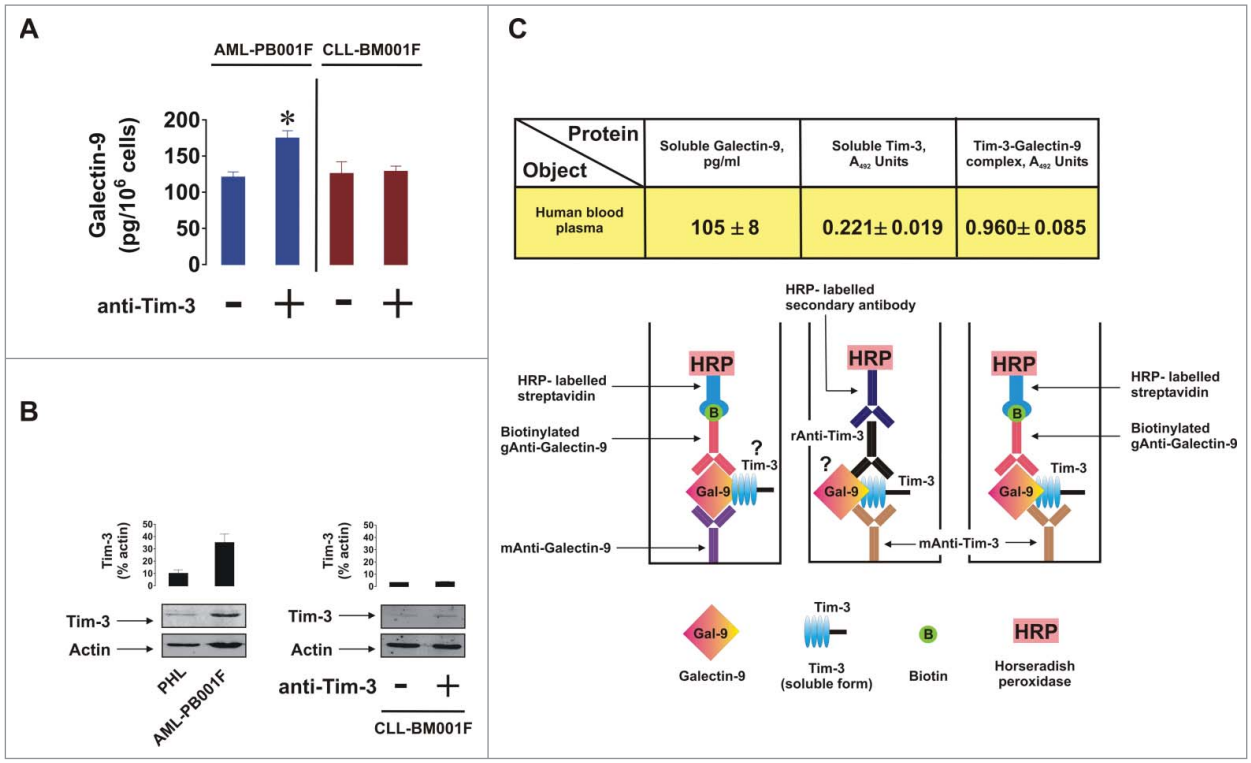

Figure 6. Galectin-9 and Tim-3 levels in primary human AML, CLL, and PHL cells as well as in blood plasma. (A) Non treated primary human AML and CLL cells, as well as those exposed for 4 h to anti-Tim-3, were precipitated and medium was subjected to measurement of galectin-9 by ELISA. Data represent mean values ± SEM of three independent experiments; $^{*}p < 0.05$ vs. control. (B) PHL, primary human AML, and CLL cells were subjected to Western blot analysis for Tim-3. Images are from one experiment representative of four which gave similar results. Data are mean values ± SEM of four independent experiments. (C) Blood plasma of six healthy donors was subjected to ELISA assays for galectin-9, soluble Tim-3, and Tim-3-galectin-9 complex (for details, please see Materials and Methods and diagrams underneath the table). Data are mean values ± SEM of 3–5 independent experiments.

there is evidence that galectin-9 may cause Tim-3-independent effects (including apoptosis) in lymphoid cells.[10,21]

In human blood plasma obtained from healthy donors, we found that both galectin-9 and soluble Tim-3 are present (Fig. 6C). However, anti-Tim-3 detection antibodies also gave rise to a positive signal to visualize the product captured by anti-galectin-9 antibody (Fig. 6C). This clearly indicates that a Tim-3/galectin-9 complex is present in human blood plasma. However, our results do not provide any indication at which point the complex was formed.

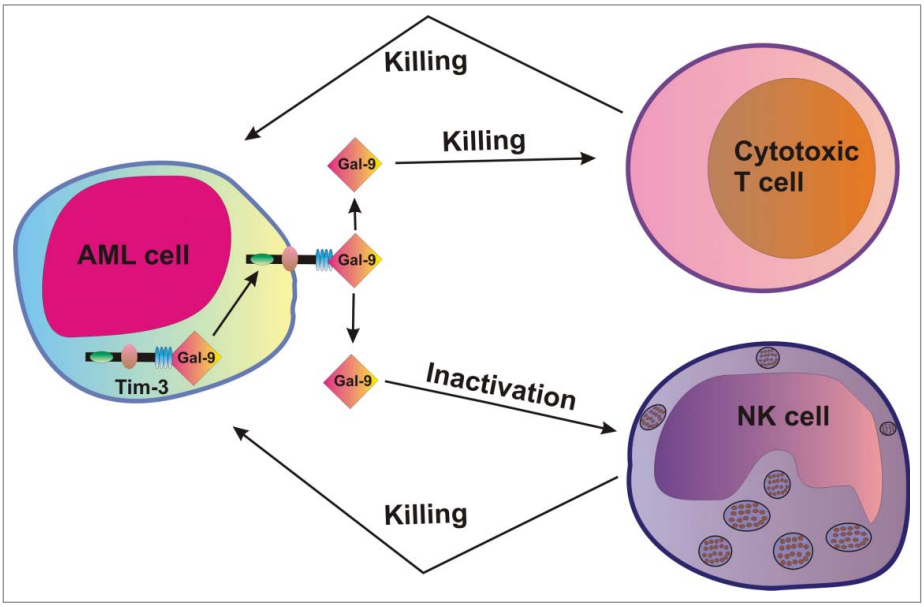

Figure 7. Tim-3-dependent secretion of galectin-9 in human AML cells could potentially impair the anti-leukemic activity of cytotoxic T cells and NK cells.

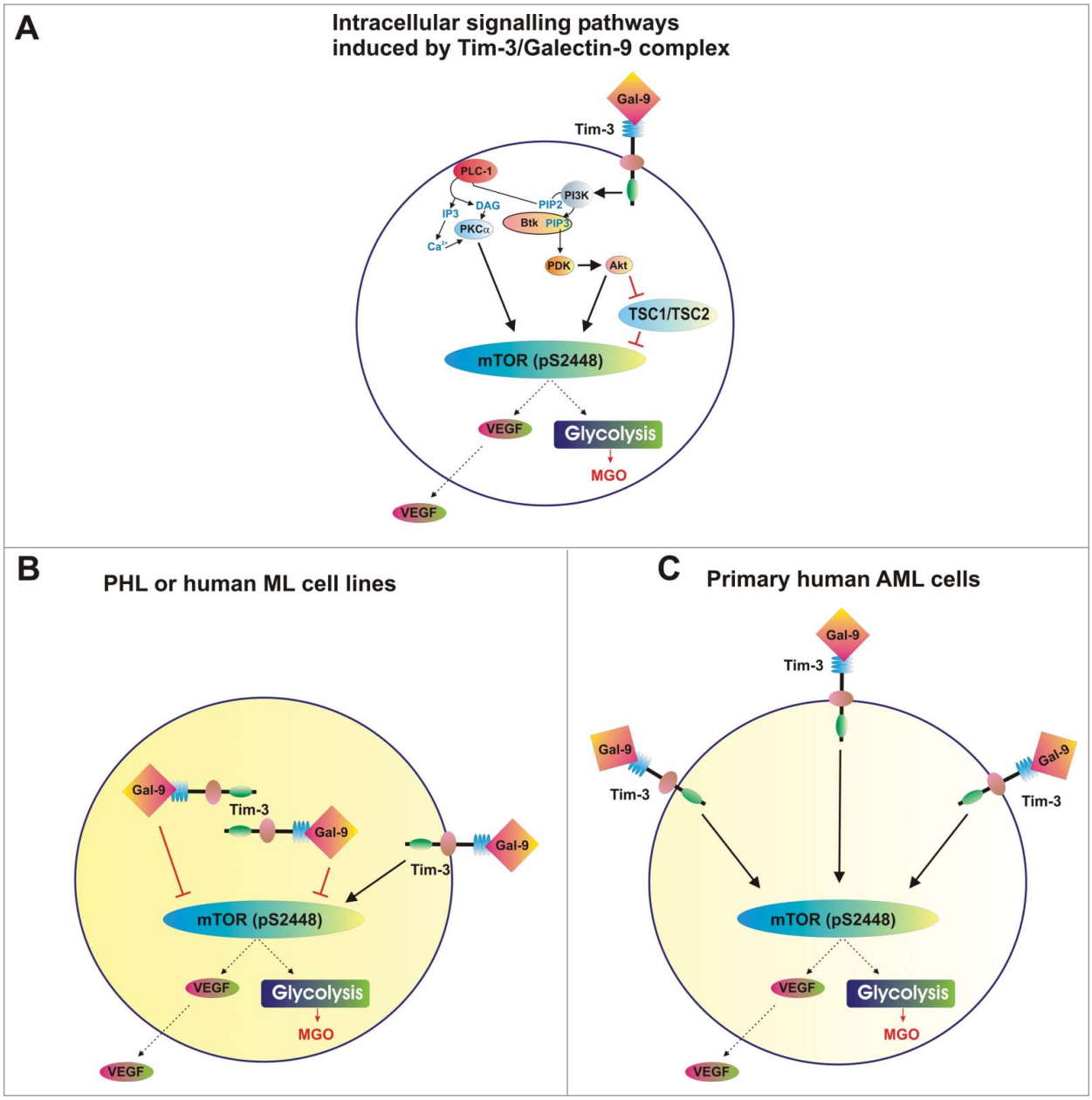

Figure 8. Distribution of complexes and corresponding effects of Tim-3 and galectin-9 in healthy and malignant human white blood cells. (A) Scheme demonstrating intracellular signaling pathways induced by Tim-3-galectin-9 complexes. (B) Tim-3/galectin-9 distribution and corresponding effects in PHL and human myeloid leukemia cell lines (THP-1 and U-937). (C) Tim-3/galectin-9 distribution and corresponding effects in primary human AML cells.

Our results suggest that Tim-3 is required for galectin-9 secretion in AML cells and this mechanism may be then used to impair the anticancer activity of cytotoxic T cells and NK cells, which might allow malignant blood cells to escape immune attack. Our hypothesis is summarized in the Fig. 7.

Our findings also demonstrated that decrease in intracellular galectin-9 level increases mTOR activity and its downstream effects (efficient glycolysis and VEGF production, Fig. 4A). In myeloid leukemia cell lines as well as in PHL, the activity of the mTOR pathway is always lower than in primary AML cells.[4,5] One of the reasons for this might be externalisation of the Tim-3/galectin-9 complex in primary AML cells (confirmed in our studies—see Fig. 3). In this case, while there are lower amounts of galectin-9 inside the cells Tim-3/galectin-9 complexes are externalized on the cell surface, which can initiate signaling events before further modification or proteolytic shedding. These effects are presented in Fig. 8, which summarizes Tim-3 signal transducing activities in PHL/AML cell lines compared with primary human AML cells.

Our results also highlight that both Tim-3 and galectin-9 are promising therapeutic targets for possibly curing AML. Absence of the Tim-3/galectin-9 autocrine loop or the timely capture and subsequent inactivation of biologically active galectin-9 may reduce the ability of AML cells to impair the anticancer activities of NK cells and cytotoxic T cells. This may therefore result in the natural eradication of cancer cells by functional NK cells and cytotoxic T cells.

Materials and methods

Materials

RPMI-1640 medium, foetal bovine serum and supplements, LPS (from *P. aeruginosa*), DOTAP transfection reagent, primers and galectin-9 silencing RNA (siRNA) were purchased from Sigma (Suffolk, UK). Maxisorp™ microtitre plates were provided either by Nunc (Roskilde, Denmark) or were a kind gift of Oxley Hughes Ltd (London, UK). Mouse monoclonal antibodies directed against mTOR and β-actin as well as rabbit polyclonal antibodies against phospho-S2448 mTOR, galectin-9, Tim-3, and HRP-labeled rabbit anti-mouse secondary antibody were purchased from Abcam (Cambridge, UK). Goat anti-mouse and goat anti-rabbit fluorescence dye-labeled antibodies were obtained from Li-Cor (Lincoln, Nebraska USA). ELISA-based assay kits for the detection of VEGF were purchased from Bio-Techne (R&D Systems, Abingdon, UK). All other chemicals purchased were of the highest grade of purity.

Primary human AML and CLL cells

Primary human AML mononuclear blasts (AML-PB001F, newly diagnosed/untreated) were purchased from AllCells (Alameda, CA, USA) and handled in accordance with manufacturer's instructions. Primary human bone marrow derived CLL mononuclear cells (CLL-BM001F, newly diagnosed/untreated leukemia) were also obtained from AllCells (Alameda, CA, USA) and handled in accordance with manufacturer's protocol. Cells from six different patients were analyzed following ethical approval (REC reference: 16-SS-033).

THP-1 and U937 human myeloid cell lines

THP-1 human myeloid leukemia monocytes and U937 human myeloid monocytes were obtained from the European Collection of Cell Cultures (Salisbury, UK). Cells were cultured in RPMI 1640 media supplemented with 10% foetal bovine serum, penicillin (50 IU/mL) and streptomycin sulfate (50 μg/mL).

Primary human leukocytes obtained from healthy donors (buffy coats)

PHL were obtained from buffy coat blood (originated from healthy donors undergoing routine blood donation) which was purchased from the National Health Blood and Transfusion Service (NHSBT, UK) following ethical approval (REC reference: 16-SS-033). Mononuclear-rich leukocytes were obtained by Ficoll-density centrifugation according to the manufacturer's protocol. Cell numbers were counted using a haemocytometer and diluted accordingly with HEPES-buffered Tyrode's solution before the indicated treatments.[4]

Stem cell factor

Human SCF protein was produced in *E. Coli* and purified in accordance with previously published protocols.[20]

Transfer of Galectin-9/Tim-3 siRNA into U-937 cells and qRT-PCR

We employed a galectin-9-specific siRNA target sequence (uga ggu gga agg cga ugu ggu ucc c) which was previously described.[14] For Tim-3 knockdown, we used commercially available siRNA purchased from Santa Cruz Biotechnology, CA, USA, as described before.[7] As a control, we used corresponding random siRNA (uac acc guu agc aga cac c dtdt[22]). Transfection into U-937 cells was performed using DOTAP reagent according to the manufacturer's protocol.

To monitor galectin-9 and Tim-3 mRNA levels, we used qRT-PCR.[21] Total RNA was isolated using a GenElute™ mammalian total RNA preparation kit, followed by a target protein mRNA reverse transcriptase–polymerase chain reaction (RT-PCR) performed in accordance with the manufacturer's protocol (Sigma). This was followed by quantitative real-time PCR. Primer selection was as follows: Galectin-9, 5′-CTTTCATCACCACCATTCTG-3′, 5′-ATGTGGAACCTCTGAGCACTG-3′ Tim-3, 5′-CATGTTTTCACATCTTCCC-3′ actin, 5′-TGACG GGGTCACCCACACTGTGCCCATCTA-3′, 5′-CTAGAAGC ATTTGCGGTCG-ACGATGGAGGG-3′. Reactions were performed using a LightCycler® 480 real-time PCR system and respective SYBR Green I Master kit (obtained from Roche, Burgess Hill, UK). Analysis was performed according to the manufacturer's protocol. Values representing galectin-9 and Tim-3 mRNA levels were normalized against β-actin.

Western blot analysis

Expressions of Tim-3 and galectin-9 were determined by Western blot analysis and compared to β-actin in order to determine equal protein loading, as previously described.[4] Li-Cor goat secondary antibodies, conjugated with fluorescent dyes, were used in accordance with manufacturer's protocol to visualize target proteins (using a Li-Cor Odyssey imaging system). Western blot data were quantitatively analyzed using Odyssey software and values were subsequently normalized against those of β-actin.

Detection of phospho-S2448 mTOR in cell lysates by ELISA

Phosphorylation of mTOR was analyzed by ELISA as described before.[23] Briefly, 96-well ELISA plates were coated with mouse anti-mTOR antibodies followed by blocking with 2% BSA. Cell lysates were then added to the wells and incubated at room temperature for 2 h (with constant agitation). Plates were then washed with Tris-Buffered Saline containing Tween 20 (TBST). Following washing with TBST buffer plates were incubated with HRP-labeled goat anti-rabbit IgG for 1 h at room temperature. Plates were then washed using TBST and bound secondary antibodies were visualized by the peroxidase reaction (ortho-phenylenediamine/H_2O_2).

In-cell Western and in-cell (on-cell) assay

We employed a standard Li-Cor in-cell Western assay to analyze total Tim-3 and galectin-9 expressions in the studied cells.[4] The in-cell (also called on-cell) assay was employed to

characterized Tim-3 and galectin-9 surface presence in the studied cells.

Characterization of Tim-3 and galectin-9 interactions in cell lysates

An ELISA-based analysis was used where plates were first coated with anti-galectin-9 antibody followed by blocking with 2% BSA. Cell lysates were then applied and incubated for at least 4 h at room temperature after which plates were extensively washed with TBST. A glycine-HCl pH lowering buffer (pH 2.0) was then applied to extract the bound proteins. Extracts were mixed with equal volumes of lysis buffer (pH 7.5) and with 4× sample buffer for SDS-PAGE at a ratio of 1:3. Samples were then subjected to Western blot analysis, using rabbit anti-galectin-9 and mouse anti-Tim-3 primary antibodies, as described above. The plate was subjected to analysis with galectin-9 detection antibody followed by standard ELISA steps to ensure that no galectin-9 remained in the wells. Signals obtained were similar to those where PBS was used instead of the sample confirming that all the protein was extracted.

Detection of galectin-9 and VEGF secretion, soluble forms of Tim-3 and Tim-3-galectin-9 complexes

Galectin-9 and VEGF levels released into the medium were analyzed by ELISA (R&D Systems assay kits) according to the manufacturer's instructions. Soluble Tim-3 was detected using similar approach where mouse anti-Tim-3 (mAnti-Tim-3) was employed as a capture antibody and rabbit anti-Tim-3 (rAnti-Tim-3)—for detection (Fig. 6C, scheme). HRP-labeled anti-Rabbit secondary antibody (Abcam) was used to visualize the reaction. Tim-3-galectin-9 complexes in blood plasma were detected by ELISA. Mouse anti-Tim-3 (mAnti-Tim-3) was employed as a capture antibody and biotinylated goat anti-galectin-9 (gAnti-Galectin-9, R&D Systems) as detection antibody. The reaction was visualized using HRP-labeled streptavidin (R&D Systems; Fig. 6C, scheme). In all cases plates were washed using TBST and bound secondary antibodies visualized by the peroxidase reaction (ortho-phenylenediamine/H_2O_2).

Characterization of glycolysis and MGO levels

Glycolytic degradation of glucose was analyzed using a colorimetric assay as described before.[20] Briefly, the approach was based on the ability of cell lysates, used as a multi-enzyme preparation, to convert glucose into lactate in the absence of oxygen (this was achieved by employing an anaerobic chamber). Cell lysates were incubated for 1 h at 37°C with 1% glucose solution within the anaerobic chamber. 2% trichloroacetic acid solution was then used to precipitate proteins. This was followed by carbohydrate precipitation using saturated $CuSO_4$ solution in combination with $Ca(OH)_2$ (at a final concentration of 60 mg/mL). Lactate was then converted into acetic aldehyde using concentrated H_2SO_4 at 90°C for 1 min and cooled the samples down on ice. We then detected acetaldehyde using the veratrole (1,2-dimethoxybenzene) test. MGO was also detected colorimetrically following biochemical modifications.[24,25] Briefly, MGO was condensed with reduced glutathione (GSH, 1 mM) for 10 min at 37°C. The complex was then converted into lactate by Glyoxalases I and II at pH 8.0 (Glyoxalase I converted the complex in D-lactoyL-glutathione, which was then transformed into lactate by Glyoxalase II[26]). The whole process is highlighted in Fig. S2). Lactate was then measured colorimetrically as described above.

Statistical analysis

Each experiment was performed at least three times and statistical analysis was conducted using a 2-tailed Student's t test. Statistical probabilities (p) were expressed as $^{*}p < 0.05$, $^{**}p < 0.01$, and $^{***}p < 0.001$.

Disclosure of potential conflicts of interest

No potential conflicts of interest were disclosed.

Funding

L.V. and M.B. were supported by a grant from Oncosuisse (KFS 3728082015).

References

1. Kikushige Y, Miyamoto T. TIM-3 as a novel therapeutic target for eradicating acute myelogenous leukemia stem cells. Int J Hematol 2013; 98:627-633; PMID:24046178; http://dx.doi.org/10.1007/s12185-013-1433-6
2. Kikushige Y, Miyamoto T. Identification of TIM-3 as a Leukemic Stem Cell Surface Molecule in Primary Acute Myeloid Leukemia. Oncology 2015; 89 Suppl 1:28-32; PMID:26551150; http://dx.doi.org/10.1159/000431062
3. Kikushige Y, Miyamoto T, Yuda J, Jabbarzadeh-Tabrizi S, Shima T, Takayanagi S, Niiro H, Yurino A, Miyawaki K, Takenaka K et al. A TIM-3/Gal-9 Autocrine Stimulatory Loop Drives Self-Renewal of Human Myeloid Leukemia Stem Cells and Leukemic Progression. Cell Stem Cell 2015; 17:341-352; PMID:26279267; http://dx.doi.org/10.1016/j.stem.2015.07.011
4. Gonçalves Silva I, Gibbs BF, Bardelli M, Varani L, Sumbayev VV. Differential expression and biochemical activity of the immune receptor Tim-3 in healthy and malignant human myeloid cells. Oncotarget 2015; 6:33823-33833; PMID:26413815; http://dx.doi.org/10.18632/oncotarget.5257
5. Prokhorov A, Gibbs BF, Bardelli M, Ruegg L, Fasler-Kan E, Varani L, Sumbayev VV. The immune receptor Tim-3 mediates activation of PI3 kinase/mTOR and HIF-1 pathways in human myeloid leukaemia cells. Int J Biochem Cell Biol 2015; 59:11-20; PMID:25483439; http://dx.doi.org/10.1016/j.biocel.2014.11.017
6. Ma CJ, Li GY, Cheng YQ, Wang JM, Ying RS, Shi L, Wu XY, Niki T, Hirashima M, Li CF et al. Cis association of galectin-9 with Tim-3 differentially regulates IL-12/IL-23 expressions in monocytes via TLR signaling. PLoS One 2013; 8:e72488; PMID:23967307; http://dx.doi.org/10.1371/journal.pone.0072488
7. Zhang Y, Ma CJ, Wang JM, Ji XJ, Wu XY, Moorman JP, Yao ZQ. Tim-3 regulates pro- and anti-inflammatory cytokine expression in human CD14+ monocytes. J Leukoc Biol 2012; 91:189-196; PMID:21844165; http://dx.doi.org/10.1189/jlb.1010591
8. Moller-Hackbarth K, Dewitz C, Schweigert O, Trad A, Garbers C, Rose-John S, Scheller J. A disintegrin and metalloprotease (ADAM) 10 and ADAM17 are major sheddases of T cell immunoglobulin and mucin domain 3 (Tim-3). J Biol Chem 2013; 288:34529-34544; PMID:24121505; http://dx.doi.org/10.1074/jbc.M113.488478
9. Clayton KL, Douglas-Vail MB, Nur-ur Rahman AK, Medcalf KE, Xie IY, Chew GM, Tandon R, Lanteri MC, Norris PJ, Deeks SG et al. Soluble T cell immunoglobulin mucin domain 3 is shed from CD8+ T

cells by the sheddase ADAM10, is increased in plasma during untreated HIV infection, and correlates with HIV disease progression. J Virol 2015; 89:3723-3736; PMID:25609823; http://dx.doi.org/10.1128/JVI.00006-15
10. Golden-Mason L, McMahan RH, Strong M, Reisdorph R, Mahaffey S, Palmer BE, Cheng L, Kulesza C, Hirashima M, Niki T et al. Galectin-9 functionally impairs natural killer cells in humans and mice. J Virol 2013; 87:4835-4845; PMID:23408620; http://dx.doi.org/10.1128/JVI.01085-12
11. Wang F, He W, Zhou H, Yuan J, Wu K, Xu L, Chen ZK. The Tim-3 ligand galectin-9 negatively regulates CD8+ alloreactive T cell and prolongs survival of skin graft. Cell Immunol 2007; 250:68-74; PMID:18353298; http://dx.doi.org/10.1016/j.cellimm.2008.01.006
12. Akira S, Takeda K. Toll-like receptor signalling. Nat Rev Immunol 2004; 4:499-511; PMID:15229469; http://dx.doi.org/10.1038/nri1391
13. Broudy VC. Stem cell factor and hematopoiesis. Blood 1997; 90:1345-1364; PMID:9269751
14. Hsu YL, Wang MY, Ho LJ, Huang CY, Lai JH. Up-regulation of galectin-9 induces cell migration in human dendritic cells infected with dengue virus. J Cell Mol Med 2015; 19:1065-1076; PMID:25754930; http://dx.doi.org/10.1111/jcmm.12500
15. Khaznadar Z, Henry G, Setterblad N, Agaugue S, Raffoux E, Boissel N, Dombret H, Toubert A, Dulphy N. Acute myeloid leukemia impairs natural killer cells through the formation of a deficient cytotoxic immunological synapse. Eur J Immunol 2014; 44:3068-3080; PMID:25041786; http://dx.doi.org/10.1002/eji.201444500
16. Tandon R, Chew GM, Byron MM, Borrow P, Niki T, Hirashima M, Barbour JD, Norris PJ, Lanteri MC, Martin JN et al. Galectin-9 is rapidly released during acute HIV-1 infection and remains sustained at high levels despite viral suppression even in elite controllers. AIDS Res Hum Retroviruses 2014; 30:654-664; PMID:24786365; http://dx.doi.org/10.1089/aid.2014.0004
17. Chabot S, Kashio Y, Seki M, Shirato Y, Nakamura K, Nishi N, Nakamura T, Matsumoto R, Hirashima M. Regulation of galectin-9 expression and release in Jurkat T cell line cells. Glycobiology 2002; 12:111-118; PMID:11886844; http://dx.doi.org/10.1093/glycob/12.2.111
18. Yoon SJ, Lee MJ, Shin DC, Kim JS, Chwae YJ, Kwon MH, Kim K, Park S. Activation of mitogen activated protein kinase-Erk kinase (MEK) increases T cell immunoglobulin mucin domain-3 (TIM-3) transcription in human T lymphocytes and a human mast cell line. Mol Immunol 2011; 48:1778-1783; PMID:21621846; http://dx.doi.org/10.1016/j.molimm.2011.05.004
19. Sahin U, Weskamp G, Kelly K, Zhou HM, Higashiyama S, Peschon J, Hartmann D, Saftig P, Blobel CP. Distinct roles of ADAM10 and ADAM17 in ectodomain shedding of six EGFR ligands. J Cell Biol 2004; 164:769-779; PMID:14993236; http://dx.doi.org/10.1083/jcb.200307137
20. Porakishvili N, Roschupkina T, Kalber T, Jewell AP, Patterson K, Yong K, Lydyard PM. Expansion of CD4+ T cells with a cytotoxic phenotype in patients with B-chronic lymphocytic leukaemia (B-CLL). Clin Exp Immunol 2001; 126:29-36; PMID:11678896; http://dx.doi.org/10.1046/j.1365-2249.2001.01639.x
21. Moritoki M, Kadowaki T, Niki T, Nakano D, Soma G, Mori H, Kobara H, Masaki T, Kohno M, Hirashima M. Galectin-9 ameliorates clinical severity of MRL/lpr lupus-prone mice by inducing plasma cell apoptosis independently of Tim-3. PLoS One 2013; 8:e60807; PMID:23585851; http://dx.doi.org/10.1371/journal.pone.0060807
22. Wang C, Liu J, Wang L, Geng X. Solubilization and refolding with simultaneous purification of recombinant human stem cell factor. Appl Biochem Biotechnol 2008; 144:181-189; PMID:18456949; http://dx.doi.org/10.1007/s12010-007-8112-0
23. Yasinska IM, Gibbs BF, Lall GS, Sumbayev VV. The HIF-1 transcription complex is essential for translational control of myeloid hematopoietic cell function by maintaining mTOR phosphorylation. Cell Mol Life Sci 2014; 71:699-710; PMID:23872956; http://dx.doi.org/10.1007/s00018-013-1421-2
24. Chaplen FW, Fahl WE, Cameron DC. Detection of methylglyoxal as a degradation product of DNA and nucleic acid components treated with strong acid. Anal Biochem 1996; 236:262-269; PMID:8660503; http://dx.doi.org/10.1006/abio.1996.0165
25. Chaplen FW, Fahl WE, Cameron DC. Method for determination of free intracellular and extracellular methylglyoxal in animal cells grown in culture. Anal Biochem 1996; 238:171-178; PMID:8660607; http://dx.doi.org/10.1006/abio.1996.0271
26. Thornalley PJ. The glyoxalase system in health and disease. Mol Aspects Med 1993; 14:287-371; PMID:8277832; http://dx.doi.org/10.1016/0098-2997(93)90002-U

SUPPLEMENTARY INFORMATION

The immune receptor Tim-3 acts as a trafficker in a Tim-3/galectin-9 autocrine loop in human myeloid leukaemia cells

Isabel Gonçalves Silva[1], Laura Rüegg[1], Bernhard F. Gibbs[1]*, Marco Bardelli[2], Alexander Fruewirth[2], Luca Varani[2] , Steffen M. Berger[3], Elizaveta Fasler-Kan[3]* and Vadim V. Sumbayev[1]*

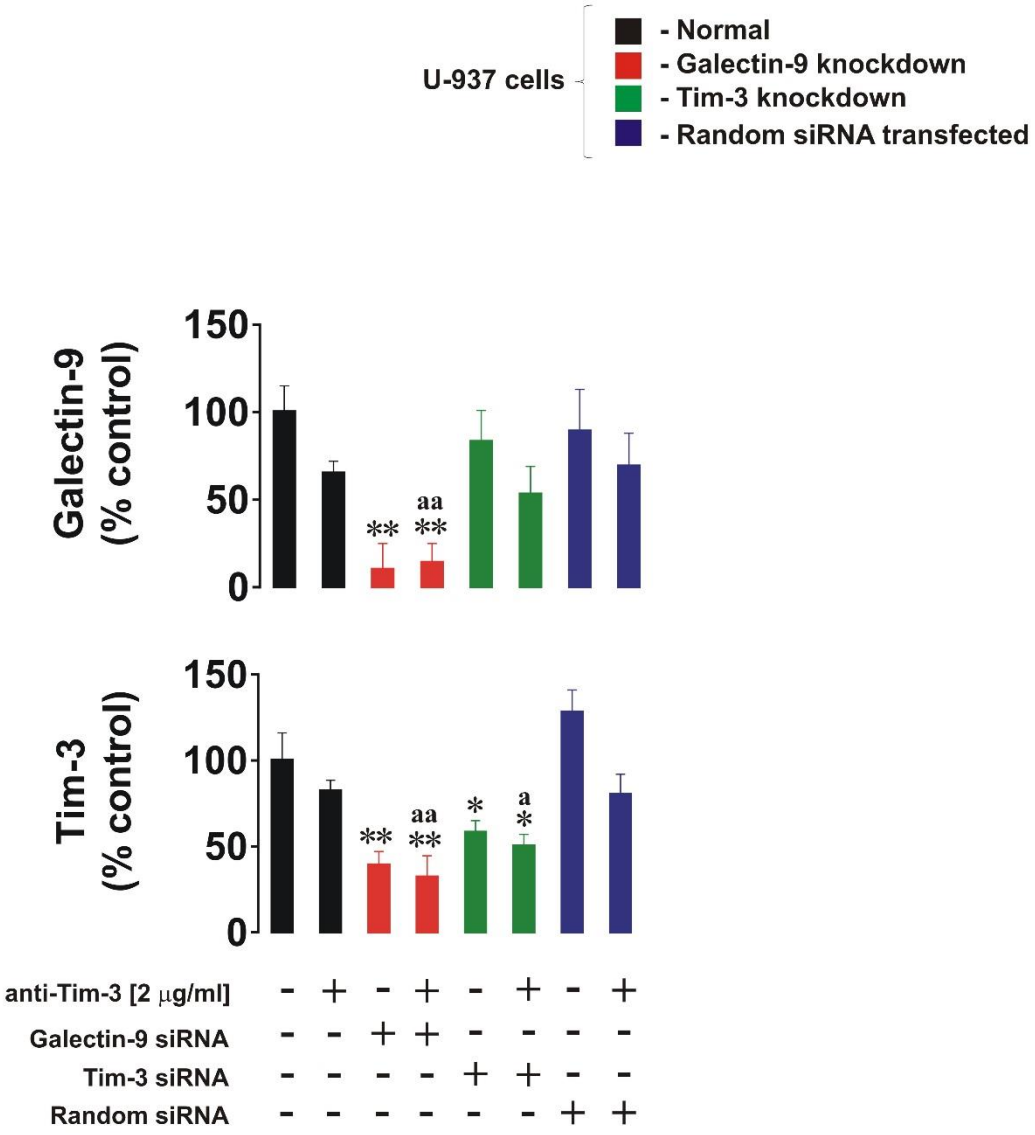

Supplementary Figure 1. qRT-PCR analysis of galectin-9 and Tim-3 mRNA levels in U-937 cells. Non-treated normal (wild type), galectin-9 knockdown, Tim-3 knockdown and transfected with random siRNA U-937 cells, as well as the same cells which underwent 4 h treatment with 2 μg/ml anti-Tim-3, were used. Total RNA was isolated and subjected to qRT-PCR analysis of Tim-3 and galectin-9 mRNA levels as outlined in Materials and Methods. Data are mean values ± SEM of eight independent reactions; * – $p < 0.05$; ** – $p < 0.01$ vs. control; ^{a} – $p < 0.05$; ^{aa} – $p < 0.01$ vs. anti-Tim-3.

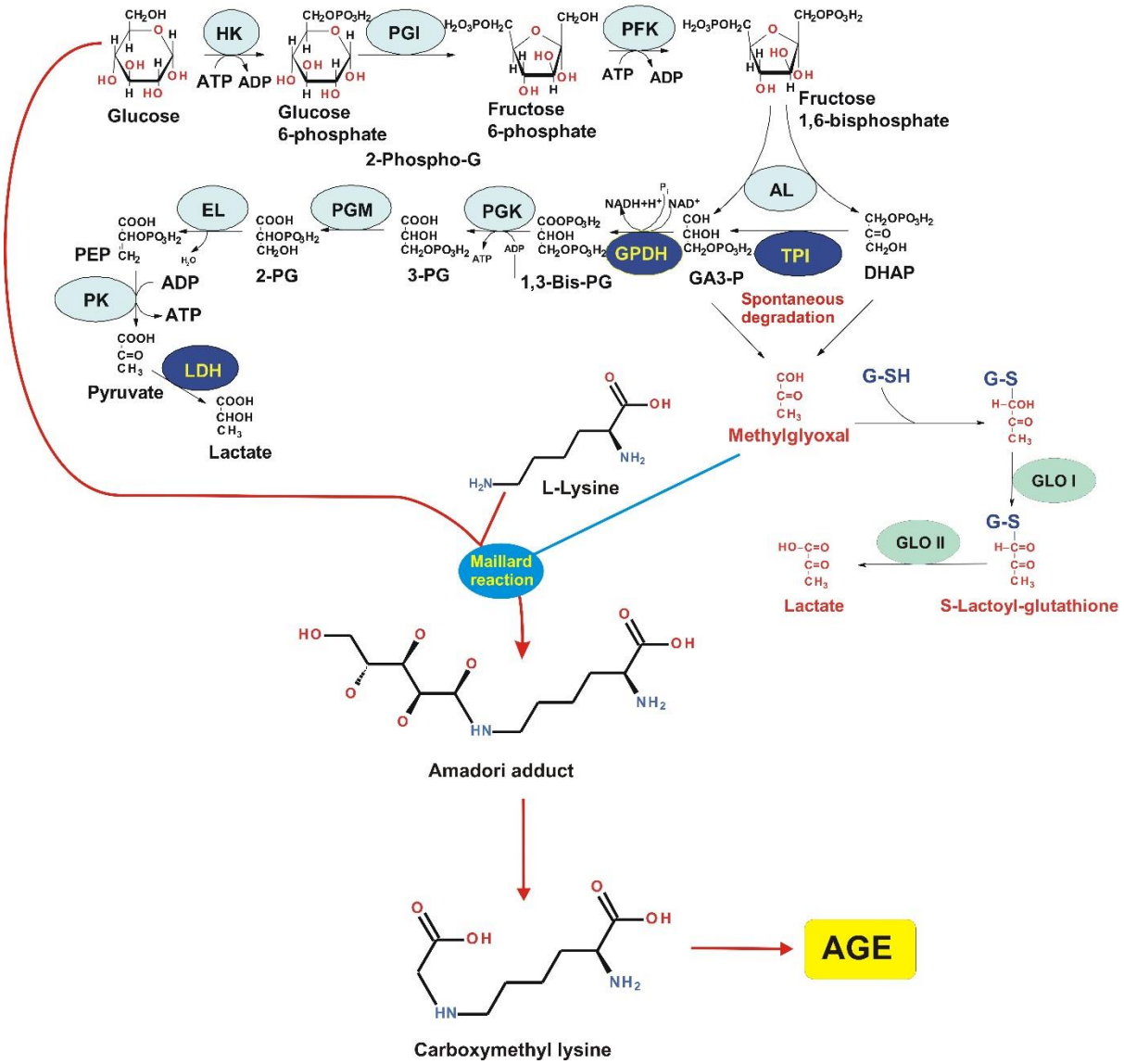

Supplementary figure 2. Biochemistry of glycolytic degradation of glucose, generation of methylglyoxal (MGO) and MGO-dependent formation of advanced glycation end (AGE) products. The scheme contains the biochemistry of glycolysis, shows spontaneous conversions of dihydroxyacetone phosphate -and possibly glyceraldehyde-3-phosphate- into MGO. The scheme highlights (in red) the process of conversion of MGO into lactate (used also to design the biochemical assay to detect MGO levels). The Maillard reaction between glucose and L-lysine leading to the generation of the Amadori adduct followed by conversion into carboxymethyl lysine and then into AGE is presented.

Additional abbreviations used: HK – hexokinase, PGI – phosphoglucose isomerase, PFK – phosphofructokinase, AL – Aldolase, TPI – Triose-phosphate isomerase, GPDH – glyceraldehyde-3-phosphate dehydrogenase, PGK – phosphoglycerate kinase, PGM – phosphoglycerate mutase, EL – enolase, PK – pyruvate kinase, LDH – lactate dehydrogenase, DHAP – dihydroxyacetone phosphate, GA3-P – glyceraldehyde-3-phosphate, 3-PG – 3-phosphoglycerate, 2-PG – 2-phosphoglycerate, PEP – phosphoenolpyruvate, G-SH – reduced glutathione, GLO (I or II) – glyoxalases I and II.

EBioMedicine xxx (2017) xxx–xxx

Contents lists available at ScienceDirect

EBioMedicine

journal homepage: www.ebiomedicine.com

Research Paper

The Tim-3-galectin-9 Secretory Pathway is Involved in the Immune Escape of Human Acute Myeloid Leukemia Cells

Isabel Gonçalves Silva [a,1], Inna M. Yasinska [a,1], Svetlana S. Sakhnevych [a], Walter Fiedler [b], Jasmin Wellbrock [b], Marco Bardelli [c], Luca Varani [c], Rohanah Hussain [d], Giuliano Siligardi [d], Giacomo Ceccone [e], Steffen M. Berger [f], Yuri A. Ushkaryov [a,*], Bernhard F. Gibbs [a,g,*], Elizaveta Fasler-Kan [f,h,*], Vadim V. Sumbayev [a,*]

[a] School of Pharmacy, University of Kent, Chatham Maritime, UK
[b] Department of Oncology, Hematology and Bone Marrow Transplantation with Section Pneumology, Hubertus Wald University Cancer Center, University Medical Center Hamburg-Eppendorf, Germany
[c] Institute for Research in Biomedicine, Universita' della Svizzera italiana (USI), Bellinzona, Switzerland
[d] Beamline 23, Diamond Light Source, Didcot, UK
[e] European Commission Joint Research Centre, Ispra, Italy
[f] Department of Pediatric Surgery and Department of Clinical Research, Children's Hospital, Inselspital, University of Bern, Switzerland
[g] Department of Dermatology, University of Oldenburg, Germany
[h] Department of Biomedicine, University of Basel, Switzerland

ARTICLE INFO

Article history:
Received 16 June 2017
Received in revised form 12 July 2017
Accepted 17 July 2017
Available online xxxx

Keywords:
Acute myeloid leukemia
Tim-3
Galectin-9
NK cells
Anti-leukemia immunity

ABSTRACT

Acute myeloid leukemia (AML) is a severe and often fatal systemic malignancy. Malignant cells are capable of escaping host immune surveillance by inactivating cytotoxic lymphoid cells. In this work we discovered a fundamental molecular pathway, which includes ligand-dependent activation of ectopically expressed latrophilin 1 and possibly other G-protein coupled receptors leading to increased translation and exocytosis of the immune receptor Tim-3 and its ligand galectin-9. This occurs in a protein kinase C and mTOR (mammalian target of rapamycin)-dependent manner. Tim-3 participates in galectin-9 secretion and is also released in a free soluble form. Galectin-9 impairs the anti-cancer activity of cytotoxic lymphoid cells including natural killer (NK) cells. Soluble Tim-3 prevents secretion of interleukin-2 (IL-2) required for the activation of cytotoxic lymphoid cells. These results were validated in ex vivo experiments using primary samples from AML patients. This pathway provides reliable targets for both highly specific diagnosis and immune therapy of AML.

1. Introduction

Acute myeloid leukemia (AML) is a blood/bone marrow cancer originating from self-renewing malignant immature myeloid precursors, which rapidly becomes a systemic malignancy. It is often a fatal disease because malignant cells are capable of suppressing anti-cancer immunity by impairing the functional activity of natural killer (NK) cells and cytotoxic T cells (Golden-Mason et al., 2013; Wang et al., 2007; Khaznadar et al., 2014). Recent evidence clearly demonstrated an involvement of the T cell immunoglobulin and mucin domain 3 (Tim-3) - galectin-9 pathway in this immune escape mechanism (Golden-Mason et al., 2013; Kikushige et al., 2015; Gonçalves Silva et al., 2016). Galectin-9 is a β-galactoside-binding lectin, which has a tandem structure and contains two carbohydrate recognition domains (CRDs) fused together by a peptide (Delacour et al., 2009). Galectin-9 has a specific receptor on AML cells known as Tim-3 which also could act as its possible trafficker (galectin-9 as all other galectins lacks a signal sequence required for transport into the endoplasmic reticulum (ER) and thus requires a trafficking protein for its secretion (Hughes, 1999; Delacour et al., 2009)). However, the mechanisms underlying the activation of biosynthesis of the components of the Tim-3-galectin-9 autocrine loop, galectin-9 secretion and its effects on cytotoxic lymphocytes (NK cells and T cells) remain poorly understood.

Recently, we discovered that human AML cells – but not healthy leukocytes – express physiologically active latrophilin 1 (LPHN1; Sumbayev et al., 2016). LPHN1, an adhesion G-protein-coupled receptor, is highly expressed in neuronal axon terminals and in many secretory cells (Davletov et al., 1998; Silva and Ushkaryov, 2010). In all cells expressing this receptor, LPHN1 activation by its most potent agonist, α-latrotoxin (LTX) from black widow spider venom (Ushkaryov, 2002), triggers intracellular Ca^{2+} signaling and exocytosis of neurotransmitters and hormones (Volynski et al., 2003). Similarly, ligand-

* Corresponding authors.
E-mail addresses: Ushkaryov@kent.ac.uk (Y.A. Ushkaryov), bernhard.gibbs@uni-oldenburg.de (B.F. Gibbs), elizaveta.fasler@insel.ch (E. Fasler-Kan), V.Sumbayev@kent.ac.uk (V.V. Sumbayev).
[1] IGS and IMY contributed equally to this work.

http://dx.doi.org/10.1016/j.ebiom.2017.07.018

induced activation of LPHN1 in AML cells facilitates exocytosis of cytokines and growth factors (Sumbayev et al., 2016). Production of LPHN1 in AML cells is controlled by the mammalian target of rapamycin (mTOR) (Sumbayev et al., 2016), a highly conserved serine/threonine kinase that acts as a central regulator of growth and metabolism in healthy and malignant human myeloid cells (Yasinska et al., 2014). To function in cell-cell interactions and cell signaling, LPHN1 can interact with at least two endogenous ligands, Lasso/teneurin-2 (Silva et al., 2011) and fibronectin leucine rich transmembrane protein 3 (FLRT3) (Boucard et al., 2014), although only FLRT3 seems to be expressed in peripheral tissues. In addition to triggering exocytosis by increasing cytosolic Ca^{2+}, LPHN1 can enhance the sensitivity of the release machinery by activating protein kinase C (Liu et al., 2005), which is also thought to be involved in galectin-9 secretion (Chabot et al., 2002). Based on these observations, we hypothesized that activation of LPHN1 by its ligands can induce secretion of galectin-9, thus protecting AML cells against NK and cytotoxic T cells. This hypothesis has been studied experimentally in the present study.

Here we report that the Tim-3-galectin-9 autocrine loop is activated in AML cells through protein kinase C (PKC)/mTOR pathways. These pathways trigger translation of both Tim-3 and galectin-9 and induce high levels of galectin-9 secretion as well as the release of soluble Tim-3. Importantly, this effect was also verified in the AML patients studied. Galectin-9 was found to impair AML cell killing by primary human NK cells. Soluble Tim-3 reduced the ability of T cells to secrete IL-2, a cytokine, which is required for the activation of both NK cells and cytotoxic T cells (Dhupkar and Gordon, 2017). Blood plasmas of AML patients contained significantly lower amounts of IL-2 compared to those of healthy donors. We confirmed that PKC activation occurred in AML cells in a LPHN1-dependent manner. The LPHN1 agonist LTX and natural ligand FLRT3 upregulated the Tim-3-galectin-9 autocrine loop in a PKC-dependent manner. Based on our findings, we conclude that LPHN1/PKC/mTOR/Tim-3-galectin-9 is a biosynthetic and secretory pathway which is operated by human AML cells resulting in a decrease of immune surveillance and promotion of disease progression.

2. Materials and Methods

2.1. Materials

RPMI-1640 medium, fetal bovine serum and supplements and basic laboratory chemicals were purchased from Sigma (Suffolk, UK). Maxisorp™ microtitre plates were provided either by Nunc (Roskilde, Denmark) and Oxley Hughes Ltd. (London, UK). Mouse monoclonal antibodies directed against mTOR and β-actin, as well as rabbit polyclonal antibodies against phospho-S2448 mTOR, galectin-9, HRP-labelled rabbit anti-mouse secondary antibody were purchased from Abcam (Cambridge, UK). Mouse monoclonal antibody against FLRT3 was obtained from Santa Cruz Biotechnology (Heidelberg, Germany). The polyclonal rabbit anti-peptide antibody (PAL1) against LPHN1 was described previously (Davydov et al., 2009). LTX was purified as previously described (Ashton et al., 2000). Goat anti-mouse and goat anti-rabbit fluorescence dye-labelled antibodies were obtained from LI-COR (Lincoln, Nebraska USA). ELISA-based assay kits for the detection of galectin-9, Tim-3 and IL-2 were purchased from Bio-Techne (R&D Systems, Abingdon, UK). Anti-Tim-3 mouse monoclonal antibody, its single chain variant as well as human Ig-like V-type domain of Tim-3 (amino acid residues 22–124), expressed and purified from *E. coli* (Prokhorov et al., 2015) were used in our work. Secondary antibodies for confocal laser microscopy and imaging flow cytometry (goat anti-mouse and goat anti-rabbit Alexa 488, Alexa 555 and Alexa 647) were from Invitrogen (Carlsbad, USA). All other chemicals purchased were of the highest grade of purity.

2.2. Cell Lines and Primary Human Cells

THP-1 human myeloid leukemia monocytes, K562 chronic myelogenous leukemia cells and Jurkat T cells were obtained from the European Collection of Cell Cultures (Salisbury, UK). Renal clear cell carcinoma RCC-FG1 cells were obtained from CLS Cell Lines Service (Eppelheim, Germany). Cells were cultured in RPMI 1640 media supplemented with 10% fetal bovine serum, penicillin (50 IU/ml) and streptomycin sulfate (50 μg/ml). LAD2 mast cells were kindly provided by A. Kirshenbaum and D. Metcalfe (NIH, USA). Cells were cultured in StemPro-34 serum-free media in the presence of 100 ng/ml SCF (Kirshenbaum et al., 2003).

Primary human AML mononuclear blasts (AML-PB001F, newly diagnosed/untreated) were purchased from AllCells (Alameda, CA, USA) and handled in accordance with the manufacturer's instructions. Primary human NK cells were purified from buffy coat blood (prepared from healthy donors) obtained from the National Health Blood and Transfusion Service (NHSBT, UK) following ethical approval (REC reference: 16-SS-033). Primary CD34-positive HSCs were obtained from Lonza (Basel, Switzerland).

Femur bones of six-week-old C57 BL16 mice (25 ± 2.5 g, kindly provided by Dr. Gurprit Lall, School of Pharmacy, University of Kent) were used for the experiments following approval by the Institutional Animal Welfare and Ethics Review Body. Animals were handled by authorized personnel in accordance with the Declaration of Helsinki protocols. Bone marrow was isolated from femur bone heads as described before (Swamydas and Lionakis, 2013) and whole extracts (1 mg protein/ml) were then obtained.

2.3. Primary Human Plasma Samples

Blood plasma of healthy donors was obtained from buffy coat blood (originated from healthy donors undergoing routine blood donation) which was purchased from the National Health Blood and Transfusion Service (NHSBT, UK) following ethical approval (REC reference: 16-SS-033). Primary human AML plasma samples were obtained from the sample bank of University Medical Centre Hamburg-Eppendorf (Ethik-Kommission der Ärztekammer Hamburg, reference: PV3469).

2.4. Western Blot Analysis

Tim-3, galectin-9, FLRT3, LPHN1 and Gαq were analyzed by Western blot and compared to β-actin in order to verify equal protein loading, as previously described (Yasinska et al., 2014). Briefly, cells were lysed using lysis buffer (50 mM Tris–HCl, 5 mM EDTA, 150 mM NaCl, 0.5% Nonidet-40, 1 mM PMSF, pH 8.0). After centrifugation, the protein content in the supernatants was analyzed. Finally, samples were added to the same volume of 2× sample buffer (125 mM Tris–HCl, 2% sodium dodecyl sulfate (SDS), 10% glycerine, 1 mM dithiothreitol (DTT), 0.002% bromophenol blue, pH 6.9) and boiled for 5 min. Proteins were resolved using SDS–polyacrylamide gels followed by blotting onto nitrocellulose membranes. Molecular weights were calibrated in proportion to the running distance of rainbow markers. For all primary antibodies (see Materials section) a 1:1000 dilution was used, except those against LPHN1 and FLRT3 (where a 1:500 dilution was used). β-actin staining was used to confirm equal protein loading as described previously (Yasinska et al., 2014). LI-COR goat secondary antibodies (dilution 1:2000), conjugated with fluorescent dyes, were used in accordance with manufacturer's protocol to visualize target proteins (using a LI-COR Odyssey imaging system). Western blot data were quantitatively analyzed using Odyssey software and values were subsequently normalized against those of β-actin.

Please cite this article as: Gonçalves Silva, I., et al., The Tim-3-galectin-9 Secretory Pathway is Involved in the Immune Escape of Human Acute Myeloid Leukemia Cells, EBioMedicine (2017), http://dx.doi.org/10.1016/j.ebiom.2017.07.018

2.5. Characterization of Tim-3 and Galectin-9 in Tissue Culture Medium

Secreted Tim-3 and galectin-9 were characterized in the RPMI-1640 medium used to culture THP-1 cells. The proteins were first precipitated on Maxisorp ELISA plates (see Materials section). For this purpose ELISA plates were coated overnight using single-chain antibody against Tim-3. Plates were then blocked with 2% BSA. Tissue culture medium was then applied and incubated for 4 h at room temperature, followed by extensive washing with TBST buffer. Proteins were then extracted using 0.2 M glycine-HCl buffer (pH 2.0). Extracts were neutralized using lysis buffer and subjected to Western blot analysis using mouse anti-Tim-3 and rabbit anti-galectin-9 antibodies as described before (Gonçalves Silva et al., 2016) and above.

2.6. Enzyme-linked Immunosorbent Assays (ELISAs)

Galectin-9, sTim-3 and IL-2 were measured by ELISA using R&D Systems kits according to manufacturer's protocols. In all cases the procedure involves specific detection of captured target proteins using biotinylated detection antibody. The interaction was then analyzed using streptavidin conjugated with horseradish peroxidase (HRP) according to the manufacturer's protocol. Tim-3-galectin-9 complex was also analyzed by ELISA. Single-chain antibody (described above, dilution 1:100) was used to capture the complex and biotinylated goat R&D Systems antibody against galectin-9 (detection antibody) was used to detect galectin-9 bound to Tim-3. HRP-labelled streptavidin was then used to perform quantitative analysis according to the R&D Systems protocol for the galectin-9 assay kit. Phosphorylation of mTOR was analyzed by ELISA as previously described (Yasinska et al., 2014).

2.7. In Cell Assays and in Cell Westerns

We employed a standard LI-COR in-cell Western (ICW) assay (methanol was used as permiabilization agent) to analyze total Tim-3 and galectin-9 expressions in the studied cells. The in-cell (ICA, also called on-cell) assay was employed to characterize Tim-3 and galectin-9 surface presence in the studied cells. We also used this assay to visualize binding of LAD2 cells to NK cells. IgE-sensitized LAD2 cells were exposed for 5 min to 1 μg/ml, carefully washed with sterile PBS and exposed to LI-COR goat anti-mouse labelled secondary antibody. Following washing with PBS, cells were scanned using a LI-COR Odyssey imaging system (Gonçalves Silva et al., 2016).

2.8. Confocal Microscopy and Imaging Flow Cytometry

THP-1 cells were grown on 12 mm cover glasses in 24-well plates. Cells were treated (o/n) with PMA and then fixed/permeabilized for 20 min with ice-cold MeOH or MeOH/acetone. Alternatively cells were fixed in a freshly prepared 2% paraformaldehyde, washed 3 times with PBS and then permeabilized with 0.1%TX-100. Cover glasses were blocked for 1 h at RT with 10% goat serum in PBS. 1 μg/ml anti-Tim-3 antibody and anti-galectin-9 antibody were used as primary antibodies and incubated o/n at 4 °C. Goat-anti-mouse Alexa Fluor 488 and goat-anti-rabbit Alexa Fluor 555 were used as secondary antibodies. Cells were incubated with secondary antibodies for 45 min at RT. The preparations were examined on Olympus laser scanning confocal microscope as described (Prokhorov et al., 2015; Fasler-Kan et al., 2010). Images were collected and analyzed using proprietary image acquisition software. Imaging flow cytometry was performed in accordance with a previously described protocol (Fasler-Kan et al., 2016). Briefly, permiabilized cells were stained with mouse anti-Tim-3 and rabbit anti-galectin-9 antibodies for 1 h at room temperature. Goat anti-mouse Alexa Fluor 647 and goat-anti-rabbit Alexa Fluor 488 were used as secondary antibodies. Images were collected and analyzed using IDEAS analytical software on ImageStream X mark II (Amnis-EMD-Millipore, USA).

2.9. Synchrotron Radiation Circular Dichroism Spectroscopy

Human recombinant Tim-3, human recombinant galectin-9 and Tim-3-galectin-9 complex were analyzed using SRCD spectroscopy at beam line 23, Diamond Light Source (Didcot, UK). SRCD measurements were performed using 0.2 μg/ml of samples in 10 cm path length cell, 3 mm aperture diameter and 800 μl capacity using Module B with 1 nm increment, 1 s integration time, 1.2 nm bandwidth at 23 °C (Hussain et al., 2012a, 2012b; Siligardi and Hussain, 2015). The results obtained were processed using CDApps (Hussain et al., 2015) and OriginLab™.

2.10. PKCα Activity Assay

The catalytic activity of PKCα was measured as described before based on its ability to phosphorylate specific substrate in a reaction buffer containing 20 mM Tris-HCl (pH 7.5), 20 μM ATP, 5 mM $MgCl_2$ and 200 μM $CaCl_2$ (Micol et al., 1999). Phosphate groups attached to the substrate were detected using colorimetric assay (Abooali et al., 2014).

2.11. Cell Viability Assay

Cell viability was analyzed using the Promega UK Ltd. (Southampton, UK) assay kit. We used an MTS colorimetric assay for assessing cell metabolic activity. NAD(P)H-dependent cellular oxidoreductase enzymes playing crucial role in human myeloid cell survival (Sumbayev and Nicholas, 2010), reflect the number of viable cells present. Cells were incubated with 3-(4,5-dimethylthiazol-2-yl)-5-(3-carboxymethoxyphenyl)-2-(4-sulfophenyl)-2H-tetrazolium (MTS) and then absorbance was measured at 490 nm in accordance with the manufacturer's protocol.

2.12. Leukemia Cell Protection Assay

K562 and NK cells were cultured separately or as a 1:2 co-culture (K562:NK) for 16 h, at 37 °C, in the absence or presence of 0.5–5 ng/ml of galectin-9. The unfixed cell cultures were then imaged under an inverted microscope (TE200, Nikon), using phase-contrast lighting, a digital camera and the WinFluor image acquisition software (J. Dempster, University of Strathclyde). Raw images were analyzed using the ImageJ software (Schindelin et al., 2015), including illumination correction, background subtraction, overlapping cells separation, edge artefacts elimination, and particle size optimization (based on the size difference between K562 and NK cells). The selected areas were then applied to the raw images for automatic cell counting.

2.13. Statistical Analysis

Each experiment was performed at least three times and statistical analysis when comparing two events at a time was conducted using a two-tailed Student's *t*-test. Multiple comparisons were performed using ANOVA test. Post-hoc Bonferroni correction was applied. Statistical probabilities (p) were expressed as * where $p < 0.05$; **, $p < 0.01$ and *** when $p < 0.001$.

3. Results

3.1. Differential Proteolytic Enzymes are Involved in the Secretion of the Tim-3 and Galectin-9 Complex in Human AML Cells

We investigated differential proteolytic shedding of free and galectin-9-bound Tim-3 from the surface of human AML cells as a possible mechanism for the secretion of these proteins. Firstly, we examined the medium used to culture THP-1 human AML cells with or without 16 h exposure to 100 nM phorbol 12-myristate 13-acetate (PMA) known to activate proteolytic shedding of Tim-3 (Moller-

Please cite this article as: Gonçalves Silva, I., et al., The Tim-3-galectin-9 Secretory Pathway is Involved in the Immune Escape of Human Acute Myeloid Leukemia Cells, EBioMedicine (2017), http://dx.doi.org/10.1016/j.ebiom.2017.07.018

Hackbarth et al., 2013). We then immunoprecipitated Tim-3 from the medium and extracted the precipitate as outlined in the Materials and Methods. Extracts were subjected to Western blot analysis followed by specific detection of galectin-9 and Tim-3. Specific galectin-9 bands appeared at around 32 kDa (molecular weight of galectin-9) as well as 52 kDa (Fig. 1A). Interestingly, the 52 kDa band was also detectable by anti-Tim-3 antibody (Fig. 1A), suggesting that this band corresponds to the unbroken Tim-3-galectin-9 complex. Furthermore, specific Tim-3 bands appeared at around 33 kDa (molecular weight of soluble Tim-3 – sTim-3) and around 20 kDa. This 20 kDa band is likely to be a fragment of Tim-3 shed together with galectin-9 being released from the complex during the Western blot procedure (Fig. 1A). This suggests that the Tim-3 protein fragment complexed with galectin-9 might be shed at different cleavage site(s). Interestingly, the amount of all the proteins detected was clearly higher in PMA-treated samples.

It has recently been found that Tim-3 can be shed from the cell surface by a disintegrin and metalloproteinase domain-containing proteins (ADAM) 10/17 (Moller-Hackbarth et al., 2013). We therefore investigated whether these proteases are associated with release of free Tim-3 and/or of the galectin-9-Tim-3 complex. We exposed THP-1 cells for 16 h to 100 nM PMA, after which the PMA-containing medium was removed and replaced with the same medium containing 100 μM GI254023X (ADAM 10 and 17 inhibitor) or 100 μM BB-94, a matrix metalloproteinase inhibitor. The cells were incubated for 4 h and levels of Tim-3 and galectin-9 were then measured in the culture medium by ELISA. We also measured soluble Tim-3-galectin-9 complex by capturing Tim-3 using a single-chain antibody and then detecting galectin-9 using a biotinylated anti-galectin-9 antibody. We found that PMA treatment significantly upregulated sTim-3 release as well as the release of galectin-9 (a similar increase was observed in the Tim-3-galectin-9 complex, Fig. 1B). GI254023X and BB-94 decreased PMA-induced sTim-3 release but did not affect the release of either galectin-9 or the Tim-3-galectin-9 complex (Fig. 1B), suggesting that this complex is differentially shed from the cell surface.

3.2. Protein Kinase C is Involved in the Activation of Tim-3 and Galectin-9 co-secretion by AML Cells

We considered the levels of Tim-3 and galectin-9 remaining in THP-1 cells following 16 h of exposure to specific PKC activator PMA. It was found that, despite the levels of released sTim-3, galectin-9 and Tim-3-galectin-9 complex were increased in PMA-treated cells, the levels of respective cell-associated proteins decreased (Fig. 2). Interestingly, a specific band in the range of 70 kDa detectable by both anti-Tim-3 and anti-galectin-9 antibodies was present in all the assays (Fig. 2). This molecular weight corresponds to a sum of those of uncleaved Tim-3 and galectin-9. This indicates that a complex between full Tim-3 and galectin-9 is first formed before undergoing shedding, which results in a release of its soluble form corresponding to the 52 kDa species, as described above. Our observations were confirmed by co-localization assays using confocal microscopy (Fig. 3). Following 24 h exposure to 100 nM PMA, paraformaldehyde-fixed non-permeabilized and methanol-permeabilized THP-1 human AML cells were investigated. We found that both galectin-9 and Tim-3 were present on the cell surface. In permeabilized cells there was clear evidence of co-localization

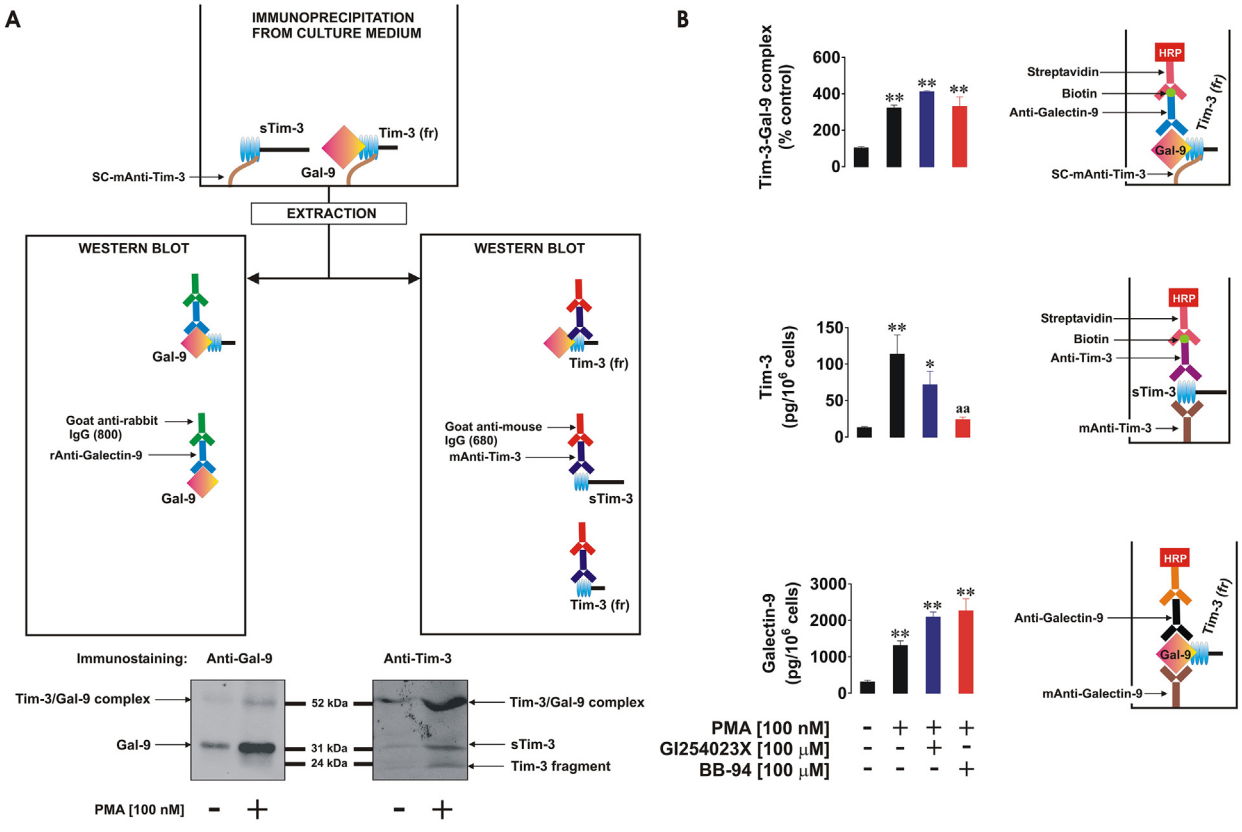

Fig. 1. Free and galectin-9-bound Tim-3 is shed differentially from the cell surface. THP-1 cells were exposed for 16 h to 100 nM PMA; medium was then exchanged for fresh PMA-free medium and cells exposed to the indicated concentrations of GI254023X (ADAM10/17 inhibitor) and BB-94 (matrix metalloproteinase inhibitor). Non treated THP-1 cells were incubated for 16 h after which medium was changed and cells incubated for further 4 h and used as a control. Western blot characterization of galectin-9 and Tim-3 variants (20 kDa fragment (Tim-3 (fr)) and 33 kDa (sTim-3)) was performed in medium collected after final 4 h of incubation of resting and PMA-pre-treated THP-1 cells as outlined in the Materials and Methods (A). All the samples were subjected to ELISA-based detection of galectin-9, soluble Tim-3 and Tim-3-galectin-9 complex (B). Images are from one experiment representative of six which gave similar results. Quantitative data represent mean values ± SEM of six independent experiments; $^{*}p < 0.05$; $^{**}p < 0.01$ vs. control.

Please cite this article as: Gonçalves Silva, I., et al., The Tim-3-galectin-9 Secretory Pathway is Involved in the Immune Escape of Human Acute Myeloid Leukemia Cells, EBioMedicine (2017), http://dx.doi.org/10.1016/j.ebiom.2017.07.018

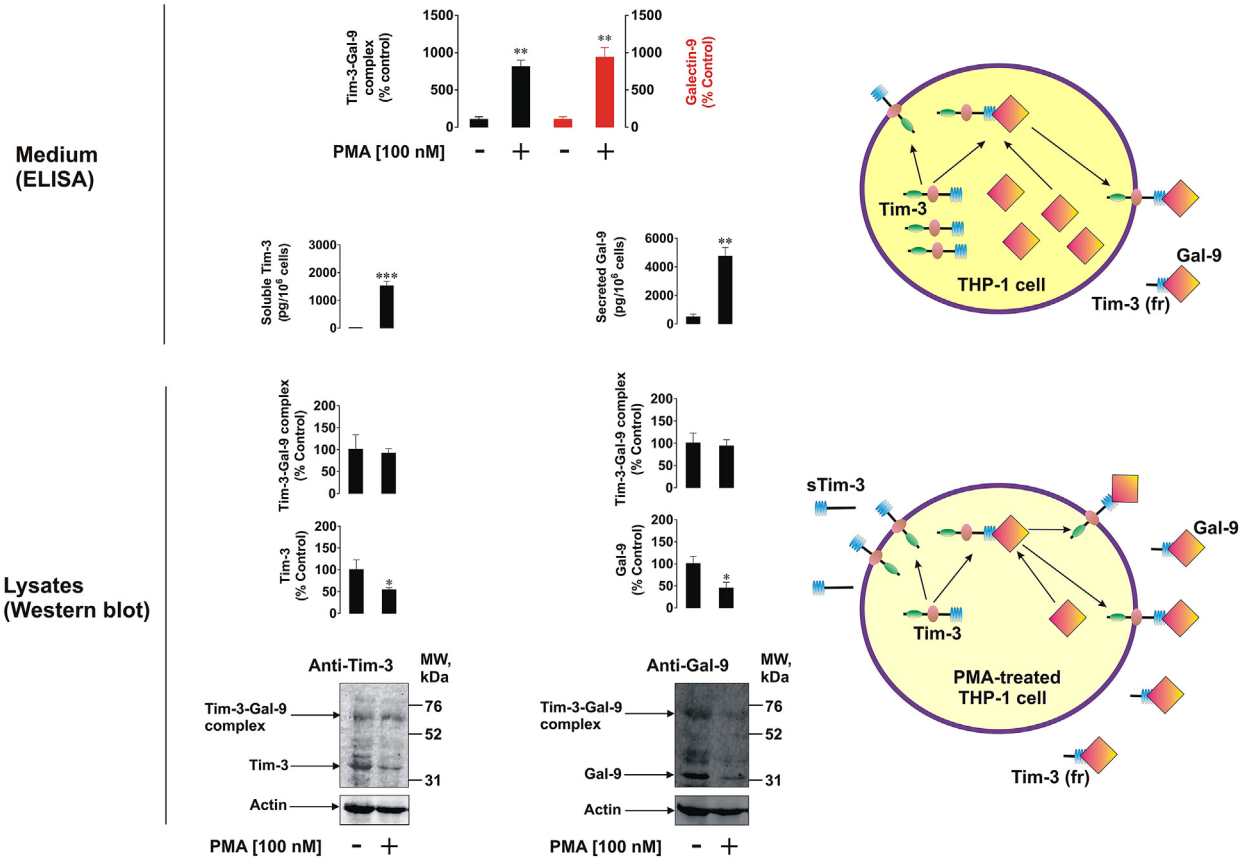

Fig. 2. PMA activates Tim-3 and galectin-9 production and release as well as generation of Tim-3-galectin-9 complex. THP-1 cells were treated with 100 nM PMA for 16 h. Non-treated THP-1 cells were used as a control. Cells were then harvested and galectin-9 as well as Tim-3 were analyzed in whole cell extracts by Western blot. Both proteins and Tim-3-galectin-9 complexes were analyzed by ELISA in the medium used to treat the cells. The bar diagram on the top shows the comparative analysis (expressed in % control) of galectin-9 and Tim-3-galectin-9 complex levels released by non-treated and PMA-treated THP-1 cells. Images are from one experiment representative of three which gave similar results. Quantitative data are the mean values ± SEM of three independent experiments; $^{*}p < 0.05$; $^{**}p < 0.01$; $^{***}p < 0.001$ vs. control.

of both proteins. These findings were confirmed using imaging flow cytometry (Supplementary Fig. 1). In non-permeabilized cells we saw sectors full of either Tim-3 or galectin-9, without substantial co-localization. Given that galectin-9 is soluble, it can remain on the cell surface only if it is bound to its receptor, Tim-3 (Fig. 3). Taken together our findings suggest that Tim-3 is either externalized on its own or acts as a trafficker for galectin-9 (which lacks the signal domain required for secretion and thus requires a trafficker). Given that PMA, a specific PKC activator, significantly increases Tim-3 and galectin-9 secretion, it is likely that PKC is involved in the Tim-3 and galectin-9 co-secretion process.

3.3. Levels of Soluble Tim-3 and Galectin-9 are Highly Increased in the Blood Plasma of AML Patients: Characterization of the Tim-3-galectin-9 Complex in Human Blood Plasma

We then sought to confirm our findings in primary samples collected from AML patients. We analyzed plasma samples from 98 AML patients versus healthy donors and found that galectin-9 and Tim-3 levels were strikingly increased in blood plasma of AML patients (Fig. 4A, B, E and F). Five randomly selected plasma samples from the group of studied AML patients and five from healthy donors were then subjected to detection

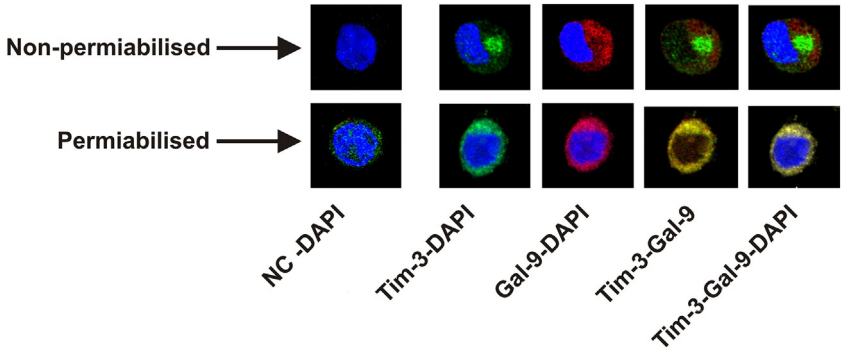

Fig. 3. Co-localization of Tim-3 and galectin-9 in PMA-activated THP-1 cells. Co-localization of Tim-3 and galectin-9 was analyzed in non-permeabilized and permeabilized THP-1 cells following 24 h of exposure to 100 nM PMA using confocal microscopy (see Materials and Methods for details). Images are from one experiment representative of six which gave similar results.

Please cite this article as: Gonçalves Silva, I., et al., The Tim-3-galectin-9 Secretory Pathway is Involved in the Immune Escape of Human Acute Myeloid Leukemia Cells, EBioMedicine (2017), http://dx.doi.org/10.1016/j.ebiom.2017.07.018

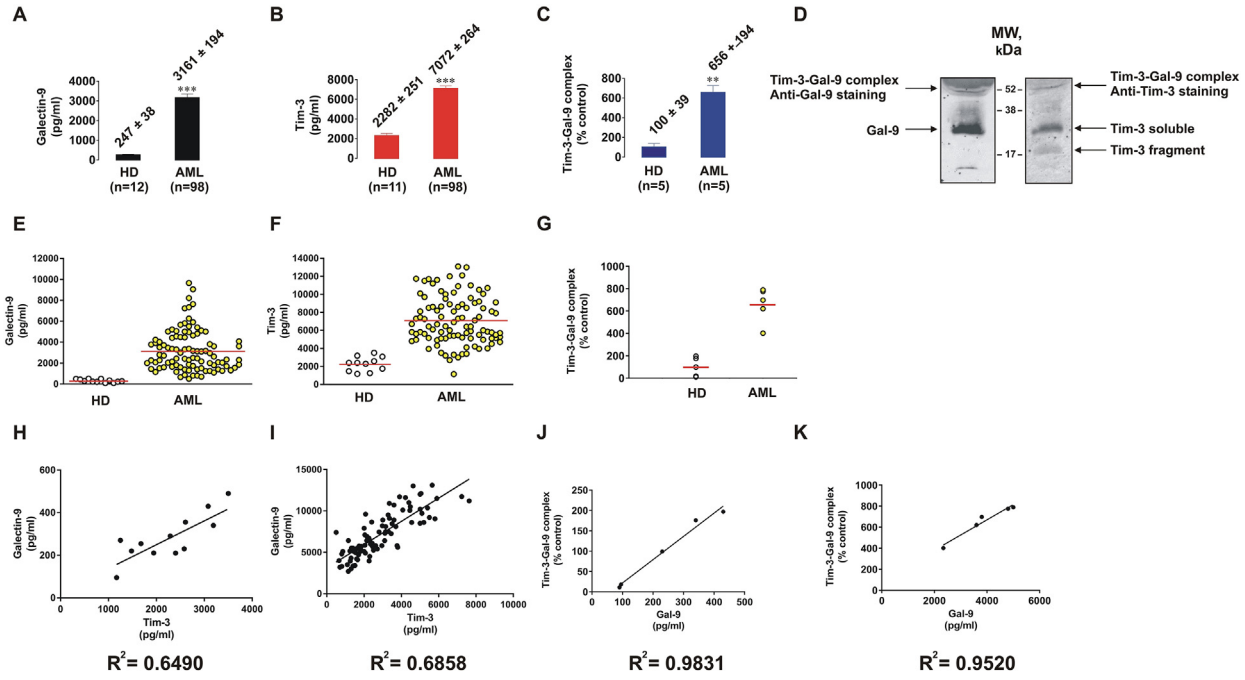

Fig. 4. Levels of galectin-9 and soluble Tim-3 are highly increased in blood plasma of AML patients. Galectin-9 and Tim-3 were measured by ELISA in blood plasma obtained from healthy donors and AML patients (A, B, E and F). The levels of Tim-3-galectin-9 complex were measured by ELISA in blood plasma of five randomly picked healthy donors and AML patients (C and G). Tim-3 and galectin-9 were characterized by Western blot in blood plasma from five randomly chosen AML patients (D). Correlations between Tim-3 and galectin-9 as well as between galectin-9 and Tim-3-galectin-9 complex was then determined (H, I, J and K). Images are from one experiment representative of five which gave similar results. Quantitative data represent mean values ± SEM of three independent experiments; $^{*}p < 0.05$; $^{**}p < 0.01$; $^{***}p < 0.001$ vs. control.

of Tim-3-galectin-9 complex by ELISA as described above. The level of increase in Tim-3-galectin-9 complex in AML samples was similar to that of galectin-9 (Fig. 4C and G). We then randomly chose five plasma samples from the group of studied AML patients and analyzed Tim-3 and galectin-9 levels by Western blot (Fig. 4D). Prior to loading onto the SDS-PAGE, samples were sonicated and boiled for 5 min at 95 °C. We found that sTim-3 and galectin-9 were clearly detectable. We could also see a clear band (probably representing the soluble form of the Tim-3-galectin-9 complex) at around 52 kDa (detectable by both anti-Tim-3 and anti-galectin-9 antibodies). This suggests that the complex released by THP-1 cells (Fig. 1) and the one found in blood plasma is unlikely to be formed after secretion. If this had been the case, its molecular weight would have been around 65 kDa (33 kDa for sTim-3 and 32 kDa for galectin-9) rather than 52 kDa. A specific band was also detectable at around 20 kDa (Fig. 4D). These results are in line with those obtained for soluble forms of Tim-3, galectin-9 and Tim-3-galectin-9 complex released by THP-1 cells confirming that sTim-3 and Tim-3 complexed with galectin-9 are likely to be differentially shed from plasma membranes of AML cells. Interestingly, there is a clear evidence of a correlation between Tim-3 and galectin-9 levels in the plasma of both healthy donors and AML patients and these correlation levels were very similar to each other (Fig. 4H and I) suggesting a co-release of both proteins in both cohorts.

3.4. Tim-3 Binding Alters the Conformation of Galectin-9

In order to assess the biophysical properties of Tim-3, galectin-9 and the Tim-3-galectin-9 complex we investigated them using synchrotron radiation circular dichroism (SRCD) spectroscopy at Diamond Light Source (Beam Line 23, Supplementary Fig. 2). Structural organization of Tim-3 and galectin-9 as well as their interaction are schematically presented in the Fig. 5A. Galectin-9 interacts with non-glycosylated Tim-3 with nanomolar affinity (Kd = 2.8×10^{-8} M); the binding can be further strengthened by interaction of galectin-9 with glycosylated Tim-3 (Prokhorov et al., 2015). Indeed, the complex is detectable by Western blot, which means that interaction between a lectin and sugar is taking place. SRCD spectroscopy was also performed on galectin-9 and Tim-3 mixed to a stoichiometry of 1:1 molar ratio (Fig. 5B). Galectin-9 when mixed with Tim-3 showed a CD spectrum significantly different from the simulated spectrum indicating that the interaction of galectin-9 with Tim-3 causes significant conformational change of the proteins with a clear increase in β-strand component. Based on the above, one might speculate that Tim-3 binding could alter the conformation of galectin-9, resulting in increased ability to interact with receptors in target cells. Since galectin-9 is a tandem protein with two sugar binding domains, one domain could bind Tim-3 (or other proteins) and leave the other domain open for interaction with a receptor molecule associated with the plasma membrane of a target cell (for example membrane associated Tim-3).

3.5. Latrophilin 1, Protein Kinase C and mTOR-Dependent Translation Play a Crucial Role in Tim-3 and Galectin-9 Production and Secretion

LPHN1 mRNA was found in primary human CD34-positive stem cells (Maiga et al., 2016). We were able to detect LPHN1 protein in them (at a slightly higher molecular weight than in THP-1 cells (around 140 kDa)), while in THP-1 it is detectable at 130 kDa (Supplementary Fig. 3) as well as in primary AML cells (Sumbayev et al., 2016). No Tim-3 or galectin-9 protein expression was detectable in primary human CD34-positive stem cells (Supplementary Fig. 3).

For this experimental set-up we used THP-1 cells and exposed them to 100 nM PMA or 250 pM α-latrotoxin (LTX, a highly specific and potent ligand of LPHN1 (Sumbayev et al., 2016)). We found that both PMA and LTX downregulated intracellular Tim-3 and galectin-9 levels (though not significantly) and significantly increased activating phosphorylation of the mammalian target of rapamycin (mTOR) at S2448 (Fig. 6A and B). One hour pre-treatment of THP-1 cells with 70 nM Gö6983 (PKCα inhibitor) before exposure to PMA or LTX led to attenuation of stimulus-induced mTOR activation and downregulation of intracellular Tim-3 and galectin-9 levels. Interestingly, in the cells exposed just to Gö6983, phospho-S2448 mTOR and intracellular Tim-3/galectin-9 levels were not different

Please cite this article as: Gonçalves Silva, I., et al., The Tim-3-galectin-9 Secretory Pathway is Involved in the Immune Escape of Human Acute Myeloid Leukemia Cells, EBioMedicine (2017), http://dx.doi.org/10.1016/j.ebiom.2017.07.018

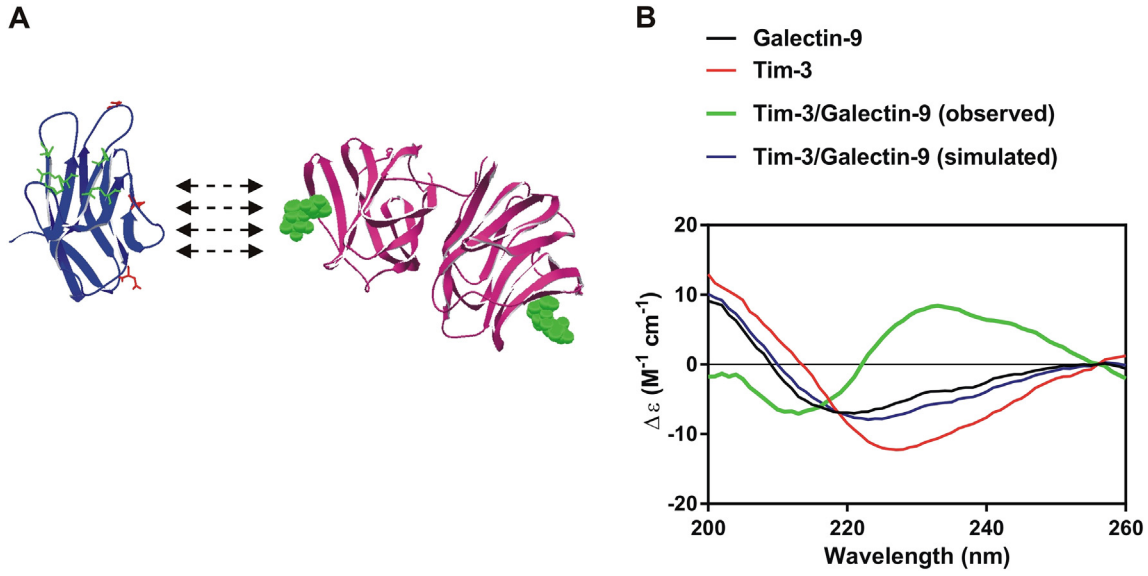

Fig. 5. Interaction of Tim-3 with galectin-9 leads to major conformational changes increasing solubility of the protein complex. (A) The schematic structural models of Tim-3 extracellular domain (left) and galectin-9 (right). In the Tim-3 structure, amino acid residues involved in galectin-9-independent binding are highlighted in green. Residues, which are potential targets for glycosylation, are highlighted in red. In galectin-9, sugar molecules, which could potentially bind the protein, located close to the carbohydrate binding sites are shown in green. (B) The SRCD spectroscopy of Tim-3, galectin-9 and Tim-3-galectin-9 interaction (both simulated and real curves are presented). (For interpretation of the references to color in this figure legend, the reader is referred to the web version of this article.)

from the control. Both PMA and LTX highly upregulated release of both sTim-3 and galectin-9 from THP-1 cells. Gö6983 completely attenuated this increase in both cases, but did not change basic levels of Tim-3 and galectin-9 secretion, which suggests that basic (background) release of galectin-9 and Tim-3 does not depend on PKCα (Fig. 6D).

In summary, both PMA and LTX induce production of both Tim-3 and galectin-9 in THP-1 cells. We confirmed that THP-1 cells express Gαq (Supplementary Fig. 4A) and PMA as well as LTX induce highly significant upregulation of PKCα kinase activity (Supplementary Fig. 4B). Pre-treatment of THP-1 cells with 10 μM AZD2014 (a highly specific mTOR inhibitor) before exposure to PMA or LTX reduced intracellular Tim-3 and galectin-9 levels as well as release of both proteins (Fig. 6C and D). This indicates that PMA or LTX-induced translation of both proteins depends on the mTOR pathway. Importantly, the solvents used to dissolve pharmacological inhibitors had no effect on any of the studied protein levels or their secretion (data not shown).

These results were validated using primary human AML cells. For this purpose we exposed primary human AML mononuclear blasts AML-PB001F for 24 h to LTX followed by detection of secreted galectin-9 and Tim-3. We found that AML-PB0011F expressed LPHN1 and the secreted levels of both proteins were significantly increased in LTX-treated AML cells (Supplementary Fig. 5) confirming the findings obtained in THP-1 cells.

To confirm the physiological role of LPHN1 in galectin-9 release we exposed THP-1 cells to FLRT3, which is one of physiological ligands of LPHN1 (Boucard et al., 2014). We found that 10 nM FLRT3 induced significant upregulation of galectin-9 and sTim-3 release (Fig. 7A, a scheme of the experiment is presented in Supplementary Fig. 6A); it also upregulated PKCα activity in THP-1 cells (Supplementary Fig. 4B). To confirm

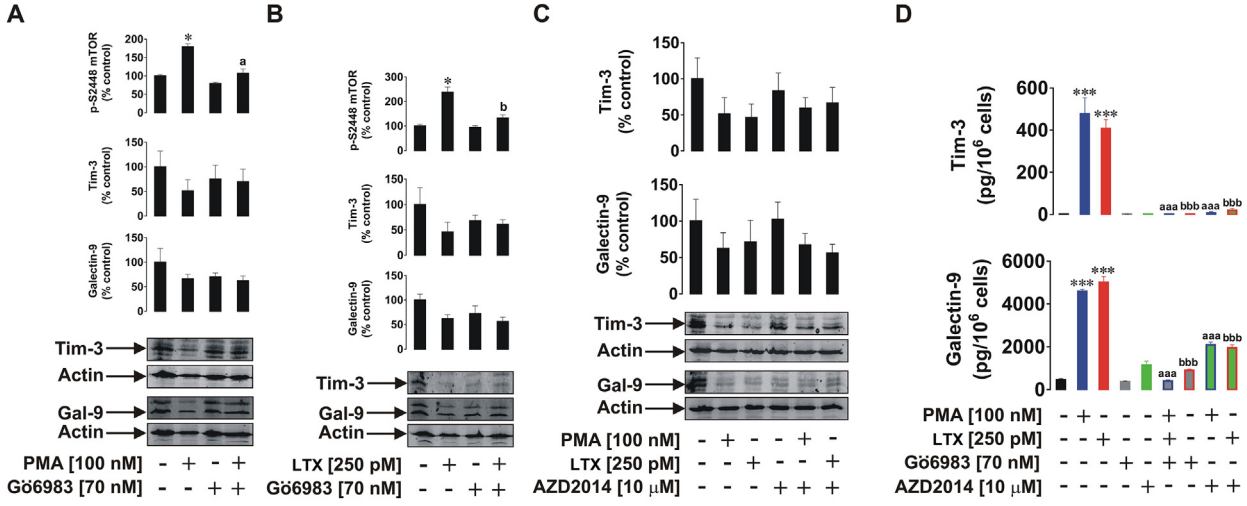

Fig. 6. LPHN1, PKCα and mTOR pathways are involved in Tim-3 and galectin-9 production and secretion in AML cells. THP-1 cells were exposed to the indicated concentrations of PMA or LTX for 16 h with or without 1 h pre-treatment with the PKCα inhibitor Gö6983 (A, B, D) or the mTOR inhibitor AZD2014 (C, D). Cellular levels of Tim-3 and galectin-9 were analyzed by Western blot. Released Tim-3 and galectin-9 were detected by ELISA. Images are from one experiment representative of three which gave similar results. Quantitative data are the mean values ± SEM of three independent experiments; $^{*}p < 0.05$; $^{**}p < 0.01$; $^{***}p < 0.001$ vs. control. Symbols "a" or "b" are used instead of "*" to indicate differences vs. PMA and LTX-treated cells, respectively.

Please cite this article as: Gonçalves Silva, I., et al., The Tim-3-galectin-9 Secretory Pathway is Involved in the Immune Escape of Human Acute Myeloid Leukemia Cells, EBioMedicine (2017), http://dx.doi.org/10.1016/j.ebiom.2017.07.018

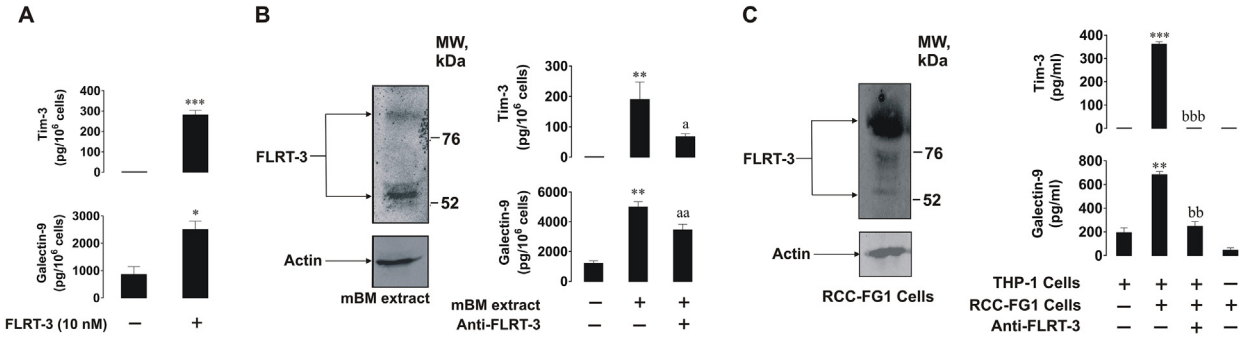

Fig. 7. FLRT3, a physiological ligand of LPHN1, induces galectin-9 and Tim-3 secretion. (A) THP-1 cells were exposed for 16 h to 10 nM extracellular domain of human recombinant FLRT3 followed by measurement of released Tim-3 and galectin-9 by ELISA. (B) THP-1 cells were exposed to mouse bone marrow (mBM) extracts for 16 h with or without 1 h pre-treatment with 5 μg/ml anti-FLRT3 antibody. The presence of FLRT3 in mBM extracts was confirmed by Western blot analysis. Secreted Tim-3 and galectin-9 were measured by ELISA. (C, left) RCC-FG1 cells express FLRT3 as confirmed by Western blotting. (C, right) RCC-FG1 cells were co-cultured with THP-1 cells at a ratio of 1 THP-1:2 RCC-FG1 with or without 1 h pre-treatment with 5 μg/ml FLRT3 neutralizing antibody. Secreted galectin-9 and Tim-3 were measured by ELISA. Images are from one experiment representative of three which gave similar results. Quantitative data depict mean values ± SEM of three independent experiments; $^{*}p < 0.05$; $^{**}p < 0.01$; $^{***}p < 0.001$ vs. control. Symbols "a" or "b" are used instead of "*" to indicate differences vs. cells treated with mBM extracts or co-cultured with RCC-FG1 cells, respectively.

that this effect was physiologically relevant, we exposed THP-1 cells for 16 h to mouse bone marrow (mBM) extracts (10 μg protein/ml, which contain FLRT3, Fig. 7B, a scheme of the experiment is presented in Supplementary Fig. 6B) obtained as outlined in the Materials and Methods. Treatments were conducted with or without 1 h pre-treatment with 5 μg/ml FLRT3 neutralizing mouse antibody. We found that mBM extracts significantly upregulated galectin-9 and sTim-3 secretion in THP-1 cells. FLRT3 neutralizing mouse antibody reduced the effects of mBM extracts but did not block them (Fig. 7B). This means that BM contains several activators of galectin-9 secretion in AML cells. Finally, we co-cultured THP-1 cells with RCC-FG1 renal carcinoma cells (which are highly adherent) in the ratio 1 THP-1:2 RCC-FG1. RCC-FG1 cells express high levels of FLRT3 and release almost undetectable amounts of galectin-9 (Fig. 7C, a scheme of the experiment is presented in Supplementary Fig. 6C). Cells were kept together for 16 h in the absence or presence of 5 μg/ml FLRT3 neutralizing antibody and then galectin-9 and sTim-3 secretion levels were analyzed. We found that the presence of RCC-FG1 cells significantly increased galectin-9 and sTim-3 release and FLRT3 neutralization attenuated these effects. The presence of RCC-FG1 cells significantly upregulated PKCα activity, an effect that was also attenuated by neutralization of the FLRT3 (Supplementary Fig. 4C). These results suggest that FLRT3 stimulates the release of galectin-9 from AML cells.

3.6. Galectin-9 and sTim-3 Attenuate AML Cell Killing Activity of NK Cells

Recent evidence suggested that galectin-9 (either soluble or cell surface associated) can interact with Tim-3 or possibly other receptors on

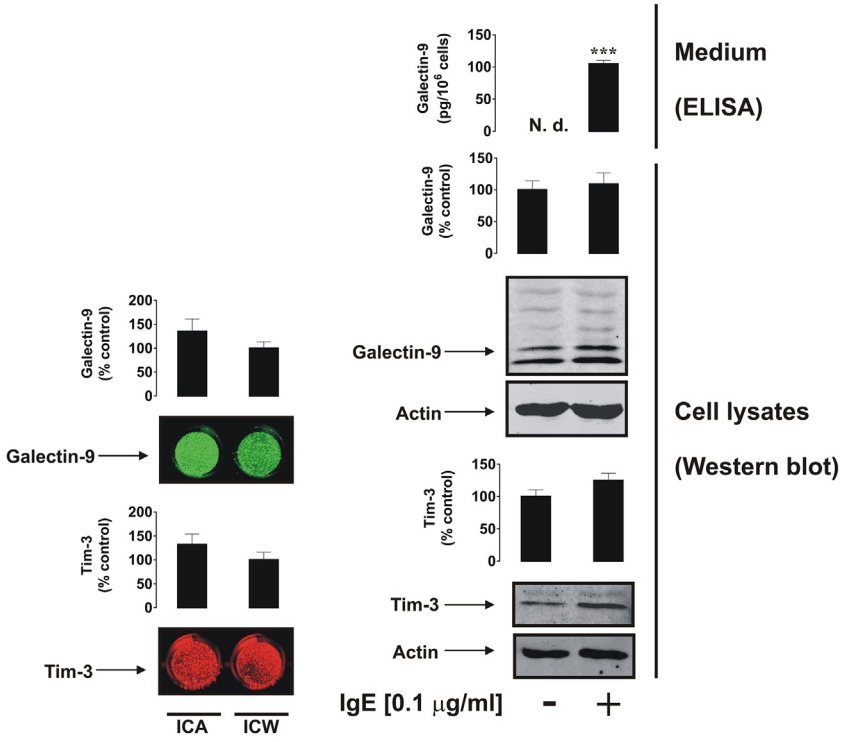

Fig. 8. LAD2 cells express and externalize Tim-3 and galectin-9. Left panel: surface-based and total Tim-3 and galectin-9 were measured in LAD2 human mast cell sarcoma cells using LI-COR in cell assay (ICA, non-permeabilized cells) and in cell Western (ICW, permeabilized cells). Right panel: protein levels of Tim-3 and galectin-9 were measured in resting and IgE-sensitized LAD2 cells by Western blot. Galectin-9 release was characterized using ELISA. Images are from one experiment representative of three which gave similar results. Quantitative data show mean values ± SEM of three independent experiments; $^{***}p < 0.001$ vs. control.

cytotoxic lymphoid cells including NK cells and cytotoxic T cells (Gleason et al., 2012). It may be proposed that Tim-3-galectin-9 interaction is involved in the creation of immunological synapses between target cells and cytotoxic lymphoid cells. To investigate this we used LAD2 human mast cell sarcoma cells kindly provided by Prof. Metcalfe and Dr. Kirshenbaum (NAID, NIH, USA; Kirshenbaum et al., 2003). These cells express both Tim-3 and galectin-9 with both proteins located mostly on the cell surface (Fig. 8) and not rapidly shed. This can thus be used to visualize the formation of immunological synapses between the two cell types. They also express high affinity IgE receptors (FcεRI) which are not expressed by NK cells and thus can be used to distinguish between the two cell types.

Resting LAD2 cells do not release detectable amounts of galectin-9 and sensitization with IgE (which was used in order to label the cells for visualization) does not augment galectin-9 secretion considerably (Fig. 8). We therefore immobilized primary human NK cells isolated from buffy coats of human blood on ELISA plates as outlined in Materials and Methods. NK cells express Tim-3 (several glycosylation variants, Supplementary Fig. 7) but do not produce detectable amounts of galectin-9 protein. We applied IgE-sensitized LAD2 cells (Sumbayev et al., 2012) to the NK cells at a ratio of 1:1 with or without 15 min pre-incubation with galectin-9 neutralizing antibody. Isotype control antibody was also used instead of galectin-9 antibody to rule out the IgG effect. LAD2 cells were then flagged using mouse IgM anti-IgE followed by visualization using anti-mouse LI-COR secondary antibody (which recognizes IgM, see Materials and Methods for further details). We found that LAD2 cells were binding to NK cells and the presence of galectin-9 neutralizing antibody (but not isotype control antibody) abrogated this effect (Fig. 9, a scheme of the experiment is presented in Supplementary Fig. 8). These results confirm that galectin-9 produced by LAD2 cells participates in their interactions with NK cells. Furthermore, abrogation of the effect by anti-galectin-9 antibodies may indicate that the Tim-3-galectin-9 interaction is the only pathway through which these cells could interact. This is most likely a result of IgE sensitization of LAD2 cells which highly increases the presence of galectin-9 on their surface.

We then used K562 chronic myeloid leukemia cells which do not release detectable amounts of galectin-9 (as confirmed by ELISA). K562 cells were exposed to PMA for 24 h in 96 well Maxisorp plates. Medium was replaced with PMA-free RPMI-1640 medium containing isolated primary human NK cells at a ratio of 1 K562:2 NK in the absence or presence of 5 ng/ml human recombinant galectin-9. Cells were co-incubated for 16 h and their viability was then assessed using an MTS test. We found that the presence of NK cells significantly reduced the viability of K562 cells however, the presence of galectin-9 attenuated K562 killing effect (Fig. 10A). Viability of NK cells was not affected in any of the cases (Fig. 10A). Interestingly, the cytotoxic attack by NK cells also led to a dramatic change in the behavior of K562 cells, causing their massive aggregation. Using phase contrast microscopy, we determined the effect of galectin-9 on cell aggregation in individual or combined K562 and NK cell cultures. In the absence of galectin-9, there was clear evidence of K562 cells aggregating in the presence of NK cells (Fig. 10B). Galectin-9, in a dose-dependent manner, decreased the aggregation of K562 cells by NK cells, such that no K562 cell aggregation was detectable in the presence of 5 ng/ml galectin-9 (Fig. 10C). Galectin-9 itself had no visible effect on either of the two cell types alone. Thus, galectin-9 clearly protects myeloid leukemia cells from being killed by NK cells.

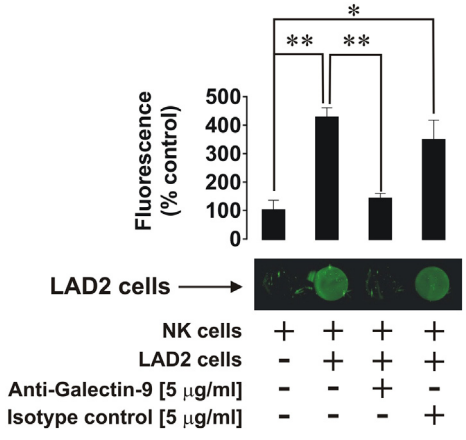

Fig. 9. Galectin-9 participates in the formation of an "immunological synapse" between NK cells and LAD2 cells. Primary human NK cells were immobilized on the surface of Maxisorp plates. Cells were then co-incubated for 30 min with LAD2 cells with or without 30 min pre-treatment of LAD2 cells with 5 μg/ml galectin-9 neutralizing antibody (or the same amount of isotype control antibody). LAD2 cells were then visualized using LI-COR assay as outlined in Materials and Methods. Images are from one experiment representative of five which gave similar results. Quantitative data represent mean values ± SEM of five independent experiments; $^{*}p < 0.05$; $^{**}p < 0.01$.

We then investigated the interactions between AML THP-1 cells and primary human NK cells. THP-1 cells were exposed to 100 nM PMA for 16 h. The medium was then replaced with PMA-free medium containing NK cells at a ratio of 2 NK cells:1 THP-1 cells and left for 6 h in the absence or presence of 5 μg/ml galectin-9-neutralizing antibody. Tim-3 and galectin-9 were then measured in the NK cells by Western blot analysis, and viability of THP-1 cells, activities of granzyme B, caspase-3 and galectin-9 release were monitored. We found that THP-1 cell viability was reduced when galectin-9 was neutralized (Fig. 11). This was in line with increased caspase-3 activity and granzyme B activities. Galectin-9 release was not affected (Fig. 11, galectin-9 bound to neutralizing antibody is detectable in our system). We confirmed that resting NK cells did not produce detectable amounts of galectin-9. However, this protein on its own, and in the form of unbroken Tim-3-galectin-9 complex, was detectable in NK cells co-cultured with THP-1 cells and was reduced in the presence of galectin-9 neutralizing antibody. This suggests that THP-1 cells were the source of galectin-9, which was most likely bound to Tim-3 on the surface of NK cells, preventing the delivery of NK cell-derived granzyme B into THP-1 cells and inhibiting the caspase-3-dependent apoptotic pathway.

Recently, a possible reciprocal link between levels of sTim-3 and IL-2, a cytokine, which activates cytotoxic activity of NK cells and T cells, was reported (Geng et al., 2006). We also found that in the plasma of healthy donors the levels of sTim-3 were significantly lower compared to AML patients (Fig. 4) whereas the levels of IL-2 were significantly higher (Fig. 12A and B). To investigate a possible direct influence of sTim-3, we exposed Jurkat T cells (resting Jurkat T cells produce detectable amounts of IL-2) to increasing concentrations of Tim-3 for 24 h. We found a striking sTim-3 concentration-dependent and significant reduction of IL-2 release from Jurkat T cells. This indicates that sTim-3 is capable of binding a target protein (or a group of target proteins) and reducing IL-2 production thus preventing induction of NK cell and T lymphocyte anti-cancer activities.

Taken together, our results demonstrate a pathobiochemical pathway in AML cells. It is associated with activation of PKCα by LPHN1 (or any other receptors with similar activity) leading to the expression and exocytosis of sTim-3 and galectin-9, which prevent the activation of cytotoxic lymphocytes and impair their malignant cell killing activity.

4. Discussion

AML is a malignancy affecting bone marrow and blood and is a severe, and often fatal, systemic disease. AML cells escape host immune attack involving NK and cytotoxic T cells by impairing their activity (Golden-Mason et al., 2013; Kikushige et al., 2015; Gonçalves Silva et al., 2016). However, the biochemical mechanisms underlying the immune escape of malignant white blood cells remain unclear. Recently, it was shown that AML cells express high levels of the immune receptor Tim-3 and release galectin-9 which impairs the activity of NK cells and cytotoxic T cells (Gonçalves Silva et al., 2016). We have also suggested that Tim-3, as a membrane associated glycoprotein, might act as a trafficker for galectin-9 (Gonçalves Silva et al., 2016). As for all galectins,

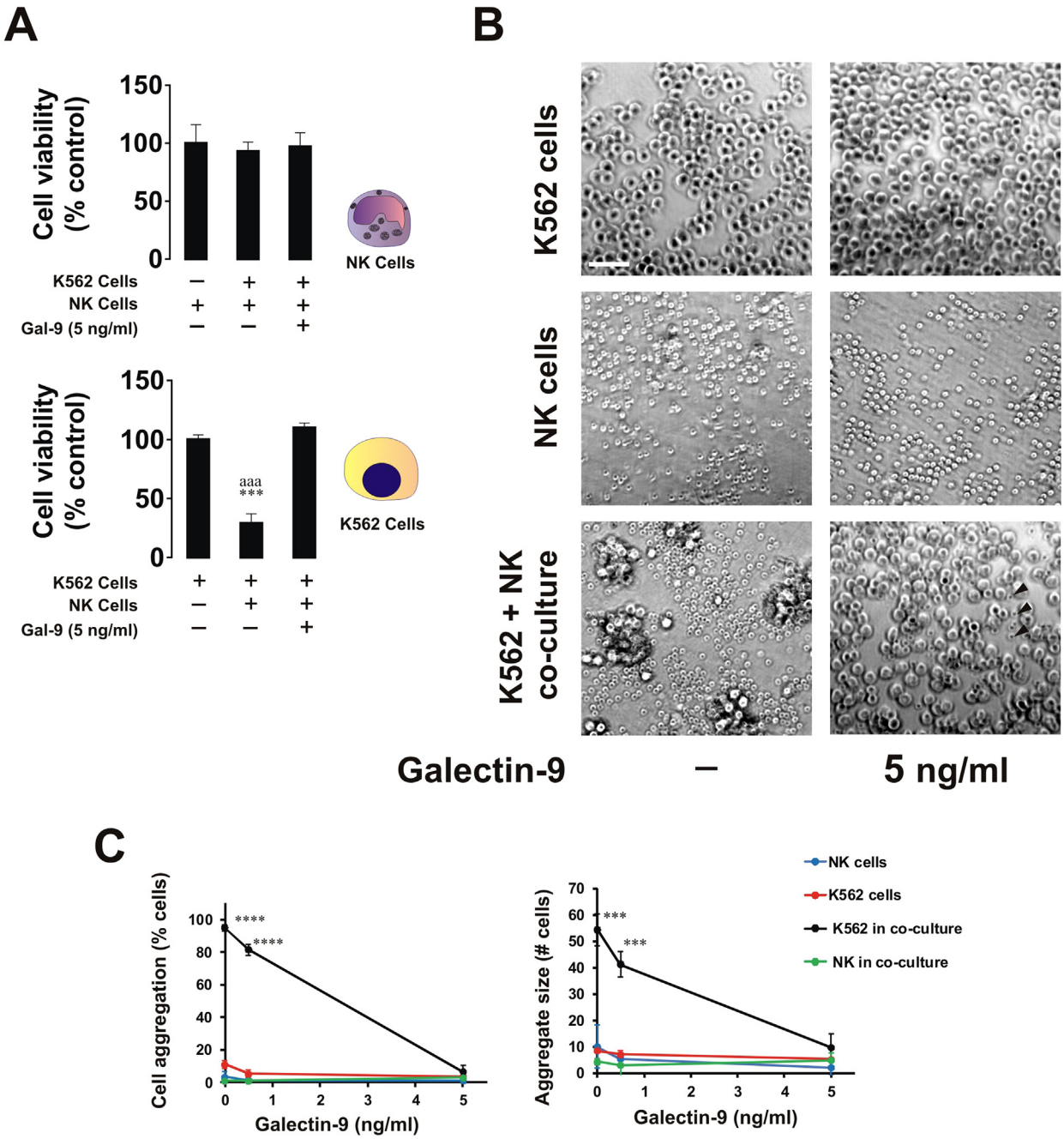

Fig. 10. Galectin-9 protects myeloid leukemia K562 cells from being killed by primary human NK cells. (A) K562 cells were co-cultured for 16 h with primary human NK cells (at a ratio of 1 K562:2 NK) in the absence or presence of 5 ng/ml galectin-9. Viability of K562 and NK cells was then measured using an MTS test. Images are from one experiment representative of three which gave similar results. Quantitative data represent mean values ± SEM of three independent experiments; ***$p < 0.001$ vs. control. (B) K562 cells were co-cultured for 16 h with primary human NK cells (at a K562:NK ratio of 1:2) in the presence of different concentrations of galectin-9 (0–5 ng/ml). Cells were imaged using phase-contrast microscopy. The images are from one representative experiment of six ($n = 6$), which gave similar results. Scale bar (the same for all images), 50 μm. (C) The NK cell-induced aggregation of K562 cells was quantified as a function of galectin-9 concentration. Left panel: percent of cells found in aggregates in individual cultures and in co-culture. Right panel: the size of cell aggregates in individual cultures and in co-culture. The data represent the mean values ± SD of six independent experiments; *, $p < 0.05$; **, $p < 0.01$; ****, $p < 0.0001$.

galectin-9 is synthesized on free ribosomes and since it lacks the signal domain required for secretion it thus needs a trafficker in order to be released (Delacour et al., 2009). When on the cell surface, Tim-3 is known to be shed by ADAM 10/17 proteolytic enzymes thus producing sTim-3, the function of which remains unknown (Moller-Hackbarth et al., 2013). We found, that Tim-3 could be shed in its free form as well as in complex with galectin-9; however, differential shedding is taking place. The Tim-3 fragment in the complex is about 20 kDa molecular weight, while sTim-3 is around 33 kDa. SRCD analysis of the complex suggests that the interaction between Tim-3 and galectin-9 proteins leads to major conformational change, possibly increasing the ability of galectin-9 to interact with the target proteins. Since galectin-9 is a tandem protein containing two domains (Delacour et al., 2009), one of them might be interacting with Tim-3, while the other one could bind to a target receptor molecule, for example another molecule of Tim-3 associated with the plasma membrane of the target cell (Nagae et al., 2006). This may explain the high efficiency of galectin-9 in triggering Tim-3 on NK cells, which do not express galectin-9 and thus contain unoccupied Tim-3 on their surface.

Since we can observe the Tim-3-galectin-9 complex on Western blots following denaturing SDS-gel electrophoresis (Figs. 1, 2 and 4; ~52 kDa soluble form and ~70 kDa cell-derived form), it is likely that

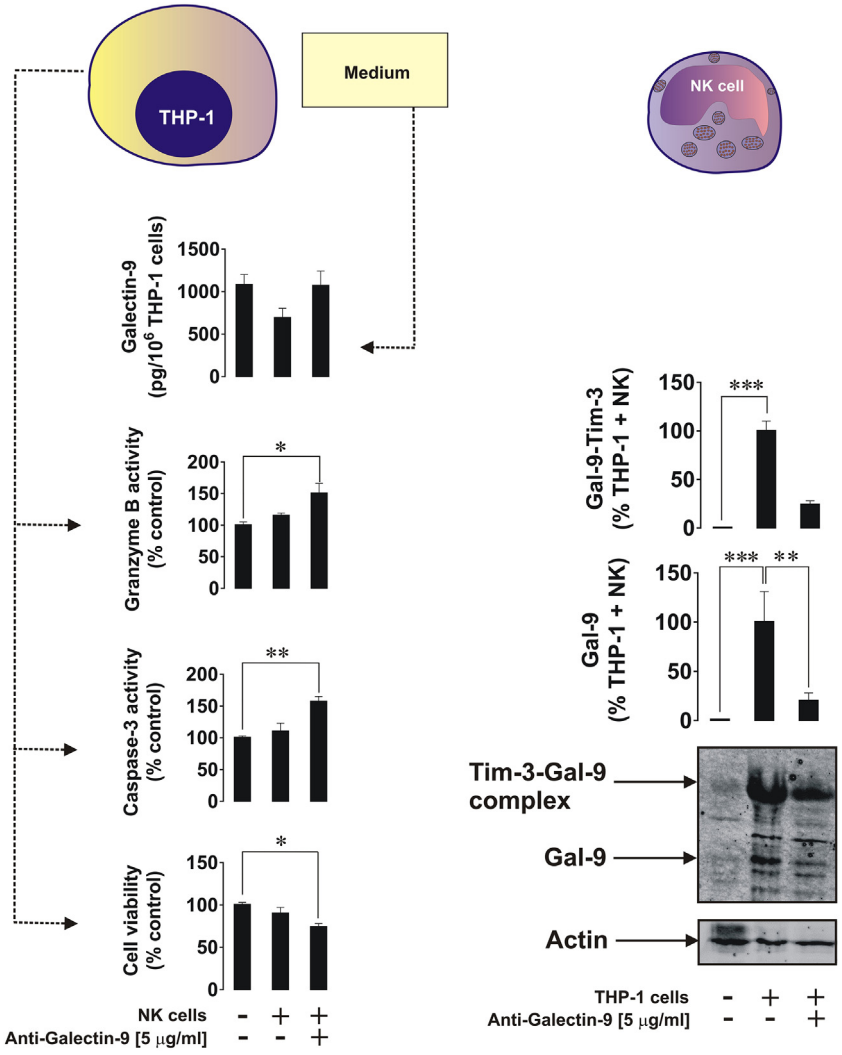

Fig. 11. Cell-derived galectin-9 attenuates AML cell killing activity of primary human NK cells. THP-1 cells were co-incubated with primary human NK cells (ratio – 1 THP-1:2 NK) for 6 h followed by detection of THP-1 cell viability by the MTS test, measurement of activities of granzyme B and caspase 3 in THP-1 cell lysates and released galectin-9 (left panel). Galectin-9 levels from NK cells were determined by Western blot (right panel). Images are from one experiment representative of three which gave similar results. Quantitative data show mean values ± SEM of three independent experiments; $^{*}p < 0.05$; $^{**}p < 0.01$; $^{***}p < 0.001$ vs control.

the binding between proteins is further strengthened by the interaction of galectin-9 with Tim-3-associated glycosides. Interestingly, the complex is detectable by Western blot with both anti-Tim-3 and anti-galectin-9 antibodies. However, when these antibodies are sequentially applied to the same blot, the second antibody fails to detect the respective protein in the same band (unless the first antibody is stripped off), due to steric hindrance. This effect explains why Tim-3 located on the cell surface and covered by galectin-9 cannot be co-stained by the antibody in confocal microscopy co-localization analysis (Fig. 3). Another point supporting this conclusion is that there was also clear evidence of co-localization of Tim-3 and galectin-9 in permiabilized THP-1 cells upon exposure to PMA (Fig. 3, Supplementary Fig. 1).

Previously it was reported that the release of both Tim-3 and galectin-9 depends on PKCα and proteolysis (Chabot et al., 2002). Our

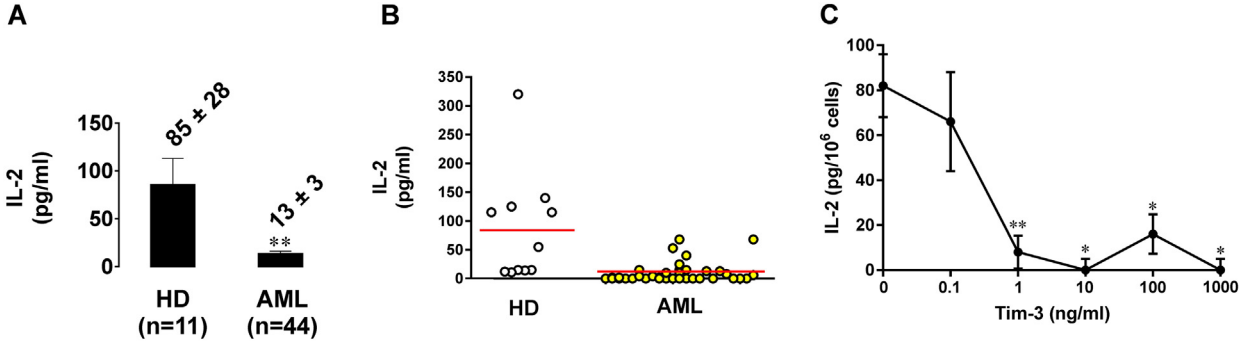

Fig. 12. Soluble Tim-3 attenuates IL-2 release. (A and B) IL-2 levels were measured by ELISA in blood serum of healthy donors and AML patients. (C) Jurkat T cells were exposed to the increasing concentrations of Tim-3 for 24 h followed by detection of secreted IL-2 by ELISA. Data show mean values ± SEM of three independent experiments; $^{*}p < 0.05$; $^{**}p < 0.01$.

Please cite this article as: Gonçalves Silva, I., et al., The Tim-3-galectin-9 Secretory Pathway is Involved in the Immune Escape of Human Acute Myeloid Leukemia Cells, EBioMedicine (2017), http://dx.doi.org/10.1016/j.ebiom.2017.07.018

results confirmed these findings. PMA treatments induced PKCα activation, which activated exocytosis of Tim-3 and galectin-9 as well as their mTOR-dependent production in THP-1 AML cells (Fig. 6).

Interestingly, natural and exogenous ligands of LPHN1, a G-protein coupled neuronal receptor expressed also in CD34-positive human stem cells (Supplementary Fig. 3) and AML cells but not healthy white blood cells, activated the PKCα pathway. They also induced both mTOR-dependent translation of Tim-3 and galectin-9 as well as their exocytosis. The effect was observed in THP-1 and primary human AML blasts. PKCα is known to provoke agglomeration of SNARE complex responsible for exocytosis (Stockli et al., 2011; Morgan et al., 2005). Since FLRT3, one of natural ligands of LPHN1, is present in bone marrow (Fig. 7) it might explain how LPHN1 causes PKCα activation. Interestingly, constitutively active PKCα in malignant primary AML cells correlates with a very poor prognosis and high mortality rate of patients (Kurinna et al., 2006). This suggests that AML cells constantly release high levels of Tim-3 and galectin-9. Bone marrow also expresses other PKCα-activating proteins. When we exposed THP-1 cells to mouse bone marrow extracts, galectin-9 release was significantly higher compared to resting THP-1 cells. FLRT3 neutralizing antibody significantly reduced but did not abolish FLRT3 induced PKCα-dependent galectin-9 release. This suggests that galectin-9 and Tim-3 are synthesized and exocytozed by AML cells in a PKCα and mTOR-dependent manner, using available plasma membrane-associated PKCα activating receptors (for example LPHN1) to induce the whole pathway.

Galectin-9 prevents the delivery of granzyme B into AML cells (this is a perforin and mannose-6-phosphate receptor-dependent process (Supplementary Fig. 9)). Inside AML cells granzyme B performs cleavage of the protein Bid into tBid, thus inducing mitochondrial dysfunction and cytochrome C release followed by caspase 3 activation. Proteolytic activation of caspase 3, in addition to the classic pathway, might also be directly catalyzed by granzyme B (Lee et al., 2014). Our results with galectin-9 confirmed this concept (Fig. 11). Recently it was reported that galectin-9 induces interferon-gamma (IFN-γ) release from NK cells (Gleason et al., 2012). IFN-γ interacts with AML cells inducing the activity of indoleamine 2,3-dioxygenase (IDO1), an enzyme which converts L-tryptophan into formyl-L-kynurenine, which is then converted into L-kynurenine and released (Corm et al., 2009; Folgiero

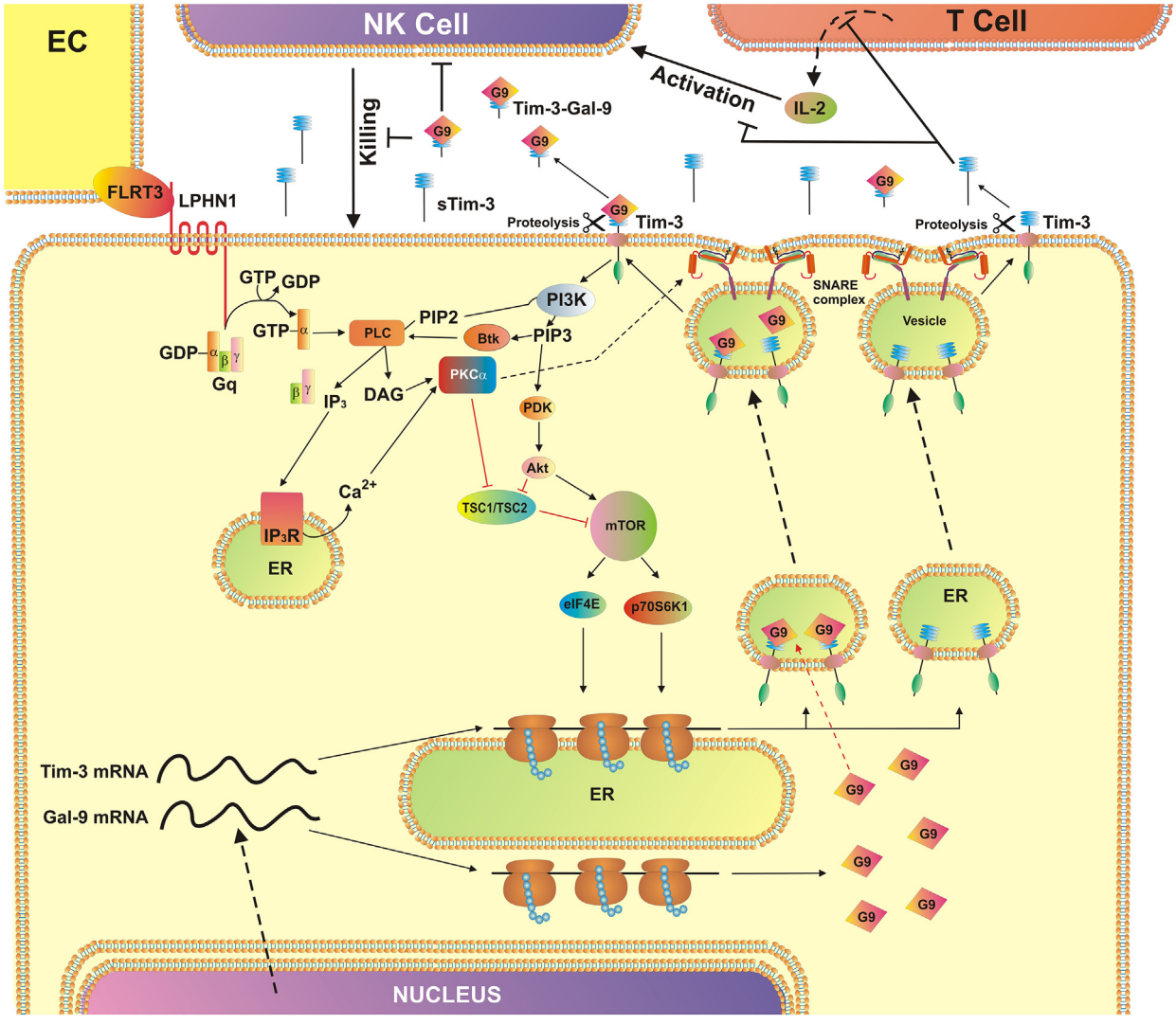

Fig. 13. AML cell-based pathobiochemical pathway showing LPHN1-induced classic activation of PKCα, which triggers translation of Tim-3 and galectin-9 as well as their secretion which is required for immune escape. The interaction of FLRT3 located on the surface of endothelial cells (EC) with LPHN1 leads to the activation of PKCα through the classic Gq/PLC/Ca^{2+} pathway. Ligand-bound LPHN1 activates Gq, which in then stimulates PLC. This leads to phosphatidyl-inositol-bisphosphate (PIP2) degradation and production of inositol-trisphospate (IP_3) and diacylglycerol (DAG). IP_3 interacts with ER-associated IP_3 receptor (IP3R) leading to Ca^{2+} mobilization. PKCα is activated by DAG and Ca^{2+} activates mTOR translational pathway through downregulation of TSC1/TSC2. mTOR controls translation of Tim-3 and galectin-9. PKCα also phosphorylates Munc18 exocytosis regulator protein which provokes formation of SNARE complexes that tether vesicles to the plasma membrane. This pre-activates the release machinery, and elevated cytosolic Ca^{2+} lead to exocytosis of free and galectin-9-complexed Tim-3. Both types of Tim-3 are differentially shed from the cell surface by proteolytic enzymes. Soluble Tim-3 prevents IL-2 secretion required for activation of NK cells and cytotoxic T cells. Galectin-9 impairs AML cell killing activity of NK cells (and other cytotoxic lymphocytes).

Please cite this article as: Gonçalves Silva, I., et al., The Tim-3-galectin-9 Secretory Pathway is Involved in the Immune Escape of Human Acute Myeloid Leukemia Cells, EBioMedicine (2017), http://dx.doi.org/10.1016/j.ebiom.2017.07.018

et al., 2015; Mabuchi et al., 2016). L-kynurenine affects the ability of NK cells to kill AML cells, an effect which was seen in our experiments and presented in Supplementary Fig. 9. Soluble Tim-3 was shown to significantly downregulate production of IL-2, a cytokine required for activation of NK cells and cytotoxic T lymphocytes.

Taken together, our results show that human AML cells possess a secretory pathway which leads to the production and release of sTim-3 and galectin-9. Both proteins prevent the activation of NK cells and impair their AML cell-killing activity. This pathway, which involves the LPHN1-dependent activation of Tim-3 and galectin-9 production is summarized in Fig. 13. The described pathway presents both biomarkers for AML diagnostics and potential targets (both sTim-3 and galectin-9) for AML immune therapy and thus can be considered as a fundamental discovery.

Grant Support

This work was supported by a Daphne Jackson Trust postdoctoral fellowship (to IMY), University of Kent Faculty of Sciences Research Fund (to VVS and YAU), Batzebär grant (to EFK and SB) and Oncosuisse grant KFS-3728-08-2015 (to LV and MB). Funders had no role in study design, data collection, data analysis, interpretation or writing of the report.

Acknowledgements

We thank Prof. Michelle D. Garrett (School of Biosciences, University of Kent, UK) for generously providing us with AZD2014. We are grateful to Dr. Gurprit S. Lall (School of Pharmacy, University of Kent, UK) for kindly providing us with biological materials for bone marrow extraction. Antibody against Gαq was generously provided by Dr. Emma Veale, School of Pharmacy, University of Kent, UK. We are most grateful to Dr. Natasha S. Barteneva, School of Science and Technology, Nazarbayev University, Astana, Kazakhstan for her generous help with imaging flow cytometry. We thank Diamond Light Source for access to B23 beamline (SM12578).

Conflict of Interest

The authors declare no potential conflicts of interest.

Author Contributions

IGS and IMY conducted most of the experiments, analyzed the data and contributed to manuscript writing, data interpretation and figure assembly. SSS conducted the experiments reported in Figs. 2 and 7 as well as Supplementary Figs. 4 and 6, analyzed the data, contributed to manuscript writing and figure assembly. WF and JW were collecting plasma/providing blood plasma samples obtained from AML patients. MB and LV generated antibodies against Tim-3 and human recombinant Tim-3 protein fragment used in the study. RH, GS and GC conducted the experiments associated with SRCD and analyzed the data. SB contributed to the study design and concept development. YAU and BFG designed the experiments associated with cell-cell interactions, analyzed and interpreted the data, contributed to the concept development and manuscript writing. EFK designed and interpreted co-localization experiments, strongly contributed to design of experiments associated with Tim-3 and galectin-9 secretion, concept development and manuscript writing. VVS – designed the whole study, strongly participated in all the data collection, data analysis and interpretation, developed the concept and wrote the manuscript.

Appendix A. Supplementary data

Supplementary data to this article can be found online at http://dx.doi.org/10.1016/j.ebiom.2017.07.018.

References

Abooali, M., Lall, G.S., Coughlan, K., Lall, H.S., Gibbs, B.F., Sumbayev, V.V., 2014. Crucial involvement of xanthine oxidase in the intracellular signalling networks associated with human myeloid cell function. Sci. Rep. 4, 6307.

Ashton, A.C., Rahman, M.A., Volynski, K.E., Manser, C., Orlova, E.V., Matsushita, H., Davletov, B.A., van Heel, M., Grishin, E.V., Ushkaryov, Y.A., 2000. Tetramerisation of α-latrotoxin by divalent cations is responsible for toxin-induced non-vesicular release and contributes to the Ca^{2+}-dependent vesicular exocytosis from synaptosomes. Biochimie 82, 453–468.

Boucard, A.A., Maxeiner, S., Sudhof, T.C., 2014. Latrophilins function as heterophilic cell-adhesion molecules by binding to teneurins: regulation by alternative splicing. J. Biol. Chem. 289, 387–402.

Chabot, S., Kashio, Y., Seki, M., Shirato, Y., Nakamura, K., Nishi, N., Nakamura, T., Matsumoto, R., Hirashima, M., 2002. Regulation of galectin-9 expression and release in Jurkat T cell line cells. Glycobiology 12, 111–118.

Corm, S., Berthon, C., Imbenotte, M., Biggio, V., Lhermitte, M., Dupont, C., Briche, I., Quesnel, B., 2009. Indoleamine 2,3-dioxygenase activity of acute myeloid leukemia cells can be measured from patients' sera by HPLC and is inducible by IFN-gamma. Leuk. Res. 33, 490–494.

Davletov, B.A., Meunier, F.A., Ashton, A.C., Matsushita, H., Hirst, W.D., Lelianova, V.G., Wilkin, G.P., Dolly, J.O., Ushkaryov, Y.A., 1998. Vesicle exocytosis stimulated by α-latrotoxin is mediated by latrophilin and requires both external and stored Ca^{2+}. EMBO J. 17, 3909–3920.

Davydov, I.I., Fidalgo, S., Khaustova, S.A., Lelyanova, V.G., Grebenyuk, E.S., Ushkaryov, Y.A., Tonevitsky, A.G., 2009. Prediction of epitopes in closely related proteins using a new algorithm. Bull. Exp. Biol. Med. 148, 869–873.

Delacour, D., Koch, A., Jacob, R., 2009. The role of galectins in protein trafficking. Traffic 10, 1405–1413.

Dhupkar, P., Gordon, N., 2017. Interleukin-2: old and new approaches to enhance immune-therapeutic efficacy. Adv. Exp. Med. Biol. 995, 33–51.

Fasler-Kan, E., Barteneva, N., Ketterer, S., Wunderlich, K., Huwyler, J., Gygax, D., Flammer, J., Meyer, P., 2010. Activation of the JAK-STAT intracellular pathway in human retinal pigment epithelial cell line ARPE-19. Int. J. Interf. Cytokine Mediat. Res. 2, 127–136.

Fasler-Kan, E., Baiken, Y., Vorobjev, I.A., Barteneva, N.S., 2016. Analysis of nucleocytoplasmic protein shuttling by imaging flow cytometry. Methods Mol. Biol. 1389, 127–137.

Folgiero, V., Cifaldi, L., Li Pira, G., Goffredo, B.M., Vinti, L., Locatelli, F., 2015. TIM-3/Gal-9 interaction induces IFNgamma-dependent IDO1 expression in acute myeloid leukemia blast cells. J. Hematol. Oncol. 8, 36.

Geng, H., Zhang, G.M., Li, D., Zhang, H., Yuan, Y., Zhu, H.G., Xiao, H., Han, L.F., Feng, Z.H., 2006. Soluble form of T cell Ig mucin 3 is an inhibitory molecule in T cell-mediated immune response. J. Immunol. 176, 1411–1420.

Gleason, M.K., Lenvik, T.R., McCullar, V., Felices, M., O'Brien, M.S., Cooley, S.A., Verneris, M.R., Cichocki, F., Holman, C.J., Panoskaltsis-Mortari, A., et al., 2012. Tim-3 is an inducible human natural killer cell receptor that enhances interferon gamma production in response to galectin-9. Blood 119, 3064–3072.

Golden-Mason, L., McMahan, R.H., Strong, M., Reisdorph, R., Mahaffey, S., Palmer, B.E., Cheng, L., Kulesza, C., Hirashima, M., Niki, T., et al., 2013. Galectin-9 functionally impairs natural killer cells in humans and mice. J. Virol. 87, 4835–4845.

Gonçalves Silva, I., Ruegg, L., Gibbs, B.F., Bardelli, M., Fruehwirth, A., Varani, L., Berger, S.M., Fasler-Kan, E., Sumbayev, V.V., 2016. The immune receptor Tim-3 acts as a trafficker in a Tim-3/galectin-9 autocrine loop in human myeloid leukemia cells. Oncoimmunology 5, e1195535.

Hughes, R.C., 1999. Secretion of the galectin family of mammalian carbohydrate-binding proteins. Biochim. Biophys. Acta 1473, 172–185.

Hussain, R., Javorfi, T., Siligardi, G., 2012a. Circular dichroism beamline B23 at the Diamond Light Source. J. Synchrotron Radiat. 19, 132–135.

Hussain, R., Jávorfi, T., Siligardi, G., 2012b. Spectroscopic analysis: synchrotron radiation circular dichroism. Compr. Chiral. 8, 438–448.

Hussain, R., Benning, K., Myatt, D., Javorfi, T., Longo, E., Rudd, T.R., Pulford, B., Siligardi, G., 2015. CDApps: integrated software for experimental planning and data processing at beamline B23, Diamond Light Source. J. Synchrotron Radiat. 22, 862.

Khaznadar, Z., Henry, G., Setterblad, N., Agaugue, S., Raffoux, E., Boissel, N., Dombret, H., Toubert, A., Dulphy, N., 2014. Acute myeloid leukemia impairs natural killer cells through the formation of a deficient cytotoxic immunological synapse. Eur. J. Immunol. 44, 3068–3080.

Kikushige, Y., Miyamoto, T., Yuda, J., Jabbarzadeh-Tabrizi, S., Shima, T., Takayanagi, S., Niiro, H., Yurino, A., Miyawaki, K., Takenaka, K., et al., 2015. A TIM-3/Gal-9 autocrine stimulatory loop drives self-renewal of human myeloid leukemia stem cells and leukemic progression. Cell Stem Cell 17, 341–352.

Kirshenbaum, A.S., Akin, C., Wu, Y., Rottem, M., Goff, J.P., Beaven, M.A., Rao, V.K., Metcalfe, D.D., 2003. Characterization of novel stem cell factor responsive human mast cell lines LAD 1 and 2 established from a patient with mast cell sarcoma/leukemia; activation following aggregation of FcepsilonRI or FcgammaRI. Leuk. Res. 27, 677–682.

Kurinna, S., Konopleva, M., Palla, S.L., Chen, W., Kornblau, S., Contractor, R., Deng, X., May, W.S., Andreeff, M., Ruvolo, P.P., 2006. Bcl2 phosphorylation and active PKC alpha are associated with poor survival in AML. Leukemia 20, 1316–1319.

Lee, J., Lee, S.J., Lim, K.T., 2014. ZPDC glycoprotein (24 kDa) induces apoptosis and enhances activity of NK cells in N-nitrosodiethylamine-injected Balb/c. Cell. Immunol. 289, 1–6.

Liu, J., Wan, Q., Lin, X., Zhu, H., Volynski, K., Ushkaryov, Y., Xu, T., 2005. α-Latrotoxin modulates the secretory machinery via receptor-mediated activation of protein kinase C. Traffic 6, 756–765.

Mabuchi, R., Hara, T., Matsumoto, T., Shibata, Y., Nakamura, N., Nakamura, H., Kitagawa, J., Kanemura, N., Goto, N., Shimizu, M., et al., 2016. High serum concentration of L-kynurenine predicts unfavorable outcomes in patients with acute myeloid leukemia. Leuk. Lymphoma 57, 92–98.

Maiga, A., Lemieux, S., Pabst, C., Lavallee, V.P., Bouvier, M., Sauvageau, G., Hebert, J., 2016. Transcriptome analysis of G protein-coupled receptors in distinct genetic subgroups of acute myeloid leukemia: identification of potential disease-specific targets. Blood Cancer J. 6, e431.

Micol, V., Sanchez-Pinera, P., Villalain, J., de Godos, A., Gomez-Fernandez, J.C., 1999. Correlation between protein kinase C alpha activity and membrane phase behavior. Biophys. J. 76, 916–927.

Moller-Hackbarth, K., Dewitz, C., Schweigert, O., Trad, A., Garbers, C., Rose-John, S., Scheller, J., 2013. A disintegrin and metalloprotease (ADAM) 10 and ADAM17 are major sheddases of T cell immunoglobulin and mucin domain 3 (Tim-3). J. Biol. Chem. 288, 34529–34544.

Morgan, A., Burgoyne, R.D., Barclay, J.W., Craig, T.J., Prescott, G.R., Ciufo, L.F., Evans, G.J., Graham, M.E., 2005. Regulation of exocytosis by protein kinase C. Biochem. Soc. Trans. 33, 1341–1344.

Nagae, M., Nishi, N., Murata, T., Usui, T., Nakamura, T., Wakarsuki, S., Kato, R., 2006. Crystal structure of the galectin-9 N-terminal carbohydrate recognition domain from Mus musculus reveals the basic mechanism of carbohydrate recognition. J. Biol. Chem. 281, 35884–35893.

Prokhorov, A., Gibbs, B.F., Bardelli, M., Ruegg, L., Fasler-Kan, E., Varani, L., Sumbayev, V.V., 2015. The immune receptor Tim-3 mediates activation of PI3 kinase/mTOR and HIF-1 pathways in human myeloid leukemia cells. Int. J. Biochem. Cell Biol. 59, 11–20.

Schindelin, J., Rueden, C.T., Hiner, M.C., et al., 2015. The ImageJ ecosystem: an open platform for biomedical image analysis. Mol. Reprod. Dev. 82, 518–529.

Siligardi, G., Hussain, R., 2015. CD Spectroscopy: An Essential Tool for Quality Control of Protein Folding. RJ Owen, ed. Methods Mol. Biol 1261. Springer, NY, pp. 255–276.

Silva, J.P., Ushkaryov, Y.A., 2010. The latrophilins, "split-personality" receptors. Adv. Exp. Med. Biol. 706, 59–75.

Silva, J.P., Lelianova, V.G., Ermolyuk, Y.S., Vysokov, N., Hitchen, P.G., Berninghausen, O., Rahman, M.A., Zangrandi, A., Fidalgo, S., Tonevitsky, A.G., Dell, A., Volynski, K.E., Ushkaryov, Y.A., 2011. Latrophilin 1 and its endogenous ligand Lasso/teneurin-2 form a high-affinity transsynaptic receptor pair with signaling capabilities. Proc. Natl. Acad. Sci. U. S. A. 108, 12113–12118.

Stockli, J., Fazakerley, D.J., James, D.E., 2011. GLUT4 exocytosis. J. Cell Sci. 124, 4147–4159.

Sumbayev, V.V., Nicholas, S.A., 2010. Hypoxia-inducible factor 1 as one of the "signaling drivers" of toll-like receptor-dependent and allergic inflammation. Arch. Immunol. Ther. Exp. 58, 287–294.

Sumbayev, V.V., Yasinska, I., Oniku, A.E., Streatfield, C.L., Gibbs, B.F., 2012. Involvement of hypoxia-inducible factor-1 in the inflammatory responses of human LAD2 mast cells and basophils. PLoS One 7, e34259.

Sumbayev, V.V., Gonçalves Silva, I., Blackburn, J., Gibbs, B.F., Yasinska, I.M., Garrett, M.D., Tonevitsky, A.G., Ushkaryov, Y.A., 2016. Expression of functional neuronal receptor latrophilin 1 in human acute myeloid leukemia cells. Oncotarget 7, 45575–45583.

Swamydas, M., Lionakis, M.S., 2013. Isolation, purification and labeling of mouse bone marrow neutrophils for functional studies and adoptive transfer experiments. JoVE e50586.

Ushkaryov, Y., 2002. α-Latrotoxin: from structure to some functions. Toxicon 40, 1–5.

Volynski, K.E., Capogna, M., Ashton, A.C., Thomson, D., Orlova, E.V., Manser, C.F., Ribchester, R.R., Ushkaryov, Y.A., 2003. Mutant α-latrotoxin (LTX^{N4C}) does not form pores and causes secretion by receptor stimulation: this action does not require neurexins. J. Biol. Chem. 278, 31058–31066.

Wang, F., He, W., Zhou, H., Yuan, J., Wu, K., Xu, L., Chen, Z.K., 2007. The Tim-3 ligand galectin-9 negatively regulates CD8+ alloreactive T cell and prolongs survival of skin graft. Cell. Immunol. 250, 68–74.

Yasinska, I.M., Gibbs, B.F., Lall, G.S., Sumbayev, V.V., 2014. The HIF-1 transcription complex is essential for translational control of myeloid hematopoietic cell function by maintaining mTOR phosphorylation. Cell. Mol. Life Sci. 71, 699–710.

Please cite this article as: Gonçalves Silva, I., et al., The Tim-3-galectin-9 Secretory Pathway is Involved in the Immune Escape of Human Acute Myeloid Leukemia Cells, EBioMedicine (2017), http://dx.doi.org/10.1016/j.ebiom.2017.07.018

Supplementary information

The Tim-3-galectin-9 secretory pathway is involved in the immune escape of human acute myeloid leukemia cells

Isabel Gonçalves Silva, Inna M. Yasinska, Svetlana S. Sakhnevych, Walter Fiedler, Jasmin Wellbrock, Marco Bardelli, Luca Varani, Rohanah Hussain, Giuliano Siligardi, Giacomo Ceccone, Steffen M. Berger, Yuri A. Ushkaryov, Bernhard F. Gibbs, Elizaveta Fasler-Kan and Vadim V. Sumbayev

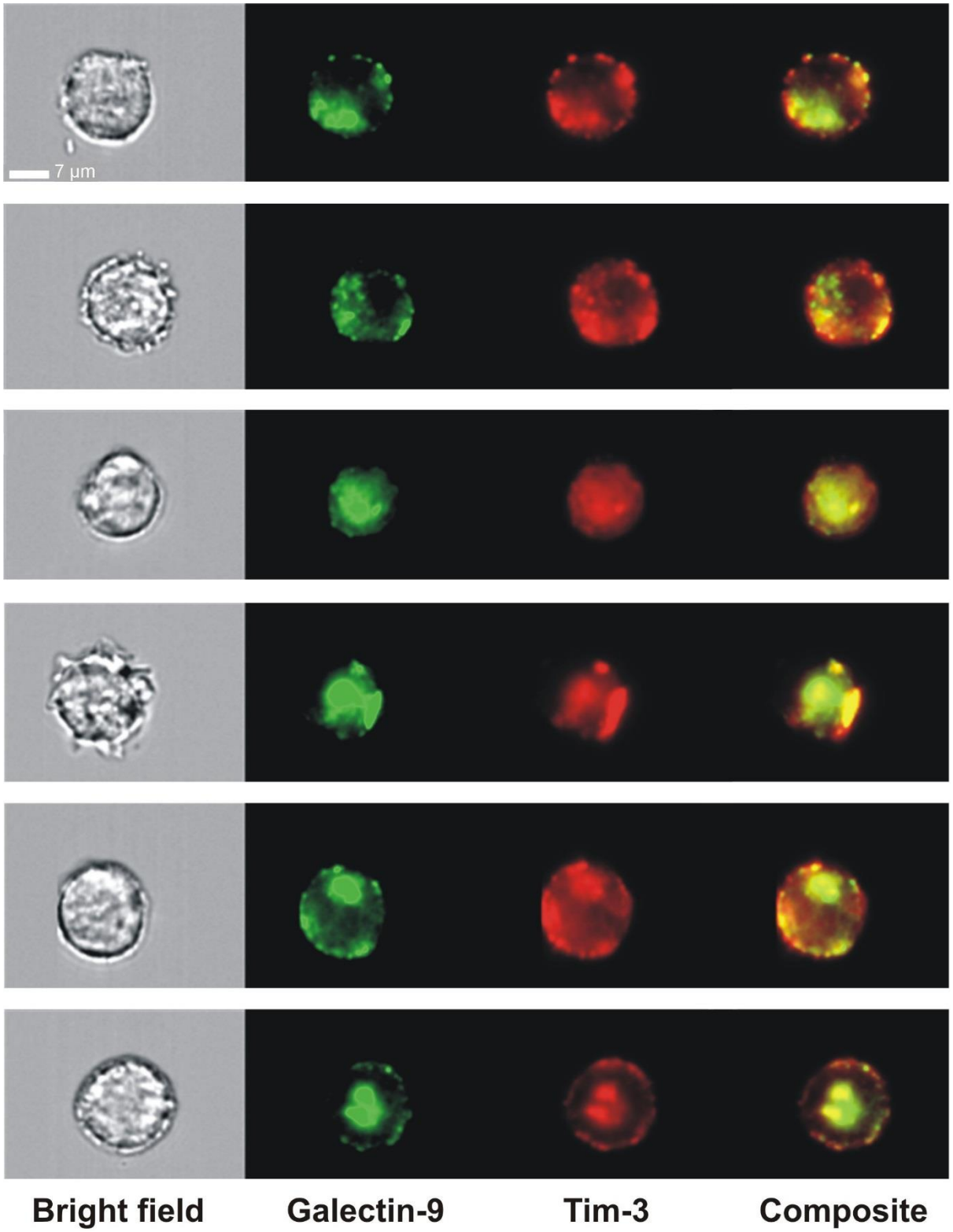

Supplementary figure 1. Co-localization of galectin-9 and Tim-3 in THP-1 human AML cells upon PKC activation. THP-1 cells stimulated with PMA (please see Figure 3 for details) were permiabilized and subjected to imaging flow cytometry as outlined in Materials and Methods. Images represent six selected single cells.

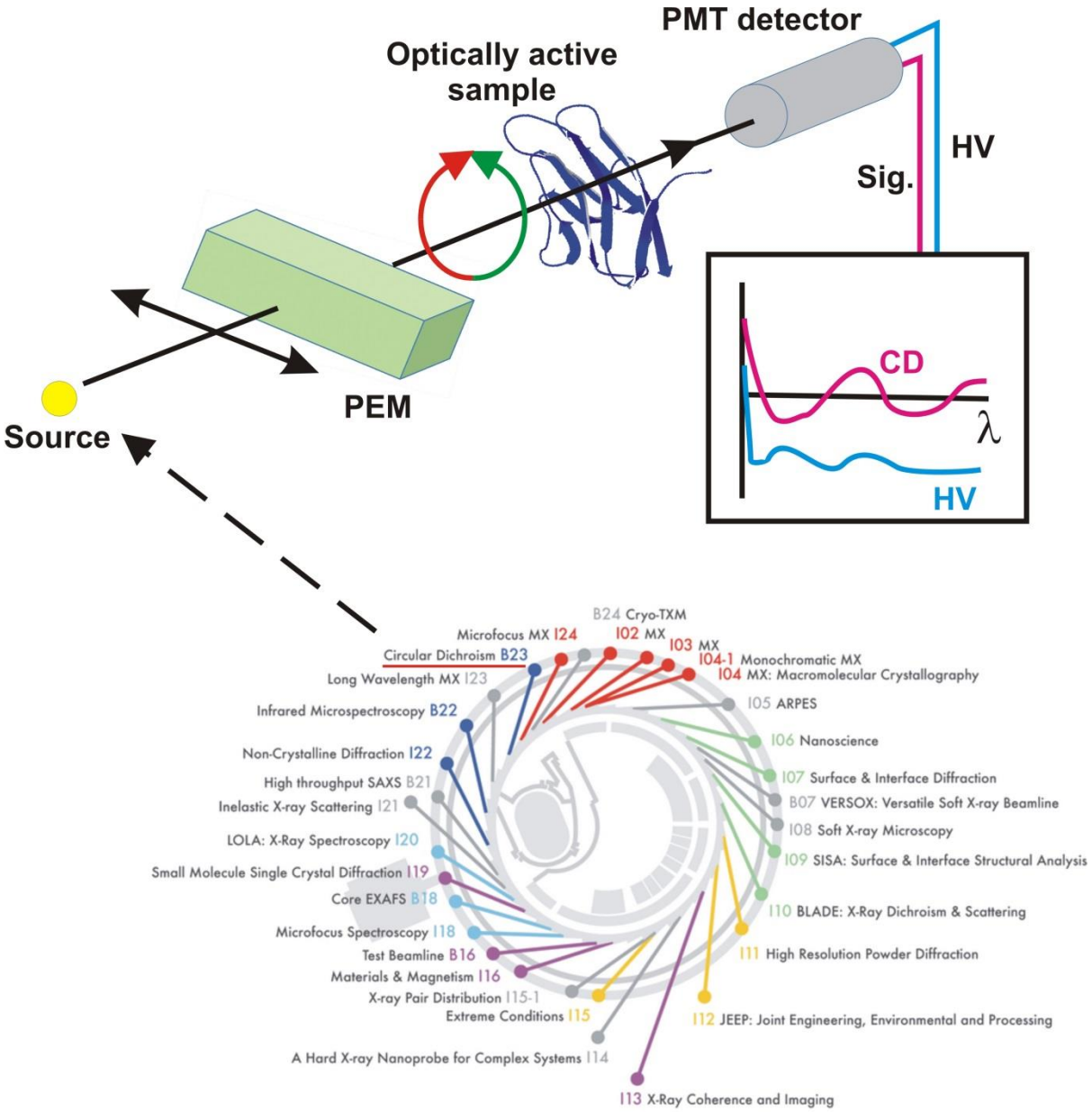

Supplementary figure 2. Beam line 23 at Diamond Light Source synchrotron and scheme of SRCD spectroscopy analysis.

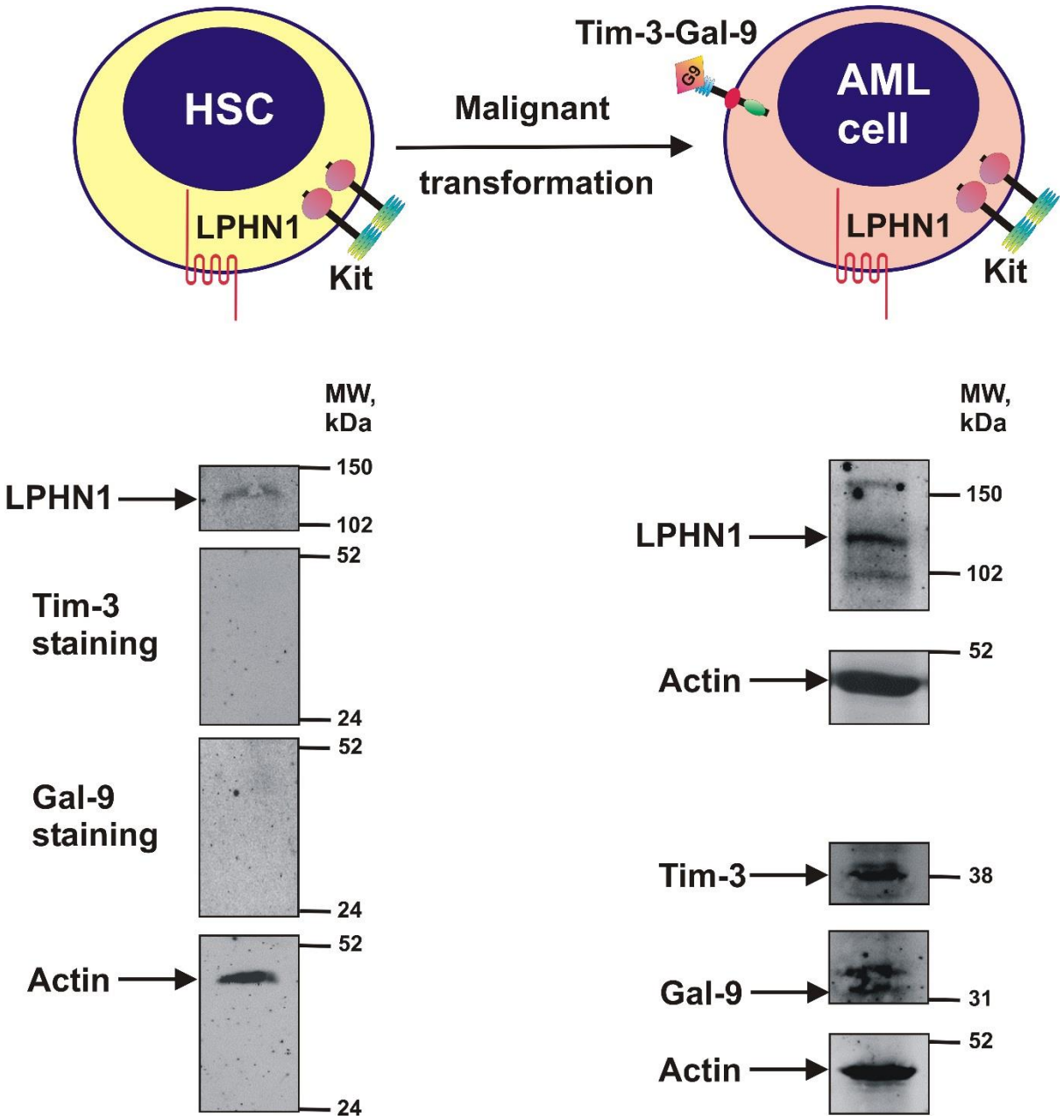

Supplementary figure 3. Characterisation of expression of LPHN1, Tim-3 and galectin-9 proteins in CD34 positive human stem cells (HSCs) and THP-1 AML cells (positive control). LPHN1, Tim-3 and galectin-9 proteins were detected in CD34-positive HSCs and THP-1 cells (positive control) using Western blot analysis. Images are from one experiment representative of three which gave similar results.

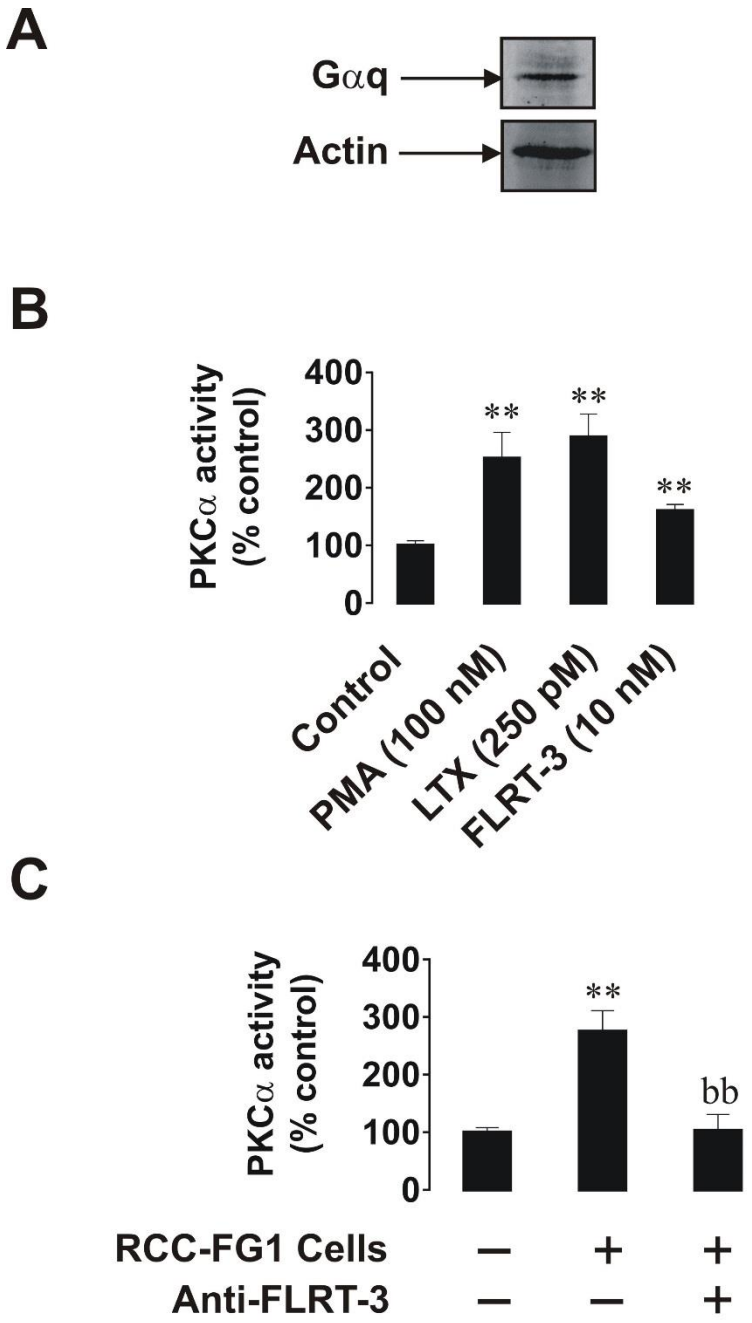

Supplementary figure 4. Expression of Gαq and activity of PKCα in THP-1 human AML cells. (A) Gαq expression was analysed by Western blot analysis in resting THP-1 cells. (B) Activity of PKCα was analysed in resting THP-1 cells as well as those exposed for 16 h to 100 nM PMA, 250 pM LTX and 10 nM FLRT-3. (C) Activity of PKCα was analysed in resting THP-1 cells and those co-cultured with RCC-FG1 cells (ratio 1 THP-1: 2 RCC-FG1) in the absence or presence of 5 µg/ml FLRT-3 neutralising antibody. Images are from one experiment representative of three which gave similar results. Quantitative data are mean values ± SEM of three independent experiments; *$p < 0.05$; **$p < 0.01$ vs. control. Symbol "bb" indicates $p<0.01$ vs. THP-1/RCC-FG1 co-culture.

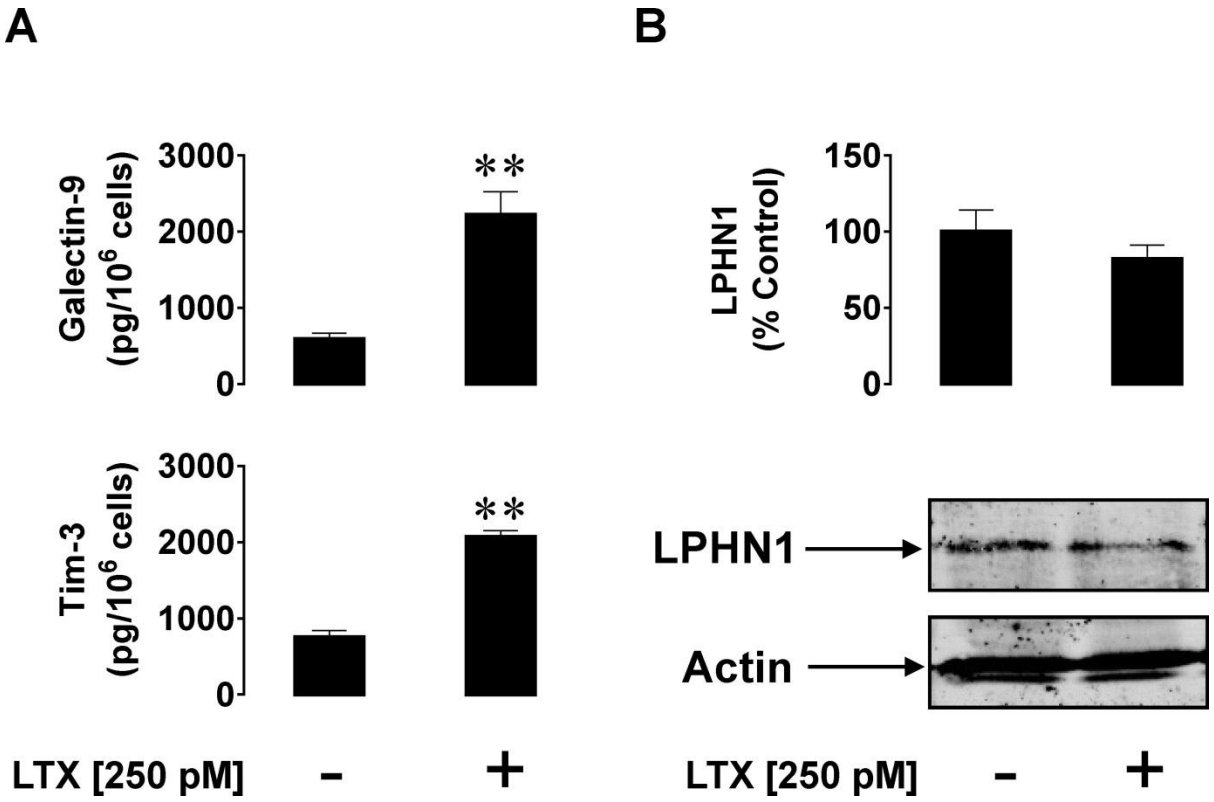

Supplementary figure 5. LTX induces on Tim-3 and galectin-9 secretion in primary human AML cells. Primary human AML blasts (AML-PB001F) were exposed for 24 h to 250 pM LTX followed by detection of secreted galectin-9 and Tim-3 levels by ELISA **(A)** as outlined in Materials and Methods. LPHN1 expression in these cells was confirmed by the Western blot analysis **(B)**. Images are from one experiment representative of six which gave similar results. Quantitative data are mean values ± SEM of six independent experiments; **p < 0.01 vs. control.

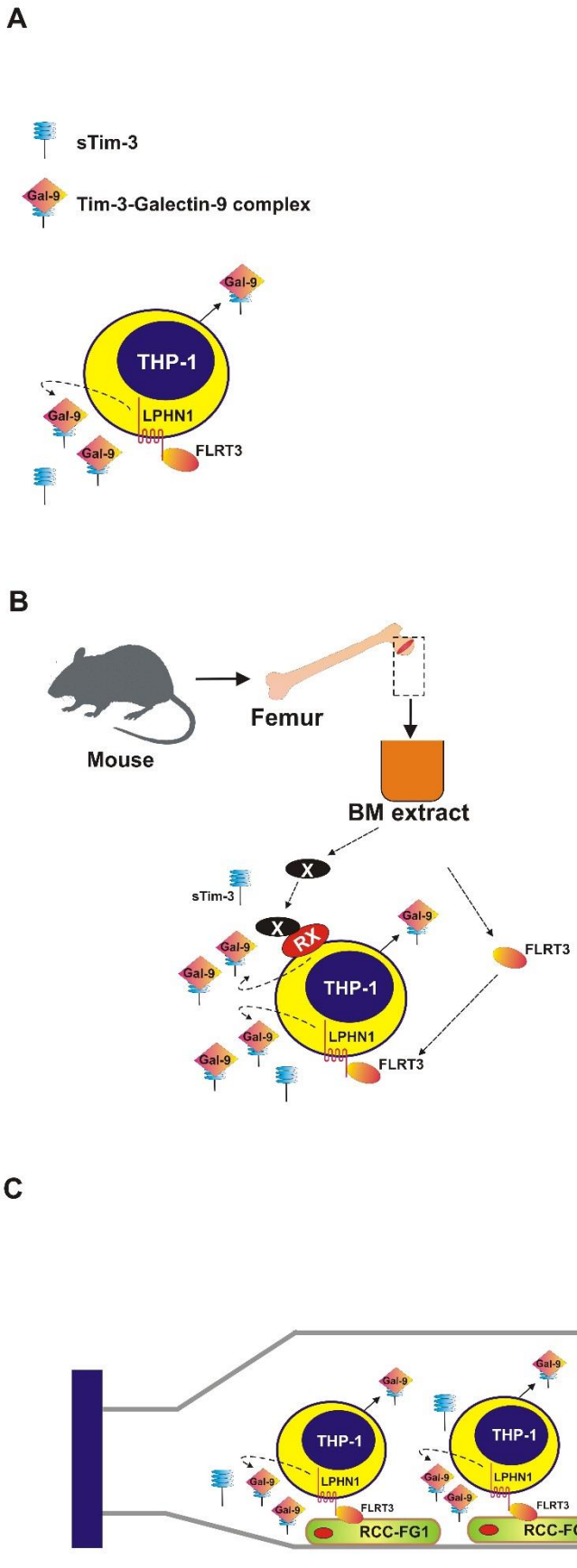

Supplementary figure 6. Schemes of the experiments presented in the Figure 7. Sections A, B and C correspond to those of the Figure 7.

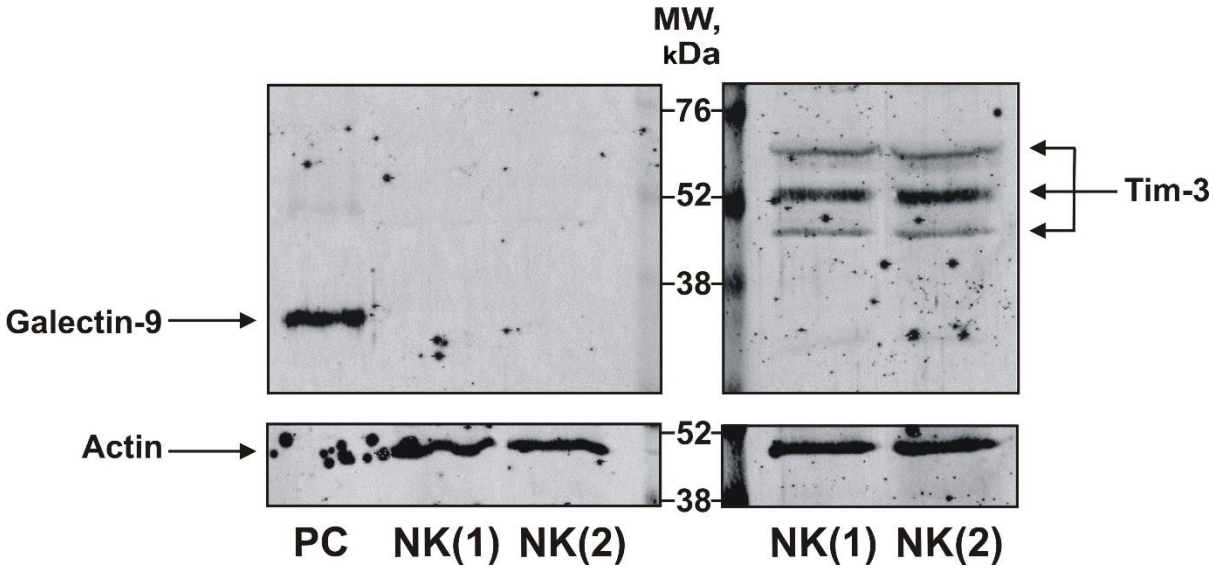

Supplementary figure 7. Expression of Tim-3 and galectin-9 in primary human NK cells. Expressions of both proteins were analysed in whole cell extracts by Western blot. Human recombinant galectin-9 was used as a positive control. Images are from one experiment representative (two donors in each) of three which gave similar results.

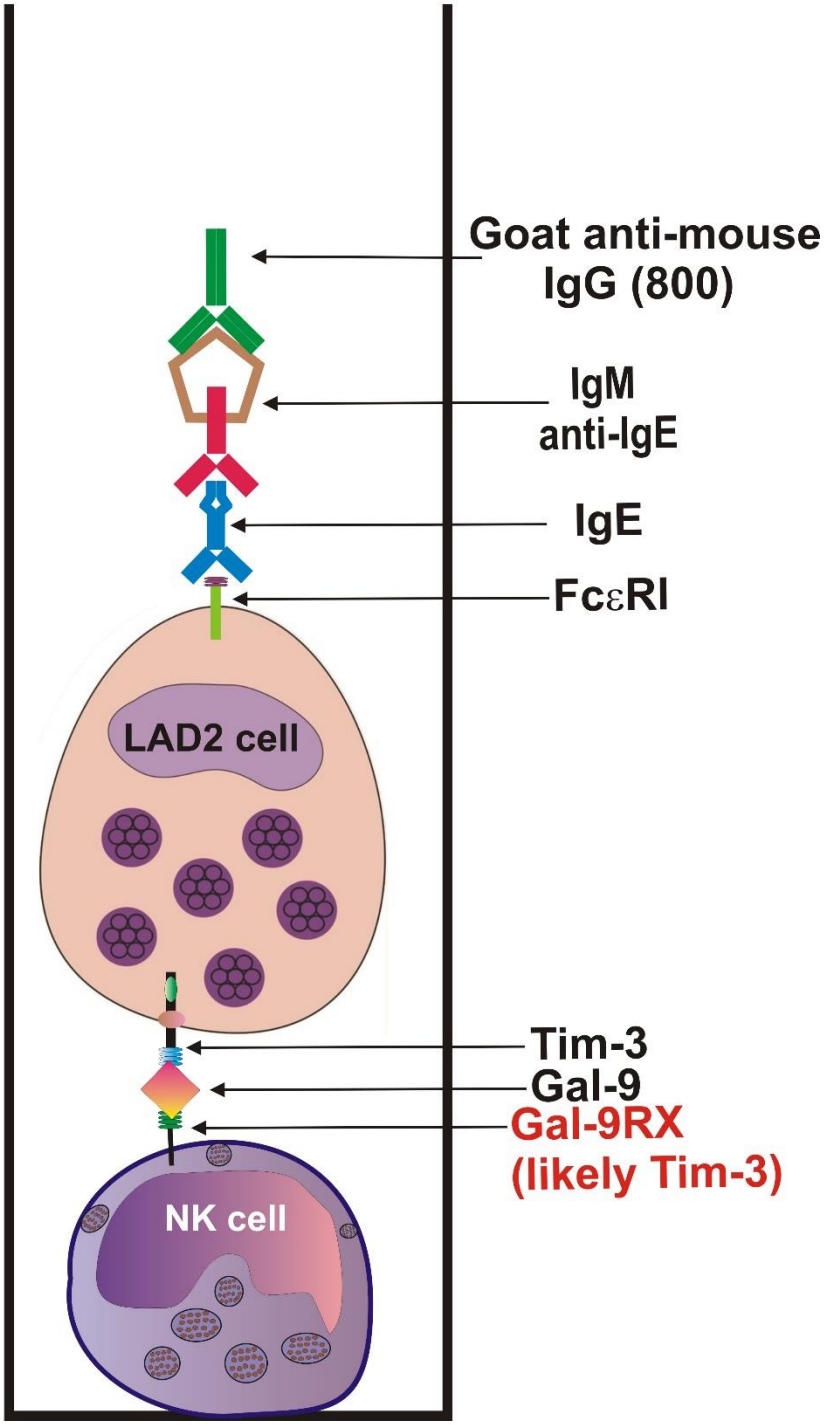

Supplementary figure 8. Scheme of the experiment presented in the Figure 9.

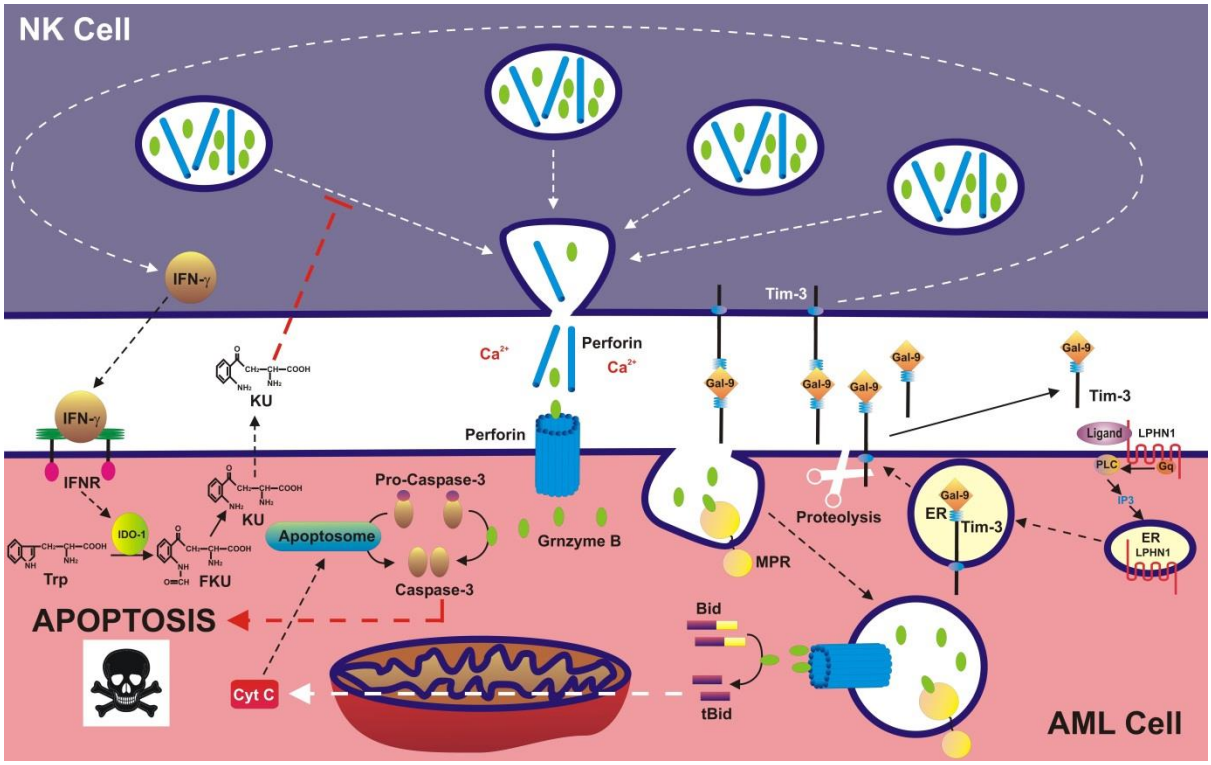

Supplementary figure 9. Possible biochemical interactions between AML and NK cells. LPHN1/Tim-3/galectin-9 pathway (Figure 14) leads to externalisation/release of galectin-9, which binds to the NK cell receptor (likely – Tim-3). In response, NK cells release IFN-γ which triggers the activation of IDO1 in AML cells. IDO1 converts tryptophan (Trp) into formyl-kynurenine (FKU), which is further degraded into L-kynurenine (KU). KU is released and is capable of attenuating the ability of NK cells to deliver granzyme B into SAML cells in perforin/mannose-6-phosphate receptor (MPR)-dependent manner. If successfully delivered, granzyme B catalysed Bid cleavage leading to cytochrome c release from mitochondria. This leads to formation of apoptosome and activation of caspase-3. Furthermore, granzyme B is capable of performing direct proteolytic activation of caspase-3. These effects lead to AML cell apoptosis. However, this process is not taking place due to galectin-9-induced impairing of NK cell activity as described above.